



HAL
open science

Study of the structural organization of humic nanocolloids

Abdul Amir Chaaban

► **To cite this version:**

Abdul Amir Chaaban. Study of the structural organization of humic nanocolloids. Hydrology. Université Paul Sabatier - Toulouse III, 2016. English. NNT : 2016TOU30062 . tel-01532223

HAL Id: tel-01532223

<https://theses.hal.science/tel-01532223v1>

Submitted on 2 Jun 2017

HAL is a multi-disciplinary open access archive for the deposit and dissemination of scientific research documents, whether they are published or not. The documents may come from teaching and research institutions in France or abroad, or from public or private research centers.

L'archive ouverte pluridisciplinaire **HAL**, est destinée au dépôt et à la diffusion de documents scientifiques de niveau recherche, publiés ou non, émanant des établissements d'enseignement et de recherche français ou étrangers, des laboratoires publics ou privés.



Université
de Toulouse

THÈSE

En vue de l'obtention du

DOCTORAT DE L'UNIVERSITÉ DE TOULOUSE

Délivré par :

Université Toulouse 3 Paul Sabatier (UT3 Paul Sabatier)

Cotutelle internationale avec :

Université Libanaise

Présentée et soutenue par :

Abdul Amir CHAABAN

Le 7 Avril 2016

Titre :

Etude de l'Organisation Structurale des Nanocolloïdes Humiques

École doctorale et discipline ou spécialité :

ED SDU2E : Hydrologie, Hydrochimie, Sol, Environnement

Unité de recherche :

Laboratoire Géosciences Environnement Toulouse (GET)-UMR 5563

Directeur/trice(s) de Thèse :

Bruno LARTIGES-Professeur-Université de Toulouse

Zeinab SAAD-Professeur-Université Libanaise

Veronique Kazpard-Professeur-Université Libanaise

Rapporteurs :

Véronique PEYRE- Maître de Conférences-Chercheur (PHENIX-UPMC)

Edith PARLANTI- Chercheur CNRS (EPOC/OASU-Université de Bordeaux)

Jose-Paulo PINHEIRO- Professeur (ENSG-LIEC- université de Lorraine)

Autre(s) membre(s) du jury :

Particia VICENDO- Chercheur CNRS (IMRCP- Université Paul Sabatier Toulouse III)

Hala Hafez SAKAKINI-Professeur (Université Libanaise)

ACKNOWLEDGEMENTS

My profound gratitude and great appreciation goes to all of those who contributed directly or indirectly in the writing of this manuscript and the progress of the course as well.

First of all, I wish to thank Mr. Michel GREGOIRE, Director of Geosciences Environment Toulouse (GET) laboratory, for his warm welcoming and permanent good mood.

My sincere gratitude's go to my supervisor and Mentor, Pr. Bruno LARTIGES, lecturer at CNRS/UPS that has closely followed the progress of my work. Your precious guidance, helps, advices and corrections remain to me the testimony of your scientific and human qualities. I was blessed to have the chance to work with a pioneer in scientific research domain. Your confidence, freedom, encouragement and valuable advices you gave me allowed me to develop myself in my work. You will always remain one of the few people whom will affect me, not only on my scientific career but also on the personal level. It was always fun working with you, especially your good mood and laughter that always made me optimistic of tomorrow. I hope you accept my sincere gratitude and appreciation.

My thanks also go to Zeinab SAAD, professor at EDST- Lebanese University, for accepting enthusiastically the direction of this work and for your guidance and support.

My sincere appreciations also go to my co-supervisor, Pr. Véronique KAZPARD, coordinator of the Master research degree in EDST- Lebanese University. To whom I am proudly to say that she was my professor throughout my university journey, you had positively affected my life and career. I really appreciate all your efforts not only in improving the quality of education and the creation of the criteria in the advanced research but also in your readiness for guidance, help and advice.

I express my sincere thanks to Mme. PEYRE Véronique, Maître de Conférences UPMC - laboratoire Phenix, Mme. PARLANTI Edith. CNRS Researcher - laboratoire EPOC University of Bordeaux I, and M. PINHEIRO Jose-Paulo, University of Lorraine Nancy-Observatoire Terre et Environnement de Lorraine, for sacrificing some of their time and accepting the heavy burden of evaluating this work and being the reporters of this thesis. I am also grateful to Mme. VICENDO Patricia, CNRS Researcher, and Mme. HAFEZ Hala, Professeur at Lebanese University, who agreed to be part of this jury.

The realization of this work was made possible through the funding from AZM and SAADE foundation- Lebanese university in the person of Pr. Mohamad KHALIL, the director of AZM centre for research in biotechnology at the Lebanese university.

My appreciations go to anyone who contributed, in one way or another, in the experimental results of this thesis. I refer in particular to Celia PLISSON-CHASTANG from Laboratoire de Biologie Moléculaire Eucaryote (METI platform-UPS) for her valuable and precious help in the cryogenic transmission electron microscopy, quality time and advices. Because of her significant qualifications we were able to acquire high quality micrographs. I have to also mention and thanks Stephanie Balor and Vanessa Soldan from the METI Platform. I appreciate the help of Isabelle BIHANNIC, from Laboratoire Interdisciplinaire des Environnements Continentaux (LIEC) from University of Lorraine- Vandoeuvre-les-Nancy, in the treatment and interpretation of small angle neutron scattering data. I also thank Celine CAILLET from LIEC for her help with the Zeta-Sizer and her valuable advices. I also mention Benedicte PRELOT, from ICGM (AIME)-University of Montpellier II, for her help with the surface tension and Isothermal Calorimetric data acquirement and spectra interpretation. Finally, I thank Patricia VICENDO from Laboratoire des Intéractions Moléculaires et Réactivité Chimique et Photochimique (IMRCP-UPS) for her valuable help and effort with the fluorescence spectroscopy.

I want to express my appreciation and acknowledgements to all the members and friends of the Geosciences Environment Toulouse (GET) laboratory and Platform for Research and Analysis in Environmental Sciences Beirut (PRASE) without which the last four years would not have been enjoyable.

I want to thank the friends who have always shown me kindness and attention especially Ashraf Nouredine, Eliane el Hayek, Josseph Bassil and Zeinab Ezzeddine.

*Finally, I will finish my gratitude and appreciation by dedicating this dissertation to my family and my fiancée **Sahar Ismail** who always told me that in a desperate situation, initiative and tranquility are the only hope to get by and that human qualities are often evaluated in the most difficult conditions.*

I dedicate this work to the scientific community and hope that it contributes to the good of science, as to who will read and appreciate the information provided in this dissertation all my gratitude.

TABLE OF CONTENTS

GENERAL INTRODUCTION.....	5
CHAPTER I: Humic Nano-Colloids “General Context”	11
I.1 HUMIC SUBSTANCES.....	13
I.1-1 Definitions and Terminologies.....	14
I.1-2 Classification of Humic Substances.....	15
I.1-2-1 Humic Acid.....	15
I.1-2-2 Fulvic Acid.....	16
I.1-2-3 Humin	17
I.1-2-4 Comparison of Humic Substance Fractions (Humic Acid, Fulvic Acid and Humin).....	17
I.2 HUMIC SUBSTANCE GENESIS	20
I.2-1 Lignin-Protein Theory (Biological or Degradative Concept)	21
I.2-2 The Poly-Phenol Theory (Biological Processes Followed by Chemical Reaction “Abiotic” or Synthetic Concept).....	23
I.2-3 Sugar-Amine Theory “Maillard Reaction” (Biological Processes Followed by Chemical Reaction “Abiotic” or Synthetic Concept)	24
I.3 ISOLATION/EXTRACTION AND FRACTIONATION.....	25
I.3-1 Isolation.....	26
I.3-2 Drawback of Isolation Processes.....	29
I.4 CHARACTERIZATION: CHEMICAL AND PHYSICAL PROPERTIES	30
I.4-1 Elemental Analyses	31
I.4-2 Functional Group Composition.....	32
I.4-3 Optical Properties.....	35
I.4-3-1 UV/Vis Spectrophotometry	35
I.4-3-2 Fluorescence Spectroscopy.....	36
I.4-4 Molecular Conformation (Size and shape) and Molecular Weight.....	40
I.4-5 Structural Organization of Humic Substances	47
I.4-5-1 Humic Substances as Polymers (Macromolecule).....	47
I.4-5-2 Humic Substances Membrane-Like Micelles	48
I.4-5-3 Humic Substances as Supramolecular Associations.....	50

I.5	MODELING REPRESENTATION OF HUMIC SUBSTANCE	53
I.6	ROLES OF HUMIC SUBSTANCES	56
I.7	SURFACTANTS	58
I.7-1	Definition and Classification.....	58
I.7-2	Applications	59
I.7-3	Interaction between Surfactants-Polymers and Surfactants-Humic Substances	60
CHAPTER II:	Materials and Experimental Methods	64
II.1	MATERIALS	67
II.1-1	Humic Substances and Dissolved Organic Matter (DOM).....	67
II.1-2	Surfactants.....	71
II.2	PREPARATION OF HS/SURFACTANT COMPLEXES	72
II.3	METHODS OF CHARACTERIZATION	74
II.3-1	Turbidity	74
II.3-2	Dynamic Light Scattering.....	76
II.3-3	Surface Tension	78
II.3-4	Electrophoretic Mobility and Zeta Potential.....	79
II.3-5	Cryogenic Transmission Electron Microscopy (Cryo-TEM)	81
II.3-5-1	Sample Preparation for Cryo-TEM Observation.....	81
II.3-5-2	Cryo-TEM Imaging Procedure.....	83
II.3-6	Small Angle Neutron Scattering (SANS)	84
II.3-7	Ultraviolet/Visible Spectrophotometer	87
II.3-8	Fluorescence Spectroscopy.....	89
CHAPTER III:	Spontaneous Vesicles in the Suwannee River Fulvic Acid/DTAC System: Implications for the Supramolecular Organization of Humic Substances.	93
III.1	PREFACE	95
III.2	PROBING THE ORGANIZATION OF FULVIC ACID USING A CATIONIC SURFACTANT.....	96
III.2-1	Abstract.....	96
III.2-2	Introduction	96

III.2-3	Experimental Section.....	98
III.2-3-1	Materials.....	98
III.2-3-2	Sample Preparation	98
III.2-3-3	Characterization of SRFA/DTAC Complexes	99
III.2-4	Results	100
III.2-4-1	Turbidity Measurements	100
III.2-4-2	Electrophoretic Mobility, DLS and Surface Tension Measurements.	102
III.2-4-3	Cryo-TEM Observations	104
III.2-5	Discussion.....	109
III.2-5-1	Self-assemblies of Fulvic Acid and DTAC.....	109
III.2-5-2	Towards Average Geometric Characteristics of SRFA Constituents	111
III.2-6	Conclusions	114
III.3	Packing Parameter of the Mixed System SRFA/DTAC: Assuming Interdigitating Alkyl Chain	114
III.4	SMALL ANGLE NEUTRON SCATTERING (SANS).....	119
III.4-1	Sample Preparation.....	119
III.4-2	Characterization of SRFA/DTAC Complexes	119
III.4-3	Small Angle Neutron Scattering Measurements	120
III.5	INTERMEDIATE CONCLUSIONS.....	123
CHAPTER IV:	Association of Suwannee River Humic Acid with a Homologous Series of Cationic Surfactants (C_n-trimethylammonium chloride): The Self-assemblies and Rearrangements.	125
IV.1	PREFACE	127
IV.2	RECONFORMATION OF HUMIC ACID INDUCED BY THE ADDITION OF CATIONIC SURFACTANTS OF VARYING ALKYL CHAIN LENGTH: EVIDENCE OF THE SUPRAMOLECULAR ORGANIZATION OF HUMIC SUBSTANCES.	128
IV.2-1	Introduction	128
IV.2-2	Experimental Section: Materials and Methods	130
IV.2-3	Results	131
IV.2-3-1	Turbidity and DLS Measurements.....	131
IV.2-3-2	Electrophoretic Mobility and Surface Tension Measurements.....	135
IV.2-3-3	Cryo-TEM Observations.....	139

IV.2-4 Discussion	143
IV.2-4-1 Interaction between Humic Acid/Surfactant: Effect of Alkyl Chain Length..	143
IV.2-4-2 Organization of Humic Substances.....	144
IV.3 EFFECT OF pH MODIFICATION	147
IV.3-1 Turbidity and Surface Tension Measurements.....	147
IV.3-2 Cryo-TEM Observations	149
IV.4 SMALL ANGLE NEUTRON SCATTERING (SANS)	150
IV.4-1 Small Angle Neutron Scattering Measurements	151
IV.4-1-1 Two Power Law	152
IV.4-1-2 Two Correlation-Length Model (Two Lorentzian Model)	154
IV.4-1-3 Corrlength Model.....	155
IV.5 INTERMEDIATE CONCLUSIONS.....	157
CHAPTER V: The Effect of Molecular Rearrangement on the Chromophores and Fluorophores of Humic Substances upon Interaction with Cationic Surfactant: A Fluorimetric Study.	159
V.1 PREFACE	161
V.2 ADDITION OF DTAC CATIONIC SURFACTANT TO HUMIC SUBSTANCES TRIGGERS THE SO-CALLED PROTEIN-LIKE FLUORESCENCE.....	162
V.2-1 Abstract.....	162
V.2-2 Introduction.....	162
V.2-3 Materials and Methods	164
V.2-4 Results.....	167
V.2-5 Discussion.....	174
V.2-5-1 Significance of Newly Formed Fluorescence Signals.....	174
V.2-5-2 Potential spectral fingerprinting of HS-DOM after DTAC addition.....	177
V.2-5-3 Assignment of T(δ) Signal	177
V.3 Conclusions	178
CHAPTER VI: General Conclusion and Perspectives.....	181
BIBLIOGRAPHIC REFERENCES	185
LIST OF FIGURES AND TABLES.....	247
ANNEXES.....	259

GENERAL INTRODUCTION

Humic substances (HS) represent more than 50% of dissolved organic compounds in natural aquatic systems (Zumstein and Buffle, 1989). They are ubiquitous organic compounds in waters, sediments and soils (Stevenson, 1994). These organic molecules are composed of heterogeneous mixture of biochemical substances (proteins, carbohydrates, lipids...) decomposed to a greater or lesser extent by microorganisms, but also formed in part from the condensation of small organic molecules (Stevenson, 1994). This diversity results in a poorly understood organization. Humic substances cannot be grouped to a specific chemical or distinctive structural category or unique functional term, so they are operationally classified into three fractions: fulvic acid, humic acid, and humin according to their solubility, acid-alkaline, at different pH level condition.

Besides their obvious role in carbon geocycling, they represent the most abundant form of organic matter on continental surface (Zumstein and Buffle, 1989), HS have been shown to be key components in the transportation/sequestration of xenobiotics and metal contaminants in the environment (Ishiguro et al., 2007 ; Wershaw, 1999 ; Sutton and Sposito, 2005 ; Nebbioso and Piccolo, 2012). Humic Substances also represent a major source of energy to microorganisms. They play an important role in soil and water environment through improving soil water retention, the development of plants through nutrients retained in their aggregates. Although humic substances themselves are not considered to be harmful, they can be source of worries in potable water production and treatment through the formation of direct-acting mutagenic products (trihalomethanes "THM").

The complex heterogeneous nature of HS has been extensively characterized and revealed various constituents that give rise to an amphiphilic nature: large proportion of carboxylic and phenolic groups that make them hydrophilic and contribute to their surface charge and reactivity, and aliphatic moieties that give them surface active and hydrophobic-binding properties. The characteristic size of HS determined by a number of techniques (e.g. AFM, TEM, SAXS...) is about 1-2 nm in diameter. The structure of HS exhibits sensitivity toward the chemical property of solution since variations in solution pH, ionic strength, adsorption and metal complexation change their conformation; this is consistent with the modeling of their charge characteristics that regards HS as soft and porous structures (Duval et al., 2005). These structural modifications may affect the fate and the bioavailability of metal-organic pollutant in the environment (Sieliechi et al., 2008).

Nevertheless, the detailed organization, *i.e.* molecular and conformational structures, of humic nanocolloids remains a matter of harsh debate. They have been long regarded as randomly coiled macromolecules or slightly branched polymers that can coil or adopt an extended conformation according to solutions properties (Stevenson, 1994 ; Swift, 1999 ; Ghosh and Schnitzer, 1980). Such description was formulated after the development of polymer science (Piccolo, 2001): at basic pH and low ionic strength, humic substances are unfolded linear macromolecules. By cons, decreased pH or increased ionic strength leads to the formation of globular structures (Stevenson, 1994). Ghosh and Schnitzer (1980) confirm this hypothesis by linking the conformation of humic substances to their concentration in the solution, such that they form spherical colloids with a high concentration, and provide flexible linear colloids at low concentrations (while respecting conditions of pH and ionic strength). In addition, other researchers support this model based on the study by Cameron et al. (1972) which showed that humic substances form helices of random conformation with average molecular weight between 20,000 to 50,000 Da with a hydrodynamic radius of 4-10 nm (Swift, 1999).

Contrary to previous data, studies of humic acids show that the model of the polymer is not consistent with the new results. These studies are based on several spectroscopic and microscopic techniques, and processes of ionization and pyrolysis (Sutton and Sposito, 2005). Moreover, even the phenomena of formation and preservation of humic substances in soils suggest a different model than that of polymers (Piccolo, 2002 ; Burdon, 2001). Humic substances are now envisioned as supramolecular associations of small heterogeneous molecules associated by hydrogen bonds and hydrophobic interactions that can be disrupted in the presence of organic acids (Piccolo, 2001 ; Piccolo and Conte, 2000 ; Simpson et al., 2002). This model is based on the use of several techniques, such as gel permeation chromatography, size exclusion chromatography at high pressure, and ultraviolet visible spectroscopy (UV). A study by Piccolo et al. (2001) sought to compare the size of humic acid following the addition of an organic acid or hydrochloric acid and they observed a considerable decrease in the size of molecules in the case of the addition of organic acid. This decrease was explained as the result of the rupture of intermolecular hydrophobic interactions within the humic acids, which lead to their disintegration into small subunit molecules forming their structure. This explanation is considered more obvious than suggested by the model polymer, which in turn explains the abrupt reduction in size by a tight coil of the polymer chains (Sutton and Sposito, 2005).

The main objective of this thesis is to identify which of the two structural concepts, polymeric/macromolecular or supramolecular, is actually appropriate for describing the structure of humic substances. For this, the structure of humic substances is probed through investigating the type of associations and reconformations induced by the combination of humic substances from various origins (fulvic acid and humic acid from the Suwannee River, Nyong humic acid and a modeled humic-like substance) and dissolved organic matter from the Amazonas-Brazil (Rio-Negro and Rio-Jutai) with a homologous series of cationic surfactants (C n-trimethylammonium chloride) with different alkyl chain length, *i.e.* Octyl (C8), Dodecyl (C12) and Hexadecyl (C16).

Humic substances are entities with anionic carboxylic and phenolic groups. They have properties of surfactant due to their amphiphilic character (Von Wandruszka, 1998). Based on these characteristics, several types of interactions may occur: a covalent amide bond between the polar head groups of surfactant (trimethylammonium) and carboxylic groups of humic substances and hydrophobic interactions between the alkyl chain of surfactant and the humic substances with an intervention their aromatic fraction. All these interactions will induce drastic molecular rearrangements in the structure of humic acids. Such reorganizations can be illustrated by the formation of aggregates resulting in new partnerships between the studied molecules.

Even though many factors influence the binding of surfactants to either a polymeric or supramolecular structure (surfactant chain length, charge density, backbone rigidity of the polymer...), the corresponding complexation behaviour (size and organization of aggregates) should be markedly different as a function of surfactant concentration. Indeed, globules, mixed micelles and **vesicles** could be found in the case of self-assemblies where it is easier for the surfactant to interact with small subunit molecules comprising the supramolecule of humic substances, whereas **chain collapse**, formation of aggregates connected by surfactant micelles and various types of precipitates could be evidenced with a polymeric structure.

In our work, two types of characterizations are implemented: first, the study of association humic substance/surfactant suspension by turbidity provides a rapid assessment of aggregates formation. Then to highlight the structures identified in turbidity, Dynamic light Scattering (DLS) is used to determine the sizes and polydispersity of particles in suspension. Surface tension and Electrophoretic mobility allow assessing the effect of neutralization and charge inversion, so as to define the various stages of reorganization of complexes formed.

On the other hand, more sophisticated investigative techniques such as cryogenic Transmission Electron Microscopy (Cryo-TEM), are used in order to achieve observations at the nanoscale and to complement with DLS, allowing a better understanding of structures permitting the identification of colloidal size, shape, molecular conformation and their corresponding aggregates in sighting the possible supramolecular nature of HS. Small Angle Neutron Scattering (SANS) is also used where it is possible to study the samples, with high level of resolution, in their natural condition (in solution) avoiding the drying process that could deform the object under study. Finally, the molecular rearrangement is investigated by fluorescence spectroscopy where new emission peaks not present in the reference HS suggest major restructuration and exposure of their intrinsic fluorophoric properties.

In the first chapter, an overview about humic substances, definitions and classification, including the modes of formation in the natural environment is presented. In addition, the various isolation and extraction procedures and their further fractionation are reported. Moreover, a detailed reviewing of the physicochemical properties is done (elemental ratios, major functional group composition, and molecular conformation, *i.e.* Size and shape, and Molecular Weight). The debate in the literature regarding the nature of structural organization of humic substances is discussed including humic substances modeling representation, *i.e.* a building block monomeric subunit of the molecular structure. Finally, surfactants are also reviewed regarding their application and interaction with Polymers and Humic Substances.

Chapter II is a description of the experimental protocols and conditions. It includes the materials and HS-DOM/Surfactants complexes preparation, as well as the various methods of characterization implemented.

In Chapter III, the molecular organization of Suwannee River Fulvic Acid (SRFA) is probed in the presence of cationic surfactant molecule (Dodecyltrimethyl ammonium Chloride, DTAC). The Self-assemblies, associations and reconformations, induced by the combination of fulvic acid with DTAC is investigated. Furthermore, an attempt to infer average geometric characteristics of HS constituent molecules according to the framework introduced by Israelachvili is presented, where the self-organization of amphiphiles can be reasonably predicted from the so-called critical packing parameter.

In Chapter IV, we extend our soft matter approach to assess the organization of Suwannee River Humic Acid (SRHA). The Self-assemblies and rearrangements, induced by the combination of humic acid with a homologous series of cationic surfactants (C n-trimethylammonium chloride) with different alkyl chain length, *i.e.* Octyl (C8), Dodecyl (C12) and Hexadecyl (C16) are investigated.

In Chapter V fluorescence spectroscopy is used to investigate and further confirm HS structural reformation and supramolecularity. The interactions between Suwannee river humic substances (SRFA and SRHA) with cationic surfactant (DTAC) are investigated to detect any molecular rearrangements that affect the native chromophoric and fluorophoric groups. The approach is then extended, for generalization of our results, with humic substances of different origins (Nyong humic acid and a modeled humic-like substance) and dissolved organic matter from the Amazonas-Brazil (Rio-Negro and Rio-Jutai).

Finally, in chapter VI, general conclusions are drawn from the results of all the studies conducted, and future perspectives are formulated.

CHAPTER *(I)*

Humic Nano-Colloids
General Context

I.1 HUMIC SUBSTANCES

Natural organic matter (NOM) represents a complex heterogeneous pool of active organic carbon compounds (Hertkorn et al., 2007 ; Woods et al., 2011 ; Buffle, 1984, 1990 ; Amon and Benner, 1996); it consists of living organisms (plants, animals, microorganisms), their secreted matters, as well as decomposed residues (plant debris, bacteria...) through biological processes that include physical breakdown and biochemical transformation of molecules such as cellulose, fats, waxes, tannin, lignin, carbohydrate and proteins (Juma, 1999). They are group into volatile (VOC) and non-volatile (NVOC) organic matter (Atkins and Jones, 1998), the latter being divided into dissolved organic carbon (DOC) and particulate organic carbon (POC), based on filtration typically using a 0.45 or 0.22 μm filter (Azam and Malfatti, 2007).

Depending on their chemical properties, they are separated into identifiable molecules that have been synthesized directly from plants or other living organisms and non-identifiable complex structures (Figure. I-1) that are not easily used by many micro-organisms as an energy source and persist in the environment for a relatively long time (Tipping, 2002 ; Jones and Bryan, 1998):

- Non- Humic Substances: are identifiable compounds that belong to specific biochemical classes (Thurman, 1985 ; Christman and Gjessing, 1983 ; Perdue et al., 1990 ; Beck et al., 1993) where they can be represented by distinct chemical formula such as carbohydrates (mono-, Oligo- and polysaccharides), cellulose and hemicellulose, lipids and Amino Acids/proteins (Piccolo, 2001 ; McDonald et al., 2004). In general, the microorganisms rapidly degrade those compounds because of the simplicity of their chemical nature. As a consequence, they do not persist for a long period in the environment. Other chemicals such as resins, waxes, and lignin, due to their complex structures, are more difficult for microorganisms to break down.
- Humic Substances (HS): are non-identifiable naturally occurring, yellow to black, biogenic organic substances of high molecular weight (Wall and Choppin, 2003 ; Lead et al., 1994 ; Redwood et al., 2005) known for being heterogeneous refractory (Gjessing, 1976 ; Aiken et al., 1985 ; Huang et al., 1986) since they resist the decomposition and breakdown (Sparks, 2003). They may persist in nature for long periods of time and are produced as byproducts of microbial metabolisms, physicochemical degradation of organic materials (plant debris, bacteria), and condensation of small organic molecules

that cannot be categorized to a definite chemical or distinctive structural group nor a unique functional term (do not carry any specific biochemical function) (Schnitzer, 1978 ; Tadros and Gregory, 2013 ; Rowell, 1994).

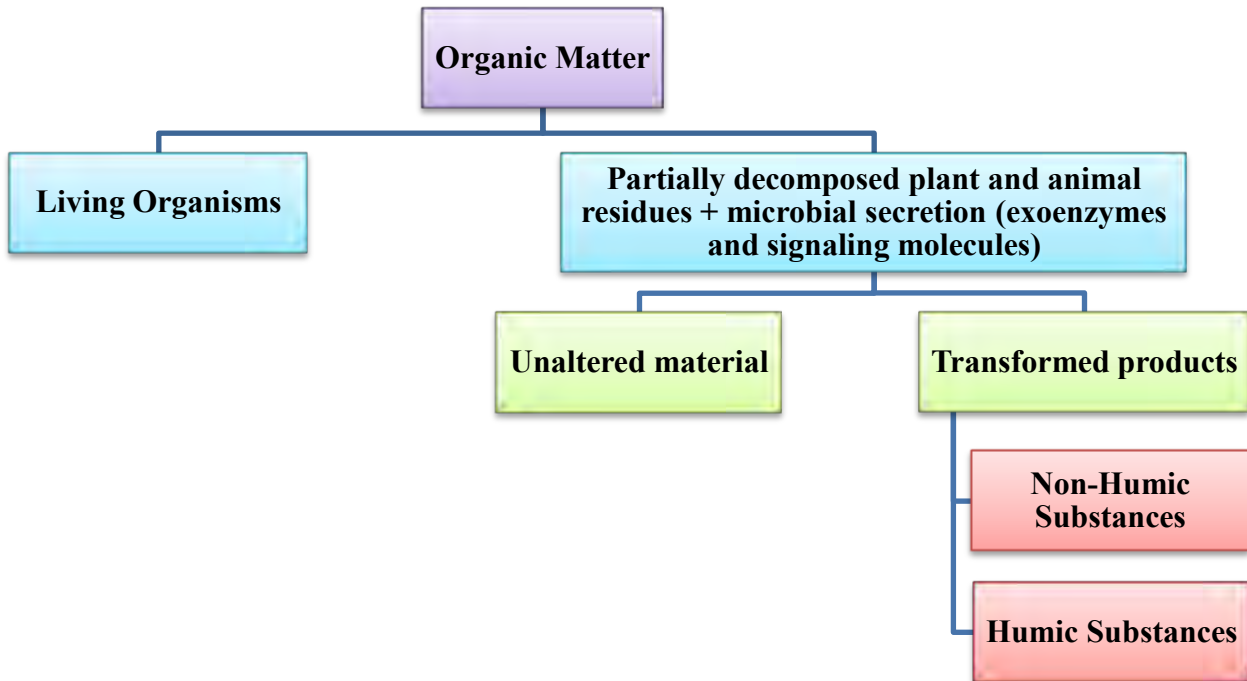


Figure I-1. Distribution of Organic matter.

I.1-1 Definitions and Terminologies

The scarcity of an explicit definition for humic substances is a problematic issue in this field, where the different terminologies are not used in a compatible manner. Some soil scientists use the term humus synonymously with soil organic matter (SOM) that is composed of both the humic and non-humic substances without the undecayed or partially decayed animal and plant debris, as well as the soil living organisms (Stevenson, 1994). Concurrently, in soil science, this term (*i.e.* humus) is used to refer only to the humic substances within which various constituents such as polysaccharides and amino acids that are usually linked with the humic materials during extraction are removed (Tan, 2011, 2014 ; MacCarthy, 2001). However, the segregation of these constituents, or excluding the partially decayed products from the isolated humic substances, is practically tedious if not impossible as it is very challenging during the decomposition process to identify the level of humification (Knicker et al., 1997 ; Wershaw, 1994). In other terms we have a pool of humic substances, where part is completely formed, some is undergoing formation, and the remaining is still subjecting to breaking down and decomposition.

Despite the discrepancies in definitions, humic substances are considered as an amorphous mixture, composed of heterogeneous biochemical substances (proteins, carbohydrates, lipids...) degraded to a greater or lesser extent by microorganisms and physicochemical processes (Stevenson, 1994). This diversity results in a poorly understood structure where they lack a definite or regular structural form. These substances are highly refractory, so they can oppose microorganisms degradation and their breaking down is slower than that of other simpler organic components (e.g. biopolymers of polysaccharides, proteins) (MacCarthy, 2001).

I.1-2 Classification of Humic Substances

The complex nature of humic substances raises a conceptual paradox when classification is considered. The lack of a unique biochemical content makes it difficult to categorize them into functional or chemical terms as any other chemical compounds (e.g. proteins, lignin, etc.) (Xing, 1998 ; Steelink, 1963). Instead, grouping is based on their solubility behavior in aqueous media (pH-dependent) that is applied during their extraction process (Rosa et al., 2000 ; Moraes and Rezende, 2008). Humic substances are then classified into three major fractions: humic acid (HA), fulvic acid (FA) and humin.

I.1-2-1 Humic Acid

Humic acid corresponds to colloidal fraction of humic substances that is insoluble under acidic conditions ($\text{pH} < 2$), which implies that they can be found in aqueous system (Hayes and Clapp, 2001 ; Chilom and Rice, 2009 ; Thorn et al., 1996). They behave as a weak acid and represent the main extractable fraction of soil humic substances. Humic acids are dark brown to black, contain essentially aromatic and aliphatic structures (Chien and Bleam, 1998), that made up 35% and 65% of their molecular composition respectively (Pettit, 2004). That gives them active surface property, allowing the establishment of hydrophobic interactions (Chen and Schnitzer, 1978 ; Engebretson and von Wandruszka, 1994). In addition, other functional groups such as carboxylic acids and phenolic give them their hydrophilic property (Ritchie and Perdue, 2003). The surface active properties are influenced by the hydrophobic and hydrophilic structures, i.e. hydrophobic/hydrophilic ratio =HB/HI, (Quadri et al., 2008 ; Adani et al., 2010 ; Salati et al., 2011 ; Quagliotto et al., 2006).

The size of humic acids have been determined by various techniques, such as transmission electron microscopy (TEM), atomic force microscopy (AFM), small angle X-

ray and neutron scattering (SAXS and SANS) (Balnois et al., 1999 ; Wilkinson et al., 1999 ; Kawahigashi et al., 1995 ; Pranzas et al., 2003 ; Osterberg et al., 1993). All of these methods suggest that humic acids are nanoscale structures with a diameter between 1 and 2 nm (Lyvén et al., 2003; Baalousha et al., 2005). They are ascribed for being a high molecular weight fraction, ranging from 10,000 to greater than 1,000,000 dalton (Da) for soil-extracted materials (Piccolo et al., 2002) and about 2000 to 3000 Da in the case of aquatic origin (Flaig and Beutelspacher, 1968 ; Malcolm, 1990 ; Aiken and Wershaw, 1985). This size can vary depending on the pH: at basic pH, they present an extended configuration due to electrostatic repulsions, whereas small aggregates begin to form with $\text{pH} < 5$ (Lead et al., 1999 ; Plaschke et al., 1999). In addition, humic acids are known to have a high cation exchange capacity and metal-chelating properties, which is crucial to understand their coagulation with cationic and inorganic minerals species (Pettit, 2004 ; El Samrani et al., 2004).

1.1-2-2 Fulvic Acid

Fulvic acids are the light yellow to yellow-brown fraction of humic substances, soluble in water under all pH conditions (Nam and Kim, 2002 ; Kim and Osako, 2004). They remain in solution when the humic acids are removed by acidification. In aquatic systems, they make up to 30-50% of the natural organic matter (Abbt-Braun and Frimmel, 2002 ; Reemtsma and These, 2005). Their size is smaller compared with humic acid, *i.e.* 1.5nm using conductimetry, 0.95nm using DLS and 0.1-2nm by AFM (Roger et al., 2010), with molecular weight ranging from 1500 to 2000 Da in streams and 1000 to 10,000 in soil-derived matter (Flaig and Beutelspacher, 1968 ; MacCarthy, 2001 ; Thurman et al., 1982 ; Plancque et al., 2001). They demonstrate colloidal properties due to their relatively small size (Tombácz et al., 1999 ; Fetsch et al., 1998), which in turn increases their availability to plants; fulvic acids are considered as mineral and trace elements chelating agent, making them very vital components for soil quality.

The high oxygen contents in the form of carboxyl (-COOH) and hydroxyl (-OH), in addition to ketonic and carbonyl groups, render them highly chemically active products, and enhance their solubility in the aquatic systems (Dixon et al., 1989 ; Lead et al., 2000a ; Hosse and Wilkinson, 2001). In addition, we can also find aliphatic chains and aromatic groups. These various constituents give rise to the amphiphilic nature, where analogy to surface-active agents can be anticipated (Leenheer et al., 2003), since they exhibit the capability of

linking various hydrophobic and hydrophilic compounds (Schulten and Schnitzer, 1995 ; Pompe et al., 1996).

1.1-2-3 Humin

The fraction of humic substances that is not soluble in water at any pH value is defined as Humin (Rice, 2001 ; Rice and Maccarthy, 1989a); humin is what is left after humic and fulvic acids extraction (Schnitzer and Khan, 1972 ; MacCarthy et al., 1990). They are black in color, long regarded as macro-organic due to their high molecular weight approximately ranging from 100,000 to 10,000,000 Da (Rice and MacCarthy, 1988 ; Rice and MacCarthy, 1989b). Due to the resemblance in the nature of functional chemical groups and similar elemental compositions (Rice and MacCarthy, 1991), humin has been viewed as humic acid linked to inorganic matter as clay (Theng, 1979 ; Shah et al., 1975a ; Shah et al., 1975b ; Banerjee, 1979 ; Cloos et al., 1981). Humin exhibits high resistance to degradation than the other fractions of humic substances and play a significant role in the sequestration of anthropogenic organic chemicals (pesticides, herbicides...) (Rice, 2001).

The biogeochemical alterations and the fate of humin in the environment are not well known, since scientific researchers gave less interest toward such studies, although humin comprises more than 50% and 70% of organic carbon in soils (Kononova, 1966) and in sediments, respectively (Peters et al., 1981 ; Durand and Nicaise, 1980 ; Hatcher et al., 1985 ; Vanderbrouke et al., 1985; Ishiwatari, 1985 ; Hedges and Keil, 1995 ; Mayer, 1994). According to C-14 dating, humin is the oldest of humic substances that may eventually convert into coal or kerogen (Tissot and Welte, 1978). It has been regarded as an intermediate product in the transition of peat into coal (Fischer and Schrader, 1921 ; Funasaka and Yokokawa, 1953 ; Van Krevelen, 1963 ; Stach, 1975), also as a precursor of kerogen that may eventually transform to petroleum in sedimentary rocks (Breger, 1960 ; Welte, 1973 ; Cane, 1976 ; Huc and Durand, 1977 ; Vanderbrouke et al., 1985).

1.1-2-4 Comparison of Humic Substance Fractions (Humic Acid, Fulvic Acid and Humin)

The different fractions of humic substances are relatively similar but not completely identical, since they can be distinguished by their solubility in aqueous solutions. Even when the physico-chemical properties are investigated, analogy can be found in between them. Although the molecular weight, elemental compositions, degree of polymerization and the

number and distribution of functional chemical groups can help to differentiate the fractions, no obvious boundary can be drawn, but rather a gradual evolution of properties should be considered when passing from one fraction of the other (Giannissis, 1987).

The chemical properties of the different fraction of humic substances are illustrated in Figure. I-2. The elemental compositions (Table I-1) show close similarity between humic acid and humin (Schnitzer and Khan, 1972 ; Gaffney et al., 1996 ; Rice and MacCarthy, 1991).

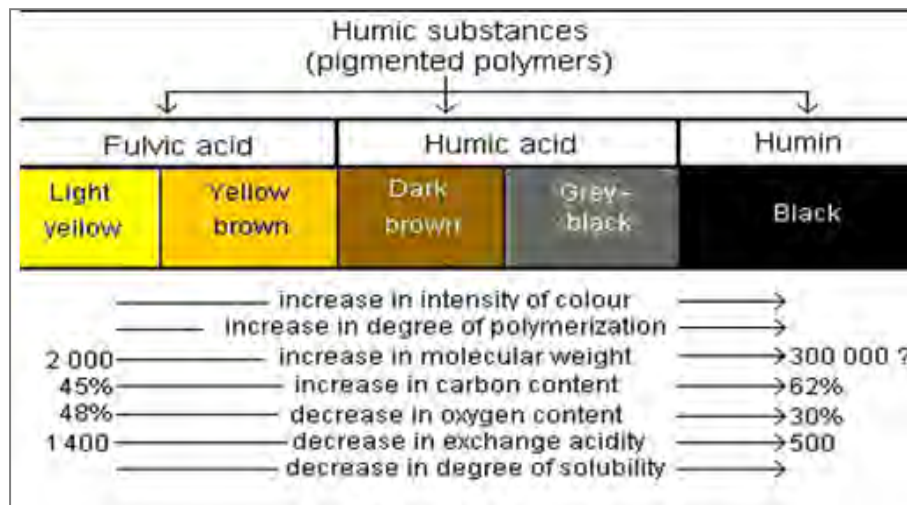


Figure I-2. Chemical properties Humic substances fractions (Stevenson, 1994).

In addition, if comparison is also made to some plant material such as lignin, the values are analogous to those of humic acids and humin constituents, which is why lignin has long been viewed as a potential precursor for humic substances (Stevenson, 1994).

Table I-1. Elemental compositions of humic substances and several plant materials (Kononova, 1966).

Elemental composition of humic substances and several plant material					
% dry ash-free basis					
Substances	C	H	O	N	Molecular weight (Da)
Fulvic acids	44 - 49	3.5 - 5.0	44 - 49	2.0 - 4.0	600-10,000
Humic acids	52 - 62	3.0 - 5.5	30 - 33	3.5 - 5.0	1,500-1,000,000
Humin	55.9	5.8	32.8	4.9	100,000-10,000,000
Proteins	50 - 55	6.5 - 7.3	19 - 24	15.0 - 19.0	
Lignin	62 - 69	5.0 - 6.5	26 - 33	-	

The higher oxygen content in fulvic acids is attributed to the fact that they are richer in acidic functional groups such as carboxylic acid, phenolic and ketonic groups, and their content in aromatic and aliphatic moieties is less than humic acids (Schulten and Schnitzer, 1995 ; Hosse and Wilkinson, 2001 ; Lead et al., 2000a) except for aquagenic fulvic acids with more aliphatic chains than humic acids (Table I-2) (Malcolm, 1990). This accounts for the solubility of fulvic acid at any pH value and the insolubility of humic acids (being more aliphatic and aromatic, and poorer in carboxylic and phenolic) at low pH where deionization and protonation of their carboxylic groups takes place to render them more hydrophobic (Pompe et al., 1996).

Table I-2. The functional chemical groups distribution (%) in humic substance fractions (Malcolm, 1990).

Humic Substances	n	Unsaturated Aliphatics	N-alkyl methoxy	Carbohydrate	Aromatic	Carboxyl	Ketonic
Soil HA	8	17-30	4-9	12-18	24-42	12-18	4-7
Soil FA	1	22	5	20	26	24	4
Aquatic HA	4	23-30	5-6	9-21	29-36	14-17	6-8
Aquatic FA	4	30-40	5-7	10-18	14-18	16-19	5-11

The amount of the various humic fractions varies noticeably from one type of soil to another. In forest soils, there is a higher content of fulvic than humic acids; whereas in peat and grassland soils, humic acids are considerably higher (Figure. I-3).

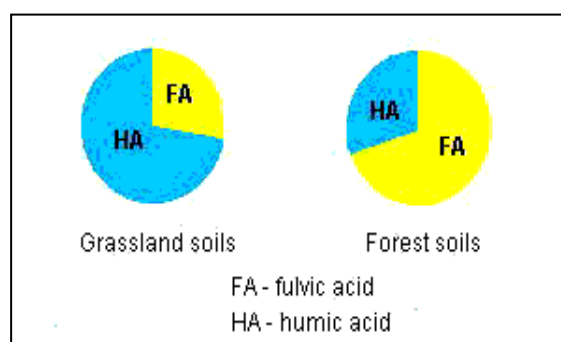


Figure I-3. Humic Substances distribution in forest and grassland soils (Stevenson, 1994).

Even in the same region, the humic acid/fulvic acid ratio can be affected by the soil profile and it decreases with increasing depth (Table I-3).

Table I-3. Humic acid/fulvic acid ratios (R) of some surface soils (Kononova, 1966).

Humic acid/fulvic acid ratios (R) of some surface soils			
Soil	R	Soil	R
Chernozem ordinary	2.0 - 2.5	Gray Forest	1.0
Chernozem deep	1.7	Sod podzolic	0.8
Chestnut dark	1.5 - 1.7	Tundra	0.3

I.2 HUMIC SUBSTANCE GENESIS

Humic substances have been a subject of interest for centuries (Schnitzer and Khan, 1972 ; Frimmel et al., 1988). Their complex nature is consented by anyone who works with these substances, as mixture of plant residues, components of microorganism and their decomposition by-products, which make it very challenging for writing a unique molecular formula representing their structures. But these humic substances are kind of similar regardless of their origin because the biochemical processes on Earth are similar (Burdon, 2001). Two modes of formation of HS have been suggested (Hayes et al., 1989a ; Hayes and Swift, 1990):

- Purely biological or Degradative concept: the breakdown and the transformation (basically lignin) of biological macromolecules under microbial (biotic) and chemical (abiotic) processes lead to humic substances that have related features to the components from which they were degraded (Hatcher and Spiker, 1988 ; Largeau et al., 1984).
- Biological processes followed by chemical reactions (abiotic) or Synthetic concept: aggregation and condensation through polymerization of smaller organic compounds released from metabolism and molecular degradation (e.g. Proteins, polysaccharides and phenols) (Flaig et al., 1975 ; Flaig, 1988 ; Hedges, 1988).

The first pathway is based on oxidation and depolymerisation, whereas the second pathway leads to the production of novel molecules that will also be subjected to oxidative degradation. Considering abiotic processes alone for the formation of humic substances is not possible since plant components are not capable of reacting with themselves, which implies that a biological step should precede the route of formation. These two concepts comprise three different pathways (Figure. I-4); the lignin theory (degradative concept) (Waksman and Iyer, 1932 ; 1933), the polyphenol theory (Hänninen et al., 1987), and the sugar-amine theory also called the “Maillard Reaction” (synthesis concept) (Stevenson, 1994).

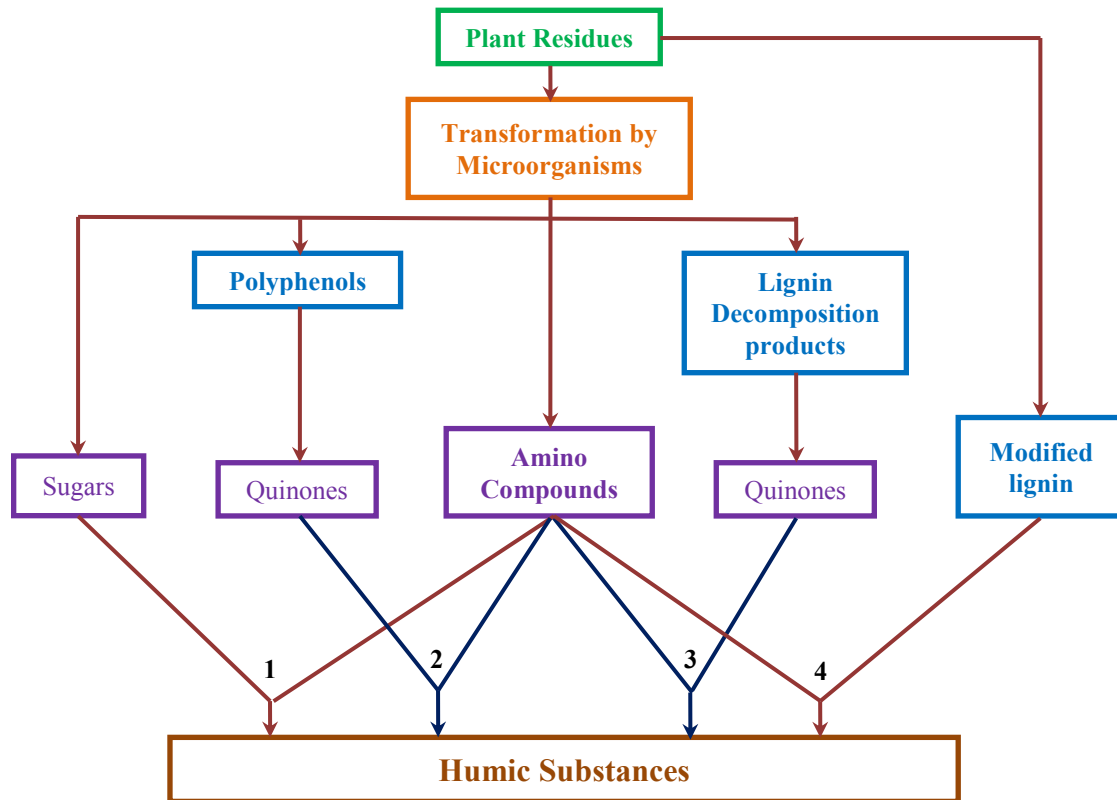


Figure I-4. Formation pathways of humic substances (Stevenson, 1994).

I.2-1 Lignin-Protein Theory (Biological or Degradative Concept)

This theory considers lignin as the primary precursor of humic substances (Waksman, 1932) because of its high molecular weight (Goring, 1971) and its resistance to decomposition (Marcusson, 1926). Lignin is incompletely degraded by microorganisms and undergoes a series of modifications where it loses, by demethylation, methoxy groups ($-\text{OCH}_3$) to produce ortho-hydroxyphenol and produces carboxyl groups ($-\text{COOH}$) through the oxidation of terminal ends of aliphatic chains (Figure. I-5) (Wershaw, 1993). The ortho-hydroxyphenol parts can produce quinones by further oxidation that is capable of reacting with amino compounds and $-\text{NH}_3$ by-product of N-containing organic compounds through condensation (pathway 4 in Figure. I-4).

In addition to lignin, other plant residues have been considered as key-components in humification (Zech et al., 1997 ; Amalfitano et al., 1992). Carbohydrates (cellulose and hemicelluloses) (Detmer, 1871 ; Rose and Lisse, 1917), cutin (Zech et al., 1990 ; Lähdesmäki and Piispanen, 1988) or wax (Nip et al., 1986), have also been linked as potential precursors of humic substances (tannin are not taken into consideration since it is not found in all plants)

(Haider et al., 1975 ; Senesi and Loffredo, 2001). Because these substances (Carbohydrates) are rapidly degraded, they cannot solely link as humic substances precursors, then interaction between these degraded matter and synthesis of new products might contribute to the formation of humic substances.

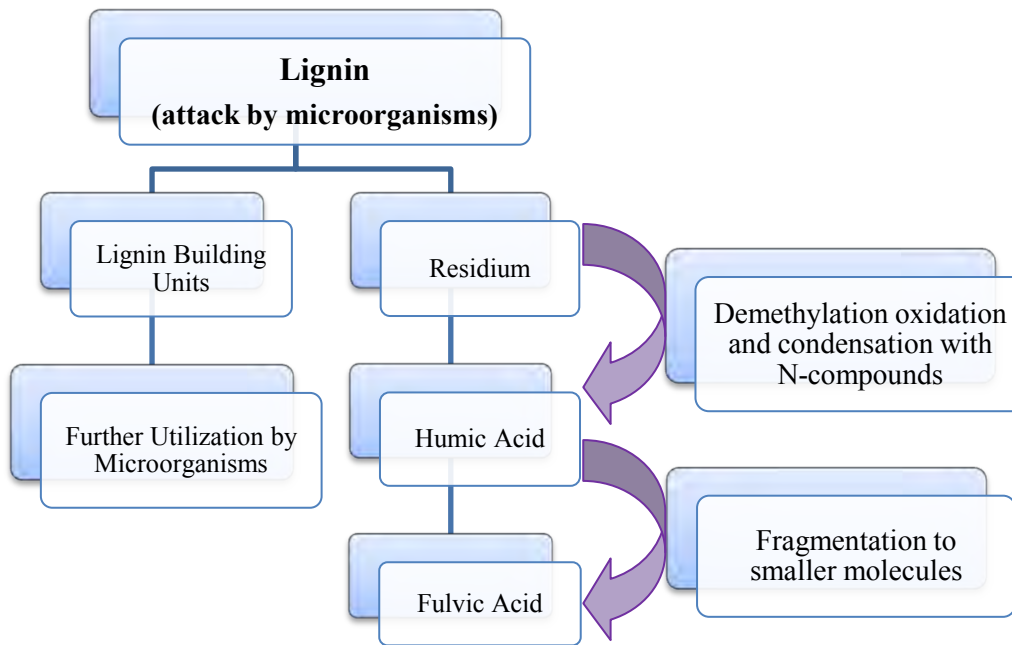


Figure I-5. The Lignin theory of humic substance genesis (Waksman, 1932).

However, this pathway has been criticized because, if lignin was the only precursor, then the structure of humic substance would have been similar to that of lignin and we would have had enough knowledge of their composition. Furthermore, the presence of various moieties that cannot be generated from lignin such as phenolic groups, nitrogen, simple sugars and amino acids (Anderson et al., 1989), were found to be released from hydrolysis experiments of humic substances (Cheshire, 1979 ; Parsons, 1989). Thus, the humic substances produced from lignin degradation alone do not account for the existence of these groups. Therefore, the degradation process should be followed by synthesis reactions, where those compounds interact with the backbone and incorporate into the structure, as the lingo-protein model in which the amino groups of proteins interact with the carboxyl groups of the modified lignin that is responsible for the presence of these groups in humic material (Jensen, 1931 ; Hobson, 1925 ; Bennett, 1949).

I.2-2 The Poly-Phenol Theory (Biological Processes Followed by Chemical Reaction “Abiotic” or Synthetic Concept)

This theory considers Polyphenols as precursors of humic substances (pathway 2 and 3 in Figure. I-4). Here, both the decomposition of plant biopolymers (e.g. cellulose) and the microbial synthesis lead to polyphenol production through oxidation and demethylation. Moreover, lignin can be a source of polyphenols under microbial degradation to produce phenolic aldehydes and phenolic acids that are converted into polyphenols by enzymatic reactions (Saiz-Jimenez et al., 1975 ; Haider et al., 1965). The Polyphenols are then converted into quinones by Polyphenol-oxidase that will also react with N-containing organic compounds and polymerize into humic substances (Figure. I-6) (Flaig, 1964 ; Martin et al., 1980).

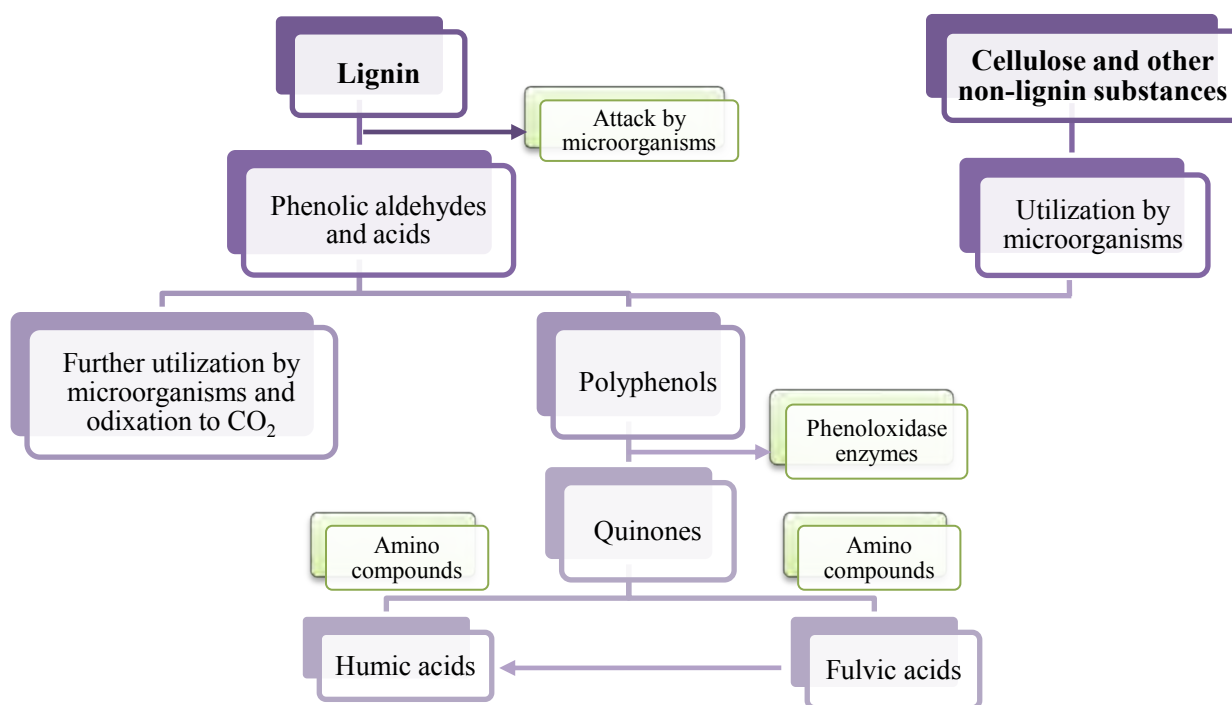


Figure I-6. The polyphenol theory of humic substance formation (Stevenson, 1994).

There are some discrepancies in this theory, because of the differences in the ^{13}C -NMR spectra of humic substance to polyphenol-derived humic substances though some similarities can be found. In addition, aliphatic parts are in a quantity insufficient if compared with humic and fulvic acid. Furthermore, we do not have a similar range of benzene-

polycarboxylic acids like that of natural humic matter when a synthetic polymerized polyphenols is oxidized (Glaser et al., 1998), and also high amounts of polyphenols are required, though they are formed in soils but not in sufficient concentrations to be considered as a major contributor to humic substances production.

I.2-3 Sugar-Amine Theory “Maillard Reaction” (Biological Processes Followed by Chemical Reaction “Abiotic” or Synthetic Concept)

The Maillard reaction is one of the most proposed process as an abiotic reaction; it takes place by polymerization between amino acids (amine) and monosaccharide (Sugar) to produce brown melanoidins (Maillard, 1912, 1917) (pathway 1 in Figure. I-4) that contains heterocyclic aromatic residues produced from biological degradation (Ledl and Schleicher, 1990) (Figure. I-7).

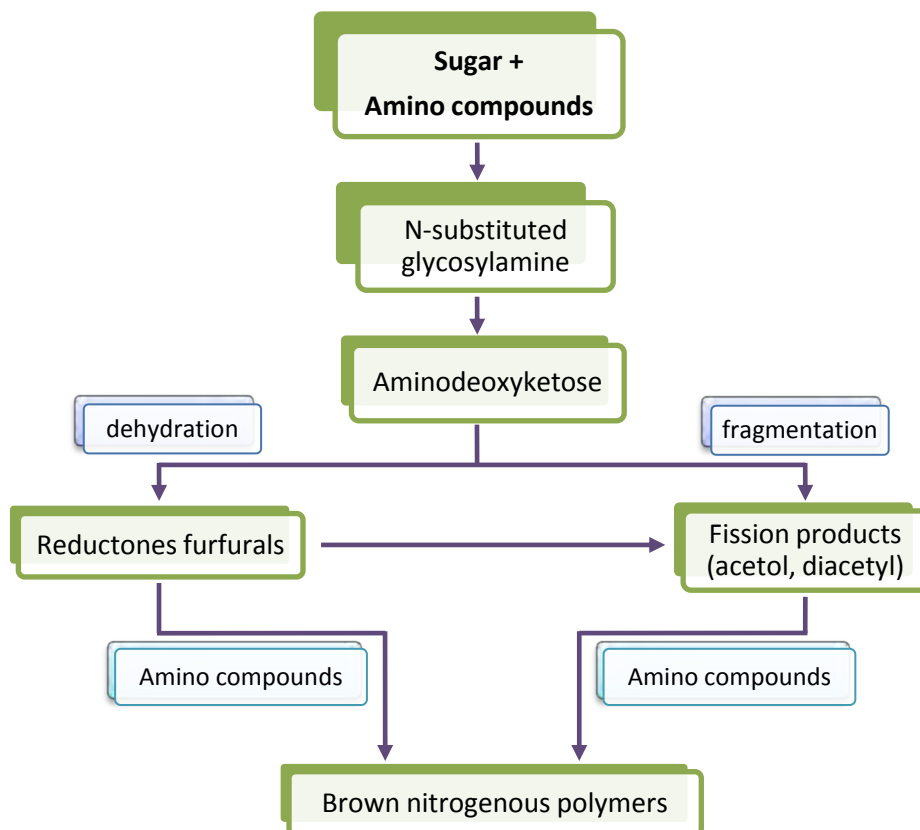


Figure I-7. Sugar-Amine theory “Maillard Reaction” for humic substances genesis (Stevenson, 1994).

Precursors such as amino acids and monosaccharide are found in the soil; then the Maillard reaction takes place but not as a major contributor to the formation of humic substances, since there has been several disagreements regarding this theory:

- First, the amounts of precursors (amino acids and monosaccharides) in soil are not enough for this reaction to occur to a great extent (Haworth, 1971).
- Second, the Maillard reaction carries on best in alkaline medium; then if this pathway is responsible for the genesis of HS, we should find more HS in basic soils than in acidic soils and there is no evidence for that (ELLIS, 1959).
- Third, nitrogen (N) is mainly found in HS in the form of amide groups as shown by ¹⁵N-NMR, and the remaining N content is in the form of ammonia or amine (Knicker and Hatcher, 1997 ; Benzing-Purdie et al., 1992 ; Hopkins et al., 1997 ; Knicker and Lüdemann, 1995 ; Knicker, 2000). The Maillard reaction yields heterocyclic-N products, which is not a significant contributor to humic substances formation.
- Fourth, the synthetic compounds obtained from Maillard reaction in the laboratory exhibit ¹³C-NMR spectra significantly different from those of natural compounds, although some similarities led to consider the Maillard reaction as a major pathway for the formation of humic substances (Benzing-Purdie and Ripmeester, 1983 ; Ikan et al., 1992).

The resemblance of molecular constituents between humic substances and various natural biopolymers (e.g. lignin, carbohydrates, sugar, and amino acids) does not necessarily validate a direct production from these materials. At any given point all of these materials are presented and both pathways (degradation and synthesis) are occurring in the environment. Thus, it is most reasonable to consider that the genesis of humic substances is made by contributions of all the previously mentioned pathways, some of which might be considered more important than others. A consensus could be reached when the biopolymers undergo degradation to its elementary units by different biochemical processes, and then reassemble/condense with each other or with other non-decomposed materials by synthesis processes (Adani and Spagnol, 2008).

I.3 ISOLATION/EXTRACTION AND FRACTIONATION

The imprecise and inconsistency of prevalent definitions of humic substances lead to an operational definition according to their mode of extraction and isolation based on their behavior in aqueous systems as function of pH, rather than on their chemical and functional

constituents, into three fractions: humic acid, fulvic acid and humin (Stevenson, 1994 ; Hayes, 1989 ; Swift, 1996).

I.3-1 Isolation

The isolation and extraction procedures of humic substances and their further fractionation have been extensively established in an attempt to provide a method for: (i) producing the most homogenous fractions (Hayes, 1985 ; Hayes and Malcolm, 2001 ; Clapp and Hayes, 1999a) and (ii) getting rid of materials that are co-linked with humic substances from inorganic colloids and to non-humic substances (Kuhn et al., 2015). Many aqueous solvents have been used to isolate humic substances from soil and the criteria for a good solvent has been discussed in previous literature (Hayes, 1997 ; Swift, 1996 ; Hayes, 1998).

Traditionally, exhaustive sequential extraction procedures are employed. Here, water is used to disperse the withdrawn soil materials. The drained materials are treated with sodium pyrophosphate ($\text{Na}_4\text{P}_2\text{O}_7$) at different pH, then nonionic hydrophobic macroporous sorbent resins, styrene-divinylbenzene (e.g. XAD-2, XAD-4) or acrylic esters (e.g. XAD-7, XAD-8), are used through which the extracts are eluted (Hayes et al., 1996 ; Gregor and Powell, 1987). Clapp and Hayes (1996, 1999) used dimethylsulfoxide (DMSO) and HCl, where DMSO is an appropriate solvent for cationic particles, and the extract retrieved after extraction with base is the humin fraction (Fagbenro et al., 1985). Hausler and Hayes (1996) reduced bonded particles to Humic acids (amino acid and sugar) when DMSO/HCl and XAD-8 is used. Ping et al. (1995) and Malcolm and MacCarthy (1992) used DMSO/HCl solvent in addition to XAD-4 and XAD-8 resins in tandem, where humic acids and fulvic acids isolation were feasible, as well as neutral hydrophobic and neutral hydrophilic fraction with XAD-8 and XAD-4 respectively. This procedure enabled the production of less polydispersed humic substances.

The isolation procedures are generally based on a manipulation of the charge of humic substances (Davies et al., 1997 ; Pierce and Felbeck, 1972 ; Davies et al., 2001). When the solvent is basic, the particles become soluble due to the increase of their electric charge. On the other hand, the adsorption/precipitation is enhanced at low pH because of charge reduction. From sediment and soils (Figure. I-8), an alkali solvent (e.g. NaOH) is used to separate humic and fulvic acids (soluble) from humin (insoluble), which can be eliminated by centrifugation/filtration. The soluble fraction is then treated with acid, *i.e.* HCl to pH=2, thus

rendering humic acid insoluble, while fulvic acids remain soluble in solution associated with different colloidal molecules (*i.e.* sugars, amino acids, polar residues). The fulvic acid is further purified to reduce the ash contents by adsorption on resin (e.g. XAD-8) and then recovered with a basic eluent. The humic acids can be further fractionated by either redissolving the precipitate with basic solvent to yield an insoluble grey humic acid and a soluble brown humic acid, or by treating with alcohol (e.g. ethanol) to produce humatmelanic acid (Hayes, 1985 ; Stevenson, 1994 ; Moraes and Rezende, 2008).

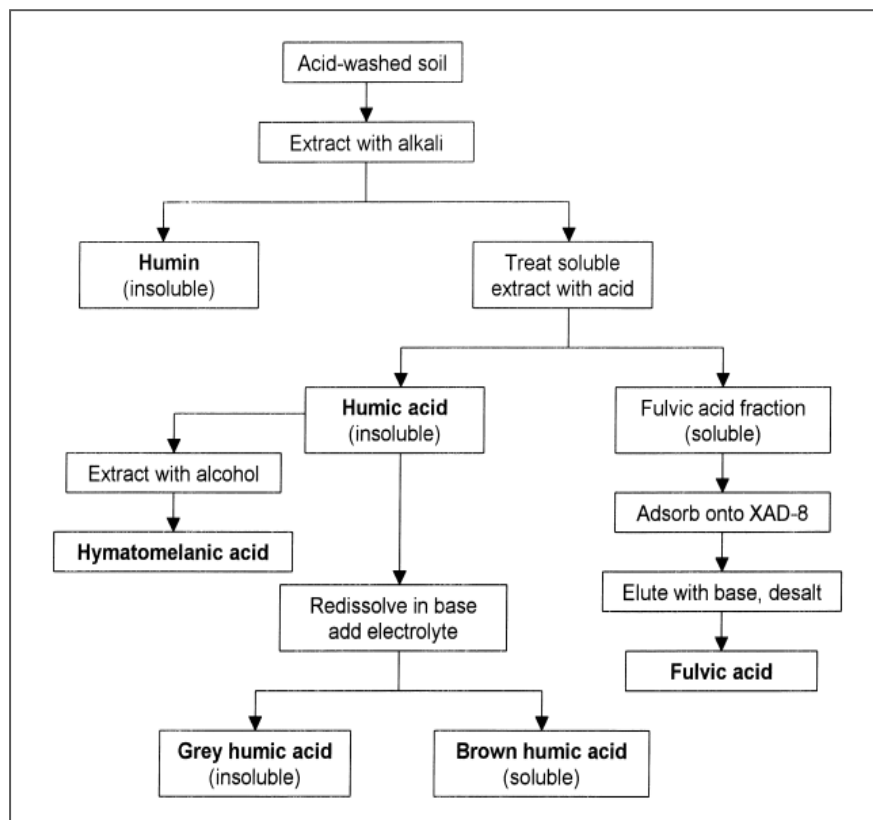


Figure I-8. Humic Substances Isolation Procedure from Soils (Stevenson, 1994).

A similar procedure can be used for aquagenic humic substances (Serkiz and Perdue, 1990 ; Riley and Taylor, 1969). The sample is first filtered (0.45 μ m) to eliminate the particulates, and the filtered sample is then acidified and passed through XAD-8 resin to separate humic from non-humic substances. The recovered humic substances can then be fractionated to humic and fulvic acids by changing the pH of the solution (HCl to pH=1 to precipitate humic acid, back-elution fulvic acid from the resin with NaOH). The outlined procedure is illustrated in Figure. I-9 (Aiken et al., 1985 ; Thurman and Malcolm, 1981 ; Hiraide et al., 1994).

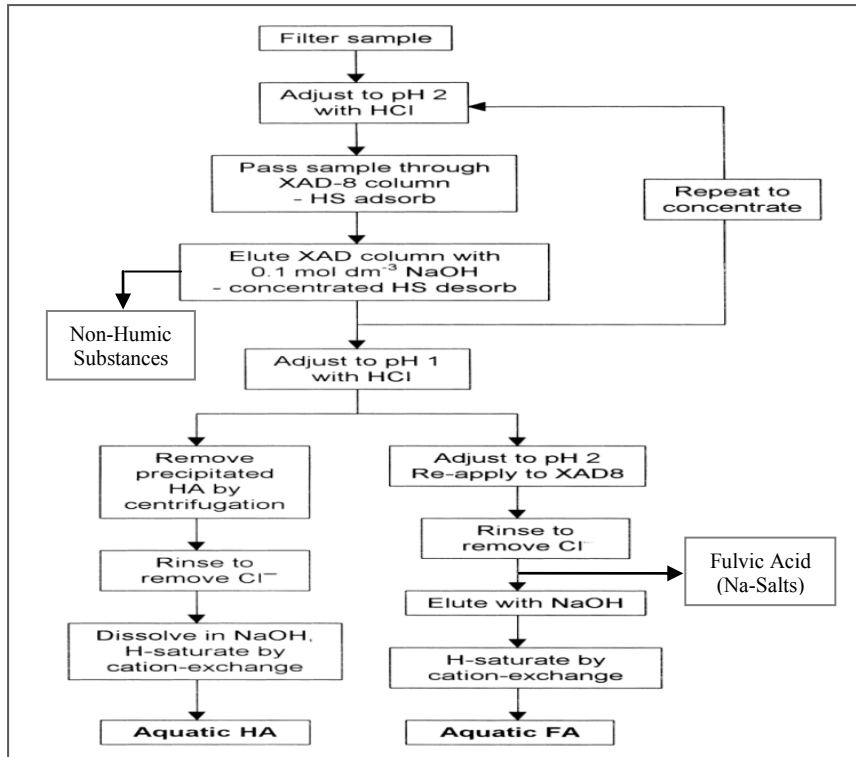


Figure I-9. Aquatic Humic Substances Isolation Procedure (Aiken, 1985).

In other procedures, IHSS applies 0.1M HCl/ 0.3M HF to segregate the inorganic colloidal matters (Figure. I-10) and to diminish the ash contents up to <1% (Swift, 1996 ; Preston et al., 1989). HF will remove most of the inorganic minerals as well as paramagnetic species such as iron. This step could lead to the hydrolysis and losses of polysaccharide and protein materials (Clapp and Hayes, 1996 ; Hayes et al., 1996). In order to preclude any biological and chemical alteration, the isolated substances are freeze-dried to stabilize them.

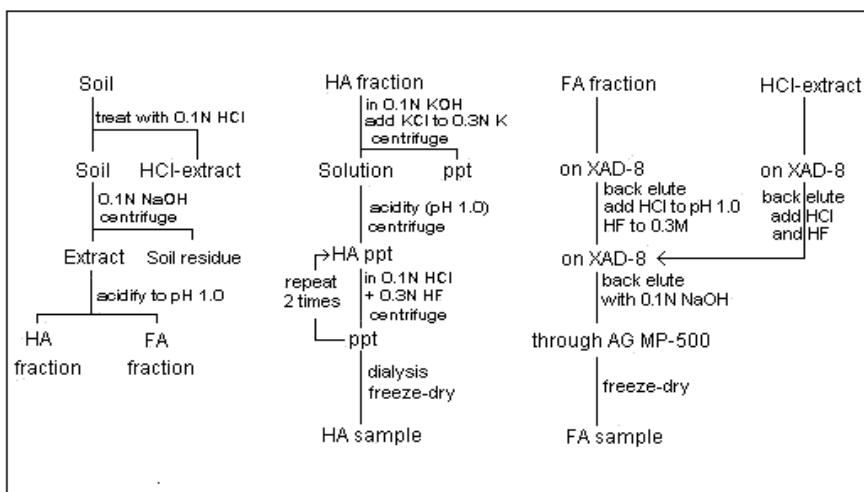


Figure I-10. Preparation of Humic and Fulvic Acid Samples (IHSS Method).

Rice and MacCarthy (1989a) employed methyl-isobutyl-ketone (MIBK) method to separate humin components (Figure. I-11B) after the exhaustive extraction procedure stated above in to bound-humic acid and bound-lipids. This procedure can be also used to segregate humin from humic and fulvic acid and from any inorganic materials (Figure. I-11A).

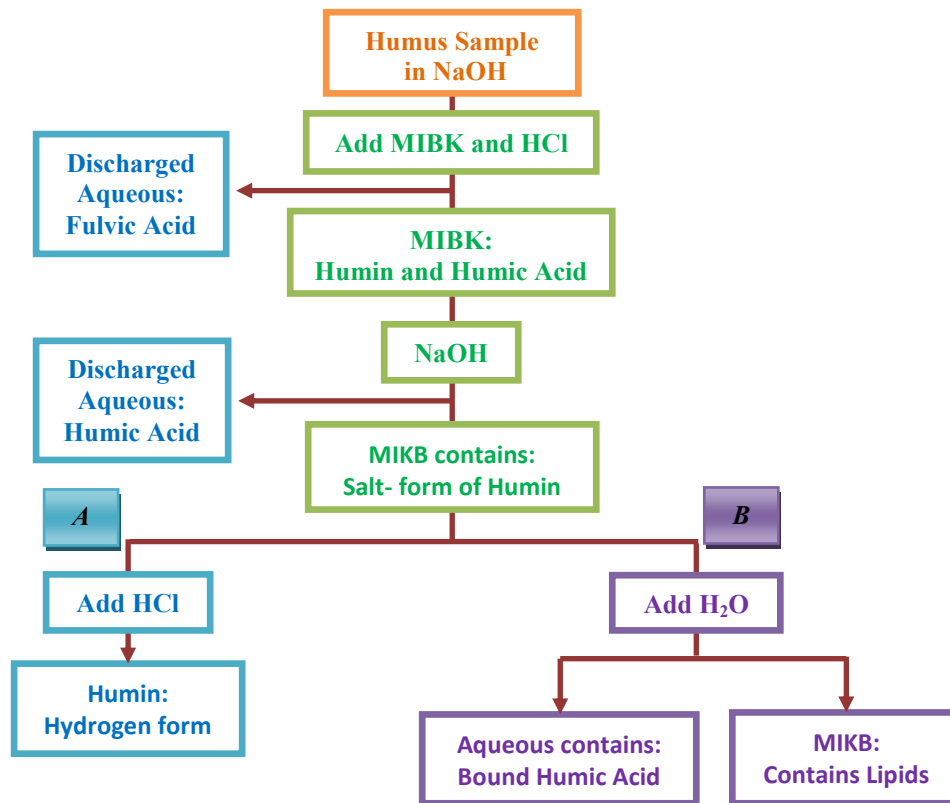


Figure I-11. Isolation of Humin Using MIBK Method (Rice and MacCarthy, 1989a).

Several alternative methods have been used, rather than the adsorption/desorption process of resin for isolation and fractionation. Gel chromatography has been successfully carried out (Swift, 1985, 1999 ; Perminova, 1999 ; De Nobili and Chen, 1999), activated carbon, as well as physical methods such as high volume ultrafiltration, membrane filtration and reverse osmosis (Sun et al., 1995 ; Nwosu and Cook, 2015 ; Green et al., 2015) have been employed for humic substances separation from aqueous solution (Dearlove et al., 1991 ; Marley et al., 1992 ; Tombacz, 1999 ; Marley et al., 1991). Leenheer (1981) summarized some of the alternative isolation technique and their advantages/disadvantages.

I.3-2 Drawback of Isolation Processes

The boundary between Humic substances and Non-Humic substances is a matter of debate because of their similar functional groups and chemical properties (MacCarthy, 2001).

Thus, it is very difficult to contrive experimental procedures that could segregate them from each other in an absolute manner where some Non-Humic Substances could be covalently bonded to HS. As a consequence, it is challenging to identify the point during the process of decomposition at which Non-Humic is transitioned to Humic substances which make it arduous to substantiate that one of the two substances does not have some of the other material mixed with it especially when dealing with low molecular weight (MW) fractions.

According to the previous statement, the following question can be raised: are the isolated materials representatives of their initial state in the natural environment? The conditions under which extraction is performed can be chemically extreme and aggressive, the organic material being possibly subjected to alteration. The strong acid and base might induce degradation, hydrolysis, condensation and decarboxylation (MacCarthy, 2001). Thus, the extracted materials are composed not only of the original substances but also of the modified forms. The solvents used could also induce some artifacts resulting from the partially oxidized and degraded humic matters, as well as from the contamination of dissolved silica materials. Although the procedures yield uniform products, they are unrepresentative due to the selectiveness of molecules with specific properties (Shuman, 1990 ; Lehmann and Kleber, 2015). Likewise, when humic substances are subjected to frequent drying process (lyophilization, evaporation) some chemical modification may occur with the production of various artifacts (e.g. carbon dioxide, anhydride, and lactones). Thus, it is very important to optimize the isolation procedures in order to obtain a well representative compound, free from artifacts and co-extracted molecules. If the purpose of extraction is questioned, then what is the use or why do we fractionate the humic matter if we definitely cannot be sure that one fraction, for example humic acid, is free from the other materials. In that case, it might be more judicious to study the DOM rather than the fractionated materials. Especially when experiments are carried out, similar properties are found that are related to the overall property of the dissolved organic matter.

I.4 CHARACTERIZATION: CHEMICAL AND PHYSICAL PROPERTIES

Understanding the basic physicochemical properties (elemental ratios, aromaticity, and major functional group composition), compositions, conformations and structures, of humic substances is critical to acknowledge their function and reactivity in the natural habitat from the interaction and complexation with different soil and aquatic components (organic

and inorganic) to the adsorption onto mineral surfaces (Avena et al., 1999 ; Pinheiro et al., 1996 ; Alvarez-Puebla et al., 2006 ; De Wit et al., 1993 ; Bohmer et al., 1990 ; Theng, 2012 ; Blaakmeer et al., 1990). Regarding physical and analytical chemistry, great advances have been achieved in humic science from which many conceptual notations were revisited regarding their origin, properties, and structures (Hayes, 1989 ; Orlov, 1985 ; Kononova, 1966). These progresses were possible due to the development in instrumental techniques of investigation (*i.e.* NMR, SANS, TEM, SEM etc.). As a result of their complex-heterogeneous nature, it is very challenging to identify unique properties for humic substances, however, average properties can be obtained (Reemtsma and These, 2005).

I.4-1 Elemental Analyses

The elemental composition of humic substances (Table I-4) is basically of carbon backbone that represents more than 50%, with hydrogen ranging around 4-5% for freshwater humics (Huffman and Stuber, 1985). Due to their aliphatic nature, this value is higher for marine substances and the oxygen content is around 30-40%, whereas groundwater humics exhibit the lowest contents in H and O. In addition, other elements are found in trace values such as sulfur (1-2%), nitrogen (1-4%), and phosphorus (0-0.3%) (Suffet and MacCarthy, 1988 ; Kurková et al., 2004 ; Conte et al., 2007 ; Peuravuori et al., 2002).

Table I-4. Humic Substances Elemental Composition (Steelink, 1985 ; Thurman, 1985 ; Hatcher et al., 1985).

Humic Substances	n	C	H	O	N	S
Soil HA	Many	52.8-58.8	2.2-6.2	32.8-38.3	0.8-4.3	0.1-1.5
Soil FA	Many	40.7-50.7	2.8-7.0	39.7-49.8	0.9-2.3	0.1-2.6
Groundwater HA	5	65.5	5.2	24.8	2.4	1.0
Groundwater FA	5	60.4	6.0	32.0	0.9	0.7
Seawater FA	1	51.8	7.0	37.7	6.6	0.5
River HA	15	52.2	4.9	41.7	2.1	–
River FA	15	52.7	5.1	40.9	1.1	0.6
Lake FA	3	54.8	5.5	41.1	1.4	1.1
Soil Humin	2	55.9	5.8	32.8	4.9	–
Peat Humin	2	56.3	5.1	36.5	2.1	–
Marine Humin	2	56.2	7.0	31.7	5.2	–

The carbon isotope fractionation (*i.e.* ^{13}C and ^{14}C) can be useful for investigating the origin and the age of humic substances. Jenkinson (1981) showed that soil fulvic acid is about 100-500 year old; whereas soil humic acid is about 700-1600 year old and finally humin is 100-2400 year old. Such observation is consistent with the proposition of humin conversion into kerogen through fulvic and humic acid condensation (Stuermer et al., 1978), and with the polyphenol theory of humic substances. In contrast, the lignin theory assume first the formation of humin, which yields humic acid and finally fulvic acid by oxidative degradation (Kögel-Knabner et al., 1988).

I.4-2 Functional Group Composition

The humic Substances are characterized by a variety of functional groups that include carboxylic (-COOH), phenolic hydroxyl and hydroxyl (-OH) groups (Ritchie and Perdue, 2003 ; Zavarzina et al., 2002 ; Buffle et al., 1990), in addition to ketones and quinones (Tate, 1987 ; Madaeni et al., 2006 ; Koopal et al., 2005 ; Tan et al., 2009). They also exhibit aliphatic chains and aromatic nuclei that form 40-50% and 35-60% of the overall molecular constituents respectively (Figure. I-12) (Chien and Bleam, 1998 ; Giasuddin et al., 2007). Using solid-state NMR and wide-angle X-ray scattering (WAXS), Hu et al. (2000) found a 3nm thickness that corresponds to 25 units of CH_2 , while Mao et al. (2002) found an aliphatic branched groups of 10nm diameter that represents up to 50% of the overall non-polar groups.

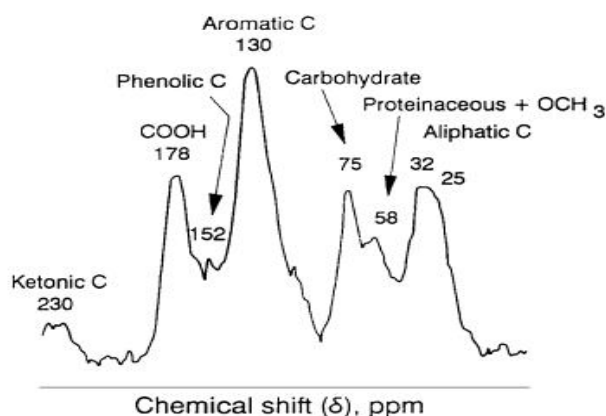


Figure I-12. The ^{13}C -NMR spectrum of a soil humic acid, showing chemical groupings and their chemical shifts (Schinitzer, 1990).

Identifying the functional groups, through degradative and non-degradative methods, is essential for their characterization (Boggs et al., 1985 ; Abbt-Braun et al., 2004 ; Nebbioso and Piccolo, 2011). The degradative methods were utilized to decompose the complex humic structure into simpler individual basic units. They include chemical oxidative degradation

with permanganate, alkaline copper (II) oxide (Schnitzer, 1991 ; Christman et al., 1989 ; Griffith and Schnitzer, 1989), hypochlorite and chlorine (Norwood et al., 1980 ; Neiswender et al., 1960), and for the core that resist the cleavage, phenol and sodium sulfide were used (Hayes and O'Callaghan, 1989). Due to the presence of non-humic matter extracted with humic material, acidic or basic hydrolytic degradation was used (Parsons, 1989 ; March, 1992 ; Schnitzer and Neyroud, 1975); likewise, reductive cleavage has been employed using metals or metal hydrides (Stevenson, 1989), hydrogen such as sodium amalgam (Burgess et al., 1963 ; Mendez and Stevenson, 1966), zinc dust distillation (Hansen and Schnitzer, 1969), sodium in liquid ammonia (Maximov and Krasovskaya, 1977), and phosphorus with hydriodic acid (Cheshire et al., 1968), as well as chemical derivatization through functional group conversion to a derivative (Leenheer and Noyes, 1989). One of the widely applied degradative methods is thermal (pyrolysis) degradation in tandem with mass spectroscopy (MS) (Meuzelaar et al., 1982), gas or liquid chromatography (GC/ LC-MS) (Abbt-Braun et al., 1989) or Fourier transform infrared spectroscopy (FTIR) (Bracewell et al., 1989).

However, degradative methods are chemically aggressive and they can lead to the destruction of some functional groups. Therefore, some alternative non-degradative analysis has been developed, such as vibrational, electronic and high energy spectroscopy (Bloom and Leenheer, 1989) including infrared (Abbt-Braun, 1992 ; Niemeyer et al., 1992 ; Marley et al., 1993), Ultraviolet/visible, fluorescence (Senesi, 1990 ; Kumke et al., 1998 ; Senesi et al., 1991), and X-ray spectroscopy, in addition to low energy radiation as electron spin resonance (Senesi and Steelink, 1989), solid and liquid nuclear magnetic resonance (NMR) (Steelink et al., 1989 ; Malcolm, 1989 ; Wilson, 1987) including ^1H and ^{13}C (Hatcher et al., 1980a , 1980b ; Newman et al., 1980 ; Nwosu and Cook, 2015), cross polarization magic angle spinning ^{13}C (CPMAS) (Conte et al., 2006, 2007), diffusion ordered spectroscopy (DOSY) (Šmejkalová and Piccolo, 2007 ; Peuravuori, 2005 ; Johnson, 1999), potentiometric titration (Driver and Perdue, 2015), and two-dimensional NMR (Hsu and Hatcher, 2005 ; Haiber et al., 2001a ; Lambert et al., 1992 ; Dixon and Larive, 1997 ; Haiber et al., 2001b ; Simpson et al., 2002a). Electrospray ionization has also recently been used coupled with mass spectroscopy (ESI/MS) (Reemtsma et al., 2006a ; Brown and Rice, 2000 ; Klaus et al., 2000 ; Kujawinski et al., 2002) or with Fourier transform ion cyclotron resonance mass spectrometry (ESI-FTICR-MS) (Fievre et al., 1997). Table I-5 shows the compositions of humic references from the International Humic Substance Society (IHSS) (Murphy and Zachara, 1995).

Table I-5. IHSS Humic Substances Properties (Murphy and Zachara, 1995).

Sample	Carbox ^a 190-165 ppm	Arom ^a 165-100 ppm	Aliph ^a 60-0 ppm	f _a	%C	%O	O/C	COOH ^b meq/g	OH ^b meq/g	Mw ^c (Da)
<i>Aquatic Humic Substances</i>										
Suwannee FA	20	24	33	0.24	53.5	41.29	0.58	6.0	1.2	829
Suwannee HA	19	37	21	0.37	54.34	39.43	0.54	4.1	2.1	1600
Nordic FA	24	31	18	0.31	53.44	40.78	0.57	5.5	1.7	2137
Nordic HA	19	38	15	0.38	55.15	38.5	0.52	4.4	1.8	3264
<i>Soil Humic Substances</i>										
Peat FA	28	34	20	0.34	51.54	42.58	0.62			
Peat HA	20	47	19	0.47	56.82	34.91	0.46			
Leonardite HA	15	58	14	0.58	63.08	30.69	0.36			7550

^a Liquid-State ¹³C-NMR used to determine carbon functional groups percentage (Thorn et al., 1989)

^b COOH and OH (meq/g) are determined by potentiometric titration

^cMw: the average molecular weight

We can find similar contents, but of different amount, of elemental and functional groups compositions in aquatic and soil humic matter ; soil humic substances exhibiting a higher degree of aromaticity (f_a), *i.e.* the relative stability of aromatic compounds (structural indices: bond order and length (Minkin et al., 1994), energy resonance: reactivity (Cyrański, 2005), or magnetic indices: π-electron current (Dauben et al., 1968 ; Chen et al., 2005), and of molecular weight than aquagenic matter. In addition, the higher O/C ratio (molecular oxygen to carbon ratio) gives an indication of the polarity and water solubility, aquagenic humics being more polar than soil humic substances (Reid et al., 1990 ; Davis and Gloor, 1981).

Although the properties of humic substances (elemental composition, number and position of functional groups) may be correlated with their origin and with the conditions of formation in the environment and/or extraction procedures, it exists however some consistency in the global properties of humics regardless of the previously stated conditions (Figure. I-13) (Schnitzer, 1977).

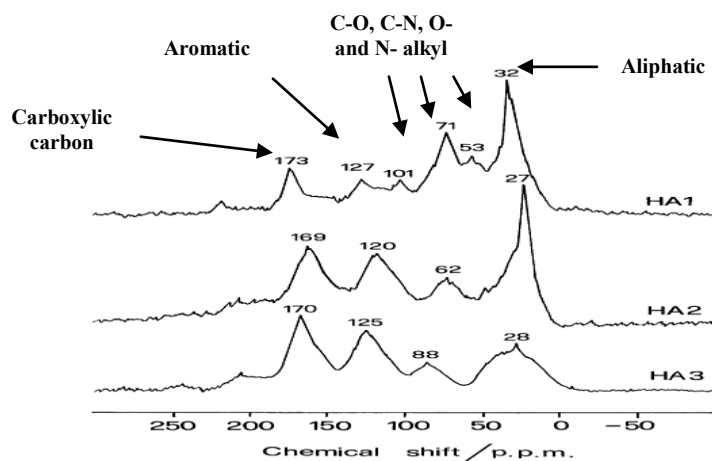


Figure I-13. CPMAS ^{13}C -NMR spectra of humic samples (HA1: volcanic soil, HA2: oxidized coal, HA3: leonardite) (Piccolo et al., 1999).

Eventually, with no unique analysis route for an absolute structural characterization, the use of a combination of numerous methods is essential to disentangle the complex nature of humic substances.

I.4-3 Optical Properties

I.4-3-1 UV/Vis Spectrophotometry

UV/Vis spectrophotometry is a rapid non-destructive assessment technique of chemical components. The two main important parameters that can be determined are the maximum absorption wavelengths (λ_{max}) and the absorptivity (ϵ) at λ_{max} estimated from a Beer Lambert law providing a semi-quantitative test of identity (Fu et al., 2007). Absorption in organic compounds is due to the presence of chromophoric groups (Sauer et al., 2010).

The humic Substances, which contain a high aromatic content with $-\text{COOH}$ and $-\text{OH}$ substituent's, are expected to have a strong absorption. The absorbance of Suwannee River humic substance, as like most HS of various origins, shows a tendency to a monotonic decrease with longer wavelengths without characteristic features (Chin et al., 1994). Although a prominent peak was not observed, a weak shoulder is identified for FA at a wavelength of 280nm and it is even weaker for HA (Figure. I-14) (Hur et al., 2011 ; Muroi et al., 2008 ; Duarte et al., 2003).

The absorbance spectra of HA in both region, *i.e.* UV and Visible, is higher than that of FA. In the UV region, absorbance is attributed to $\pi - \pi^*$ electron transitions in phenolic, carboxylic and polycyclic aromatic hydrocarbons with two or more rings (Kalbitz et al., 1999). Although FA contains a higher $-\text{COOH}$ and $-\text{OH}$ groups than HA, its absorbance is lower than that of HA, which could be due to the higher content in aromatic fraction with $-\text{COOH}$ and $-\text{OH}$ substituent's in HA that enhances the electronic transition along the unsaturated functional groups. In the visible region, the absorption spectra is generally featureless, but it has been of great interest in studying the absorbance ratio of HS at 465nm to that at 665nm (E_4/E_6), as the increase of this index indicates progressive humification and increased condensation that produce large polycondensed aromatic ring structures (Piccolo, 2001). The higher value of absorbance could also reflect a higher amount of functional groups which are responsible for color (conjugated double bonds, keto-enol functional groups, quinones) (Gjessing et al., 1998).

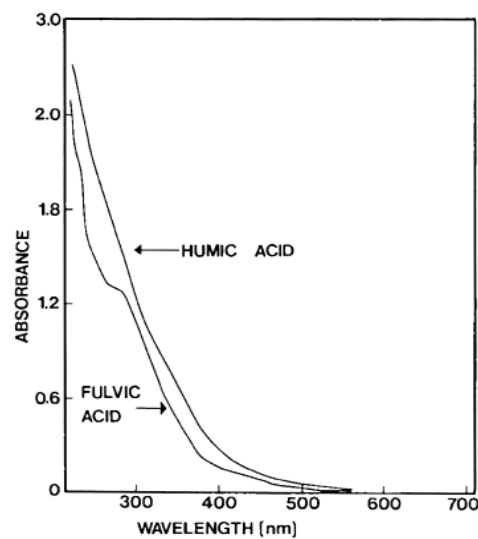


Figure I-14. UV/Visible Spectra of a poorly drained Mollisol Humic and Fulvic Acid (Bloom and Leenheer, 1989).

1.4-3-2 Fluorescence Spectroscopy

Fluorescence Spectroscopy is a sensitive technique applied to the study of selective chromophores that fluoresce efficiently. Unlike UV/visible absorption, the intrinsic fluorescence of humic substances contains some information related to structure, functional groups, conformation, and heterogeneity, as well as dynamic properties related to their intramolecular and intermolecular interactions (Mobed et al., 1996). Therefore, the relative

presence of aromatic amino acid-like, fulvic-like, and humic-like fluorescent compounds within a bulk HS can be assessed from fluorescence spectra (Baker, 2002a ; Hur et al., 2011). The major fluorescent peaks have been identified in various studies especially that with dissolved and natural organic matter (Figure. I-15) are summarized below in Table I-6.

Table I-6. Fluorescence of Organic Matter Fractions according to Excitation/Emission wavelengths.

Peak	λ_{ex} (nm)	λ_{em} (nm)	Fluorescent Component
B (γ)	230/275	310	Tyrosine, protein
T (δ)	230/290	350	Tryptophan, protein or phenolic group
A (α')	260	400-500	Humic Substances
C (α)	300-350	400-500	Humic Substances (terrestrial or lignin origin)
M (β)	310-320	380-420	Marine Humic Substances

Regarding humic fractions, humic acids are distinguished from fulvic acids by their longer emission wavelengths (red shift) and broader peaks at the same excitation wavelength (Figure. I-16) (Carstea, 2012 ; Sheng and Yu, 2006 ; Parlanti et al., 2000). The broader peak was attributed to the presence of higher molecular weight fractions (Chen et al., 2003a), electron-withdrawing substituents, and a higher degree of conjugation due to linear polycondensed aromatic ring network and unsaturated substituent in HA (Bertoncini et al., 2005 ; Kalbitz et al., 2000). The proximity of these components could explain the longer emission wavelength and the greater degree of resonance of HA (Del Vecchio and Blough, 2004) when compared to FA which is of relatively smaller molecular weight, lower degree of conjugated chromophores and humification, that will restrain the electron delocalization and energy transfer or dissipation by non-radiative processes (Elkins and Nelson, 2001 ; Baker and Genty, 1999 ; Coble, 1996). Regarding the shifting, it is accounted for the multi-fluorophores components of HS (Matthews et al., 1996), where a single fluorophore changes the intensity of the fluorescence but not the location of the emission maxima spectra as a function of the excitation wavelength (Westerhoff et al., 2001 ; Corrado et al., 2008).

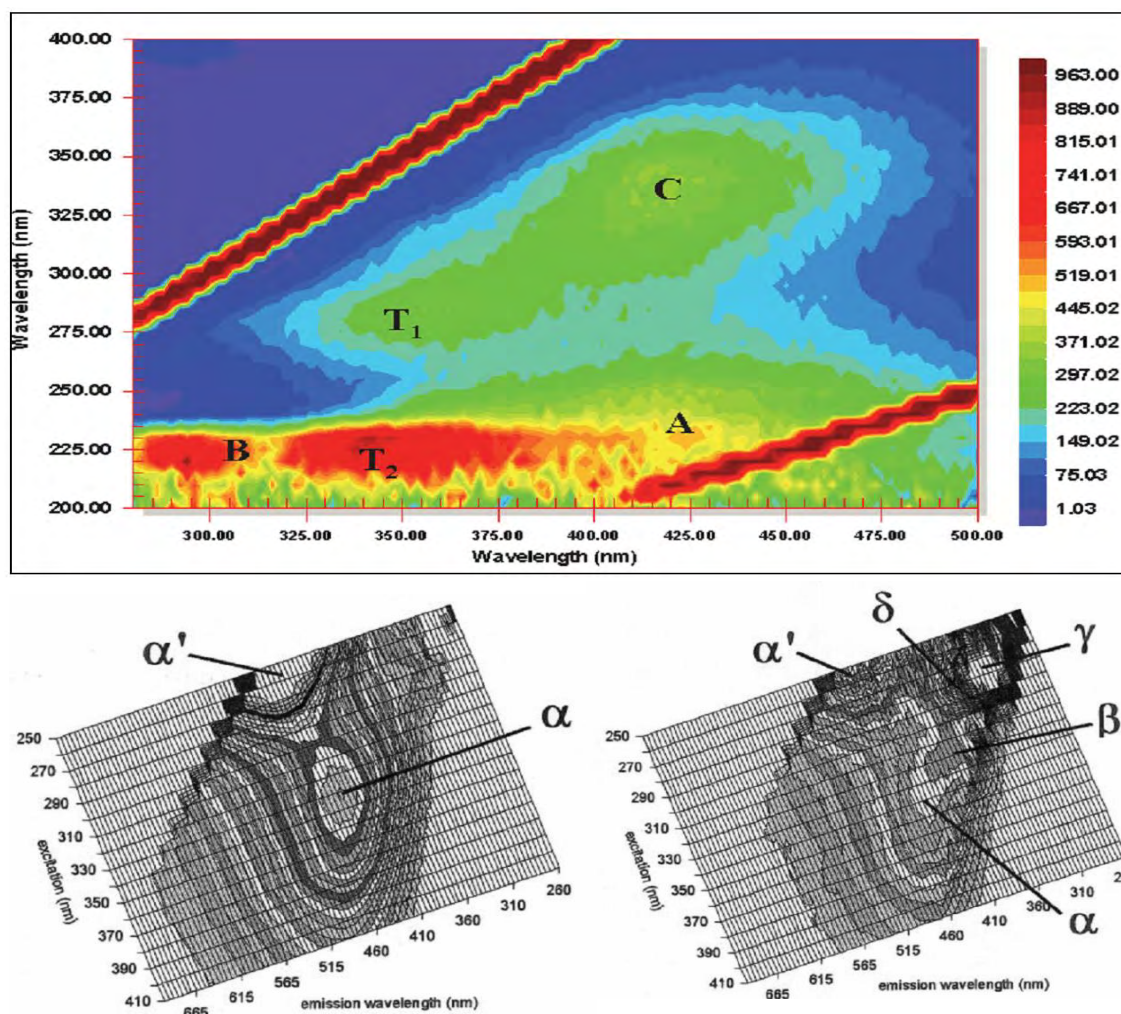


Figure I-15. Excitation-Emission matrix (EEM) of DOM (upper image) (Carstea, 2012), fresh water (lower left) and marine water (lower right) (Parlanti et al., 2000).

In general, the fluorescence intensity of FA is greater than that of HA regardless of the excitation wavelengths used (Olendzki et al., 2009 ; Sierra et al., 2005a). Although HA has a greater content in $-\text{COOH}$ and $-\text{OH}$ substituted aromatic groups with a higher degree of polycondensation that intensely fluoresces, the higher molecular weight and size of HA leads to radiative and non-radiative energy transfers (Matthews et al., 1996). In other terms, inter/intra molecular interactions caused by the proximity of aromatic chromophores, increase the probability of deactivation of the fluorescence by internal self-quenching, especially if electron-withdrawing carbonyl or carboxyl functional groups are para-oriented to the hydroxylic $-\text{OH}$ groups (Bertoncini et al., 2005 ; Chen et al., 2003a ; Mobed et al., 1996). The electron donating groups of FA such as hydroxyl and methoxyl groups have also been reported to enhance fluorescence by increasing the transition probability between the singlet

and ground state (Senesi, 1990). The presence of hydrogen bonds in FA could enhance the molecular rigidity, thus enhancing the fluorescence intensity (Xiaoli et al., 2012). Exciplex dimer-aggregate formation was previously reported for HS, characterized by the formation of bilayers (vesicles, rods) that leads to the production of excitons (Kasha et al., 1965 ; Jung, 2004 ; Huang et al., 2013 ; Chen et al., 2003b ; Baker, 2002b)

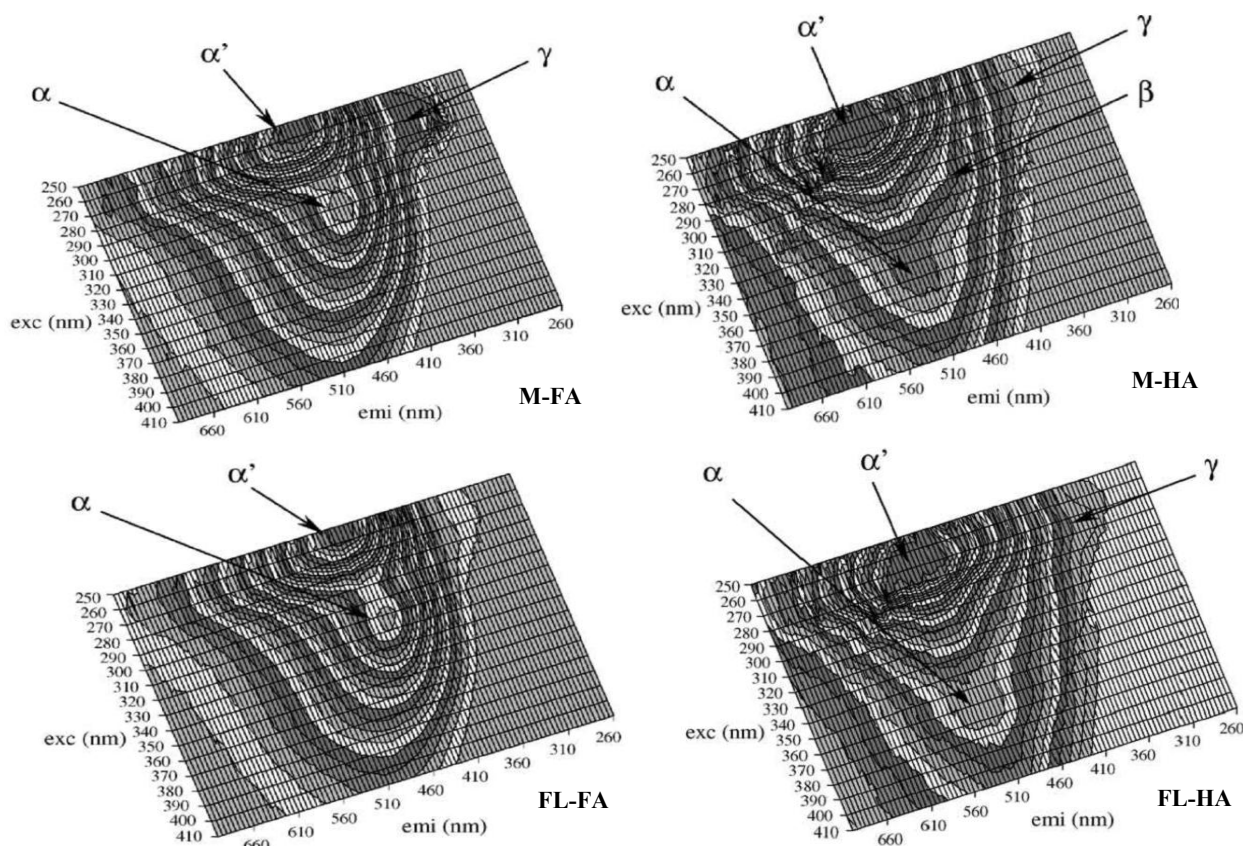


Figure I-16. EEM of marine (M) and fresh lagoon (FL) fulvic and humic acid (Sierra et al., 2005a).

Excitation/Emission Fluorescence Spectroscopy of HS interaction with heavy metals has been extensively studied (Berkovic et al., 2013 ; Fu et al., 2011 ; Orsetti et al., 2013 ; Yan et al., 2013 ; Cabaniss, 1992 ; Nakashima et al., 2008). However, until now, limited attention has been given to the interaction of HS with surfactants where Fluorescence Spectroscopy studies indicate the formation of Insoluble/soluble complexes that quench or increase the emission intensities spectra (Subbiah and Mishra, 2009 ; Muroi et al., 2008). The heterogeneous nature of HS, characterized by a variety of functional groups (catechols, quinones, phthalates, phenol amines and salicylates methoxyl...), leads to a fluorescence fingerprint of humic substances, but it remains difficult to isolate the unit that is responsible

for the fluorescence properties. Another difficulty is in the different measurement setups that use different excitation wavelengths, which then complicates the comparison between different reports (Elkins and Nelson, 2001 ; Smith and Kramer, 1999 ; Smith and Kramer, 2000).

I.4-4 Molecular Conformation (Size and shape) and Molecular Weight

The molecular conformation of HS (*i.e.* size and shape) has been intensively studied by a number of techniques (e.g. AFM, TEM, SAS, SEM...) (Manning and Bennett, 2000 ; Avena and Wilkinson, 2002 ; Guo and Ma, 2006 ; da Costa Saab et al., 2010 ; Piccolo et al., 2001 ; Chen and Schnitzer, 1989), that permits size determination of single units and aggregates (Leppard et al., 1990 ; Perret et al., 1991 ; He et al., 1996 ; Lienemann et al., 1998). Light scattering methods -static and dynamic-, can also be used to determine the small basic unit sizes ranging between 1-2.5nm (Figure. I-17) (Palmer and von Wandruszka, 2001 ; Reid et al., 1991 ; Ren et al., 1996 ; Underdown et al., 1985 ; Chin et al., 1998).

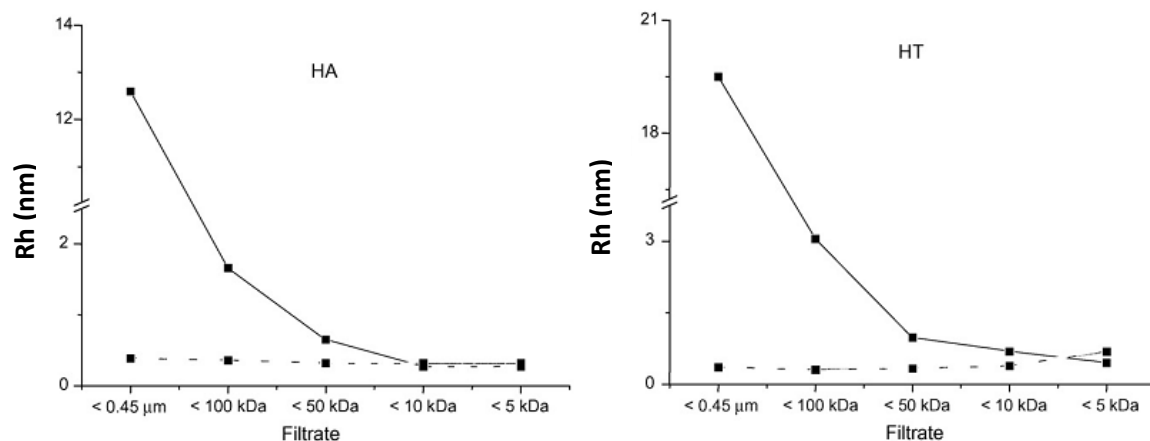


Figure I-17. Size distribution obtained by DLS, corresponding to the alkaline (solid line) and the acidified–realkalinated (dot line) samples of Aldrich humic acid (HA) and whole humic system of fulvic and humic acid extracted from peat (HT) (Baigorri et al., 2007a).

It is very crucial when dealing with humic colloid size and shape to take into consideration pH and charge effects, since these factors control the charge density by neutralization (effect of electrolyte) and ionization/deionization of functional groups (effect of pH) (Figure. I-18).

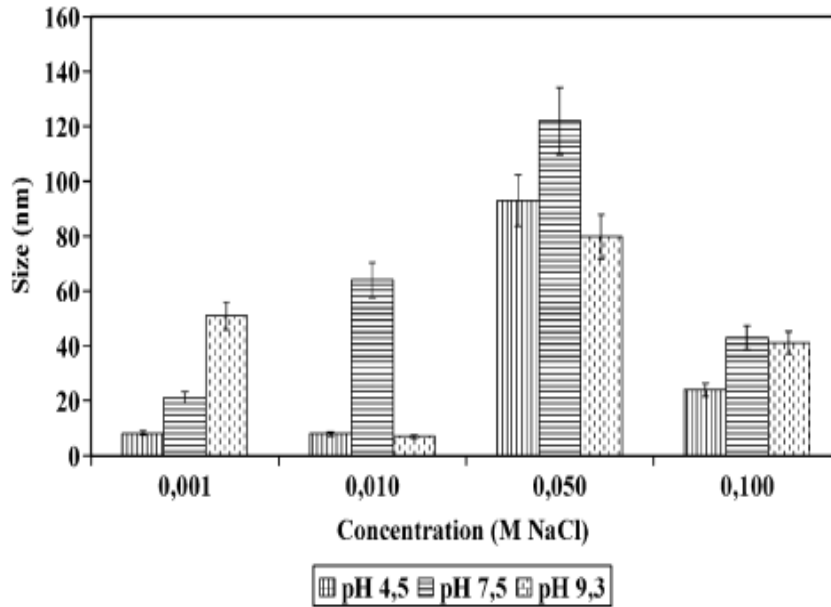


Figure I-18. Effect of Ionic strength and pH on the size of SRHA measured by photon correlation spectroscopy (PCS) (Baalousha et al., 2006).

Modifications of solution pH, ionic background, adsorption of organic pollutants and complexation with polycations, determine structural modifications of HS conformation affecting the fate and the bioavailability of metal-organic pollutant in the environment (Figure. I-19) (Glaser and Edzwald, 1979 ; Avena et al., 1999 ; Kam and Gregory, 2001). Such results are consistent with the modeling of their charge characteristics that considers HS as soft and porous structures (Duval et al., 2005). Likewise, AFM reveals that humic substances are semipermeable spheres (Marinsky and Ephraim, 1986 ; Kinniburgh et al., 1996). The effect of pH on peat humic acid aggregation was studied by dynamic light scattering: large aggregates were found in the 30-185nm range (Pinheiro et al., 1998, 1996); recently, fluorescence correlation spectroscopy has been successfully applied to assess the effect of pH and ionic strength on Suwannee humic matter, detecting 1nm size value (Lead et al., 2000b) .

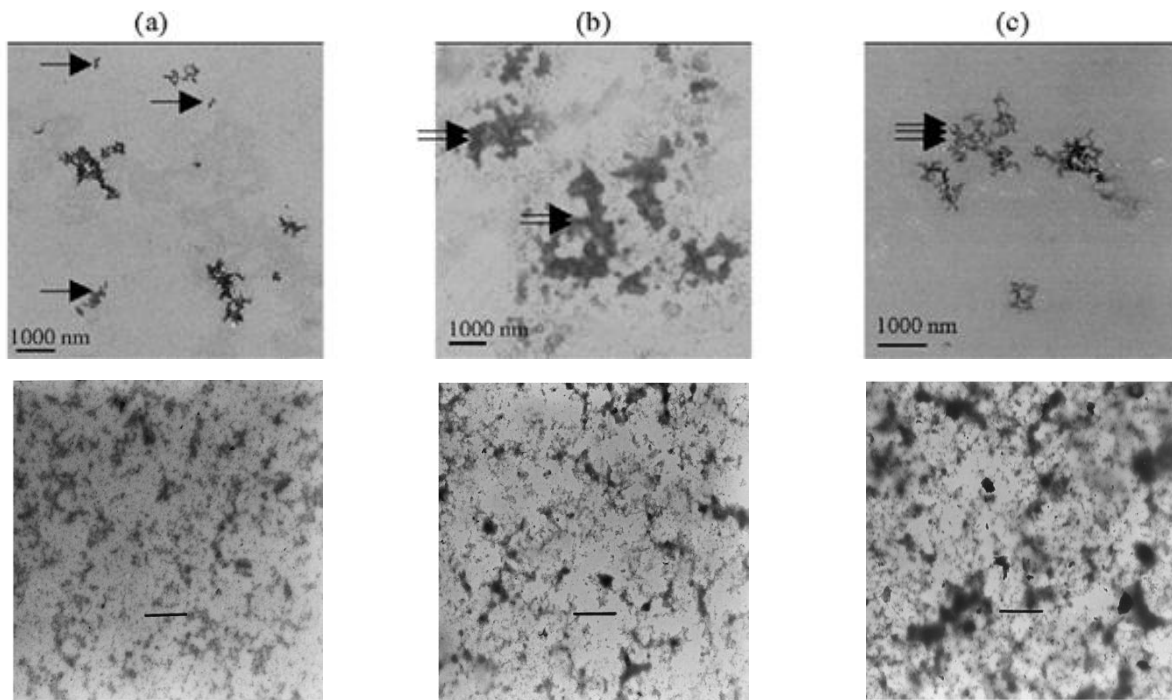


Figure I-19. Transmission electron microscopy of SRHA in (a) 0.01M, (b) 0.05M and (c) 0.1M CaCl_2 at pH 7.5 (upper images) (Baalousha et al., 2006), and soil fulvic acid in 5mM NaOH at (a) pH=10.4; (b) pH=7.2; (c) pH=5.9; Scale bars=1 μm (lower images) (Wilkinson et al., 1999).

Regarding some reported structures, Baalousha et al. (2005) and Wilkinson et al. (1997) found networks of fibrils and globules ranging from 50-300nm; Myneni et al. (1999) found globular, ring-like, sheet-like and thread-like structures ranging from 200-1200nm; Baalousha et al. (2006) identified branched networks composed of a small number of elementary units of HS with a range of sizes that increases with increasing ionic strength. In another attempt, Namjesnik-Dejanovic and Maurice (1997) found that soil fulvic acid, formed spongy-like structures consisting of rings of 15nm in size along with small spheres (10-50nm) at low concentration (Maurice and Namjesnik-Dejanovic, 1999). At higher humic concentration, the aggregated spheres formed branches and chain-like assemblies and perforated sheets at even higher concentration, whereas the aquagenic fulvic acid (SRFA) yielded spheres, aggregated branches and perforated sheet at high concentration. The interaction of cationic surfactant with extracted soil HS was studied using X-ray microscopy: spherical particles of 224 nm in size were observed at low surfactant concentration; the size of the spheroid structures increased with higher concentration and the formation of some aggregates and network-like structure occurred predominately at even higher concentration (Thieme and Niemeyer, 1998). Wilkinson et al. (1999) studied colloidal organic material

using TEM and AFM; they obtained a range of structures from linear, fibrillar, globular and reticulated OM. Some other studies were also carried out by Yu et al. (2013) on different soil profiles, where they found some regular shapes (spherical and oblong flake) and other irregular structures (Figure. I-20).

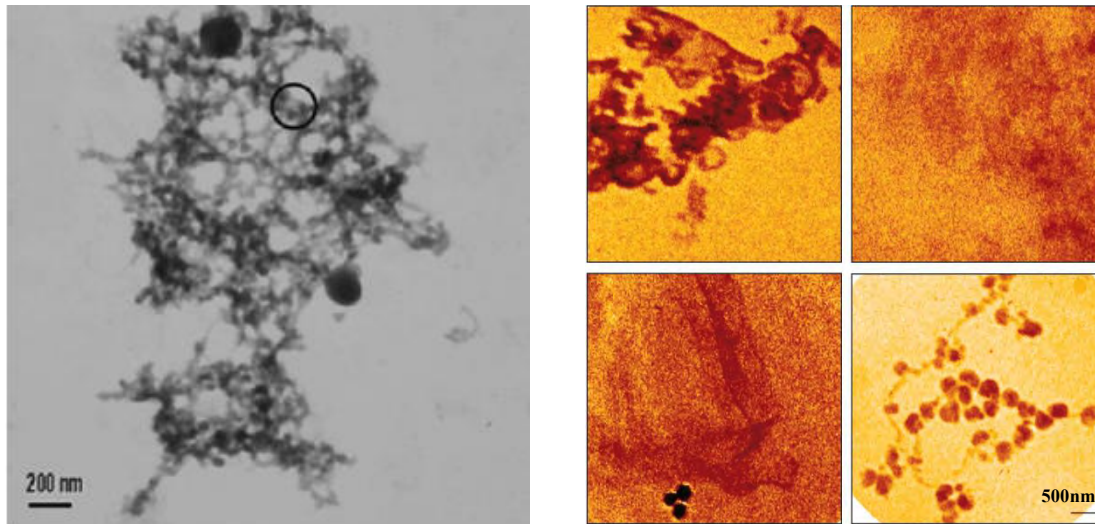


Figure I-20. Different Molecular conformation detected by TEM of Fluka HA (right image) (Baalousha et al., 2005) and X-ray microscopy of SRFA (left image) (Myneni et al., 1999).

The fractal nature of HS has been extensively reported from various SANS studies, but only a few revealed the formation of a stable or regular network. With the absence of a clear Guinier region, the primary particles were difficult to determine, and instead, a lower limit of radius of gyration was provided (Jarvie and King, 2007 ; Osterberg and Mortensen, 1994, 1992 ; Diallo et al., 2000). Clusters consisting of spherical structures ≤ 2.5 nm with soil humic acid were obtained with no significant difference in structure upon increasing the ionic strength (Diallo et al., 2005).

One of the essential physical characteristics of any chemical compound, such as humic substances, that should be measured is the molecular weight that gives an insight in to the mobility, dynamics and reactivity with various organic and inorganic components (Her et al., 2002 ; Peuravuori and Pihlaja, 1997 ; McInnis et al., 2015). The molecular weight influences the behavior of HS towards trace metals and nutrients binding, hydrophobic organic pollutants sequestration, adsorption to mineral surfaces and disinfection byproducts formation (Amy et al., 1987 ; De Wit et al., 1993 ; Vermeer and Koopal, 1998 ; Tanaka et al.,

1997 ; Cabaniss et al., 2000 ; Kreller et al., 2015). High molecular weight humic substances are found to be richer in aliphatic chains which implies a decrease in solubility and a partitioning of hydrophobic organic groups (Zhou et al., 2000). Smaller molecular weights exhibit high contents in aromatic and carboxyl functional groups that enhance their solubility, bioavailability and metal binding properties (Shin et al., 1999 ; Hur and Schlautman, 2003 ; Wang et al., 1997 ; Meier et al., 1999 ; Namjesnik-Dejanovic et al., 2000 ; Zhou et al., 2001 ; Christl et al., 2000).

The assessment of molecular weight in the case of HS is a tedious procedure due to their complex/heterogeneous nature, and the presence of a distribution range of weights reflects their polydispersity. To find appropriate standards for instrumental calibration is also a great concern (Swift and Posner, 1971 ; Sutton and Sposito, 2005). A high molecular weight is a characteristic feature of humic substances although some indecision remains when dealing with the range obtained from different studies (Sparks, 1998). Experiments done by Stevenson et al. (1953), PIRET et al. (1960) and Flaig and Beutelspacher (1968) using an ultracentrifugation technique (sedimentation velocity) on soil humic substances yielded MWs of 53,000, 25,000 and 77,000 daltons respectively. On the other hand, Stevenson, (1994) found MWs for soils humic substances from several hundred to more than 300,000 Da. Although many efforts have been done to reduce the dispersity, the fractions that are considered to be homogenous are substantially heterogeneous and not even close to monodispersity with values between 2000 up to more than 1,000,000 Da (Cameron et al., 1972 ; Posner and Creeth, 1972 ; Ritchie and Posner, 1982 ; Piccolo and Conte, 1999). Hence, for such heterogeneous materials, the average molecular weights are determined (Martin, 1964 ; Guéguen and Cuss, 2011 ; Swift, 1989a), including: Number-average molecular weight (M_n) (Aiken and Gillam, 1989); Weight-average molecular weight (M_w) (Swift, 1989b ; Wershaw, 1989 ; Moore, 1972) and z -average molecular weight (M_z) (Lansing and Kraemer, 1935).

Various techniques have been used for molecular weight measurement, such as ultrafiltration (Duarte et al., 2003; Kawahigashi et al., 2005 ; Buffle et al., 1978) , field flow fractionation (Williams and Giddings, 1987), dynamic light scattering (Palmer and von Wandruszka, 2001), ultracentrifugation (Visser, 1985 ; Wagoner et al., 1997), size exclusion chromatography (SEC), gel permeation chromatography (GPC) (Clapp et al., 2001 ; Baigorri et al., 2007a ; Song et al., 2010 ; Gjessing, 1965 ; Stuermer and Harvey, 1974 ; Tuschall and

Brezonik, 1980) and Electrophoresis (Curvetto and Orioli, 1982) (Figure. I-21). In addition, colligative property measurements (vapor pressure osmometry and cryoscopy) (Cronan and Aiken, 1985 ; Morris, 1977 ; Glover, 1975 ; Figini and Marx-Figini, 1981 ; Pavlik and Perdue, 2015) and viscosimetry (Clapp et al., 1989 ; Kawahigashi et al., 2005 ; Ghosh and Schnitzer, 1980 ; Relan et al., 1984) have also been used. Table I-7 presents the measured molecular weights of organic matter and its fractions from various origins with various techniques.

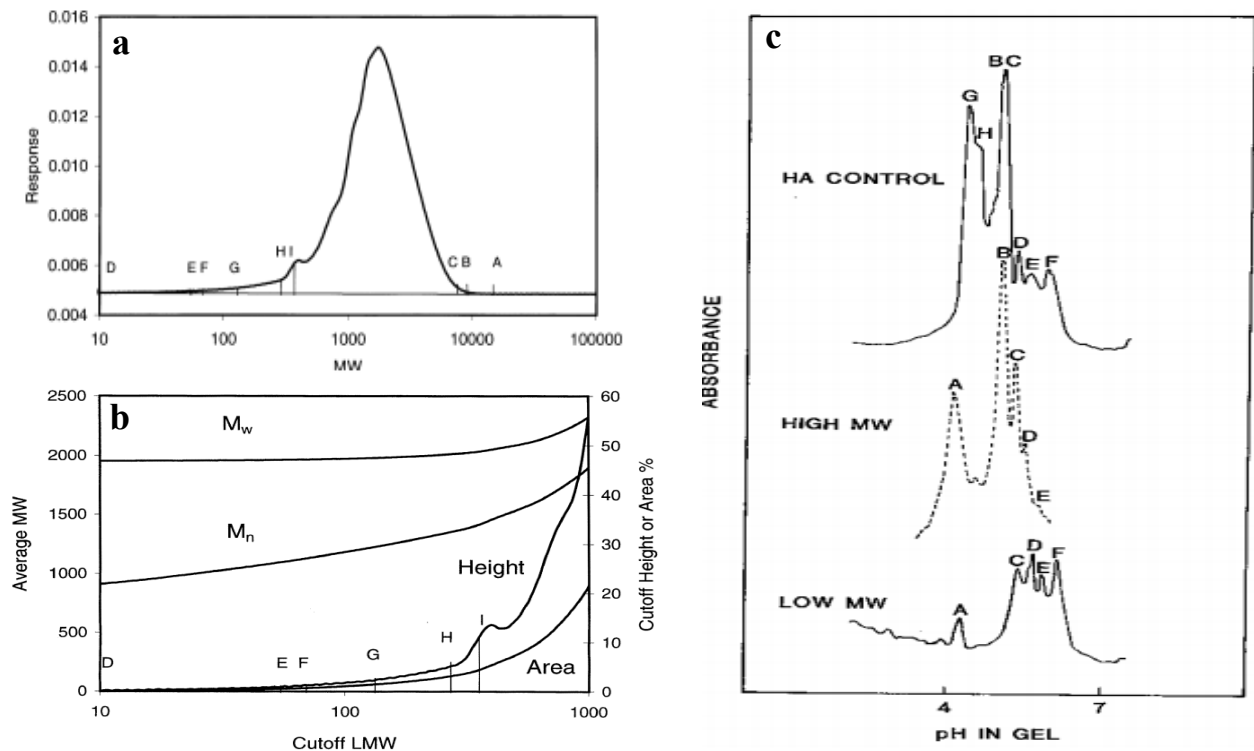


Figure I-21. HPSEC chromatogram of SRFA (left images) (Zhou et al., 2000) and Electrophoresis in pH 4-7 gradient of soil humic acid with high and low molecular weight component obtained from discontinuous pore sized gel (right image) (Curvetto and Orioli, 1982).

(a) MWs at A, B, and C are 18,000, 8804 and 8401 daltons. LMW cutoffs at D, E, F, G, H, and I corresponded to 0.11, 0.90, 1.00, 2.01, 5.01, and 10.00% of the maximum, respectively.

(b) Change in M_n and M_w of SRFA as a function of LMW cutoff, fixed HMW at 1% of the maximum height.

In general, humic substances (fulvic and humic acid) from aquatic origin, as well as dissolved organic matter, are of smaller molecular weight than that from soil HS. Fulvic acids produce more reliable values (500-2300 Da) since their hydrophilic nature hinder aggregation. Indeed, the hydrophobic interactions often interfere with the measurement of

molecular weight yielding a polydisperse molecular weight distribution, such effect being more pronounced for humic acids.

Table I-7. Molecular weights of Organic matter: Fulvic and Humic Acid.

sample	M _n (Da)	M _w (Da)	Methods	References
Freshwater FA	600-1,400	1,000-2,300	Cry, FFF, VPO, HPSEC, UC,	6-10, 12,14
Freshwater HA		4,000-8,000	UC	12
Freshwater DOM	500-1,300	800-2,200	Abs, HPSEC, UC	13,14
Marine FA	500-800		VPO	7
Soil water DOM	850-1,800	1,200-3,300	HPSEC	11
Soil FA	600-1,000		Cry, VPO	2-4
Aldrich HA	1,500-3,100	4,000-20,000	FFF, HPSEC, Visc	10,14
Soil HA		25,000-200,000+	DGU, UC, Visc	1, 2, 5
Peat HA		8,000-17,000	UC	12

Key to methods: *Abs*: molar absorptivity correlation; *Cry*: cryoscopy; *DGU*: density gradient ultracentrifugation; *FFF*: field flow fractionation; *UC*: ultracentrifugation; *Visc*: viscosity; *HPSEC*: high-pressure size-exclusion chromatography; *VPO*: vapor pressure osmometry

References: *1*-(PIRET et al., 1960); *2*-(Visser, 1964); *3*-(DeBorger and DeBacker, 1968); *4*-(Hansen and Schnitzer, 1969); *5*-(Cameron and Posner, 1974); *6*-(Wilson and Weber, 1977); *7*-(Gillam and Riley, 1981); *8*-(Reuter and Perdue, 1981); *9*-(Aiken and Malcolm, 1987); *10*-(Beckett et al., 1987); *11*-(Berdén and Berggren, 1990); *12*-(Reid et al., 1990); *13*-(Wilkinson et al., 1993); *14*-(Chin et al., 1994)

Even for a same sample examined with different techniques, a broad range of molecular weights can be obtained (Table I-8). These discrepancies have been ascribed to the limitation of the technique, e.g. electrostatic and hydrophobic interaction between humic substance and dextran gel or stationary face in case of chromatography (Cameron et al., 1972a ; De Nobili et al., 1989 ; Lindqvist, 1967), or because of the origin and type of humic matter (Figure. I-22).

Table I-8. Suwannee River Fulvic Acid Molecular Weights.

Analytical Methods	M _n (Da)	M _w (Da)	References
LDFTMS	463		(Novotny et al., 1995)
VPO	829		(Aiken and Malcolm, 1987)
GFC	960		(Novotny et al., 1995)
UC		1,460±80	(Reid et al., 1990)
X-ray Scattering		1,000-1,500	(Thurman et al., 1982)
FFF	1150	1910	(Beckett et al., 1987)
HPSEC	1,360; 14,00 1,900; 8,100	2,310; 1,700 2,500; 9,700	(Chin et al., 1994); (Chin and Gschwend, 1991)
HPSEC-MALLS	15,050±1,500 16,595±3,500	20,185±1,500 25,715±7,500	(Wagoner et al., 1997)

Key to methods: *LDFTMS*: laser-desorption Fourier transform mass spectrometry; *GFC*: gel filtration chromatography; *MALLS*: multi-angle laser light scattering

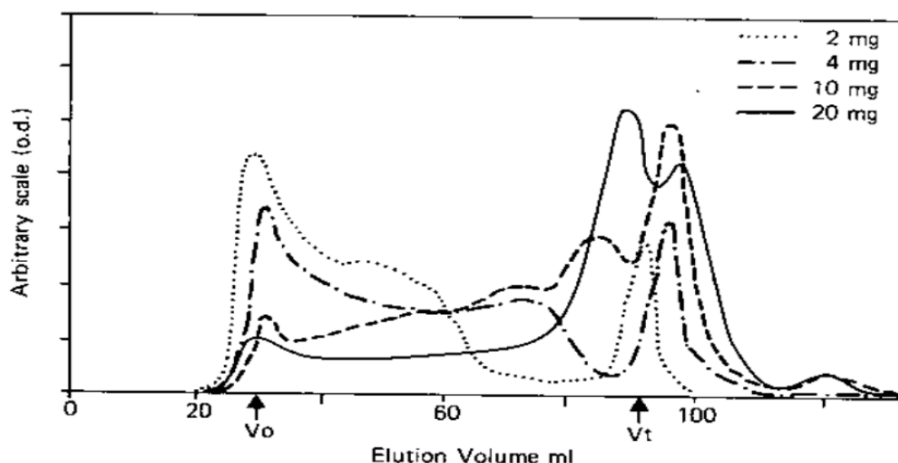


Figure I-22. Humic acids fractionation on Sephadex G-100 at different concentrations (Swift and Posner, 1971).

I.4-5 Structural Organization of Humic Substances

The nature of structural organization of humic substances represents a matter of debate in the literatures. Currently, two competing structural models are involved: a traditional assumption proposes HS as Polymers (Macromolecule) (Swift, 1999 ; Senesi, 1999 ; Schnitzer and Khan, 1972 ; Stevenson, 1994) and a new concept defends a Supramolecular organization (Wershaw, 1999 ; Piccolo, 2002 ; Simpson et al., 2002b ; Sutton and Sposito, 2005).

I.4-5-1 Humic Substances as Polymers (Macromolecule)

Humic substances have long been regarded as anionic polyelectrolytes (Cleven, 1984 ; Ephraim et al., 1986). This macromolecular concept was introduced as the rigid globular form (Visser, 1964), but later on a random polymeric coiling model was proposed (Cameron et al., 1972), as well as an ellipsoidal flexible structure (Orlov et al., 1975). These models were the base on which experimental data were interpreted, *i.e.* humic can have a flexible linear or spherical compact coiling structure depending on the solution conditions (concentration of humic substance, ionic strength and pH) (Table I-9) (Chen and Schnitzer, 1976 ; Buffle and Leppard, 1995a, 1995b ; Ghosh and Schnitzer, 1980). At basic pH and low ionic strength, humic substances should be considered as linear macromolecules that unfold because of increasing electrostatic repulsions as a result of functional group ionization (-OH). On the other hand, at acidic pH or increased ionic strength, globular structures are formed. Such hypothesis was substantiated by linking the conformation of humic substances to their concentration in solution, forming spherical colloids at a high concentration, and flexible

linear colloids at low concentrations without modifying the pH and ionic strength (Klucáková et al., 2012 ; Christl et al., 2005 ; Hosse and Wilkinson, 2001).

Table I-9. Effect of Humic Concentration, Ionic Strength and pH on the Polymeric Macromolecular Structure (Ghosh and Schnitzer, 1980).

Acid	Sample Concentration	Electrolyte Concentration (M)				pH		
		0.001	0.005	0.010	0.050	2.0	3.5	6.5
Fulvic	Low	~~~~~	~~~~~	~~~~~	~~~~~	~~~~~	~~~~~	~~~~~
	High	~~~~~	~~~~~	~~~~~	~~~~~	~~~~~	~~~~~	~~~~~
Humic	Low	~~~~~	~~~~~	~~~~~	~~~~~	~~~~~	~~~~~	~~~~~
	High	~~~~~	~~~~~	~~~~~	~~~~~	~~~~~	~~~~~	~~~~~

Despite the absence of a definite proof, many researchers support this model (Swift, 1999) where humic substances are supposed to be synthesized biologically as many macromolecules in living cells, and because of their refractory characteristics that can correspond to a coiling of their polymeric structure (Insam, 1996). Another argument was based on the polymerization of polyphenol and Maillard reaction that were achieved in the laboratory. Several authors also suggested that the polydispersity of humic substances results from the folding and unfolding of their polymeric structure (Cameron et al., 1972 ; Cornel et al., 1986 ; De Haan et al., 1987 ; Becher et al., 1985 ; Ceccanti et al., 1989).

I.4-5-2 Humic Substances Membrane-Like Micelles

The amphiphilic nature of humic substances opposes to the polymeric model. In that case, humic substances are composed of various small subunits that can rearrange to form a membrane-like micelle (Wershaw, 1986) linked by weak hydrophobic and H-bond forming hydrophobic interior domains (Figure. I-23) (Engebretson et al., 1996).

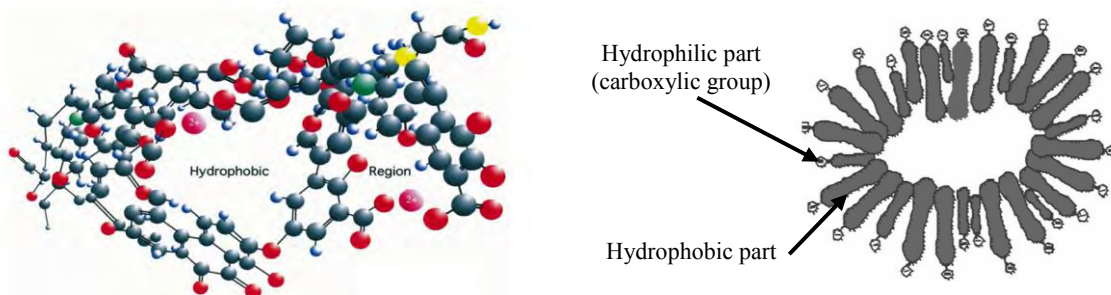


Figure I-23. Micelle-Like Structure of Humic Substances; left (Engebretson and von Wandruszka, 1994), right (Wershaw, 1986).

Humic substances are well known to be surface active compounds due to their amphiphilic nature (*i.e.* hydrophobic/hydrophilic moieties) (Yonebayashi and Hattori, 1987 ; Hayano et al., 1982 ; Vogt and Taugbrf, 1994 ; von Wandruszka, 2000 ; Klavins and Purmalis, 2010). They have the ability to reduce the surface tension of an aqueous solution (Terashima et al., 2004a ; Sierra et al., 2005b), and the formation of micelle-like aggregates, governed by intra and intermolecular aggregation of humic components held by weak hydrophobic interactions, above a critical micellar concentration (CMC) is suggested by surface tension and hydrophobic compounds solubility (Guetzloff and Rice, 1994 ; Chilom et al., 2009 ; Terashima et al., 2004b ; Yates and von Wandruszka, 1999 ; Shinozuka and Lee, 1991 ; Shinozuka et al., 1987). CMC values from 0.5-10g/L have been reported depending on various conditions (pH, temperature, HS and Surfactant nature and concentration) (Figure. I-24) (Jung et al., 2010 ; Ghosh et al., 2012 ; Anderson et al., 1995 ; Hayase and Tsubota, 1983).

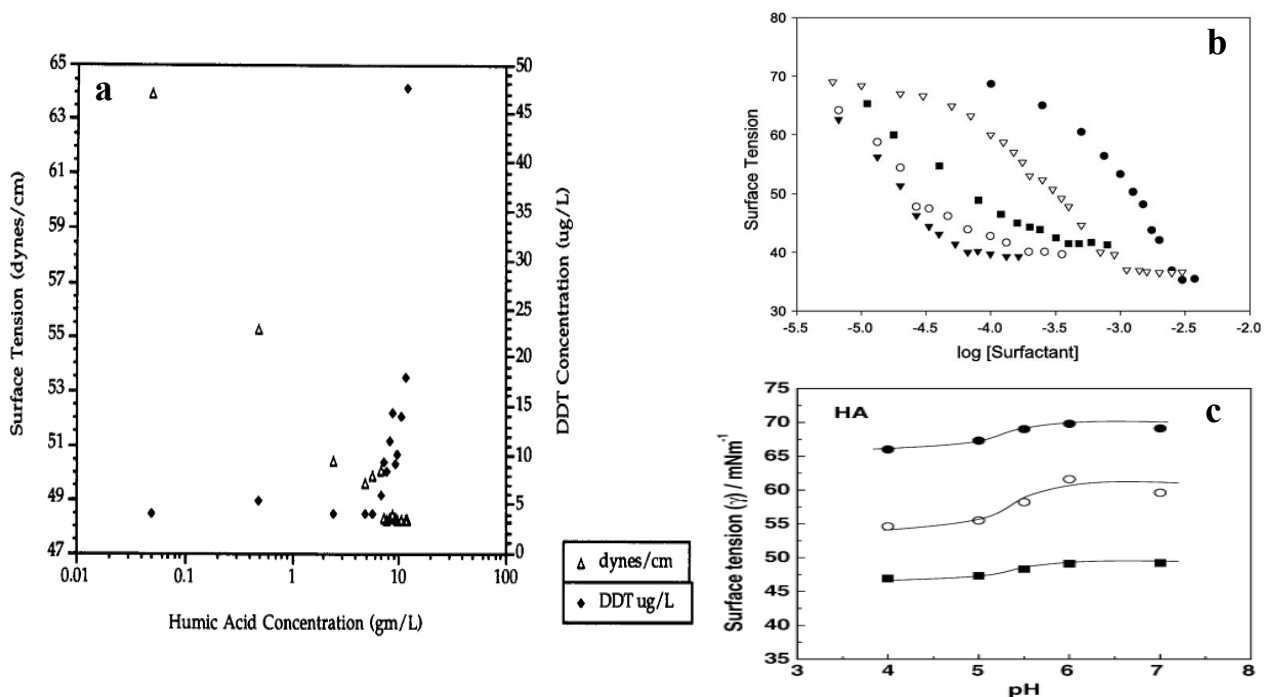


Figure I-24. Variation of the surface tension (γ) and DDT solubility as a function of HA concentration (a) (Guetzloff and Rice, 1994), and the effect of experimental conditions; surfactant (b) (Gamboa and Olea, 2006) and pH (c) (Terashima et al., 2004a).

(b) (\bullet) C_{14} TAB, (∇) C_{16} TAB; and in the presence of humic acid (\blacksquare) C_{12} TAB/HA, (\circ) C_{14} TAB/HA, (\blacktriangledown) C_{16} TAB/HA;

(c) HA: 4 mg/L (\bullet); 21 mg/L (\circ); 214 mg/L (\blacksquare).

Shaffer and Von Wandruszka (2014) carried out single-scan fluorescence emission spectroscopy on Latah Co Silt Loam Humic Acid (LSLHA), excited at 245 nm. The addition of multivalent cations (Mg^{2+} , Ca^{2+} and lanthanide ions) produced distinct changes in the native fluorescence of dissolved humic materials. The intensity of the typical broad emission spectra gradually increases, as well as a distinct peak centered at 400 nm rather than featureless emission spectra (Figure. I-25).

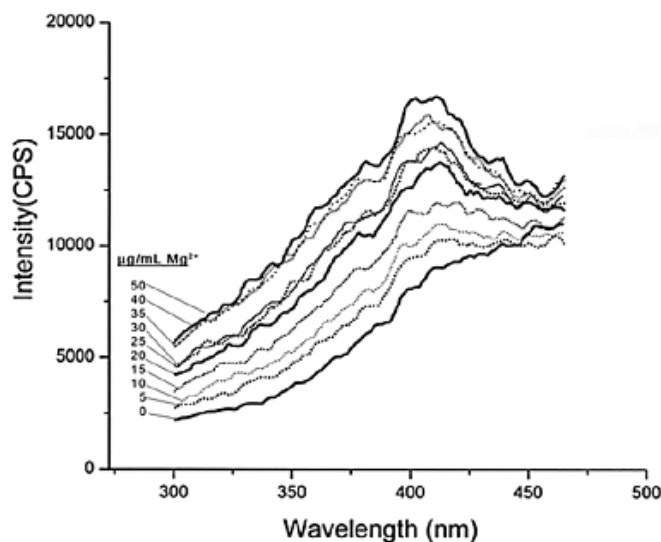


Figure I-25. Effect of different concentrations of Mg^{2+} on the intrinsic fluorescence of LSLHA in the 300-465 nm range; $\lambda_{ex} = 245nm$; 10 $\mu g/mL$ LSLHA (Shaffer and Von Wandruszka, 2014).

They suggest the formation of microaggregation where the multivalent cations cause the aqueous humates to undergo progressive intra- and intermolecular aggregation that manifest the previously quenched fluorophores centered at 400 nm. Such observation is consistent with a pseudomicellar model of the humic material, in which the aggregates have a relatively polar exterior and a nonpolar interior and the 400-nm peak may be considered a marker for the formation of pseudomicelles.

1.4-5-3 Humic Substances as Supramolecular Associations

Unlike previous data, the recent studies of humic substances suggest that the polymeric model is not consistent with the new results. These studies are based on several spectroscopic and microscopic techniques, gel permeation and size exclusion chromatography at high pressure, and processes of ionization and pyrolysis (Piccolo et al., 2002 ; Reemtsma et al., 2006b ; Sutton and Sposito, 2005 ; Piccolo and Spiteller, 2003).

Moreover, even the phenomena of formation and preservation of humics' in soils can be explained by a different model than that of polymers (Piccolo, 2002 ; Burdon, 2001). This new concept suggests that HS are defined as a supramolecular assembly of small heterogeneous organic molecules (<1000 Da) of different chemical nature associated by weak hydrogen bonds and hydrophobic interactions (Figure. I-26) (Simpson et al., 2002b ; Piccolo, 2001 ; Conte and Piccolo, 2002 ; Simpson et al., 2001a).

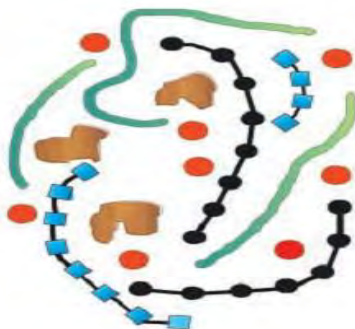


Figure I-26. Supramolecular Assembly of HS. The red spheres represent generic metal cations, the black units polysaccharides, the blue units polypeptides, the green units aliphatic chains, and the brown units aromatic lignin fragments (Simpson et al., 2002b).

This model was initially proposed based on GPC and SEC experimental results, in which the size of humic substances drastically changed following the addition of a small amount of organic acid. The decrease in size was explained by a rupture of intermolecular hydrophobic interactions between smaller subunit molecules that form the structure of the humic substances (Figure. I-27) (Piccolo and Conte, 1999 ; Cozzolino et al., 2001 ; Piccolo et al., 1999 ; Conte and Piccolo, 1999). The disaggregation processes was also detected by numerous techniques such as turbidimetry (Senesi et al., 1997), fluorescence and NMR spectroscopy (Simpson et al., 2001b), dynamic light scattering (Tombacz et al., 1997) and microscopy (transmission electron and atomic force) (Balnois et al., 1999). It has then been linked to the presence of basic subunits that form the humic matter. Baigorri et al., (2007a, 2007b) has reported the presence of both model; macromolecular polymer where he noted aggregation/flocculation process, and supramolecular assembly where disaggregation was observed.

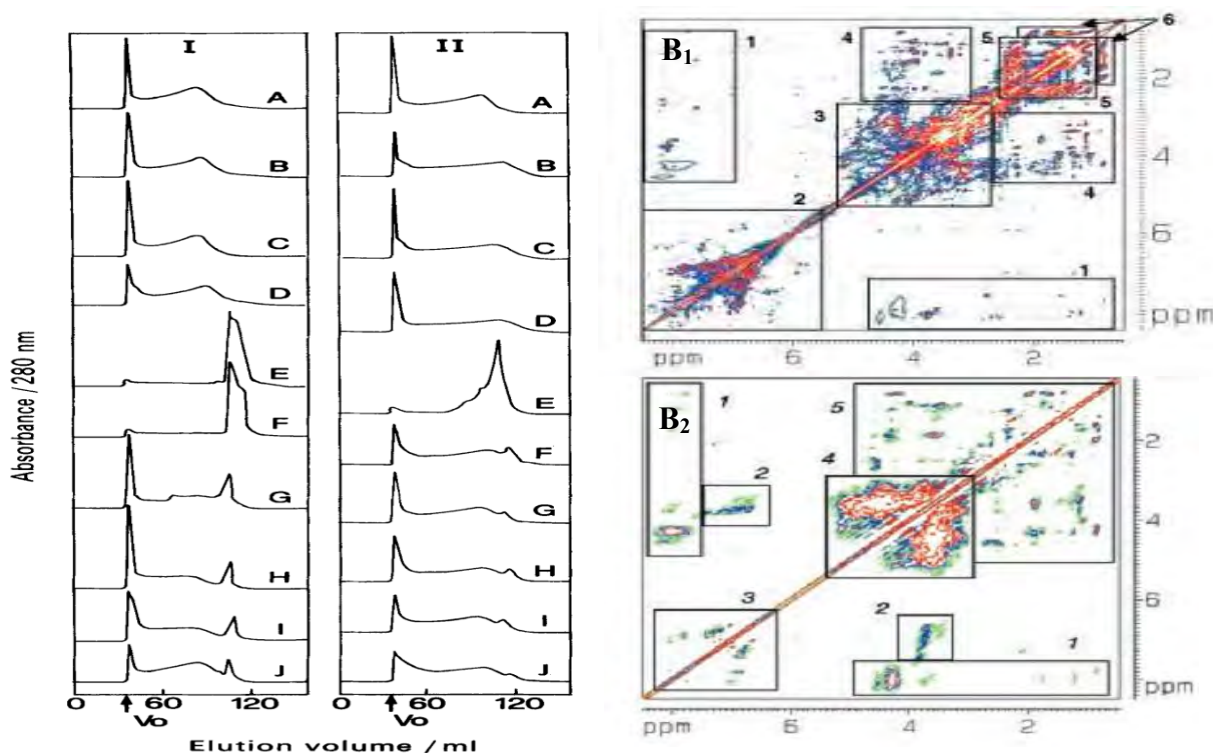


Figure I-27. Gel permeation chromatograms of HS₁ (I) and HS₂ (II) humic material (left) (Piccolo et al., 1996b) and NMR spectra of humic substances (HS) isolated from oak forest HS (right) (Simpson et al., 2002b).

Left: before elution in 0.02M Na₄B₂O₇ at pH 9.2, materials were treated as follows: (A) dissolved at pH 11.8; (B-E) titrated with acetic acid to pH 6, 4.5, 3.5 and 2; (F) the material brought to pH 2 was further back-titrated with KOH to pH 3.5; (G-I) back-titrated to pH 4.5, 6 and 8.5; (J) the latter material at pH 8.5 was further roto-evaporated to attempt the elimination of the residual acetic acid.

Right: “B₁” Total correlation spectroscopy (TOCSY) NMR spectra of humic substances (HS) isolated from oak [1 amino acids (amide-side chains), 2 aromatics, 3 sugars, methine units bridging lignin aromatics, amino acids (α - β couplings), 4 methylene units adjacent to ethers, esters, and hydroxyls in aliphatic chains, amino acids (α - β - γ couplings), 5 methylene in aliphatic chains, and 6 methyl units in amino acids and aliphatic Chains]; “B₂” NOESY NMR spectra [1 amino acids, 2 lignin aromatics (methoxyl-aromatic interactions), 3 lignin aromatic structures (interactions between aromatic protons), 4 methylene and methyl units in amino acids and aliphatic structures].

To substantiate such model, a polymerization was carried out using oxidative enzymes (e.g. peroxidase and phenoloxidase) in order to stabilize the weakly bonded humic subunits by increasing the number of covalent linkages. By further treating the resulting humics with organic acids, larger molecular weights were detected by size exclusion chromatography with a lesser disaggregation effect of the organic acids on the stabilized humic matter (Piccolo et al., 2000 ; Cozzolino and Piccolo, 2002).

I.5 MODELING REPRESENTATION OF HUMIC SUBSTANCE

It is essential to understand the molecular structure of organic matter to comprehend their biogeochemical role in the environment. This process can be readily achieved when dealing with matter of unique biochemical content (e.g. carbohydrates or proteins), but due to the complex nature of humic substances, it is very challenging if not impossible. The development of techniques of investigation (chemical and physical methods) made the possibility of identifying the elemental and functional groups that can be implicated in writing a speculative average molecular structure (Huffman and Stuber, 1985). Some early proposed structures by Haworth (1971) and Cheshire et al. (1967), where humic substances are made of aromatic cores that is linked to different materials (peptides, metals, phenolic acids and carbohydrates), are listed below in Figure. I-28.

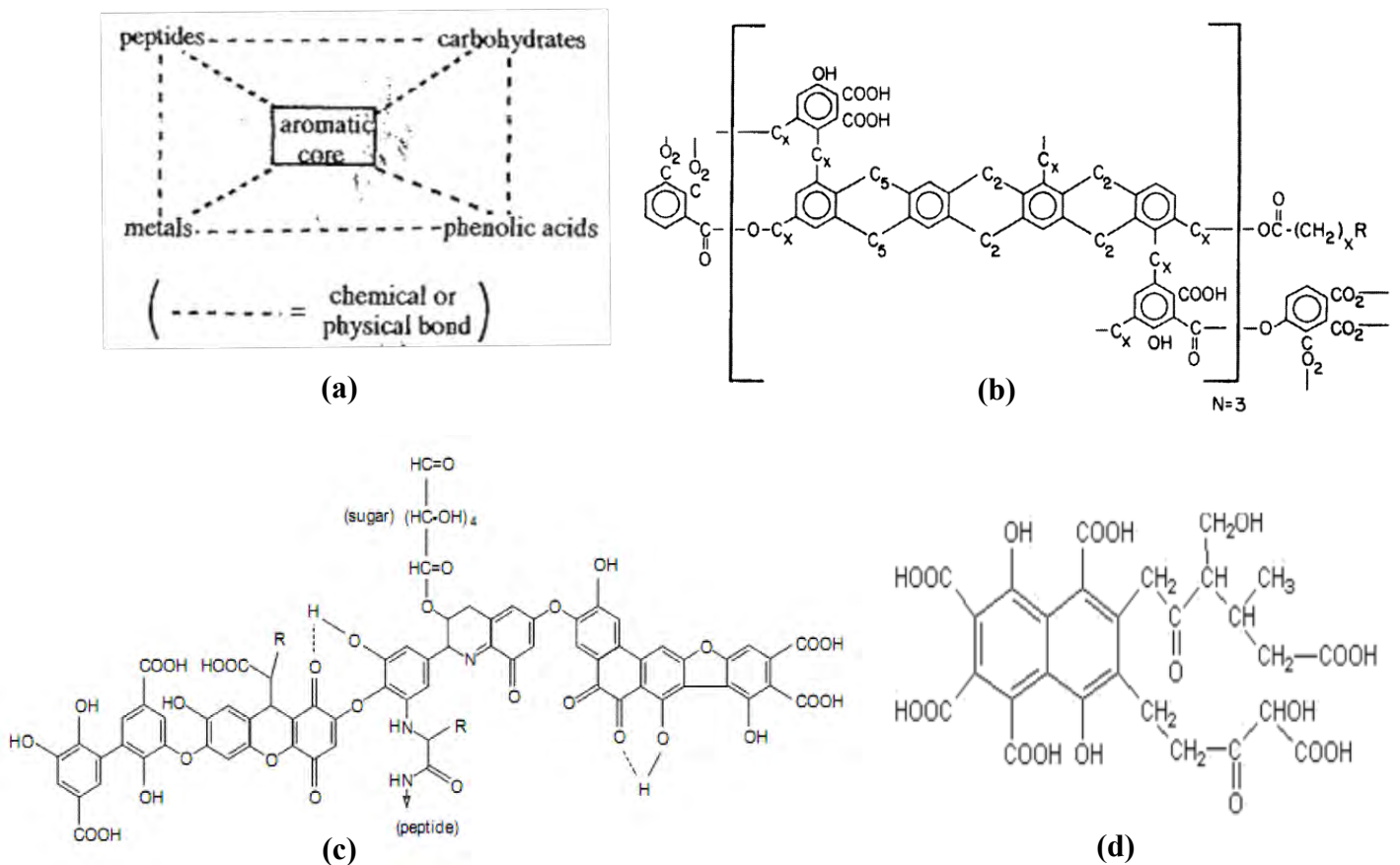


Figure I-28. Proposed Structures for Humic Substances. (a): Humic acid from Zn dust distillation and hydrolysis, oxidation, reduction and spin resonance spectroscopy (Haworth, 1971); (b): Humic acid from alkaline permanganate degradation (Christman et al., 1989); (c): Humic acid (Stevenson, 1982); (d): Fulvic acid (Buffle, 1977).

Other studies have suggested the existence of a monomer subunit, *i.e.* a building block of the molecular structure, for humic acid (Figure. I-29a) (Steelink, 1985). According to recent findings regarding the elemental composition using Liquid-NMR, Jansen et al. (1996) modified the formula proposed by Steelink for the humic monomer (Figure. I-29b). According to potentiometric titrations and NMR data, Leenheer et al. (1989) presented a 800 Da number-average molecular weight Suwannee River Fulvic Acid (SRFA) model. Recently, Leenheer, (2007) also worked on how to move from a model to actual molecular structure (Figure. I-29c, I-29d and I-29e).

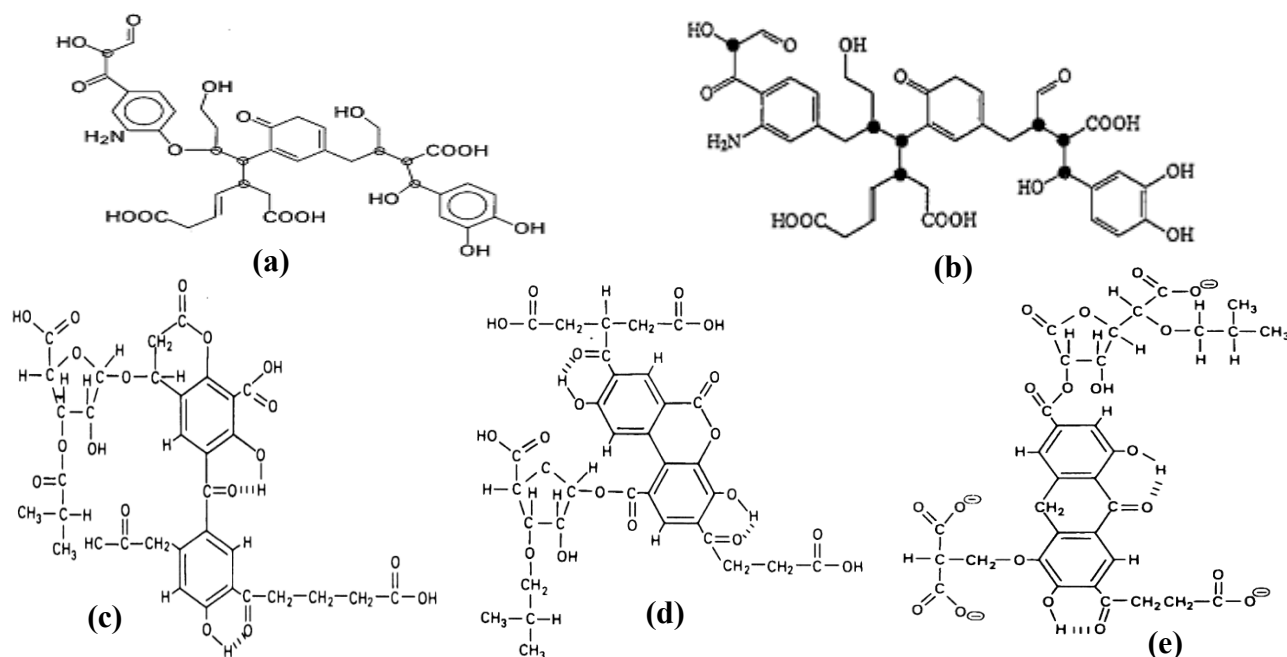


Figure I-29. The Steelink (a) and Jansens (b) Model of Humic Acid Monomer and SRFA Model of Leenheer (c, d and e).

More intricate structures have been suggested by Schulten and Schnitzer for the humic acid monomer using pyrolysis results (Schulten and Schnitzer, 1992a, 1992b), ^{13}C – NMR spectra (Schnitzer et al., 1991), oxidative and reductive degradation experiments (Hansen and Schnitzer, 1966), and electron microscopy observations (Stevenson and Schnitzer, 1982). They suggest a 2D model (Schulten and Schnitzer, 1993) and corresponding 3D structure (Schulten and Schnitzer, 1995 ; Schulten, 1995 ; Schulten and Gleixner, 1999) with a molecular formula $\text{C}_{308}\text{H}_{328}\text{O}_{90}\text{N}_5$, containing many voids (Figure. I-30) where carbohydrates and protein are adsorbed (Khan and Sowden, 1971 ; Sowden and Schnitzer, 1967 ; Martin et al., 2001 ; Zang et al., 2000). Similarly, structures for marine humic and fulvic acids have been proposed (Ehrhardt, 1984 ; Harvey et al., 1983).

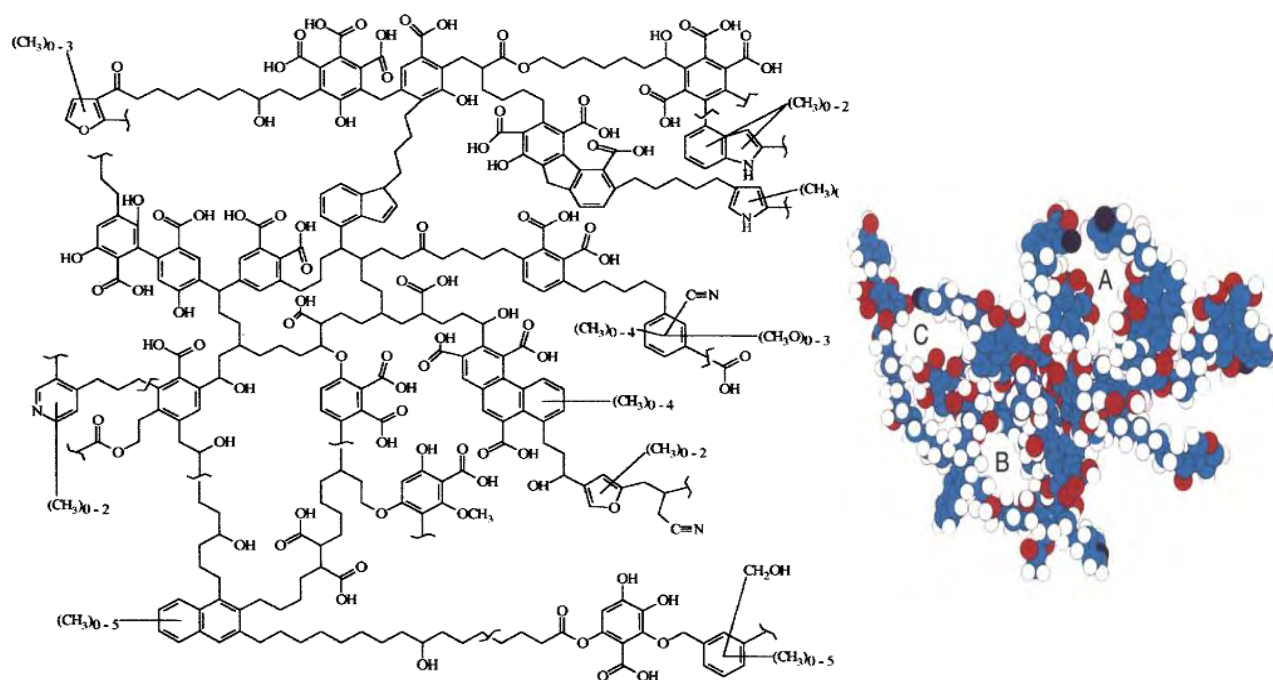


Figure I-30. 2D model (left: Schulten and Schnitzer, 1993) and corresponding 3D structure (right: Schulten and Schnitzer, 1995) of Humic Acid. Element colors: carbon=light blue; hydrogen=white; nitrogen=dark blue; and oxygen= red; A, B, and C are the voids).

From pyrolysis/GC-MS analysis, a helical conformation of Temple Northeastern Birmingham (TNB) humic acid monomer was envisioned by Sein, et al. (1999) that is similar to that proposed by Steelink (Figure. I-31), based on oxidative and cleavage reaction of lignin (Paciolla et al., 1998 ; Young and Steelink, 1973 ; Kolla et al., 1998).

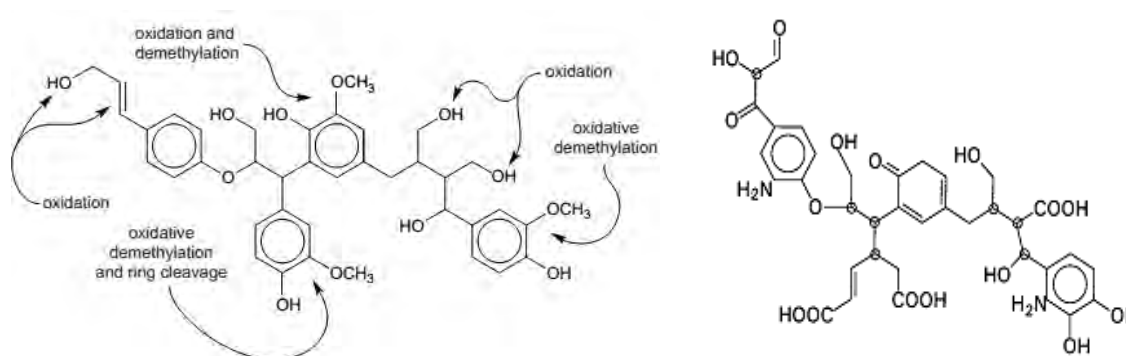


Figure I-31. Lignin Conversion (left) into Humic Acid monomer (right) (Sein et al., 1999).

The most recent model based on NMR results that accounted the complex nature of humic acid, is that proposed by Simpson et al. (2002b) (Figure. I-32).

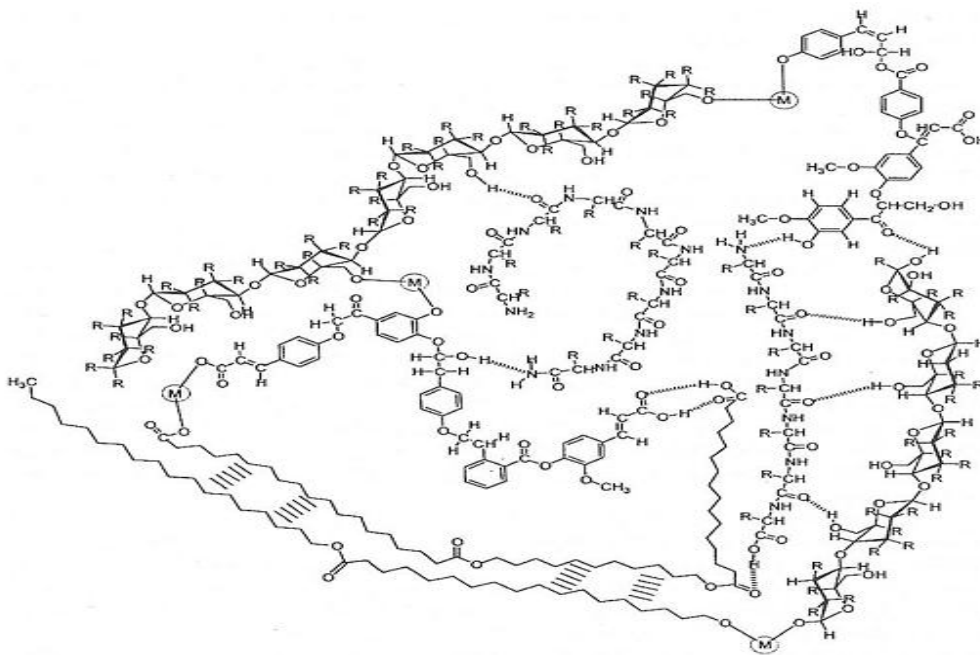


Figure I-32. Humic Acid Model suggested by Simpson et al. (2002b) M represents the metal ion or surface.

The proposed humic substances models were based on various experimental techniques. Some of which might modify the natural structure, other might destroy some of their components. For example, although Electrospray ionization couple with MS or HPLC gives insight of various chemical groups, the fragmentation complicates the process of drawing a model. Similarly, NMR also provides valuable information about different functional groups, but not the way they are linked with each other. Thus, the suggested models should not be interpreted too literally, where authors give speculation of structures that might or might not be representative or even close to what humic substance is for real.

I.6 ROLES OF HUMIC SUBSTANCES

Humic substances are widely distributed wherever the decomposition of organic matter occurs (Hayes et al., 1989b), from aquatic to terrestrial environments (soils and sediments) (Gjessing, 1976). Therefore, HS represent the major component of organic matter on earth (Woodwell and Houghton, 1977 ; Woodwell et al., 1978). They comprise from the total organic carbon around 25% and represent more than 50% of dissolved organic compounds in natural aquatic systems (Zumstein and Buffle, 1989 ; Robards et al., 1994 ; Hertkorn et al., 2002 ; Guthrie et al., 2005 ; Thurman and Malcolm, 1981 ; Herbert and Bertsch, 1995). In soils, they account for 70-80% of the organic carbon (Madaeni et al., 2006

; Orlov, 1990 ; Lal, 2004 ; Jellinek, 1974 ; Serra and Felbeck, 1972). Some values of DOC and the corresponding fraction in humic substance are given in Table I-10.

Table I-10. Concentration ranges of Dissolved Organic Carbon (DOC) and Humic Substances in some aquatic systems (Thurman, 1985).

Source	DOC (mg/L)	HS (mg/L)
Sea water	0.2-2.0	0.06-0.6
Groundwater	0.1-2.0	0.03-0.6
River	1-10	0.5-4.0
Lake	1-50	0.5-40

The wide distribution of humic substances in the ecosystem from soils, sediments and water, render them very influential (Engebretson and von Wandruszka, 1998 ; Waite et al., 1988 ; Ochs et al., 1993 ; Maurice et al., 1995) in all the biogeochemical processes that occur in the environment (Hayes and Swift, 1978 ; Nebbioso and Piccolo, 2012 ; Piccolo and Conte, 1999). HSs are a source of energy for microorganisms, thus affecting the energy flow of the food web (Fischer et al., 2002 ; Wetzel et al., 1995 ; Sun et al., 1997 ; McDonald et al., 2004). They are of importance for the proper structure of soils and they influence the fertility (Avena and Wilkinson, 2002) by controlling various biological, chemical and physical properties that affect plant growth (Kelleher and Simpson, 2006 ; Stocking, 2003 ; Flaig, 1990). Humic substances improve the water retention in soil (Lal et al., 2004) and in addition to their role in the biogeochemical cycle of carbon (Piccolo et al., 2004) and of various soil components (e.g. nitrogen, sulphur and phosphorus), they control the bioavailability of nutrients (Vigneault et al., 2000 ; Fava and Piccolo, 2002 ; Terashima et al., 2004a) by retaining and exchanging with plant roots, that is substantial for growth due to their cationic exchange capacity (Nardi et al., 2007 ; Canellas et al., 2008 ; Russell, 1962).

They also play a significant role as protons buffer (Koopal et al., 2005 ; Milne et al., 2001) and in transportation and sequestration of inorganic metal contaminants (Chiou et al., 1986 ; Magee et al., 1991 ; Schlautman and Morgan, 1993 ; Cabaniss and Shuman, 1988 ; Chiou et al., 1987 ; Hering and Morel, 1989), radionuclides (Moulin et al., 1996 ; McCarthy et al., 1998 ; Santschi et al., 1997), xenobiotic molecules (Cabaniss, 1990 ; Schroth and Sposito, 1998 ; Selim and Amacher, 1996 ; Edzwald et al., 1985) and hydrophobic organic pollutants such as pesticides, e.g. DDT, carbaryl, PCBs etc, (Šmejkalová et al., 2009 ;

Nebbioso and Piccolo, 2009 ; Nordén and Dabek-Zlotorzynska, 1996 ; Schmitt et al., 1996 ; Pestke et al., 1997 ; Shimizu et al., 1998) as well as their degradation (Holman et al., 2002 ; Linn et al., 1993). Such roles are mainly related to their amphiphilic nature (Guetzloff and Rice, 1994 ; Conte et al., 2005); the humic substances being able to form hydrophobic domains engulfing those organic matter (Tschapek and Wasowski, 1976 ; Matsuda et al., 2009), and due to their photochemical properties through the production of reactive intermediates upon solar exposure and energy absorption (Cawley et al., 2015).

In itself, the humic substance might not consider being harmful, but it can be a source of worries in potable water production and treatment where the retained contaminants could be released again into the surrounding environment. They can also enhance the development of microorganisms in distribution networks (Owen et al., 1995). They are also considered as the main precursors of disinfection byproducts (DBPs) resulting from the chlorination of drinking water, particularly halogenated compounds and direct-acting mutagenic product as trihalomethanes (THMs: chloroform, bromoform, bromodichloromethane, and chlorodibromomethane) (Wong et al., 2007; Reckhow et al., 1990 ; Leenheer et al., 2001 ; Babi et al., 2007 ; Wang et al., 2007 ; Kim and Yu, 2007 ; Gopal et al., 2007 ; Richardson et al., 2007 ; Zwiener and Richardson, 2005 ; Richardson, 2003 ; Sadiq and Rodriguez, 2004 ; Rook, 1977).

Therefore, the study of humic substances, *i.e.* their structural and molecular organization, is of major importance to better understand various chemical and biological processes occurring in natural ecosystems.

I.7 SURFACTANTS

I.7-1 Definition and Classification

Surfactants are highly surface-active agent molecules due to their amphiphilic nature, *i.e.* comprising hydrophobic alkyl chain and hydrophilic polar head. The dual nature enables their self-assembling in to micelles in solution (Tanford, 1985 ; Segota and Tezak, 2006 ; Acharya and Kunieda, 2003) and improves the solubilization of hydrophobic components (Attwood and Florence, 1983 ; Schwartz et al., 1949 ; McBain and Hutchinson, 1955 ; Hargreaves and Hargreaves, 2003 ; Nagarajan and Ruckenstein, 1991). According to the polar head charge, surfactants are classified in to different groups as Cationic (positively charged), Anionic, (negatively charged), Non-ionic (zero-charged) and Zwitterionic or

Amphoteric (containing both negative and positive charge) (Cui et al., 2006 ; Rosen and Kunjappu, 2012 ; Myers, 2005 ; Karsa, 1999 ; Rieger and Rhein, 1997 ; Lucassen-Reynders, 1982).

I.7-2 Applications

Surfactants are widely used in a range of products such as domestical (soaps and shampoo), industrial (paints, cosmetics and foods), biochemical and pharmaceutical industries as a drug delivery systems (Penfold et al., 2003 ; Nieuwkerk et al., 1998 ; Cottrell and Van-Peij, 2004 ; Kato et al., 2008). It is then crucial to identify certain parameters that control their phase behavior in solution, *i.e.* the critical micellar concentration (cmc) and the effect of temperature especially the Krafft point (Schramm et al., 2003). Their physico-chemical properties alter significantly below (being similar to electrolytes) and above (cooperative binding) the cmc (Tanford, 1980 ; Lingafelter, 1949 ; Ben-Naim, 1980 ; Stigter and Mysels, 1955 ; Mukerjee and Mysels, 1971) (Figure. I-33).

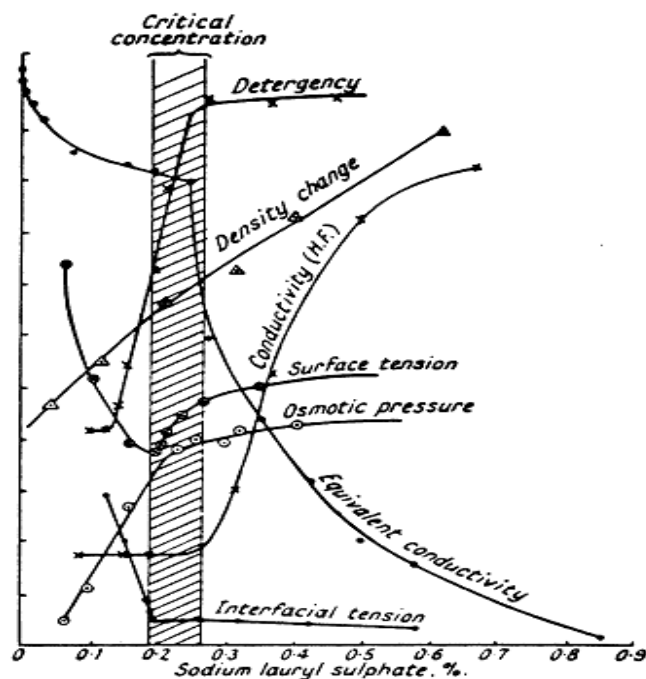


Figure I-33. Effect of Surfactant concentration (below and above cmc) on their Physico-Chemical Properties (Preston, 1948).

Similarly, below the Krafft temperature, surfactants are insoluble, lose their surface activity, and they crystallize in the form of hydrated crystals. Above this temperature their solubility is significantly increased and they self-assembled into various micellar shapes and vesicles (Figure. I-34) (Moroi, 1988 ; Bales et al., 2002).

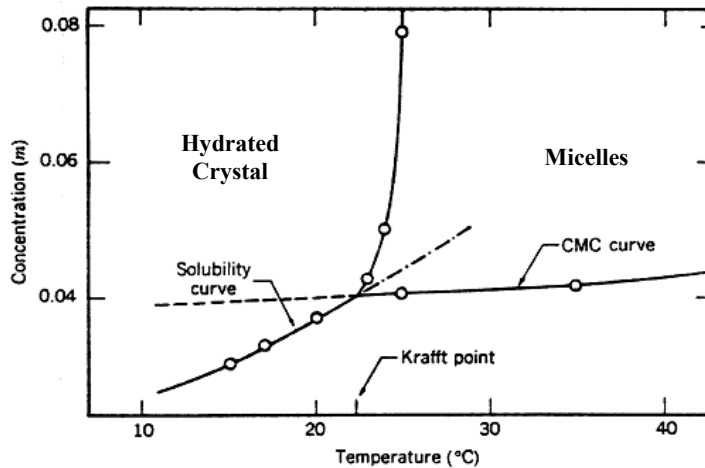


Figure I-34. Effect of Temperature (Krafft point) on Surfactant Solubility (Shinoda et al., 1963).

I.7-3 Interaction between Surfactants-Polymers and Surfactants-Humic Substances

The interaction of surfactants with polymers has recently been a subject of growing interest due to the wide range of applications for which such interaction affects the viscosity and stability of products through controlling the rheological properties (gel-like structure) (Hoff et al., 2001 ; George et al., 2009 ; Bromberg et al., 2000 ; Morishima et al., 1999 ; Chew et al., 1995 ; Antunes et al., 2004 ; Chakraborty et al., 2006). The binding could be governed by a weak association in the case of nonionic polymer (Deo et al., 2005) or stronger in the case of oppositely charged polymer-surfactants system (Hansson and Almgren, 1994 ; Maurdev et al., 2002 ; Mata et al., 2006). Improving the hydrophobic properties, e.g. increasing the length of the surfactant alkyl chain (Nieuwkerk et al., 1998), enhance the binding strength by improving the cooperative binding process.

As previously mentioned, surfactants are widely used from domestic products to pharmaceutical industries. This leads to their intrusion into the ecosystem through waste water and they may accumulate in aquatic and soil system. Cationic surfactants can interact with the humic matter thus affecting the humic substance conformation, hence the fate and bioavailability of metallic and organic contaminants (Bors et al., 2001). Such structural modification was investigated by X-ray diffraction in the presence of alkylammonium-based surfactant, where coagulation of humic matter was evidenced (Tombácz et al., 1988), and in other studies a phase separation due to precipitation as a result of neutralization and

formation of hydrophobic humic/surfactant complex was reported (Adou et al., 2001). Humic acid was also found to bind more strongly to cetyltrimethylammonium bromide than fulvic acid as detected by NMR (Otto et al., 2003). Thus, studying the interaction behavior is a point of interest. Binding isotherms have been measured to estimate the amount of bound surfactant to humic substances (Figure I-35) (Ishiguro et al., 2007 ; Shirahama, 1998 ; Rodenhiser and Kwak, 1998). The addition of a cationic surfactant drastically reduces the surface activity of humic substances and produces micelles at lower concentration than that of the pure materials (Gamboa and Olea, 2006).

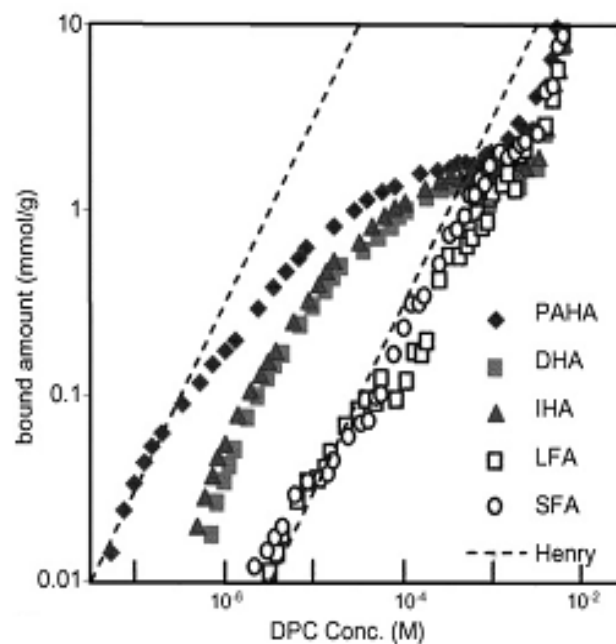


Figure I-35. Dodecyl-pyridinium chloride –HA (purified Aldrich humic acid (PAHA), Dando humic acid (DHA), Inogashira humic acid (IHA)) and –FA (Laurentian fulvic acid (LFA) and Strichen Bs fulvic acid (SFA)) binding isotherms at 0.005 M salt and pH 4.5–5 (Ishiguro et al., 2007).

From a thermodynamic point of view, humic and fulvic acid were studied using potentiometric titration using respective surfactant-ion-selective membrane electrodes, where humic acid binds more strongly to dodecylpyridinium ($C_{12}Py^+$) than fulvic acid with a cooperative interaction with the latter (Figure I-36) (Yee et al., 2006a).

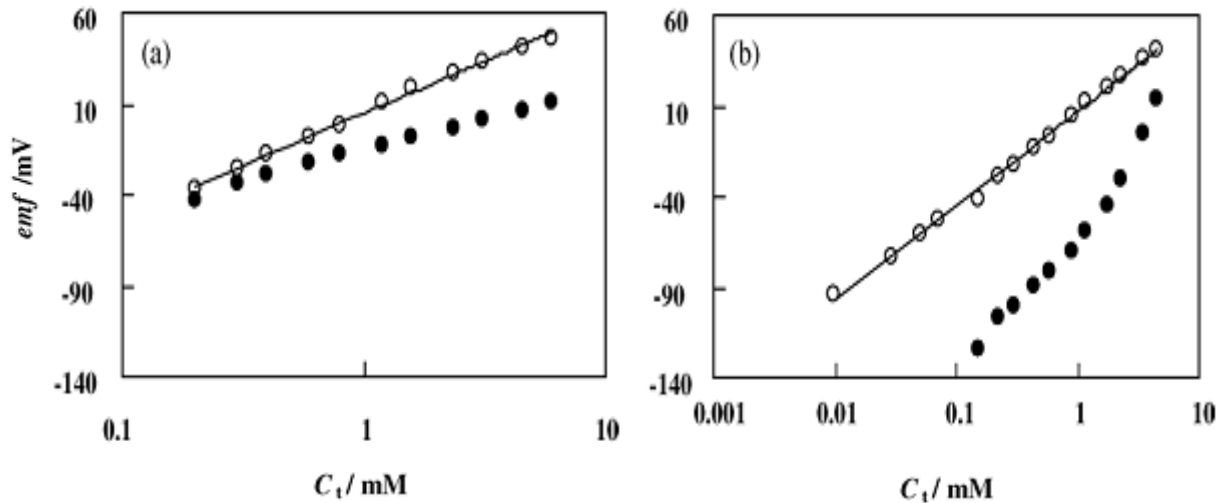


Figure I-36. Potentiograms of: (a) $C_{12}Py^+$ -AFA system and (b) $C_{12}Py^+$ system. (○) Without FA or HA; (●) with FA or HA; pH= 9.18, I= 0.03M and T=25 °C (Yee et al., 2006a).

Little interaction was found when a negatively charged surfactant (e.g. Sodium Dodecyl Sulfate) was used (Figure I-37) (Yee et al., 2009 ; Koopal et al., 2004).

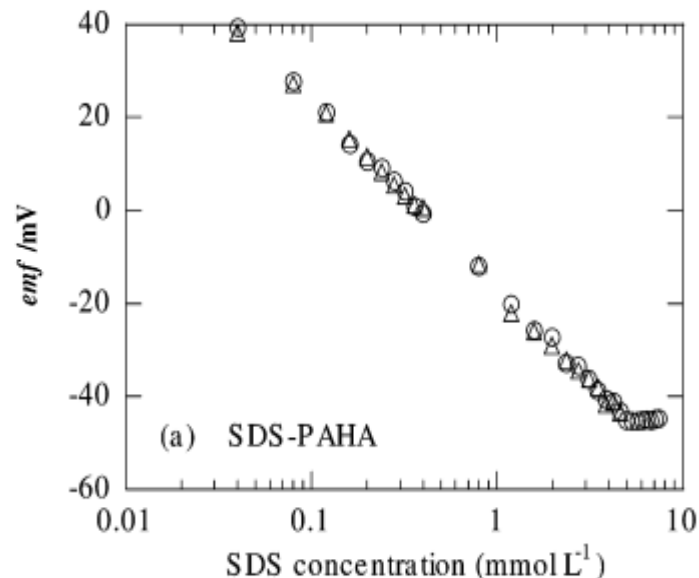


Figure I-37. Surfactant-PAHA titrations at pH=7 and I=0.025 M. The cell potential or EMF (mV) is plotted as a function of the logarithm of the total SDS (Koopal et al., 2004).

The ionic strength and pH affect the binding; indeed, an increase in pH and a decrease in ionic strength enhance the interaction by increasing the charge density and decreasing counter-ions screening effect, respectively (Figure I-38) (Yee et al., 2006b ; Yee et al., 2007).

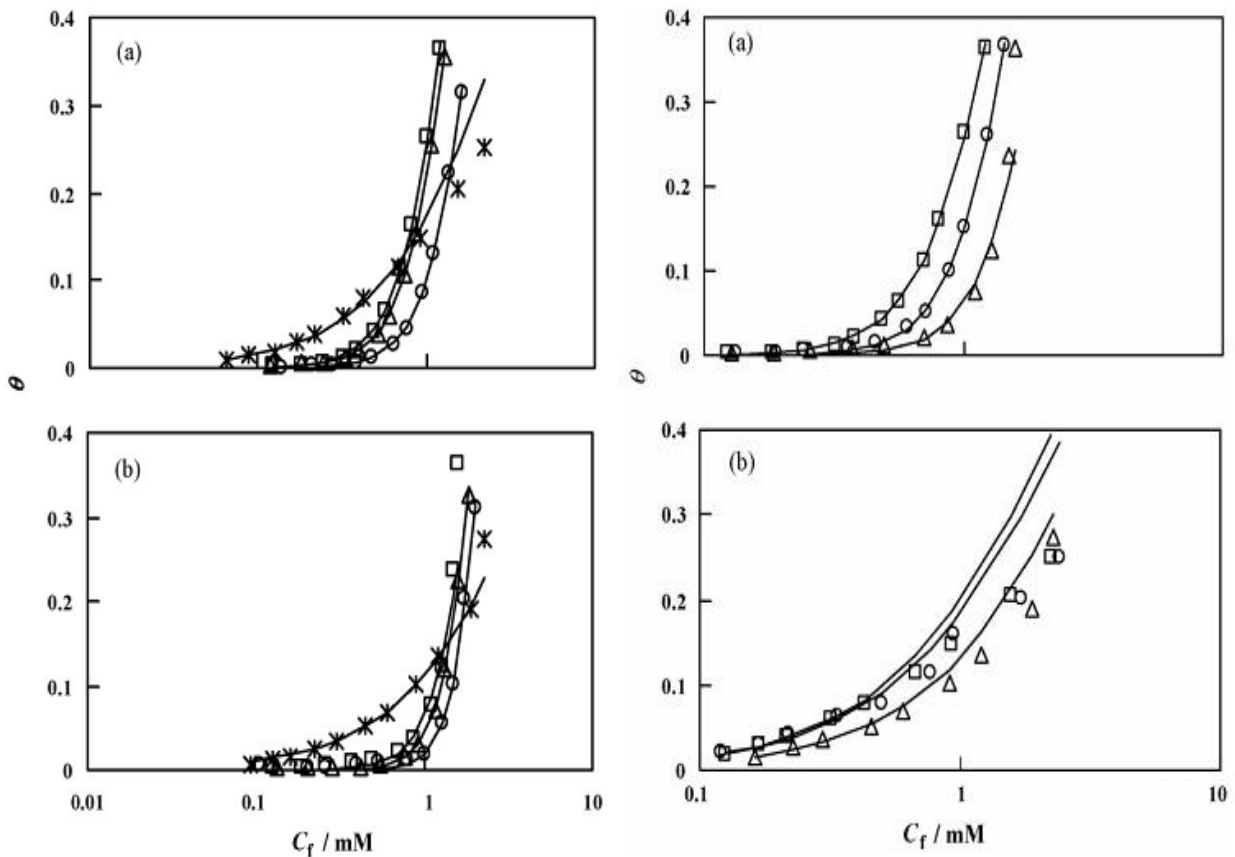


Figure I-38. Binding isotherms for $C_{12}Py^+$ -AFA system. Left image: as a function of pH at: (a) $I = 0.03 \text{ mol dm}^{-3}$ and (b) $I = 0.10 \text{ mol dm}^{-3}$, (*) pH 3.97, (○) pH 7.41, (□) pH 9.18, (Δ) pH 10.01. Right image: as a function of ionic strength at: (a) pH 9.18 and (b) pH 3.97. (□) $I = 0.03 \text{ mol dm}^{-3}$, (○) $I = 0.05 \text{ mol dm}^{-3}$, (Δ) $I = 0.10 \text{ mol dm}^{-3}$ (Yee et al., 2006b).

Based on these observations, the structure of humic substances can be probed in the presence of a cationic surfactant. Indeed, adding an oppositely charged amphiphilic molecule to humic substances is expected to induce a drastic restructuring of the humic colloid driven both by electrostatic and hydrophobic interactions. All these interactions will result in molecular rearrangement and reformation in the humic substances structure. This rearrangement can be illustrated by the formation of aggregates resulting in new partnerships between our molecules studied. If humic acids are polymers; *chain collapse*, formation of humic substance aggregates connected by surfactant micelles and various types of precipitates is expected, whereas in case of supramolecular associations, it is easier for the surfactant to interact with the small subunit molecules comprising the supramolecular organization of humic substances that will lead to major molecular rearrangement represented by the formation of globules, mixed micelles and *vesicles*.

CHAPTER *(II)*

MATERIALS
AND
EXPERIMENTAL METHODS

II.1 MATERIALS

II.1-1 Humic Substances and Dissolved Organic Matter (DOM)

In this study, the structure of Suwannee River Humic Substance (SRHS), *i.e.* Humic Acid (SRHA) and Fulvic Acid (SRFA) (Maurice, 2015), was analyzed in the presence of various cationic surfactants with different alkyl chain lengths, Octyl, Dodecyl and Cetyl trimethyl ammonium chloride (OTAC, DTAC and CTAC, respectively) using various structural characterization techniques. In addition, an attempt was also made to generalize the results obtained with SRHS by using HS of different origin (Nyong humic acids) and a modeled humic-like substance (MHS). Such comparison was made with natural organic matter from Amazonian black waters in order to understand the effect and the necessity of NOM fractionation into their various components.

Suwannee River Humic Substance, Humic Acid (Humic Acid Standard 2S101H) and Fulvic Acid (Fulvic Acid Standard 2S101F), were purchased in solid state powder from the International Humic Substances Society (IHSS). Those humic substances are extracted from the Suwannee River that passes through the Okefenokee Swamp in southern Georgia to reach the southwestern Gulf of Mexico (Figure. II-1). The extraction of the stock solution takes place at a sill where Suwannee River leaves the Okefenokee Swamp; the water of the river is dark and has a pH below 4 with a concentration of dissolved organic carbon (DOC) ranging from 25-75 mg/L (Malcolm et al., 1994a).

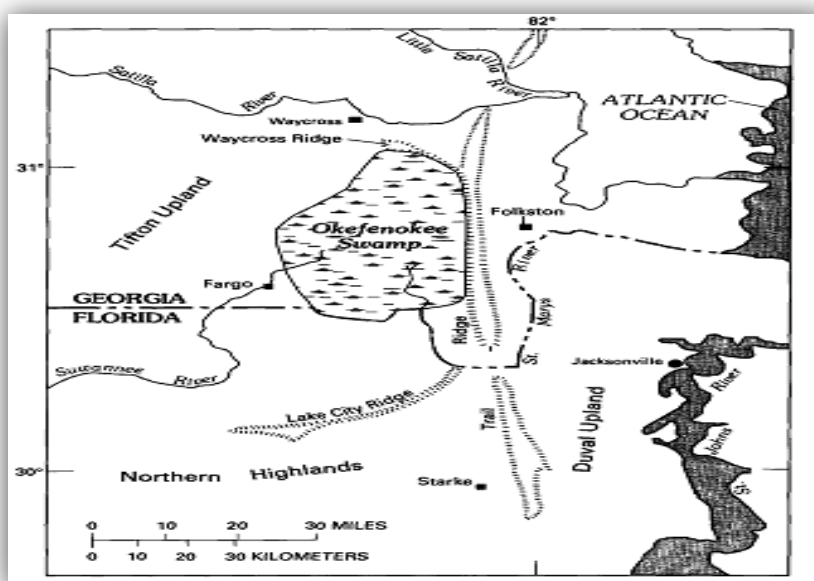


Figure II-1. Okefenokee Swamp and Suwannee River Location (Pirkle et al., 1977 ; Presley, 1984).

Both the separation and purification of the humic fractions are performed according to protocol developed by the IHSS Association (Malcolm et al., 1994b). Suwannee River Humic Substances have been intensively characterized by NMR (Noyes and Leenheer, 1994 ; Thorn, 1994), ESR (Saleh et al., 1994), Fluorescence Spectroscopy (Goldenberg and Weiner, 1994), Acid-Base titration and hydrolysis (Bowles and Antweiler, 1994). The elemental analysis (Thurman and Malcolm, 1994 ; Reddy et al., 1994), molecular size and weight (Aiken et al., 1994) as well as hypothesized molecular structures (Leenheer, 1994) have been reported by various authors (Averett et al., 1994). Their properties can be found on the IHSS website (<http://www.humicsubstances.org/>).

Nyong humic acid was extracted from Nyong River sediment at Mbalmayo in the tropical rain forest of Cameroon (Figure. II-2). The isolation and extraction was based on the procedure described by Thurman and Malcolm (1981). The river is characterized by a slightly acidic pH of 5.8 and a DOC content of about 20 mg/L. The elemental composition analysis gave 39.3% in C, 3.4% in H, 2.8% in N, and 33.1% in O. The charge density shows 2.97 meq/g total titratable charges by Potentiometric titration (Sieliechi et al., 2008).

As for the modeled humic-like substance, it was obtained by polymerization between catechol and glycine according to Andreux procedure (Andreux et al., 1980). The synthesis, characterization and relevancy to natural humic substances were discussed by Jung et al. (2005b).



Figure II-2. Location of Sampling Site of Nyong River Cameroon.

One liter black water samples were collected in the Amazonas-Brazil at two different locations, *i.e.* Rio Jutai and Rio Negro (Figure. II-3). The dark colored waters were vacuum filtered at site through a Membranfilter porafil of 0.2 μ m porosity in order to remove the particles in suspension and the microorganisms, and were then preserved at about 4 °C in glass bottles wrapped in aluminum foil to reduce the breakdown and the degradation of organic matter prior to analysis.

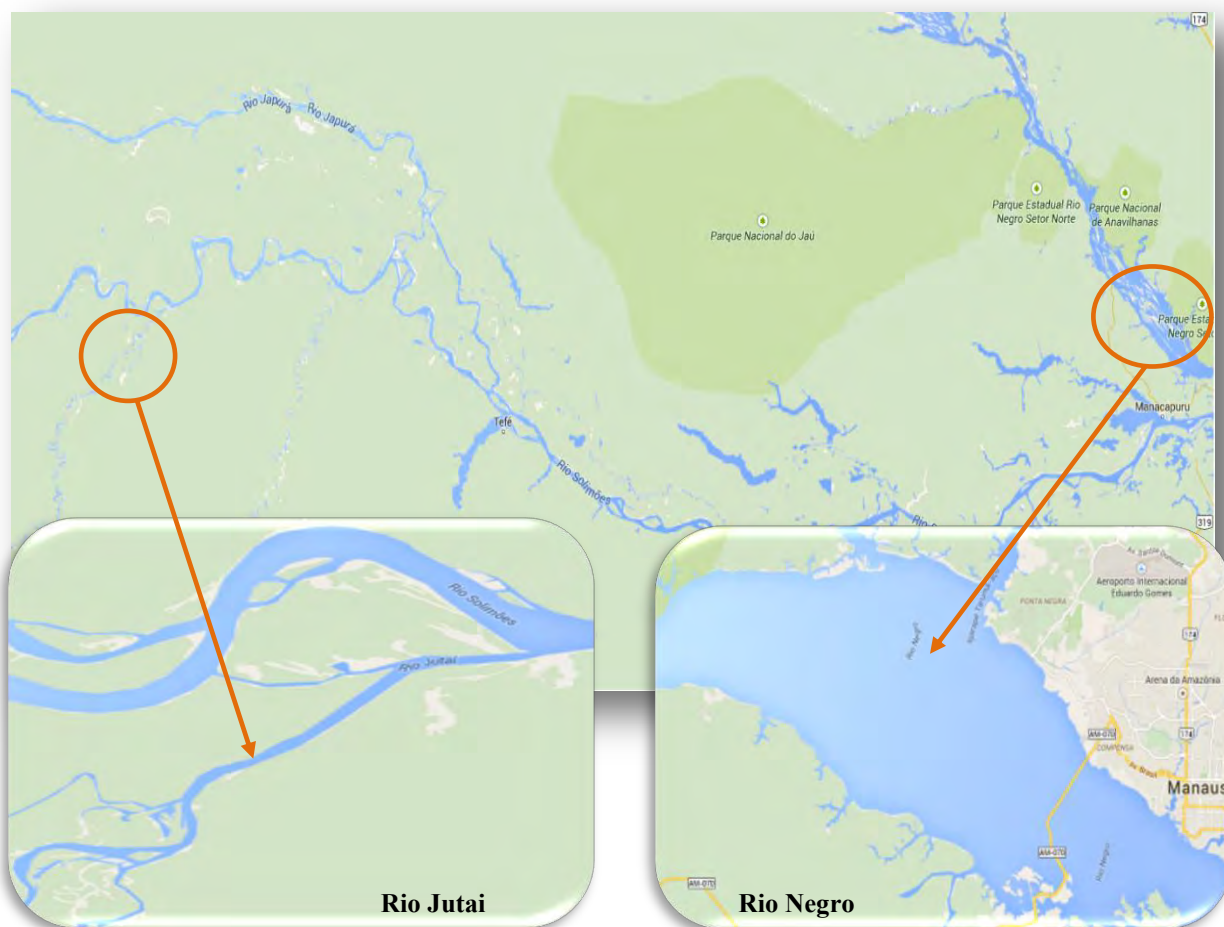


Figure II-3. Sampling Sites of black waters from the Amazonas-Brazil.

The concentration of the humic substance stock solutions (*i.e.* Suwannee River, Nyong and Modeled humic-like) was adapted to the technique of investigation used. For Turbidity, Dynamic Light Scattering (DLS), Surface Tension (ST), Electrophoretic Mobility (EM), UV/Vis Spectrophotometry and Fluorescence Spectroscopy measurements, humic substances concentrations of 0.001, 0.002 and 0.004 % w/w, *i.e.* 10, 20 and 40 mg/L respectively, were prepared by adding the appropriate mass into 500 ml of deionized water (Millipore, MilliQ 18.2 M Ω .cm) (figure II-4). For Cryogenic Transmission Electron

Microscopy (Cryo-TEM), a stock solution of 0.1 % w/w, i.e 1g/L, was freshly prepared 24 hours prior to sample analysis, whereas for Small Angle Neutron Scattering (SANS) experiments, 0.5% w/w (*i.e.* 5g/L) was dissolved in D₂O in order to minimize the incoherent background from hydrogen thus yielding a higher scattering contrast (Claesson et al. 2000 ; Aswal and Goyal 2002). All prepared stock solutions were used for two consecutive experimental days and then discarded in order to avoid any degradation of organic matter by microorganisms.

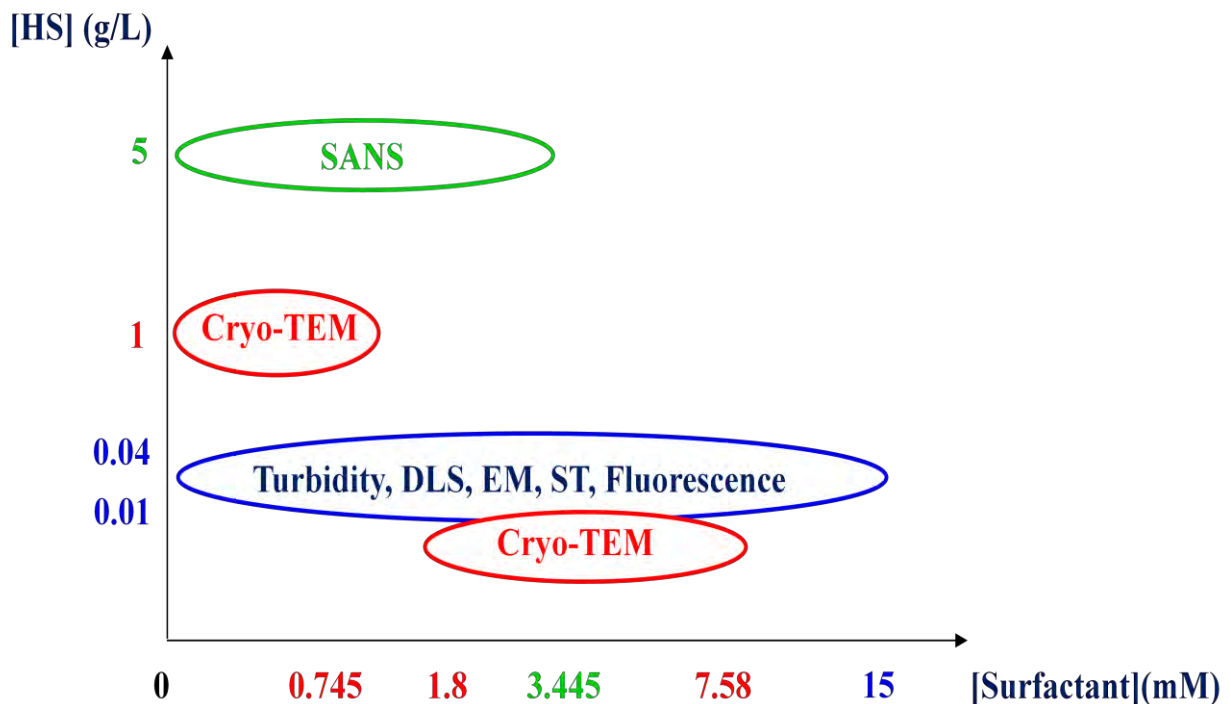


Figure II-4. The concentration of the humic substance stock solutions according to the technique of investigation used.

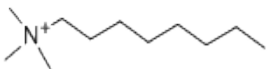


The prepared stock solutions were mechanically mixed in a 1 liter baffled reactor at 250 rpm overnight to ensure a well-dispersed suspension (Kazpard et al., 2006). The suspensions of humic acid and the Amazonas DOM were then vacuumed filtered through a membrane (Membranfilter porafil) of 0.2 μm porosity in order to remove any impurities. The DOC was checked for each prepared stock solution to ensure the consistency of preparation (Shimadzu TOC-Vcsn). When necessary, the pH of stock suspensions of the humic substances was modified from natural to neutral pH ($\text{pH}=7 \pm 0.05$) using sodium hydroxide stock solution prepared from NaOH pellets at 1N.

II.1-2 Surfactants

In this study, cationic surfactants of different alkyl chain length were used, purchased from Sigma-Aldrich; Octyltrimethyl ammonium chloride (purity $\geq 97\%$), Dodecyltrimethyl ammonium chloride (purity $\geq 99\%$) and Hexadecyltrimethyl ammonium chloride (purity $\geq 98\%$). The various properties of the surfactants are summarized in Table II-1 below. The CMCs indicated can vary depending on the purity of the surfactants and on the methods of determination (Aswal and Goyal, 2003 ; Magid et al., 2000 ; Burov et al., 2008). Deuterium oxide (D_2O 99.9 atom% in D) and Sodium hydroxide as pellets (purity $\geq 99.99\%$) were also acquired from Sigma-Aldrich. All purchased materials were used without any further purification.

The DTAC and CTAC stock solutions were prepared at 10 g/L and 200 mg/L respectively, by adding the appropriate mass of surfactant powder in 50 ml of deionized water (Millipore, MilliQ, and resistivity 18.2 M Ω .cm). In our study, we also used a concentration of 5 g/L of DTAC obtained by diluting the 10 g/L solution. For OTAC, three different concentrations were prepared at 10, 35 and 70 g/L.

Table II-1. Characteristics of the Various Cationic Surfactants Used.

Surfactant Description	Octyl Trimethyl Ammonium Chloride	Dodecyl Trimethyl Ammonium Chloride	Hexadecyl Trimethyl Ammonium Chloride (Cetyl Trimethyl Ammonium Chloride)
Symbol	OTAC	DTAC	HTAC/CTAC
Molecular Formula	C ₁₁ H ₂₆ ClN	C ₁₅ H ₃₄ ClN	C ₁₉ H ₄₂ ClN
Alkyl Chain	C ₈	C ₁₂	C ₁₆
Structural Formula			
Molar Mass (g/mol)	207.78	263.89	320
cmc (mmol/L)	250 (28 °C)	21.7(30 °C)	1.3 (30°C)
Krafft Temperature (°C)	< 0	< 0	18
Solubility (mg/L)	readily soluble	readily soluble	440
Reference	(Lindblom and Lindman, 1973 ; Rubingh and Holland, 1990 ; Łuczak et al., 2009)	(Laschewsky et al., 2005 ; Prévost et al., 2011 ; Perger and Bešter-Rogač, 2007)	(Tan et al., 2010 ; Singh and Hinze, 1982 ; Mata et al., 2005 ; Sakamoto et al., 2002 ; Karlstroem et al., 1990 ; Han et al., 2003)

II.2 PREPARATION OF HS/SURFACTANT COMPLEXES

The HS-DOM/Surfactants complexes were prepared by adding various aliquots of the concentrated surfactant solution to 10 mL (1 mL for Cryo-TEM and SANS) of the humic substance suspension and by submitting the mixture to gentle overhead agitation in order to homogenize the samples without causing the breakdown of the formed aggregates. Both Humic Substances and Surfactants stock solutions, as well as the HS/Surfactants complexes, were maintained at 30 °C in a heating bath during the experiments. The preparation procedures are summarized below (Figure. II-5).

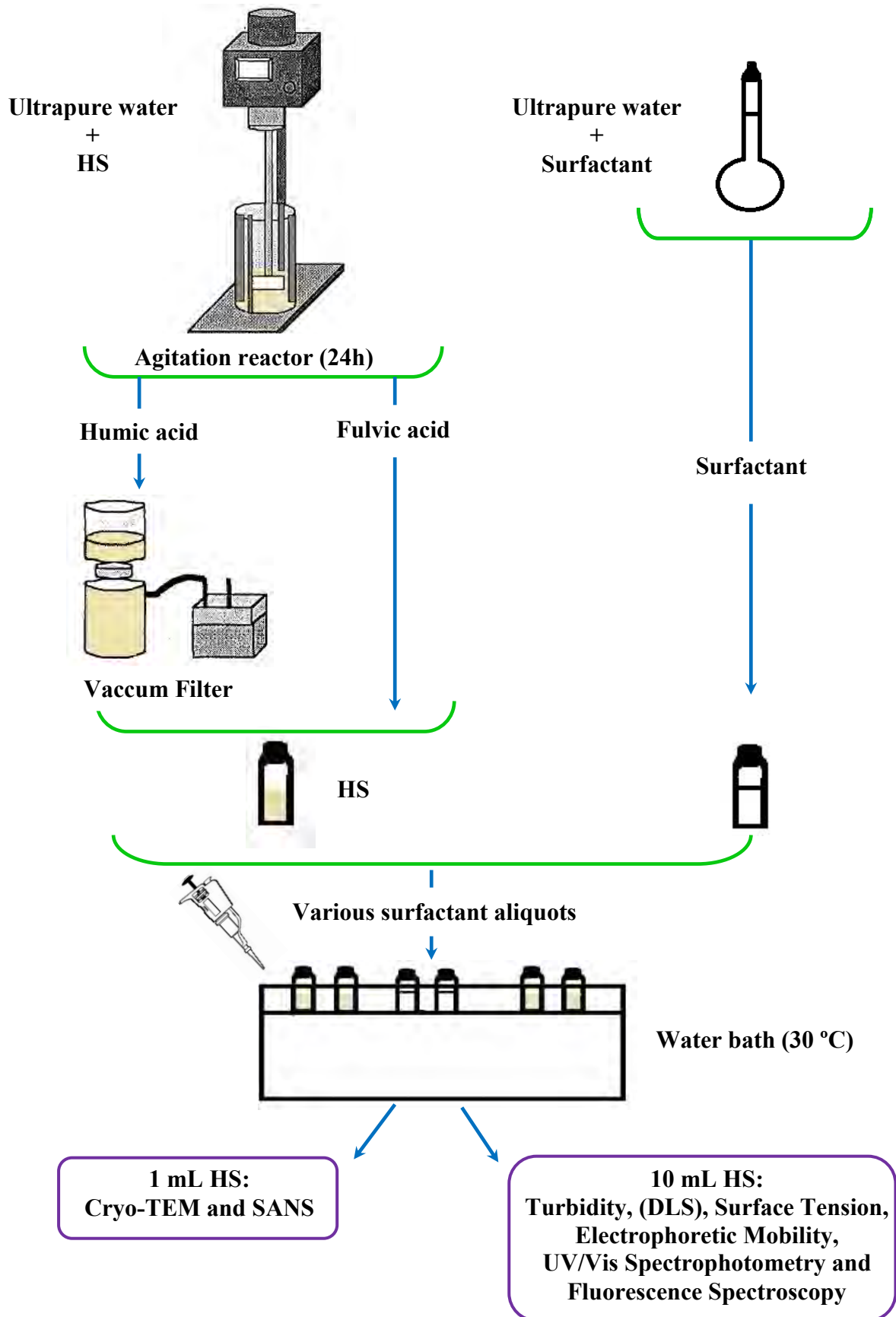


Figure II-5. The Procedures for Sample Preparation.

The pH and conductivity were measured using Multiparameter Multi 340i (WTW Multiline F/SET; SenTix 41 pH Electrode and Cellox 325 Conductivity Electrode). The calibration of the pH meter and conductivity were performed before each series of measurements. The pH meter was calibrated by two buffers, one at pH 7, and the other at pH 4 (Technical Buffer 50 ml) while the calibration of conductivity electrode was performed with a solution of potassium chloride standard of 0.01 mol/L.

II.3 METHODS OF CHARACTERIZATION

The turbidity of HS/Surfactant suspensions and the size of complexes were measured as a function of time. The pH and the conductivity, the surface tension, the electrophoretic mobility, UV/Vis and Fluorescence spectra were measured and acquired at the end of the experiment (after 1 h and/or 2 h).

II.3-1 Turbidity

The turbidity is defined by the standard DIN EN ISO 7027 as the reduction of transparency of a liquid due to undissolved material, such as colloidal particles and suspended solids. The presence of these substances in the liquid leads to the formation of a barrier to the transmittance of the incident light beam, giving rise to several optical phenomena such as diffusion, absorption, reflection or refraction of the incident light (Sadar, 1996). As a result, the principle of turbidimeter is based on the fact that an aqueous suspension is illuminated by an incident light flux and using a detector (a photocell) placed at a precise angle to the light source to capture the light beam scattered by suspended solids (Figure. II-6).

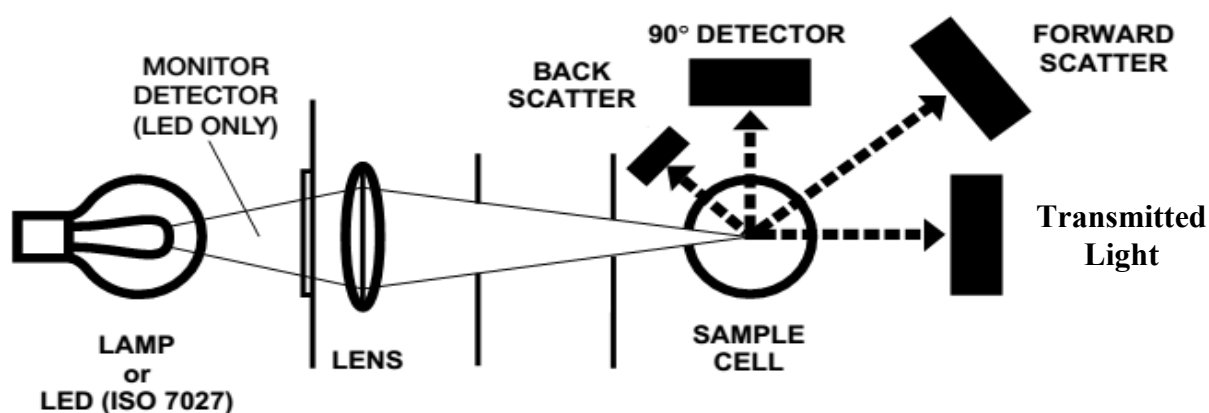


Figure II-6. Turbidimeter Principle and Optial Design of HACH LANGE 2100Q.

The turbidity of a suspension measured depends on the factors characterizing the suspended matter, such as size, shape, structure, refractive index and concentration, taking into account the wavelength of incident light that affects the intensity and pattern of the beam. Generally speaking, small particles produce symmetrical backward and forward scattering, whereas larger particles mainly give forward scattering interference (Figure. II-7).

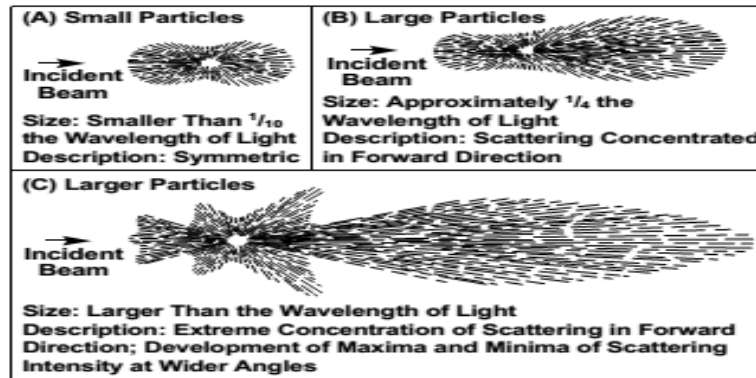


Figure II-7. Effect of Particle Sizes on the Scattering Pattern (Brumberger et al., 1968).

The turbidity is roughly proportional to the amount of colloidal particles in suspension because the higher the concentration, the higher the scattering of light. This phenomenon is described by a Beer-Lambert law which connects the turbidity light flux according to equation (2.1):

$$T = \frac{1}{L} \ln \frac{Q}{Q_0} \sim \frac{A}{L} \sim \epsilon c \quad (2.1)$$

Where T is the turbidity in (m^{-1}), L the average distance traveled by the optical beam in (m), Q the light power flux detected by the optical sensor in watts, Q_0 the luminosity of the incident flux in watts, A the measured absorbance, ϵ the molar absorptivity coefficient and c the analyte concentration.

Turbidity is an effective optical method that provides direct rapid assessment of the formation of aggregates and thus a rough measurement of interactions in our HS/Surfactants mixtures. In our study, a HACH LANGE 2100Q turbidimeter was used fitted with a tungsten filament lamp (2100Q) and a silicon photodiode detector that receives the light flux at 90° . The calibration was performed using three standard solutions: StablCal 20, 100 and 800 NTU. All the measurements are given in NTU (Nephelometric Turbidity Unit).

II.3-2 Dynamic Light Scattering

"Dynamic Light Scattering" (DLS) is a method that allows the measurement of the particle size in a diluted transparent liquid medium in a range from several nanometers to several micrometers; it also known as photon correlation spectroscopy. It analyzes the temporal fluctuations of the intensity of light scattered by suspended particles in Brownian motion (Pecora, 1985). A Light beam illuminates the sample; when photons penetrate the aqueous suspension, they interact with the particles of the medium resulting in a scattering phenomenon. The scattered photons produce a constructive interference pattern detected at a given angle of the source and obtained as peaks of intensity varying with time. The light transmission is consistent, in this case. However, Brownian motion controls the motion of suspended particles at a certain speed depending on their size and the viscosity of the medium, which modifies the constructive and destructive interference pattern, thus generating temporal fluctuations in the intensity of the scattered light (Figure. II-8).

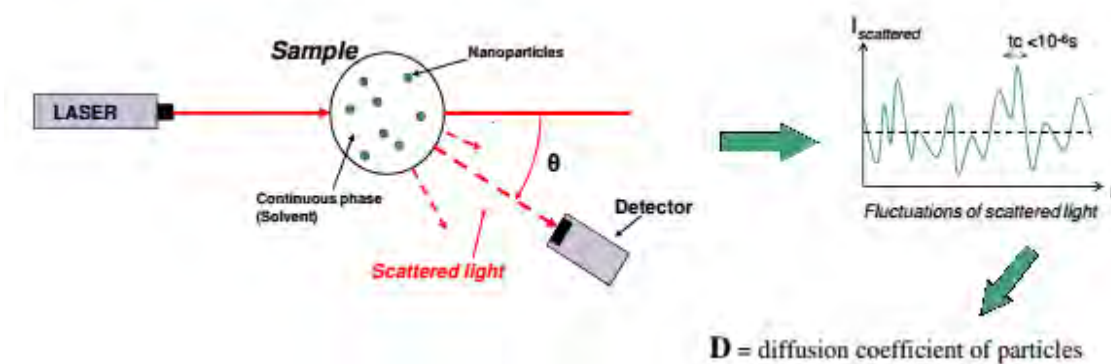


Figure II-8. Dynamic Light Scattering Setup (Maxit, Cordouan Technologies, 33400 Pessac, France).

The auto-correlation $G_2(T)$ of the scattered intensity with time is given by equation (2.2) (Pecora, 1985):

$$G_2(T) = \sum_{i=1}^{\infty} A_i e^{(-2D_i q^2 T)} \quad (2.2)$$

Where A_i is a constant, D_i is the Brownian diffusion coefficient of i^{th} particles, T is the time of decorrelation, and q is the wave vector given by the following equation (2.3):

$$q = \frac{4\pi m}{\lambda} \left(\sin \frac{\theta}{2} \right) \quad (2.3)$$

Where m is the refractive index, λ is the incident light wavelength, θ is the angle of detection. For monodisperse particles, this function decreases exponentially and according to

a characteristic time T_0 . The diffusion coefficient (D) is obtained directly from T_0 according to the equation (2.4) (Berne and Pecora, 2000):

$$D = (q^2 T_0)^{-1} \quad (2.4)$$

Knowing the diffusion coefficient, the hydrodynamic radius of spherical particles that are driven by Brownian motion is determined from the Stokes-Einstein relation (equation 2.5) (Einstein, 1956 ; Pecora, 1985):

$$r_h = \frac{K_b t^\circ}{6\pi\eta D} \quad (2.5)$$

Where t° is the absolute temperature in Kelvin (K), η is the viscosity of the medium, K_b is Boltzmann constant, and r_h is the hydrodynamic radius.

This technique, developed by Cordouan, has several drawbacks and limitations:

- the scattered photon detected should correspond to a single scattering, thus limiting the application to low concentrated particle suspensions especially for large particles with large refractive index,
- the particles motion should be only governed by Brownian motion, hence the presence of collisions or electrostatic interaction between charged particles interfere with the analysis,
- Particles under analysis should be isotropic, *i.e.* the scattering is independent of their orientation in solution (angular independence), and this property can be linked to small spherical shape, while other shape particles will exhibit anisotropy. In such case, using a fixed single angle DLS is very challenging.

DLS allows the possibility to highlight the structures identified in turbidity, determining the sizes and polydispersity of particles in a liquid medium. In this study, a "VASCO Particle Size Analyzer, Cordouan Technologies" and a "Malvern Zetasizer NANO ZS (ZEN 3600)" were used, with a single fixed detection angle; 135° and 170° respectively. The viscosity of the medium was maintained at 0.797 mPa.s⁻¹, the real part of the refractive index for organic particles was set at 1.4 (the HS/surfactant complex is equating to an oil emulsion) for a medium having a refractive index equal to 1.33, the imaginary part (material absorption, *i.e.* humic Substances) was set at 0.01 and the temperature at 30 °C. The Pade-Laplace algorithm and Cumulants analysis (ISO 13321 and ISO 22412) were used to analyze

the signal from the autocorrelation function in the case of polydisperse suspensions for Cordouan and Malvern respectively.

II.3-3 Surface Tension

The ability of a liquid surface to oppose external effects through their contractive ability, *i.e.* the cohesion attraction between liquid molecules, is known as surface tension. Its assessment reveals structural and conformational changes through the self-assembling and formation of micelle-like aggregation of amphiphilic molecules as well as the effect of various conditions such as concentration of metal ions, pH, ionic strength (Rauen et al., 2002, 2006). The plateau formation when surface tension is plotted versus concentration identifies cmc.

The surface tension was obtained with KRUSS K12 Processor Tensiometer using the Wilhelmy plate method, which is based on the force exerted on the plate due to wetting. The platinum plate of 19.9 mm length “ L ” vertically suspended touches a liquid surface or interface, then a force “ F ”, which correlates with the surface tension “ σ ” and with the contact angle “ θ ” (knowing that $\theta=0$), acts on this plate (Figure. II-9). The surface tension is then calculated according to equation (2.6):

$$\sigma \cos \theta = \frac{F}{L_w} \quad (2.6)$$

Where L_w is the wetted length, noting that we have two wetted lengths, hence $L_w = 2L$, and $\cos \theta = 1$

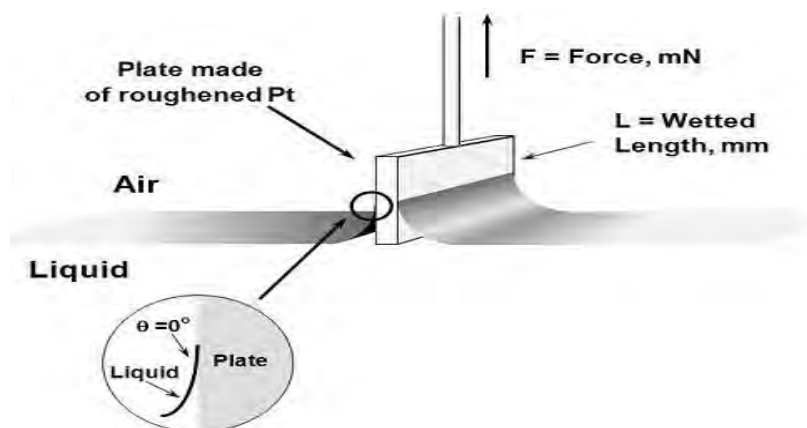


Figure II-9. Surface Tension assessment using Wilhelmy plate method.

II.3-4 Electrophoretic Mobility and Zeta Potential

The surface of suspended charged particles attracts counter ions of opposite charge forming what is called an electrical double layer. This layer is composed of two regions; an inner region called the Stern layer where the counter ions are strongly bound, and an outer layer with loosely attracted counter ions called the diffuse layer. The ions within this layer move with the particle movement, but there exist a boundary within the diffuse layer beyond which the ions do not follow the particle movement; this boundary is called the slipping plane. At the slipping plane, the potential measured is referred as Zeta Potential. The variation of ionic strength and pH may strongly influence the zeta potential measurement. Experimentally, the zeta potential is calculated from the electrophoretic mobility of particles. Such calculation is based on an appropriate model of the surface charge using Henry's equation (O'Brien and Hunter, 1981 ; Ohshima, 1995). As we cannot be sure that this model applies to the variety of self-assemblies encountered in our study, it was decided to use the experimental measurement of electrophoretic mobility to assess the surface charge (Duval et al., 2005).

The Electrophoretic mobility of a particle moving in a liquid under the action of an applied dc electric field (Figure II-10) can be determined experimentally from the migration time and the field strength according to equation (2.7 and 2.8) (Moraes and Rezende, 2008 ; Skoog et al., 1980):

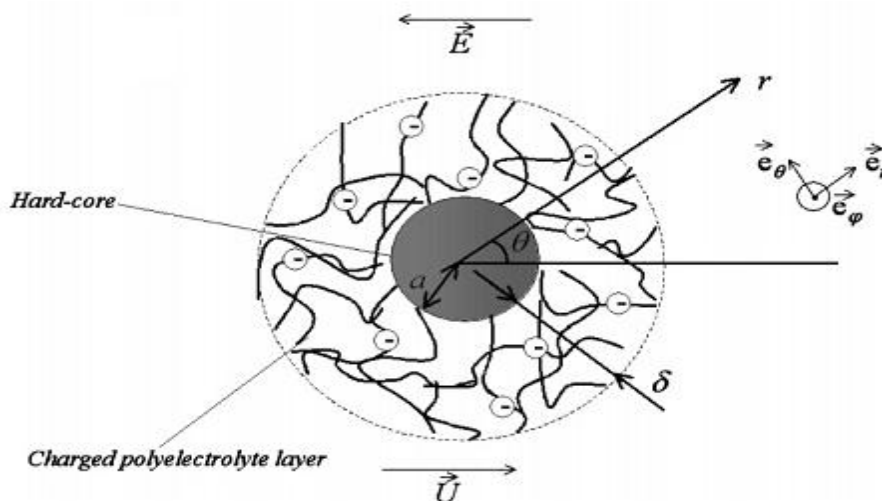


Figure II-10. Schematic representation for a diffuse soft particle, composed of a spherical hard-core and a permeable charged polyelectrolyte layer, moving with a velocity, “ U ”, in an electrolyte subject to a “dc” electric field, “ E ”. For humic substances, $a=0$, and the mode corresponds to that of a spherical polyelectrolyte (Duval et al., 2005).

$$\mu = \frac{U}{E} \quad (2.7)$$

$$\mu = \frac{(\Delta x / t)}{(V/l)} \quad (2.8)$$

where “ μ ” is the Electrophoretic mobility, “ U ” is the velocity, “ E ” is the electric field strength, “ Δx ” is the length from the capillary inlet to the detector, “ l ” is the total length of the capillary, “ V ” is the applied voltage and “ t ” is the time required for the analyte to reach the detection point (migration time).

The velocity of the moving particles is measured using Laser Doppler Velocimetry (LDV). The measurement is done at the stationary layer in order to avoid the electroosmosis effect (*i.e.* zero electroosmosis) that is created by the surface charge of the capillary cell wall that will superimpose their velocity; to counterbalance this effect, an opposite flow at the capillary center is applied (Figure. II-11).

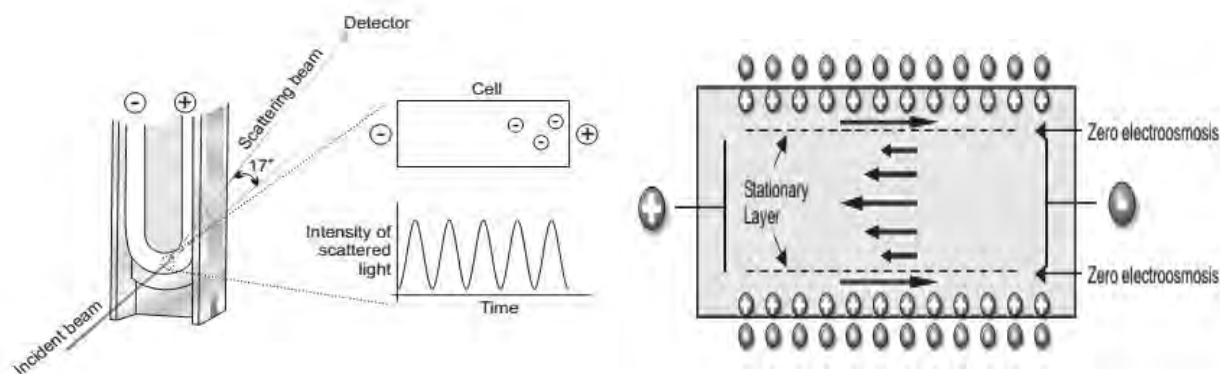


Figure II-11. LDV Principle (left) and Electroosmosis Effect (right).

A folded Capillary cell (DTS 1060) is used to carry out the electrophoresis experiment, by applying an electric field through the solution that contains electrolytes; the charged particles will be attracted to oppositely charged electrode (Figure. II-12).

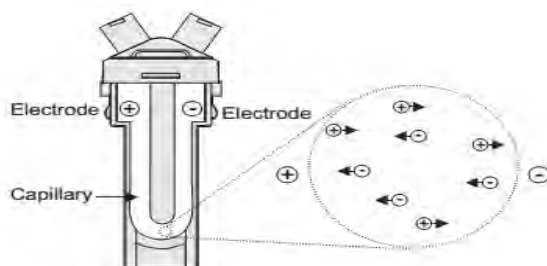


Figure II-12. Electrophoretic Movement of Electrolytes.

Malvern Zetasizer NANO ZS (ZEN 3600) was used for measuring the electrophoretic mobility of the complex HS/Surfactant. During analysis, the viscosity was set at 0.792 mPa/s, the refractive index equal to 1.33, the dispersant dielectric constant at 76.8 and the temperature at 30 °C.

II.3-5 Cryogenic Transmission Electron Microscopy (Cryo-TEM)

The transmission electron microscope (TEM) is an imaging technique which that allows a better understanding of the structures at the nanoscale with a resolution up to 1nm. In our study, before performing the TEM observations, the samples are rapidly freeze (within milliseconds) in liquid ethane maintained at -185 °C, using a fast automatic vitrification system “Leica EM GP”. This technique is designed to keep the samples in their original condition at the time of preparation and to prevent any possible molecular rearrangements preceding the analysis.

II.3-5-1 Sample Preparation for Cryo-TEM Observation

An aliquot of the sample is placed on a LACEY/CARBON FILM grid that was previously ionized or glow discharged to render it more hydrophilic, thus improving their adhesive property toward the solution, as well as allowing a uniform distribution across the grid and ensuring that the grid is properly cleaned (Figure. II-13) (Dobro et al., 2010).

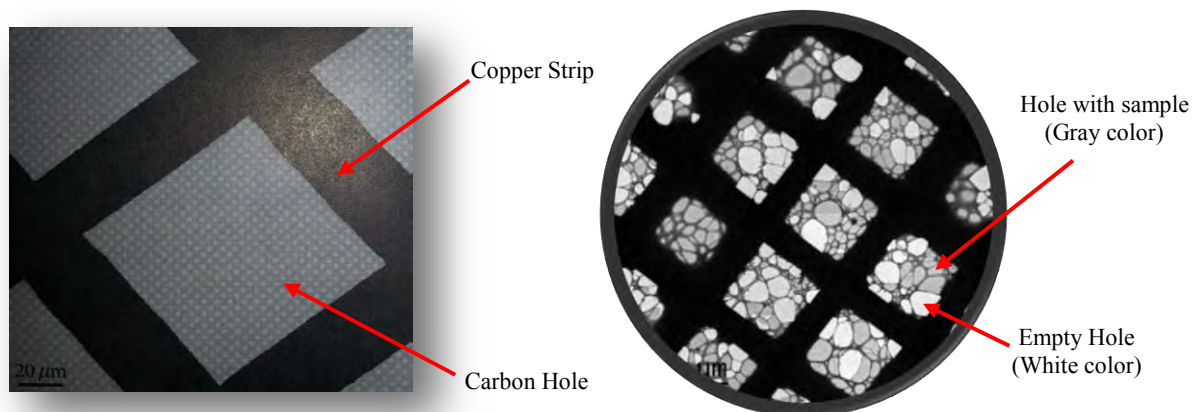


Figure II-13. LACEY/CARBON FILM Grid Showing the Carbon Holes (Left) and Sample Distribution within the Holes (Right).

The grid is attached to a forceps fixed to a clamp in the vitrification system. Before starting to freeze our samples, the Leica EM GP setting is adjusted to control various experimental condition such as the temperature and humidity in which the sample should be just before freezing and the closed chamber facilitates the ability to regulate and maintain them (Figure. II-14).

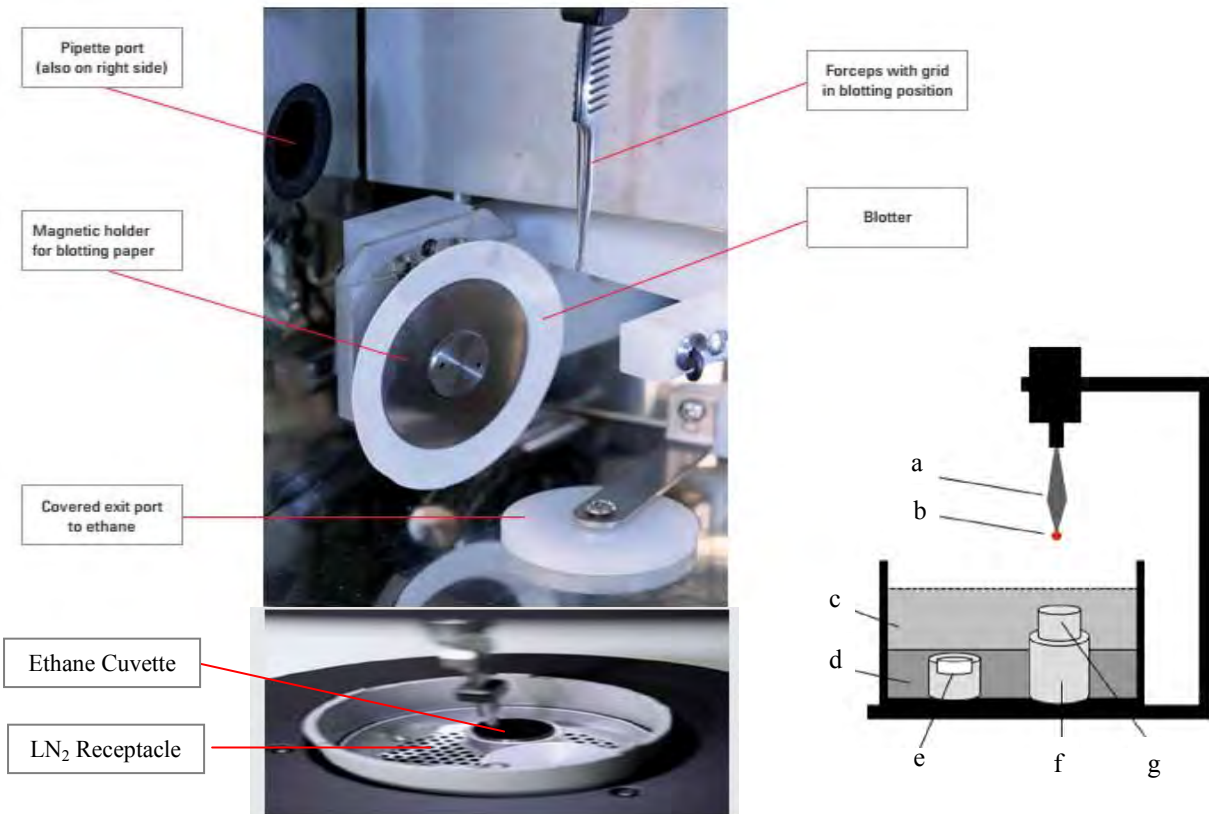


Figure II-14. Vitrification System, Photograph (left) and Scheme (right). (a): Forceps, (b): Grid, (c): N-vapour, (d): LN₂, (e): Support and Grid Receptacle, (f): Support, (g): Liquid Ethane Cuvette.

The sample is then subjected to blotting to remove the excess of added volume leaving a thin layer on the grid (Gan et al., 2008) and immediately plunged into liquid ethane at $-185\text{ }^{\circ}\text{C}$ and then stored in liquid nitrogen (LN₂). The rapid freezing preserves the sample in vitreous condition rather than crystalline ice that can produce artifacts and interact inelastically with the electrons (Cavalier et al., 2008). During freezing, liquid ethane is placed in a tank positioned near a receptacle of grids carrier, itself maintained in liquid nitrogen at all times. Indeed, the use of liquid nitrogen is designed to keep ethane in the liquid state and to prevent its evaporation. The preparation procedure is illustrated in Figure. II-15.

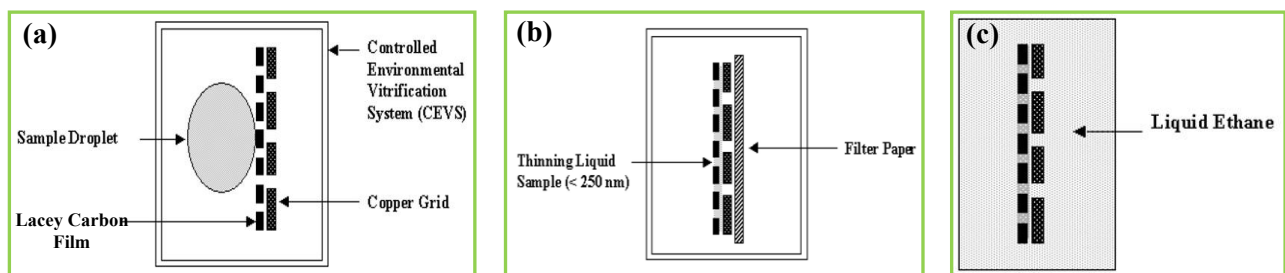


Figure II-15. Cryo-TEM Sample Preparation Procedures. (a): Liquid Sample on the Grid, (b): Thinning by Blotting, (c): Rapid Vitrification (Won, 2004).

II.3-5-2 Cryo-TEM Imaging Procedure

The prepared grid is then transferred to the electron microscope grid holder; in order to prevent any melting of the vitrified sample and formation of ice crystals, the holder is continuously cooled down using liquid nitrogen. High energy (*i.e.* 200Kev) Transmission Electron Microscopy is used and images were recorded by CCD (charged coupled device) camera (Figure. II-16) (Frank, 1996).

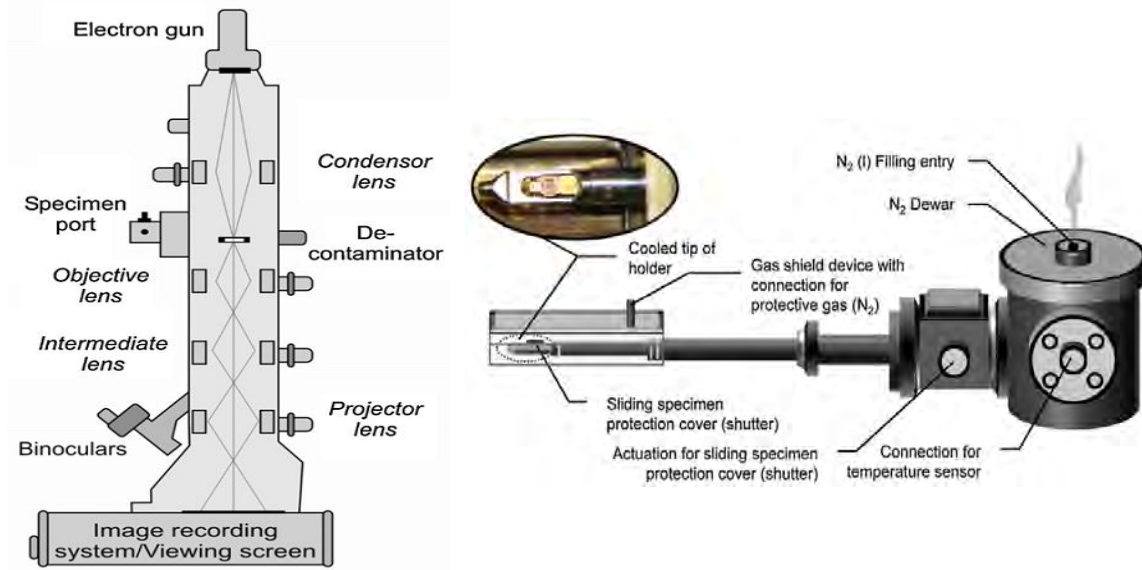


Figure II-16. Illustration of Transmission Electron Microscopy (left) and Grid's Holder (right) (Kuntsche et al., 2011).

The frozen thin layer that persists after blotting is illustrated in Figure. II-17, where we can find unequal size segregation as a result of non-uniform film thickness; large sized particles are found at the thicker edge of the film close to the copper grid, while the smaller particles remain at the thinner middle part. The size distributions are then certainly biased because the large aggregates may be drained away during the blotting step of sample preparation (Jores et al., 2004 ; Lee et al., 2012),



Figure II-17. Particles Size Segregation according to Carbon Film Thickness (Klang et al., 2012).

The transmission electron microscope (TEM) allows the assessment of colloidal size, shape, structure and the identification of aggregates including the presence of supramolecular structures. In the following study, the Cryo-TEM observations were carried out at the Multiscale Electron Imaging (METI) platform at the University of Toulouse, with the precious help of Dr. Celia Plisson-Chastang, using a *JEOL 2100 Lab6* transmission electron microscope equipped with a *Cryo-Gatan 626* electron microscope grid holder. Images were recorded with *Gatan ultrascan1000* and *Gatan ultrascan4000* CCD camera system run by Gatan Digital Micrograph and Serial-EM imaging software respectively, under low dose conditions (about 10 electrons per Å²). 4 µl of HS/Surfactant suspension was deposited onto a LACEY/CARBON FILM grid previously ionized using PELCO-easiGlow 91000TM glow discharging-cleaning system. After blotting for 0.2-0.8 seconds (depending on the initial experiment and preparation condition), to remove the excess of added volume using *Leica* EM-GP controlled vitrification system at 30 °C and 85% relative humidity, the grid was immediately plunged into liquid ethane and stored in liquid nitrogen.

The size distribution of HS/Surfactant complexes was obtained by counting the aggregates in logarithmically spaced size bins such that $d_{i+1} = 2^{1/3} d_i$, which yields equally spaced size intervals on a x-axis log scale (Frappier et al., 2010). The mean aggregate size D was calculated according to equation (2.9):

$$D = \frac{\sum_{i=1}^{i=k} n_i D_i}{\sum_{i=1}^{i=k} n_i} \quad (2.9)$$

With n_i the number of aggregates measured in the range i , D_i the middle of class range, and k the total number of bins.

II.3-6 Small Angle Neutron Scattering (SANS)

Small Angle Scattering (SANS and SAXS) is a key-technique in the study of size, shape and conformation of molecular assemblies in suspension (Liu, 2011 ; Kawahigashi et al., 1995 ; Feigin et al., 1987). It is complementary to Cryo-TEM, which provides the opportunity to study, with a high level of resolution, the samples in their natural condition (in solution) where the drying process could deform the object under study (Jacrot, 1976 ; Henderson and Unwin, 1975).

The horizontal cold source of the reactor (H512) produces the white neutron beam, which passes through neutron velocity selector (DORNIER or ASTRUM) where it undergoes monochromation (*i.e.* producing monochromatic neutron beam). Then, this beam enters a collimator in order to focus the beam and reduce its divergence. An aperture B_4C/Cd made of Boron Carbide (B_4C) and Cadmium (Cd) in front of the sample is used to fix the beam size. The neutron beam, of incident wave vector " k_i ", interacts elastically with the sample and is scattered at an angle 2θ , with a final wave vector " k_f ", which is collected on a detector. An absorbing aperture of B_4C/Cd plays a role of a beam stop suited prior the detector to avoid the damaging of the detector by the direct beam (Figure. II-18) (Svergun and Koch, 2003 ; King, 1999 ; H g lund et al., 2012).

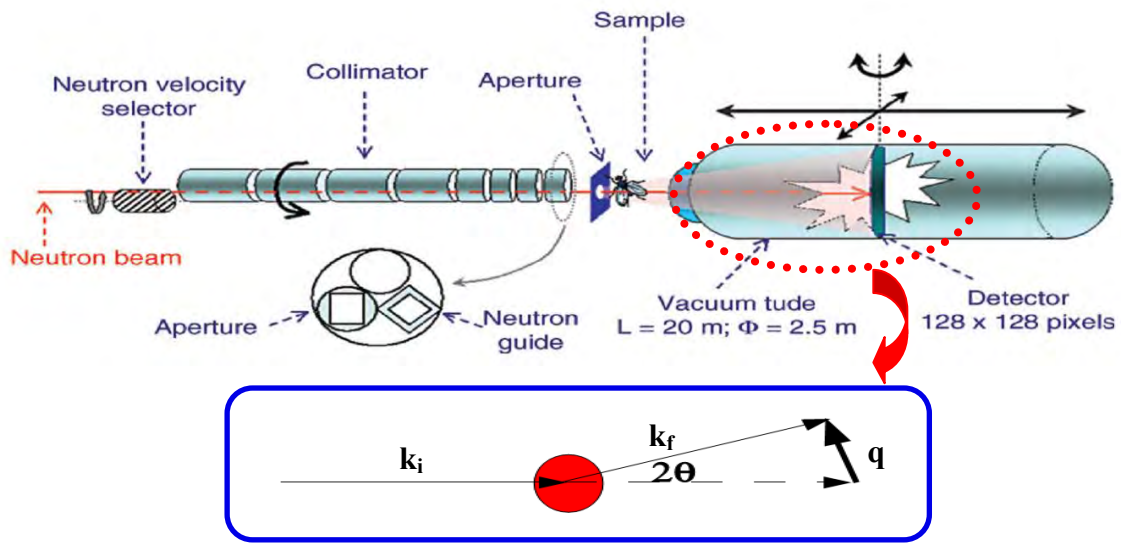


Figure II-18. Illustration of D22 SANS at the Institut Laue Langevin, Grenoble (Upper image) and the Scattering Vector (lower image) (Grillo, 2008).

The scattering vector " q " is given by the following equation (2.10):

$$\mathbf{q} = \mathbf{k}_f - \mathbf{k}_i = \frac{4\pi}{\lambda} \text{Sin}\left(\frac{\theta}{2}\right) \quad (2.10)$$

If a substitution is done to Bragg's law of diffraction, an expression of the aggregate radius " r " can be estimated (King, 1999 ; Grillo, 2008):

$$\lambda = 2r \text{Sin}\left(\frac{\theta}{2}\right) \quad (2.11)$$

$$r = \frac{2\pi}{q} \quad (2.12)$$

where “ λ ” is the wavelength of the X-ray. This simple relation links the lengths in direct and reciprocal spaces and allows one to define the observation window during the experiment.

A typical graphic representation of a scattering curve in the form of double-logarithmic plot of $I(Q)$ versus Q is shown in Figure. II-19. In the ideal case, the range of Q studied, hence the window of observation, should include all the possible sizes of particles (smallest and largest) in the investigated sample:

$$\frac{2\pi}{q_{max}} \leq r \leq \frac{2\pi}{q_{min}}$$

Each region provides some different information due to the different observation windows. At the Guinier part (low q -domain and large observation window), the particle size can be obtained (correlation length) as well as the structure and their interactions. In the absence of a well-defined Guinier region, a lower limit size can be estimated using $R=2\pi/Q_{min}$. The intermediate q -region reflects the fractal properties of aggregates; the porod region measures the dimensionality of interface, while the Bragg region (high q -domain and small observation window) provides the correlations at the atomic level (Figure. II-19).

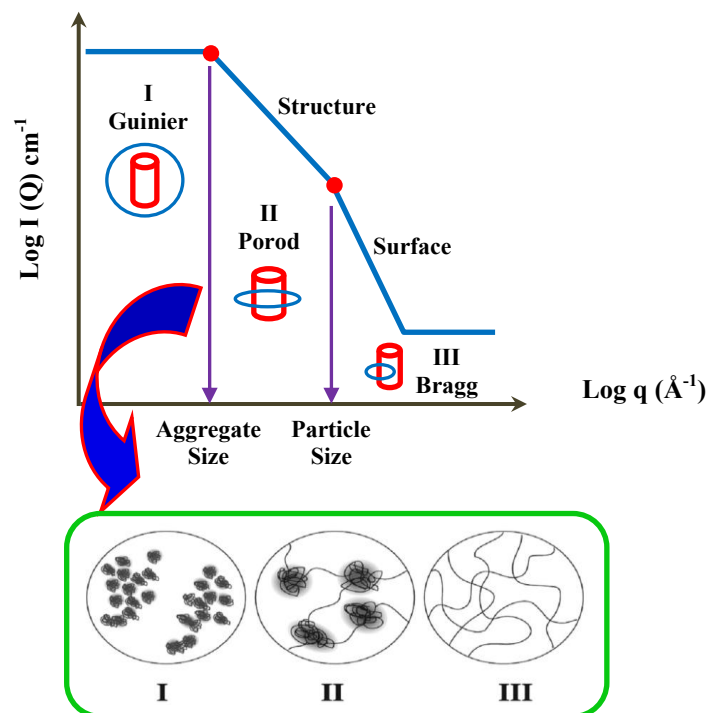


Figure II-19. A Typical Scattering Curve (upper image) and the Structures Identify from Different Region (lower image). I: low- q ; II: Intermediate- q and III: High- q region (Nasimova et al., 2004).

Our SANS experiments were carried out at the D22 SANS instrument at Institut Laue-Langevin (ILL), Grenoble, France with the valuable help of Dr. Bruno DEME. The samples were studied using incident neutron wavelength of 8 Å with three sample-to-detector distances (1.1, 5.6, and 17.6 m) used to cover the range of scattering vector from 0.001 to 0.6 Å⁻¹. The samples were kept in quartz cells (Hellma) with a path length of 2 mm for samples in D₂O and maintained at 25 °C. The raw spectra were corrected for background scattering from the sample transmission, empty sample cell (EC), detector efficiency (B₄C/Cd) and any other sources, then normalized by the corresponding corrected H₂O spectra (May et al., 1982) to produce the Q dependence of the intensity for each sample according to the equation (2.13) below (Tucker et al., 2008 ; Claesson et al., 2000):

$$\left(\frac{d\Sigma}{d\Omega}\right)_{\text{sample}} = \frac{1}{F_{sc}} \left(\frac{d\Sigma}{d\Omega}\right)_{\text{H}_2\text{O}}^{\text{real}} \frac{\left[\frac{I_{\text{sample}} - I_{\text{B4C}}}{Tr_{\text{sample}}} - \frac{I_{\text{sample-EC}} - I_{\text{B4C}}}{Tr_{\text{sample-EC}}}\right] \frac{1}{e_{\text{sample}}}}{\left[\frac{I_{\text{H}_2\text{O}} - I_{\text{B4C}}}{Tr_{\text{H}_2\text{O}}} - \frac{I_{\text{H}_2\text{O-EC}} - I_{\text{B4C}}}{Tr_{\text{H}_2\text{O-EC}}}\right] \frac{1}{e_{\text{H}_2\text{O}}}} \quad (2.13)$$

Data analysis benefitted from SasView software (DANSE/SANSview 2.1.0), originally developed by the DANSE project under NSF award DMR-0520547 ([SasView](http://www.sasview.org/), <http://www.sasview.org/>).

II.3-7 Ultraviolet/Visible Spectrophotometer

UV/Vis spectrophotometry is a rapid non-destructive assessment technique of chemical components. It is based on the absorption of Ultraviolet (180-400 nm) and visible (400-800 nm) radiation by organic compound, due to the presence of chromophoric groups. The functional groups interact with the photons, leading to electronic transitions, *i.e.* promotion of electrons from the ground state to a higher energy state. The setup is illustration below in Figure. II-20.

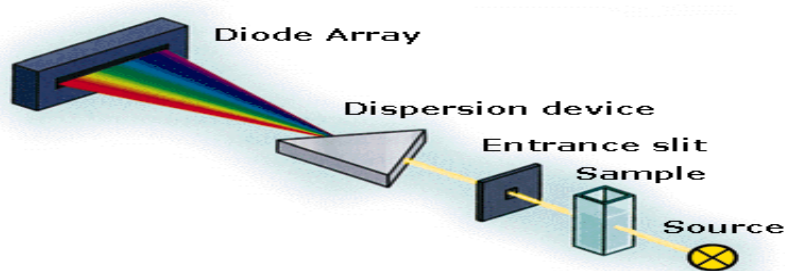


Figure II-20. Schematic Representation of UV/Vis Spectrophotometry.

Electronic transitions occur within the chromophoric orbitals, $\pi - \pi^*$, $n - \pi^*$ and $n - n^*$, where π and n are the bonding orbital in unsaturated bonds and non-bonding orbitals respectively and π^* and n^* are antibonding orbitals (Figure. II-21) (Hayes, 1989).

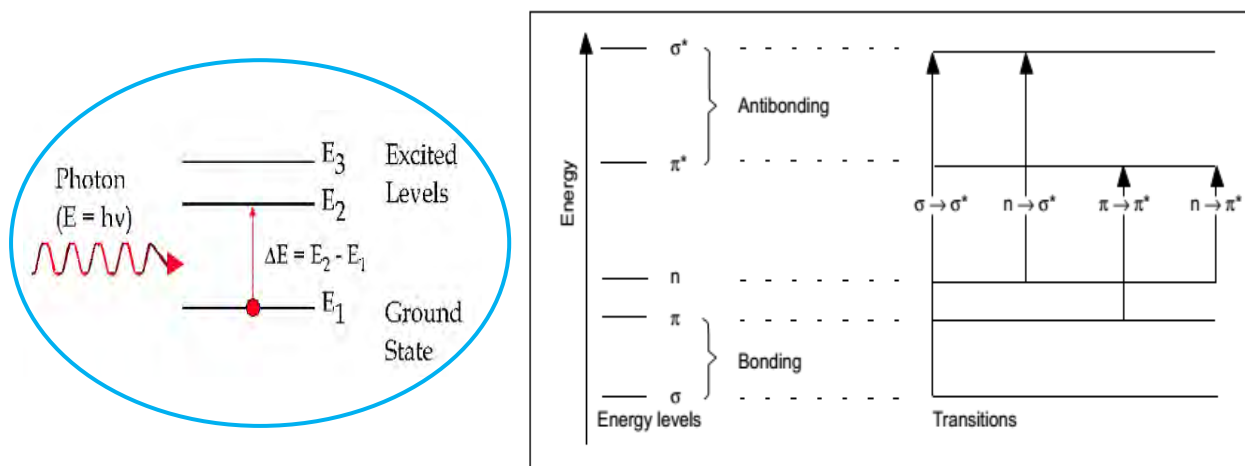


Figure II-21. Electromagnetic Wave Absorption (left) and Various Electronic Transitions (right).

The spectra in the UV/visible range give the transmittance or absorbance of the analyzed sample as a function of radiation wavelength (sometimes wavenumber). Absorbance (linearly related to the concentration) is frequently used, and it is inversely proportional to transmittance (Primer, 1996 ; Albani, 2008) (Figure. II-22):

$$A = \log \frac{I_0}{I} = \log \frac{1}{T} \quad (2.14)$$

The two main important parameters that can be determined are the maximum absorption wavelengths " λ_{max} " and the absorptivity (ϵ) at λ_{max} estimated from a Beer-Lambert law providing a semi-quantitative test of identity (Primer, 1996 ; Perkampus, 2013). This law gives a relationship between absorbance " A " and concentration " c " of the chemical species in solution. The expression of the Beer-Lambert law is given by equation (2.15):

$$A = \epsilon_{\lambda} c l \quad (2.15)$$

Where A is the Absorbance, ϵ_{λ} the molar absorptivity or molar extinction coefficient in ($L \cdot mol^{-1} \cdot cm^{-1}$), c the concentration of the absorbing species in (mol/L) and l the path length of the cuvette in (cm^{-1}).

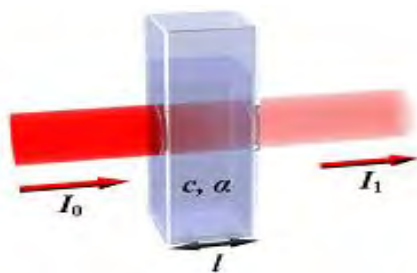


Figure II-22. Transmittance and Variation of Light Intensity through a solution.

In our study, 8452A DIODE ARRAY SPECTROPHOTOMETER (HEWLETT PACKARD), a single-beam microprocessor-controlled spectrophotometer, was used to measure the optical density (OD) or absorbance of different chromophoric components of the humic substances and the variation of the absorbance upon addition of the surfactant and formation of HS/Surfactant complex in UV/visible range of 190 to 820 nm with 2 nm resolution. When the OD of the humic substance was measured, deionized water (Millipore, MilliQ, and 18.2M Ω .cm) was set as the absorption reference, whereas for the HS/Surfactant complex, HS was set as the reference, so that any change can be related to the surfactant addition and the modification upon molecular rearrangement to the formation of HS/Surfactant complex. Spectral measurements were made in quartz cuvettes with 1 cm optical path length and 5 ml volume.

II.3-8 Fluorescence Spectroscopy

Fluorescence is a sensitive technique generally applied to the study of selective chromophores that fluoresces efficiently (Wolfbeis, 2012). It provides insights into the molecular and structural rearrangements that result from the interactions between the sample and electromagnetic waves. The fluorescence process can be decomposed in three steps.

An electromagnetic wave provided from an incandescent lamp or a laser interacts with a molecule that absorbs this photon of specific energy $E_{ex}=h\nu_{ex}=hc/\lambda_{ex}$. If the energy is sufficient, it can promote a change of the electronic state from the ground state S_0 to a higher excited electronic level ($S_1, S_2 \dots S_n$). The excited electron can either lose the absorbed energy without emitting any radiation through internal conversion (IC) and collision, which is known as non-radiative relaxation or it can return to S_0 through the emission of an electromagnetic wave ($E_{em}=h\nu_{em}=hc/\lambda_{em}$) corresponding to the energy difference between S_0 and S_1 ; this phenomenon is called fluorescence. Due to the energy loss by IC, the emission

energy is lower and the wavelength is longer than the excitation wavelength of the excitation photon (Lakowicz, 2010 ; Mondal and Diaspro, 2013). This difference causes a shift of the wavelength maximum referred to as "Stokes shift" ($\Delta\lambda_{\text{Stokes}}$) (Figure. II-23):

$$\Delta\lambda_{\text{Stokes}} = \lambda_{\text{max. em}} - \lambda_{\text{max. ex}} \quad (2.16)$$

Where " E " is the energy of the photon, " h " the Planck's constant (6.626×10^{-34} J/s), " ν " the frequency, " c " the speed of light in a vacuum (3×10^8 m/s), " λ " the wavelength (m), the indices " ex " and " em " correspond to excitation and emission photons, respectively.

Therefore, a molecule or chemical group able to absorb the photon energy and then to emit another electromagnetic wave in the range of the visible spectrum, is called a fluorophore (mainly polyaromatic hydrocarbons or heterocycles).

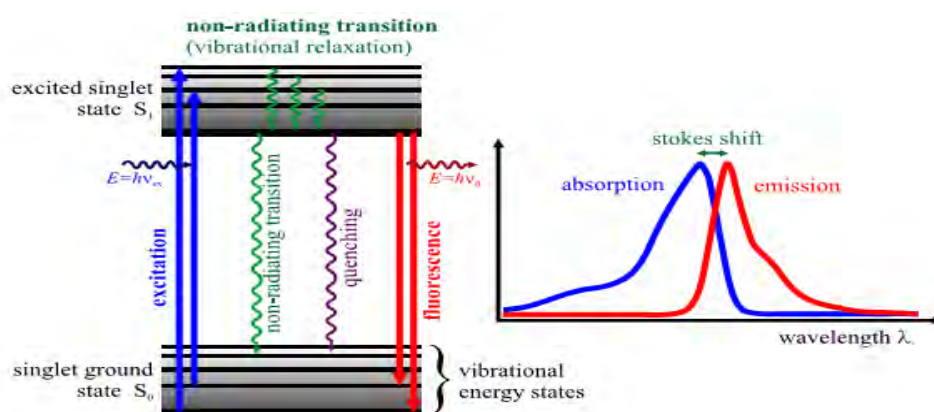


Figure II-23. Jablonski diagram illustrating the Various Processes during Electronic Excited State Formation (left) and the Stokes Shift (right).

Unlike UV/visible absorption, the intrinsic fluorescence for HS contains information about the structure, the nature of functional groups, the conformation, and the heterogeneity, as well as the dynamic properties related to their intramolecular and intermolecular interactions (Mobed et al., 1996). This provides additional information regarding the structures and the condensation of HS such as the relative presence of aromatic amino acid-like, fulvic-like and humic-like fluorescent compounds within a bulk HS (Baker, 2002a).

The emission Fluorescence Spectra were measured with Photon Technology International (PTI, QuantaMaster 30 Plus) equipped with a high power Xenon flash lamp as the light source (Figure. II-24). The emission spectra were recorded with a Slits width set at 5nm band-pass for both excitation and emission monochromators. The Gain was set at 1.5 and various excitation wavelengths of 230, 264, 350, 380 and 400 nm were used. The choice of excitation wavelengths was based on various spectra reported in the literatures about DOM fluorescence, as well as depending on the absorbance (OD) recorded previously by the UV/Visible Absorbance Spectra. A UV-Filter was used for the excitation wavelength at 264 nm to avoid the unharmony double excitation peak (situated around twice the excitation wavelength “2nd order Rayleigh”). The temperature was regulated at 30°C by a thermostat. Each aliquot was exposed to a single excitation wavelength; the cuvette was then cleaned for the next wavelength in-order to avoid any photo-bleaching (Hur et al., 2011), where irradiation probably leads to the removal of HS absorbing components, the production of non-absorbing compounds and oxidation interferences in the recorded intensities or the spectra band position.

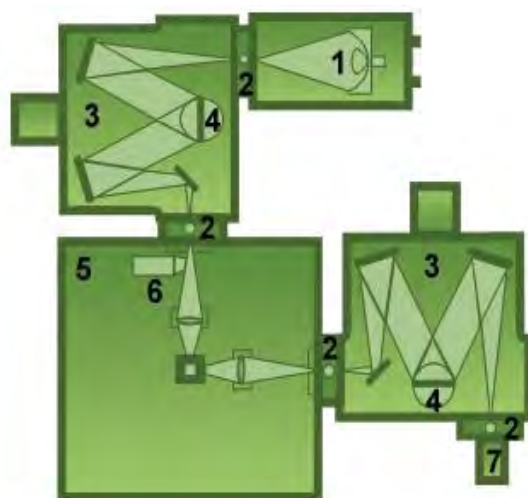


Figure II-24. Schematic Representation of PTI "Quanta-Master 30 Plus" Fluorescence Spectroscopy. (1) Light Source, (2) Adjustable slits, (3) Excitation and emission monochromator, (4) Excitation and emission grating, (5) Sample compartment, (6) Excitation and Lamp Intensity Fluctuation correction, (7) Detector.

CHAPTER

(III)

*Spontaneous Vesicles in the Suwannee
River Fulvic Acid/DTAC System:
Implications for the Supramolecular
Organization of Humic Substances*

III.1 PREFACE

The literature shows a harsh debate about the structural organization of humic nanocolloids, and surprisingly, it is not yet possible to decide between an arrangement of matter in the form of polymers (Macromolecule) more or less connected, or associations of small supramolecular molecules.

In this chapter, we are interested in identifying the structural concept that is appropriate to describe the organization of fulvic acid extracted from the Suwannee River (SRFA). For this, we will look at the reformation induced by the combination of SRFA with a cationic surfactant molecule (Dodecyl-trimethylammonium chloride (DTAC)). Two types of characterizations are to be implemented: first, the study of associations, SRFA /DTAC suspension, by turbidity, conductivity, surface tension, electrophoretic mobility and light scattering, so as to define the various reorganization stages of the complexes. On the other hand, more sophisticated investigative techniques such as cryomicroscopy was used. This chapter is presented in the form of article published in *Colloids and Surfaces A (Physicochemical and Engineering Aspects)*.

Chaaban, A.A., Lartiges, B., Kazpard, V., Plisson-Chastang, C., Michot, L., Bihannic, I., Caillet, C., and Prelot, B. (2016). *Probing the organization of fulvic acid using a cationic surfactant*. *Colloids Surf. Physicochem. Eng. Asp.* 504, 252–259.

In addition, small angle neutron scattering (SANS) was also carried out as well as an attempt to infer average geometric characteristics of SRFA/DTAC complex according to the framework introduced by Israelachvili (packing parameter). These results were not included in the article; they are presented at the end of this chapter.

III.2 PROBING THE ORGANIZATION OF FULVIC ACID USING A CATIONIC SURFACTANT

III.2-1 Abstract

The organization of Suwannee River Fulvic Acid (SRFA) is investigated through the interaction of SRFA with a cationic surfactant molecule (Dodecyl-trimethylammonium chloride (DTAC)). Turbidity measurements, Dynamic light scattering, electrophoretic mobility, surface tension, and cryo-transmission electron microscopy are combined to describe the SRFA/DTAC molecular structures thus obtained. Increasing DTAC concentration, fulvic acid-rich unilamellar vesicles, globules, aggregates of globules, disks, DTAC-rich unilamellar vesicles, and loosely aggregated spheroidal structures, are successively observed. Such sequence of molecular structures is typically found in phase diagrams of catanionic systems (mixture of oppositely charged surfactants). The strong surface activity of fulvic acid/DTAC complexes and the geometrical constraints associated with the formation of vesicles imply that a major component of SRFA is an individual amphiphile negatively charged of molecular size similar to that of DTAC. This soft matter approach supports a supramolecular organization for SRFA.

III.2-2 Introduction

Humic substances (HS), operationally classified according to their solubility into fulvic acid, humic acid, and humin, are ubiquitous organic compounds in soils and aquatic systems (Stevenson, 1994). They are formed from the by-products of organic material degradation (*e.g.* plant debris, microorganisms) but also in part from the condensation of small organic molecules (Hayes, 1989 ; Wershaw, 1999 ; Burdon, 2001 ; MacCarthy, 2001). Besides their obvious role in carbon geocycling, HS have been shown to be key components in the transport/sequestration of xenobiotics and metal contaminants in the environment (Sutton and Sposito, 2005 ; Nebbioso and Piccolo, 2012).

Extensive characterization of HS revealed that those compounds not only contain a large proportion of carboxylic and phenolic groups that make them hydrophilic, but also aliphatic moieties that give them surface active and hydrophobic-binding properties (Von Wandruszka, 1998 ; Guetzloff and Rice, 1994). A characteristic size scale of HS determined by various techniques is about 1-2.5 nm (Simpson et al., 2002b ; Palmer and von

Wandruszka, 2001 ; Lead et al., 1999 ; Balnois et al., 1999 ; Pranzas et al., 2003 ; Baalousha et al., 2005). Changes in solution pH, adsorption experiments and complexation experiments with polycations, have revealed the flexibility of HS structure (Glaser and Edzwald, 1979 ; Piccolo et al., 2003 ; Avena et al., 1999 ; Kazpard et al., 2006 ; Sieliechi et al., 2008). Furthermore, modelling of their charge characteristics suggests that HS can be regarded as soft and porous structures (Duval et al., 2005).

Still, the detailed organization of HS remains a matter of debate: molecular weight measurements performed at different stages of extensive fractionation schemes suggest that HS can be regarded as macromolecules or slightly branched polymers that can coil or adopt an extended conformation according to solution properties (Stevenson, 1994 ; Swift, 1999 ; Ghosh and Schnitzer, 1980 ; Pavlik and Perdue, 2015), whereas some Size Exclusion Chromatography experiments and NMR results suggest that HS correspond to supramolecular associations of small heterogeneous molecules that can be disrupted in the presence of organic acids (Sutton and Sposito, 2005 ; Simpson et al., 2002b ; Piccolo, 2001). To account for the surface-active properties of HS and the enhanced solubility of hydrophobic organic compounds in their presence (Carter and Suffet, 1982), such molecular aggregates have also been described as micelles with a hydrophilic exterior and a hydrophobic core (Guetzloff and Rice, 1994). A-middle-of-the-road view has also been taken, the fulvic fraction being identified as a supramolecular assembly, and the humic fraction corresponding to the coexistence of both macromolecular and supramolecular patterns (Baigorri et al., 2007b).

The main goal of the present paper is to assess which of the two structural concepts, polymeric or supramolecular, is the more appropriate for Suwanee river fulvic acid (SRFA), a reference organic material provided by IHSS. For that purpose, we investigate the association between SRFA and various concentrations of Dodecyl-trimethylammonium chloride (DTAC), a cationic surfactant molecule. Adding an oppositely charged amphiphilic molecule to SRFA is expected to induce drastic restructurations of the fulvic colloid driven by both electrostatic and hydrophobic interactions. Previous works followed a similar strategy by exploring the structure of humate/alkylammonium chloride precipitates using X-ray diffraction (Tombácz et al., 1988) and Small-Angle X-ray Scattering (Shang and Rice, 2007) whereas most other studies dealing with the association of a surfactant with humic substances were carried out in the context of contaminant transport in the environment, and focused on

the binding of the detergent to humic colloids (Adou et al., 2001 ; Koopal et al., 2004 ; Gamboa and Olea, 2006 ; Ishiguro et al., 2007).

The various molecular structures formed upon addition of DTAC to a SRFA suspension are investigated using turbidity and Dynamic Light Scattering (DLS) measurements that provide a rapid assessment of complex formation, electrophoretic mobility and surface tension measurements that yield information about the extent of neutralization and surface active properties of SRFA/DTAC complexes, and Cryogenic Transmission Electron Microscopy (Cryo-TEM) that directly images those complexes. We show that such soft matter approach provides additional tools to assess the organization of humic substances.

III.2-3 Experimental Section

III.2-3-1 Materials

Suwannee River Fulvic acid (SRFA) was obtained from the International Humic Substances Society (IHSS) (Fulvic Acid Standard 2S101F). SRFA is extracted from the Suwannee river, a blackwater river that flows from the Okefenokee Swamp (Georgia), characterized by a pH of 4 and a Dissolved Organic Carbon (DOC) content ranging from 25 to 75 mg/L (Averett et al., 1994). Dodecyltrimethyl ammonium chloride ($C_{15}H_{34}ClN$ - DTAC) was purchased from Sigma-Aldrich (purity 99%). With a Krafft temperature below 0 °C, DTAC is readily soluble in water at ambient temperature (Laschewsky et al., 2005 ; Prévost et al., 2011) and its critical micelle concentration (CMC) at 30 °C is 21.7 mmol/L (Perger and Bešter-Rogač, 2007). Both fulvic acid and surfactant were used without further purification.

III.2-3-2 Sample Preparation

The DTAC stock solution was prepared at 10 g/L in deionised water (Millipore-MilliQ 18.2 M Ω .cm). The concentration of the SRFA stock solution, and hence the range of DTAC concentrations, were adapted to the technique of investigation. For Turbidity, Dynamic Light Scattering, Surface Tension and Electrophoretic Mobility measurements, a SRFA suspension of 20 mg/L, *i.e.* 12 mg C/L, was prepared by adding the appropriate mass of fulvic acid into 500 mL of deionised water. For Cryo-TEM, stock suspensions of 20 mg/L and 1g/L were used. The SRFA stock solutions were prepared daily and mechanically mixed

overnight in the dark to obtain a well-dispersed suspension. The dissolved organic carbon was checked for each prepared stock solution (Shimadzu TOC-Vcsn).

SRFA/DTAC complexes were prepared by adding aliquots of the surfactant stock solution to 10 mL of SRFA suspension and by submitting the mixture to gentle overhead agitation (3 times). Both DTAC and fulvic acid stock solutions as well as SRFA/DTAC samples were maintained at 30°C in a heating bath during the experiments, *i.e.* a temperature at which the alkyl chain of the surfactant is flexible.

III.2-3-3 Characterization of SRFA/DTAC Complexes

The turbidity of SRFA/DTAC suspensions was measured as a function of time using a HACH LANGE 2100Q turbidimeter. Conductivity and pH (WTW Multiline F/SET), surface tension (KRUSS K12 Processor Tensiometer using a Wilhelmy plate), the electrophoretic mobility and the size of the fulvic acid-surfactant aggregates (Malvern Zetasizer Nano ZS) were measured at the end of the experiment.

Cryo-TEM observations were carried out at the Multiscale Electron Imaging (METI) platform at the University of Toulouse using a *JEOL 2100 Lab6* transmission electron microscope equipped with a *Gatan 626* cryoTEM grids holder. Images were recorded with a *Gatan ultrascan1000* camera under low dose conditions (about 10 electrons per Å²). 4 μL of SRFA/DTAC suspension was deposited onto a LACEY/CARBON FILM grid previously ionized using PELCO-easi Glow 91000 glow discharging-cleaning system. After blotting for 0.2 second to remove the excess added volume (*Leica* EM GP controlled vitrification system at 30 °C and 85% relative humidity), the grid was immediately plunged into liquid ethane at its freezing point -185 °C and then stored in liquid nitrogen. The size distribution of SRFA/DTAC complexes was obtained by counting the aggregates in logarithmically spaced size bins such that $d_{i+1} = 2^{1/3} d_i$, which yields equally spaced size intervals on a x-axis log scale (Frappier et al., 2010). The mean aggregate size D was calculated from:

$$D = \frac{\sum_{i=1}^{i=k} n_i D_i}{\sum_{i=1}^{i=k} n_i} \quad (3.1)$$

where n_i is the number of aggregates measured in range i , D_i is the middle of class range, and k is the total number of bins.

III.2-4 Results

III.2-4-1 Turbidity Measurements

Figure III-1 shows the time evolution of the turbidity of SRFA/DTAC mixtures obtained after various DTAC additions to a 20 mg/L fulvic acid solution at natural pH (4.32). At low and high DTAC concentration, the turbidity increases to reach a plateau after about 25 minutes, whereas in the 2.8-4.7 mmol/L range, the turbidity evolution is characterized by a rapid early overshoot followed by a slow stabilizing trend.

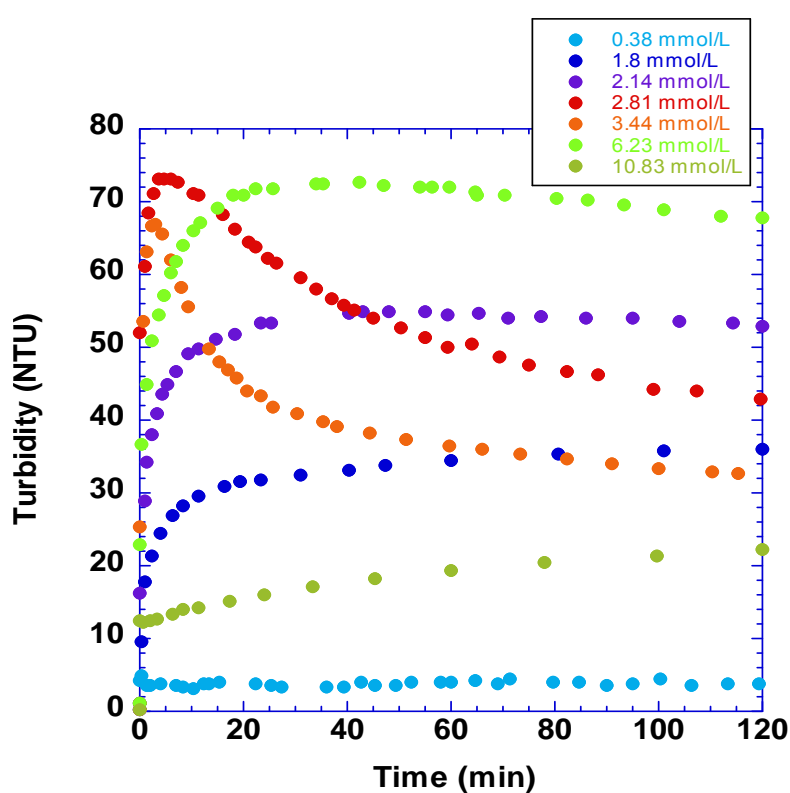


Figure III-1. Typical turbidity curves of SRFA/DTAC suspensions as a function of time for various DTAC additions; SRFA concentration = 20 mg/L.

For all surfactant additions, the pH of the SRFA/DTAC mixtures remains close to that of the initial fulvic acid solution (figure III-2).

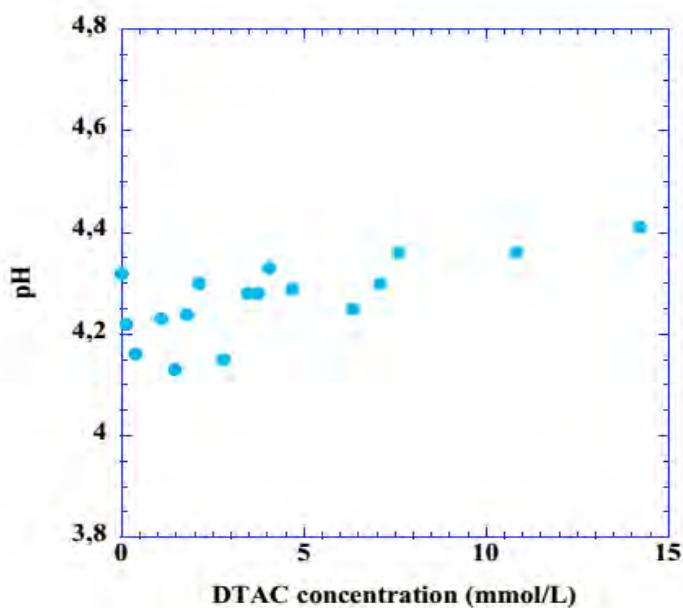


Figure III-2. pH variation of SRFA/DTAC suspensions as a function of DTAC concentration.

At steady-state, i.e. after about two hours, the variation of turbidity with DTAC concentration is characterized by two well-defined peaks (figure III-3a). Such variation may be the result of SRFA/DTAC interactions but, as DTAC is a salt, could also be related to a change in solution ionic strength.

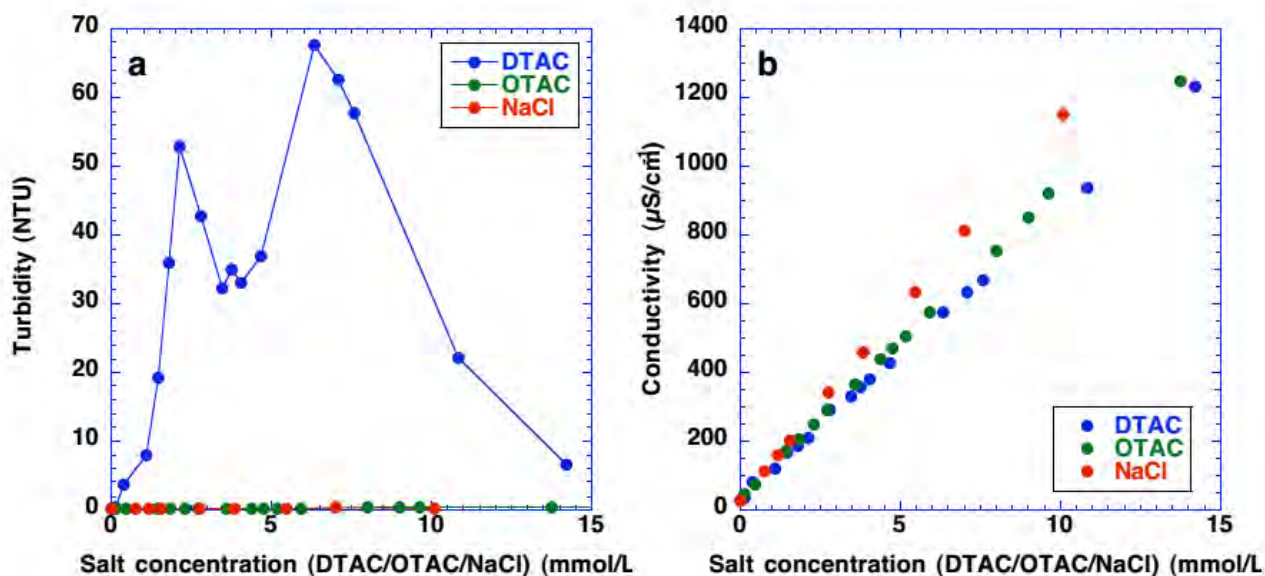


Figure III-3. Interaction of SRFA with DTAC (●), OTAC (●), and NaCl (●) as a function of salt concentration: (a) Turbidity curves; (b) Conductivity curves.

As illustrated in figure III-3, substituting either NaCl or the analogous surfactant of shorter alkyl chain Octyltrimethylammonium chloride (OTAC) to DTAC, lead to an equivalent linear increase in solution conductivity without any change in the turbidity of SRFA suspensions. Therefore, the main features of the SRFA/DTAC turbidity curve should be predominantly explained by the association of SRFA with both oppositely-charged polar head groups and hydrophobic alkyl chains of DTAC.

III.2-4-2 Electrophoretic Mobility, DLS and Surface Tension Measurements.

Figure III-4 shows the electrophoretic mobility and the particle size of SRFA/DTAC complexes as a function of surfactant concentration. In each graph, the turbidity curve is superimposed for comparison. Unexpectedly, at low DTAC concentration, the electrophoretic mobility becomes more negative upon addition of cationic surfactant to reach a minimum that coincides with the first turbidity peak. The electrophoretic mobility then increases to reach positive values above 3.5 mmol/L, and finally stabilizes in the decreasing part of the second turbidity peak. The opposite patterns followed by turbidity and electrophoretic mobility curves imply a significant reorganization of the fulvic colloid since new negatively charged sites have become electrokinetically-active during the charge neutralization of the anionic functional groups of fulvic acid with DTAC. On the other hand, the lack of correlation between those same curves in the concentration range of the second aggregation peak suggests an association between DTAC and SRFA essentially driven by hydrophobic interactions in the presence of excess surfactant.

The particle size measured by DLS at 2 h remains in the 80-130 nm range at the start of the first turbidity peak, reaches a maximum in the valley between the two turbidity peaks when neutral SRFA/DTAC complexes are formed, and then decreases substantially to stabilize around 150 nm in the DTAC concentration range of the second turbidity peak (figure III-4b). Such behaviour implies that the two increases in turbidity correspond to the formation of an increased number of individual entities rather than the formation of aggregated structures, which actually occurs around a DTAC concentration of 3.5 mmol/L in the valley between the turbidity peaks. All DLS plots exhibited a monomodal size distribution except at a DTAC concentration of 0.19 mmol/L where two populations centered on 16 nm and 80 nm were detected (inset of figure III-4b).

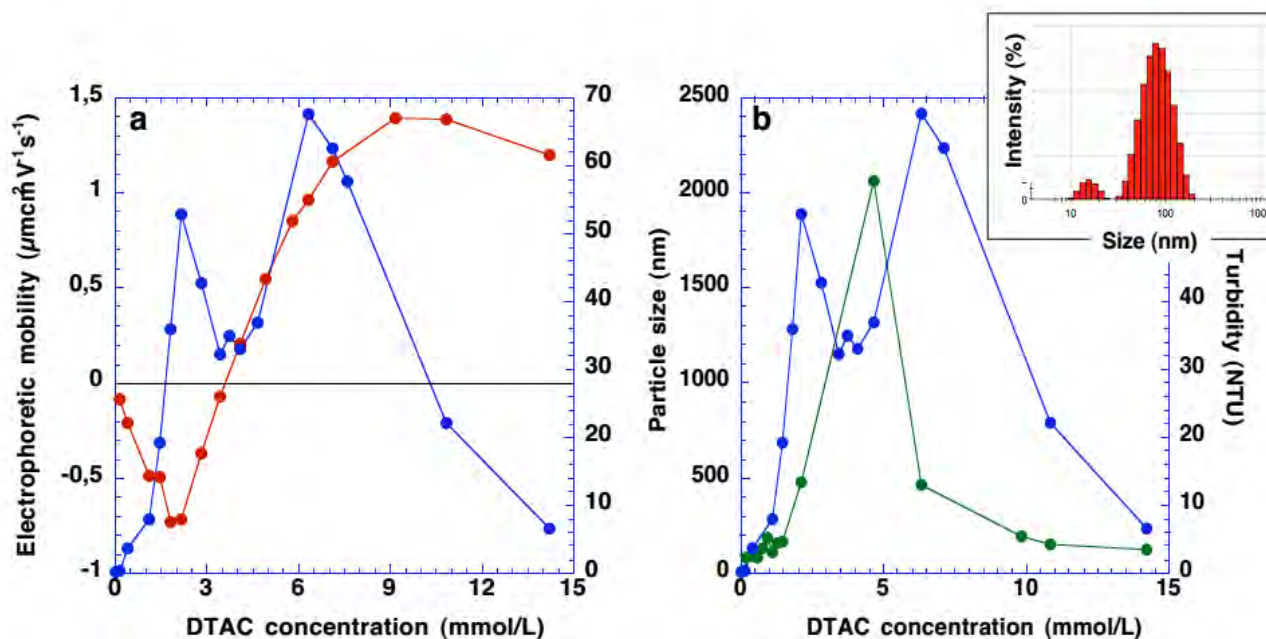


Figure III-4. (a) Electrophoretic mobility of SRFA/DTAC complexes versus DTAC concentration (●). (b) Number-average particle size of SRFA/DTAC complexes (DLS) versus DTAC concentration (●) for a SRFA concentration of 20 mg/L. The turbidity curve (●) is superimposed for comparison. The inset shows the bimodal size distribution obtained for a DTAC addition of 0.19 mmol/L.

According to Ritchie and Perdue (Ritchie and Perdue, 2003), the potentiometric proton titration of SRFA (0.36 g/L in NaCl 0.1 M) yields an acidity of 6.44 meq/g Carbon at pH 4.2. This should correspond to an initial charge of our fulvic acid solution of less than 0.077 meq (Dissolved organic carbon of 12 mgC/L), which then implies that most of the added surfactant remains in solution when neutral SRFA/DTAC complexes are obtained. Such result is consistent with the adsorption isotherms reported in the literature for similar cationic C12-surfactant/fulvic acid systems (Ishiguro et al., 2007).

Figure III-5 shows that the surface tension is drastically reduced at very low DTAC concentration, and then further diminishes gradually in successive small steps corresponding to the concentration range of turbidity peaks and the valley in between. This reveals that fulvic acid/DTAC complexes are highly surface active, since values around 40 mJ/m^2 are only attained around CMC with pure DTAC (Takata et al., 2010). Such effect, already noted by Gamboa and Olea (Gamboa and Olea, 2006), is reminiscent of the strong cooperative

effect observed between oppositely charged surfactants at the air-water interface (Nguyen et al., 2014).

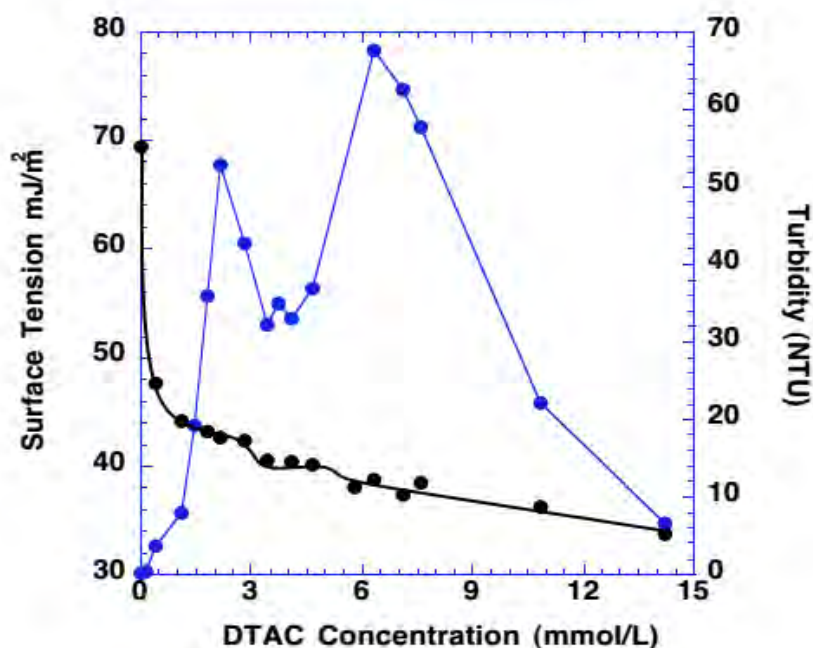


Figure III-5. Surface tension of SRFA/DTAC suspensions versus DTAC concentration (●) for a SRFA concentration of 20 mg/L. The turbidity curve (●) is shown in order to position the main variations of surface tension.

III.2-4-3 Cryo-TEM Observations

CryoTEM observations performed with 20 mg/L SRFA suspensions at DTAC concentrations of 1.8 mmol/L and 7.58 mmol/L, allow the identification of SRFA/DTAC molecular structures that make up the turbidity peaks. As illustrated in figure III-6, poorly formed unilamellar vesicles and spongy networks are formed at those DTAC concentrations. The term vesicle is used here to describe the general vesicular-like architecture and in no way implies that the wall of the vesicle is made from a lipid bilayer. It is worth noting that the size of vesicles is comparable with that of the minor population at 16 nm detected by DLS. From the electrophoretic mobility measurements, it appears that the fulvic-rich vesicles formed at low DTAC concentration are negatively charged whereas the DTAC-rich vesicles obtained at higher surfactant concentration are positively charged.

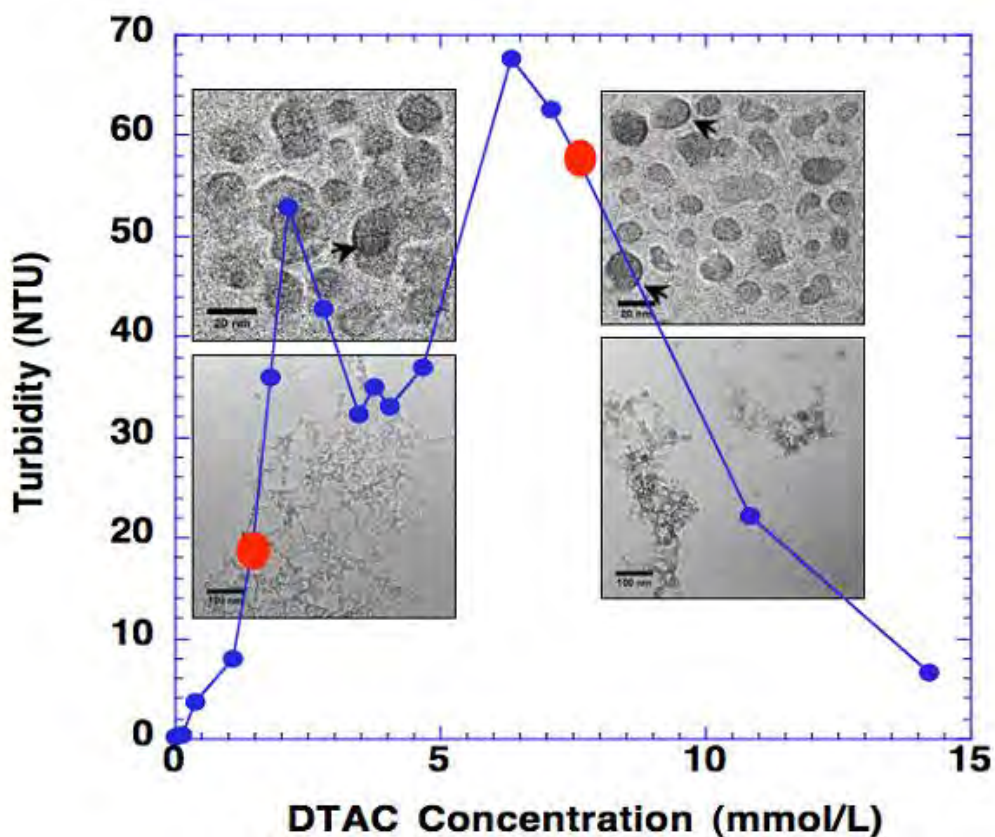


Figure III-6. CryoTEM micrographs of SRFA in presence of DTAC concentrations of 1.8 mmol/L and 7.58 mmol/L (red dots) showing spongy networks and vesicles. The arrows indicate the walls of the vesicles.

Further cryo-TEM experiments conducted with a SRFA concentration of 1g/L provide a more complete picture of the interaction of fulvic acid with DTAC. At 1g/L, the pH of the SRFA suspension is 2.95, hence the charge of fulvic acid is smaller, and the DTAC concentration range that destabilizes SRFA is much lower. Figure III-7 presents the various molecular structures obtained upon mixing SRFA with various DTAC concentrations. Unlike DTAC solutions that yield featureless micrographs (figure III-8), the reference fulvic acid suspension (fig. III-7a), *i.e.* 0 mmol/L DTAC, exhibits globular structures about 25-32 nm in diameter, as well as small aggregates of those globules (inset of fig. III-7a). The size range obtained for the individual globules is in good agreement with previous SANS measurements performed with fulvic and humic acids in similar conditions (pH 5 and about 3 g/L concentration) (Osterberg and Mortensen, 1992). Smaller values of radii-of-gyration have been reported for SRFA at higher pHs, which suggests that the globular structures correspond

to aggregates of SRFA (Wershaw and Pinckney, 1973 ; Aiken et al., 1994 ; Osterberg and Mortensen, 1994). Addition of $7.6 \cdot 10^{-3}$ mmol/L of DTAC leads to the formation of unilamellar vesicles, both complete and open, mostly in the 12-20 nm range (fig. III-7b1 and III-7b2), as well as sparse spongy networks with budding vesicles attached on the branches (fig. III-7b3 and III-7b4). Further addition of cationic surfactant, *i.e.* $3.03 \cdot 10^{-2}$ mmol/L, increases the average size of the vesicles (30.3 nm) that now coexist with globular structures of similar size and aggregates of those globules (inset of fig. III-7c). At a DTAC concentration of $5.67 \cdot 10^{-2}$ mmol/L, the unilamellar vesicles can no longer be identified and only merging aggregates of globules are found (fig. III-7d).

Another kind of morphology, *i.e.* aggregates of disk-like structures, is observed after 45 minutes at a surfactant concentration of $7.56 \cdot 10^{-2}$ mmol/L (fig. III-7e1). At longer times (101 min), cryo-TEM examination reveals that the platelets become larger and that they tend to adopt a hexagonal shape implying a well-defined local structure (fig. III-7e2). When the surfactant concentration is further increased ($18.8 \cdot 10^{-2}$ mmol/L), unilamellar vesicles (mean size around 19 nm) are again spontaneously formed (fig. III-7f1 and III-7f2). As for the 20 mg/L SRFA concentration, those vesicles are generally closed and more abundant than at lower DTAC concentration. Less developed spongy-like networks with nascent vesicles are also frequently observed (fig. III-7f3 and III-7f4). Finally, at the highest surfactant concentration investigated ($74.3 \cdot 10^{-2}$ mmol/L), loosely aggregated spheroidal structures (~22.8 nm) are found (fig. III-7g).

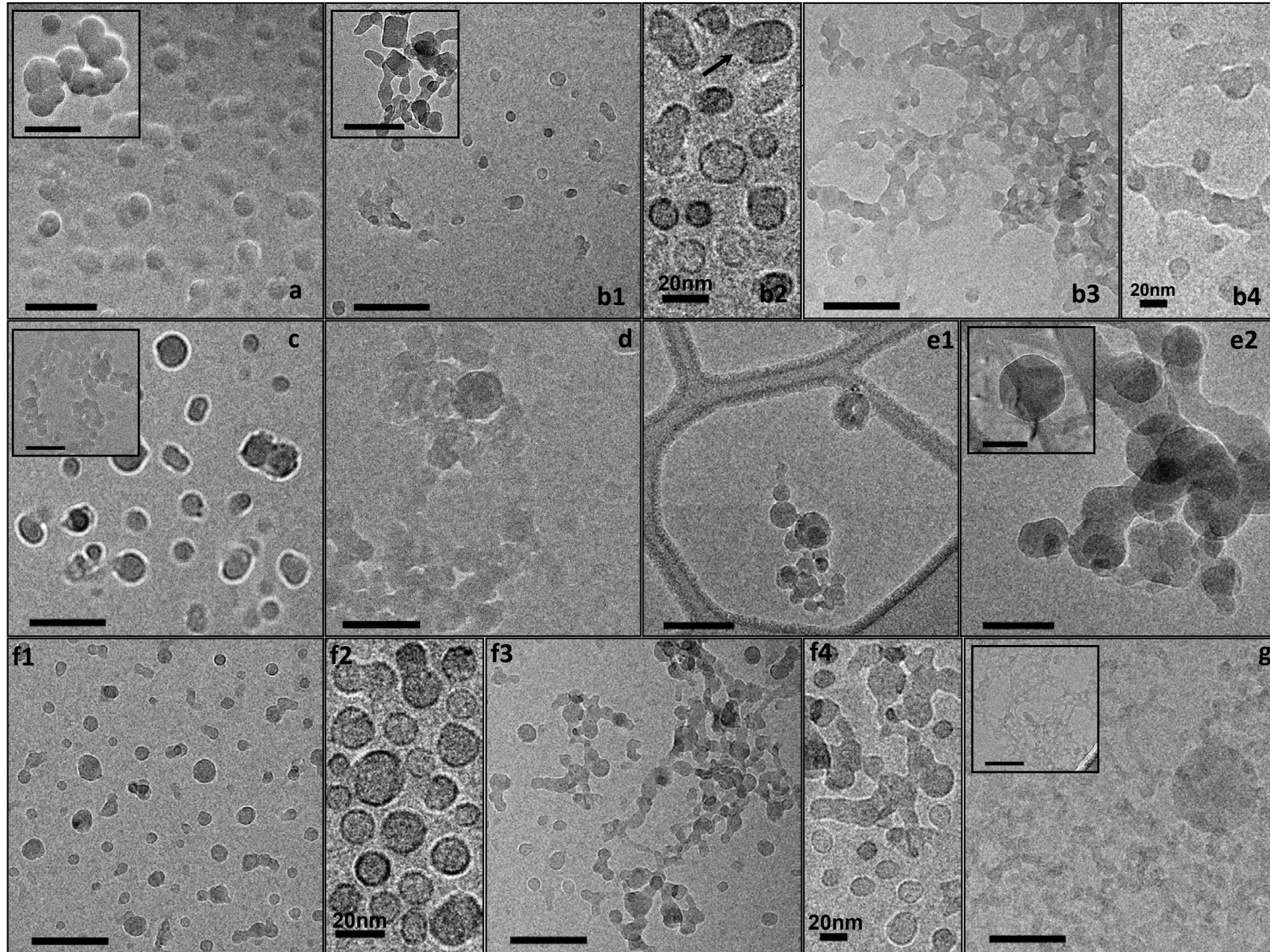


Figure III-7. CryoTEM micrographs of SRFA/DTAC molecular structures; all scale bars equal 100 nm unless otherwise indicated. (a) [DTAC] = 0 mmol/L. (b1-4) [DTAC] = $7.6 \cdot 10^{-3}$ mmol/L; the arrow indicates an open vesicle. (c) [DTAC] = $30.2 \cdot 10^{-3}$ mmol/L. (d) [DTAC] = $56.7 \cdot 10^{-3}$ mmol/L. (e1-2) [DTAC] = $75.6 \cdot 10^{-3}$ mmol/L. (f1-4) [DTAC] = $18.8 \cdot 10^{-2}$ mmol/L. (g) [DTAC] = $74.3 \cdot 10^{-2}$ mmol/L.

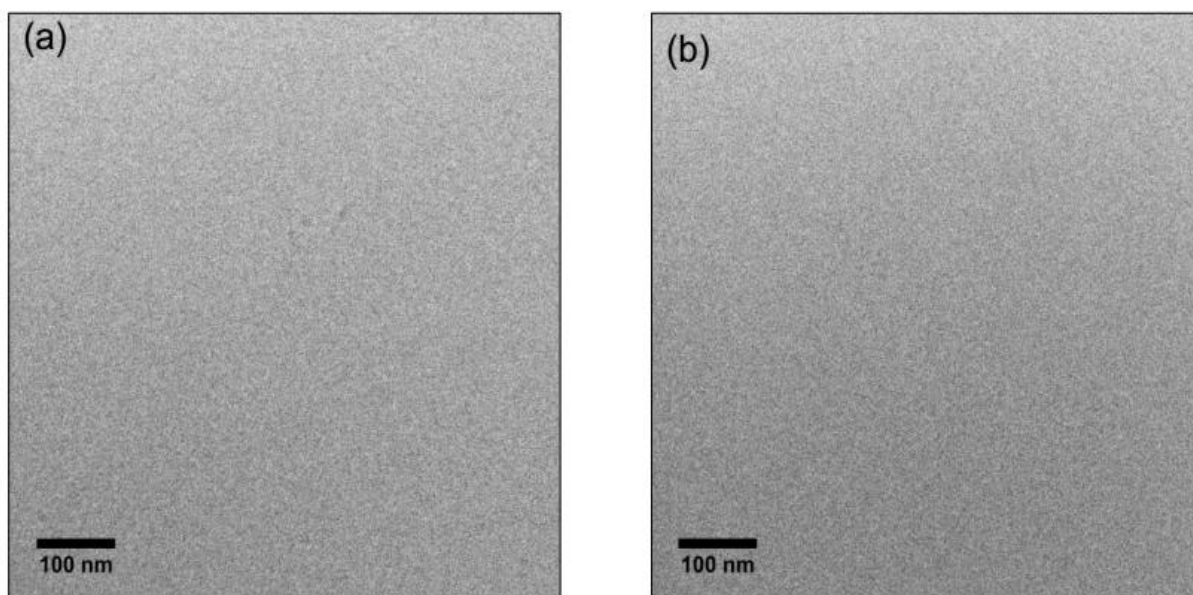


Figure III-8. CryoTEM micrographs of (a) DTAC stock solution (10g/L or 37.9 mmol/L); (b) DTAC solution at a concentration of $7.6 \cdot 10^{-3}$ mmol/L, i.e. the concentration at which fulvic-rich vesicles are formed.

The size histograms of SRFA/DTAC complexes observed by cryo-TEM and the evolution of their mean diameter as a function of surfactant concentration are shown in figure III-9. All distributions are monomodal with a slight skewness towards larger sizes when an aggregation phenomenon has been detected on the micrographs. In those cases, the size distributions are certainly biased because the large aggregates can be drained away during the blotting step of sample preparation (Lee et al., 2012).

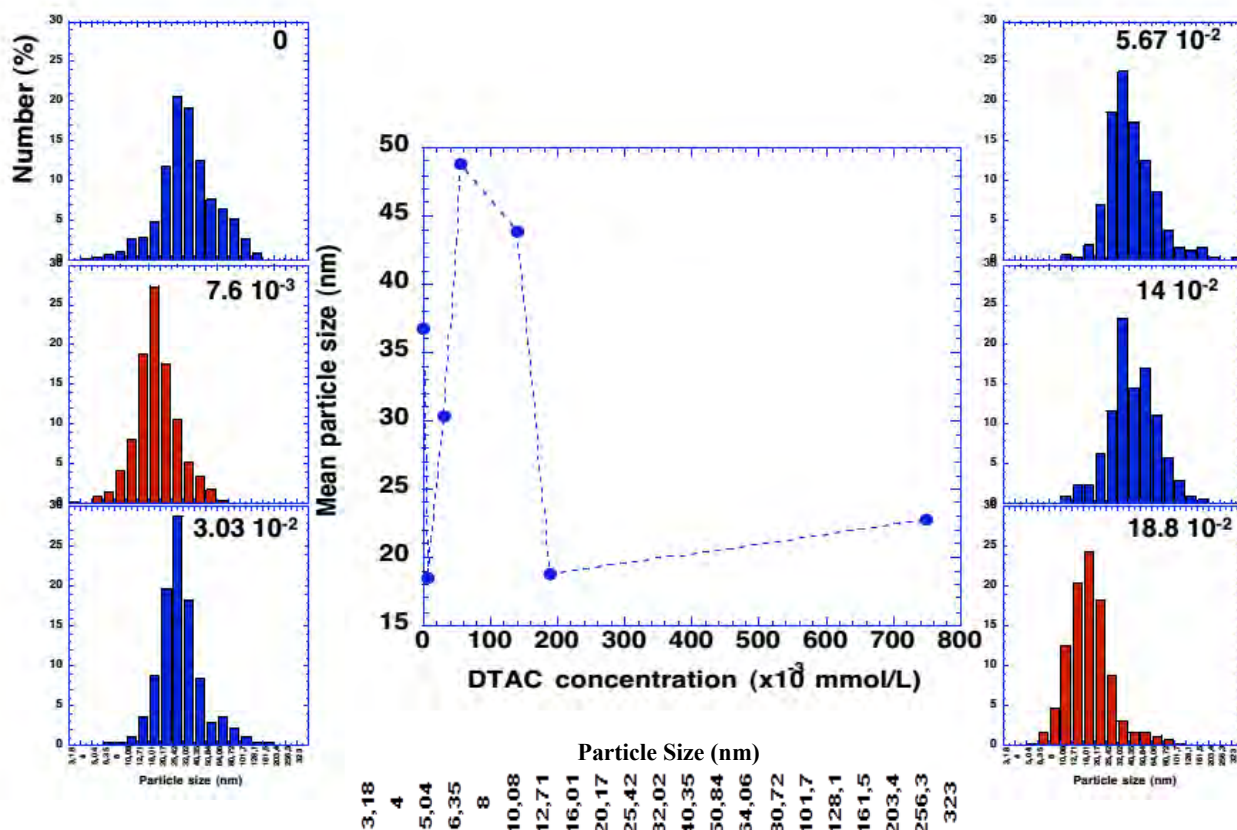


Figure III-9. Size histograms of molecular structures viewed by cryoTEM and evolution of mean particle size with DTAC concentration. The DTAC concentration is indicated in the histograms in mmol/L. The histograms in red are associated with the presence of vesicles.

III.2-5 Discussion

III.2-5-1 Self-assemblies of Fulvic Acid and DTAC

Over the years, many studies have reported a variety of molecular structures adopted by humic and fulvic acids under various conditions of pH, background electrolyte, and coagulant concentration. Using TEM, Baalousha et al. (2005) and Wilkinson et al. (1997 ; 1999) evidenced networks of fibrils and globules ranging in size from 50 to 300 nm. Above a 1gC/L in humic concentration, Myneni et al. (1999), using X-ray microscopy, found globules, ring-like, sheet-like, and thread-like structures in the 200-1200 nm size range, by varying the pH, ionic strength of the solution, and nature of the counterion. Using the same technique, Sieliechi et al. (2008) also observed the formation of 80 nm globules during the coagulation of a 10 mgC/L aquagenic humic acid in presence of hydrolyzed-Fe species.

Namjesnik-Dejanovic and Maurice (1997), Plaschke et al. (1999), used Atomic Force Microscopy to image fulvic and humic acid adsorbed on the basal plane of a freshly cleaved muscovite. Spongy-like structures consisting of 15 nm rings along with 10-50 nm spheres were found at low humic concentration, whereas aggregates of spheres, chain-like assemblies, and torus-like structures, were obtained at higher concentration. Thieme and Niemeyer (1998) investigated by X-ray microscopy an experimental system very similar to ours, *i.e.* a 10g/L soil humic acid suspension coagulated with various amounts of either Dodecyltrimethylammonium bromide (DTAB) or Hexadecyltrimethylammonium bromide (CTAB). In presence of low DTAB amounts, nearly monodispersed spheres (224 nm) were observed; those spheres doubled in size with increasing surfactant concentration. At high DTAB concentration, spongy networks were obtained. In the case of CTAB additions, micron size hollow spheres with about 240 nm thick walls were detected at low surfactant concentration.

Many of the molecular structures described in the literature are reminiscent of those found in this study. However, the formation of small unilamellar vesicles was, to our knowledge, never reported for either fulvic or humic colloids. In systems involving a cationic surfactant and an oppositely charged component, vesicles have been found to form either with an anionic surfactant, *i.e.* a catanionic system (Segota and Tezak, 2006), or an anionic polymer (Langevin, 2009). Therefore, the observation of vesicles in the mixture SRFA/DTAC is not in itself an argument for either view - supramolecular or polymeric - of SRFA. However, the sequence of molecular structures in which our vesicles are successively found, *i.e.* SRFA-rich vesicles, globules, disks, DTAC-rich vesicles, is fully consistent with phase diagrams typically encountered in catanionic systems (Marques et al., 1999 ; Marques et al., 1998). The presence of two DTAC concentration domains with disperse vesicles on both sides of neutral aggregated globules at both 20 mg/L and 1g/L, is also reminiscent of such phase diagrams. Moreover, the morphology of spongy networks observed in association with vesicles bears a close resemblance to that of the branched wormlike micelles found in aqueous surfactants solutions (Tang and Carter, 2013).

The amphiphilic character of humic substances has long been recognized (Von Wandruszka, 1998 ; Guetzloff and Rice, 1994). According to Wershaw (Wershaw, 1999), such property is even intrinsic to the formation of HS by enzymatic degradation of plant biopolymers. Recent NMR spectroscopy studies have revealed the existence of more or less

flexible alkyl segments in humic substances (Chien and Bleam, 1998 ; Cook and Langford, 1998 ; Khalaf et al., 2003). DOSY experiments performed on soil HS even indicated that the diffusion coefficients of aliphatic components are consistent with the presence of monomers to tetramers of C₁₆ – C₁₈ fatty ester units (Simpson et al., 2002b). Electrospray ionization also suggested that fulvic acid consists of more or less saturated carbon skeleton with carboxylate functional groups or even lipids (Leenheer et al., 2003 ; Reemtsma et al., 2006a ; Tfaily et al., 2015). Therefore, it does not seem unreasonable to consider SRFA as a supramolecular assembly of various anionic amphiphile molecules and the SRFA/DTAC complexes as resulting from a cationic surfactant system.

III.2-5-2 Towards Average Geometric Characteristics of SRFA Constituents

The nature of a self-assembly is essentially controlled by both electrostatic and geometric packing effects. According to the framework introduced by Israelachvili et al. (Israelachvili et al., 1976), the self-organization of amphiphiles can be reasonably predicted from the critical packing parameter P defined as the ratio between the volume v_c of the hydrophobic tail and the product of the polar head surface area a_o with the critical chain length l_c of the surfactant:

$$P = \frac{v_c}{a_o l_c} \quad (3.2)$$

Thus, for cone shaped surfactants, *i.e.* $p \leq 1/3$, spherical micelles are formed, whereas for cuplike amphiphile molecules, *i.e.* $1/2 < p < 1$, vesicles are formed. Bilayers are obtained when the packing parameter is equal to 1. For DTAC, according to the experimental values of geometrical parameters reported in the literature, $v_{DTAC} = 0.482 \text{ nm}^3$, $l_{DTAC} = 1.643 \text{ nm}$, $a_{DTAC} = 0.88 \text{ nm}^2$, $p_{DTAC} \sim 0.33$ and DTAC therefore forms spherical micelles (Prévost et al., 2011).

To carry out that kind of calculation for SRFA amphiphiles is more questionable. Even though a micelle-like organization for HS has previously been proposed in the literature (Von Wandruszka, 1998 ; Guetzloff and Rice, 1994), a pure hydrophobic interior is highly unlikely in view of the electrokinetic behaviour of SRFA/DTAC complexes at low surfactant concentration (fig. III-4a). Furthermore, the polydisperse distribution of molecular weights and a likely variety in the nature of polar head groups, can only lead to a broad estimate of

the geometrical characteristics of SRFA amphiphiles. Still, an average polar head area of SRFA can be obtained from surface tension measurements (fig. III-10) using Gibbs adsorption equation at the maximal value of $d\gamma/d\ln C$ (Chen and Schnitzer, 1978):

$$a_{SRFA} = \frac{1}{\Gamma_{\max} N} \text{ and } \Gamma_{\max} = -\frac{1}{RT} \frac{d\gamma}{d\ln C} \quad (3.3)$$

where Γ_{\max} is the maximal surface adsorption of SRFA, N Avogadro number, R the ideal gas constant, T the absolute temperature, γ the surface tension, and C the SRFA concentration.

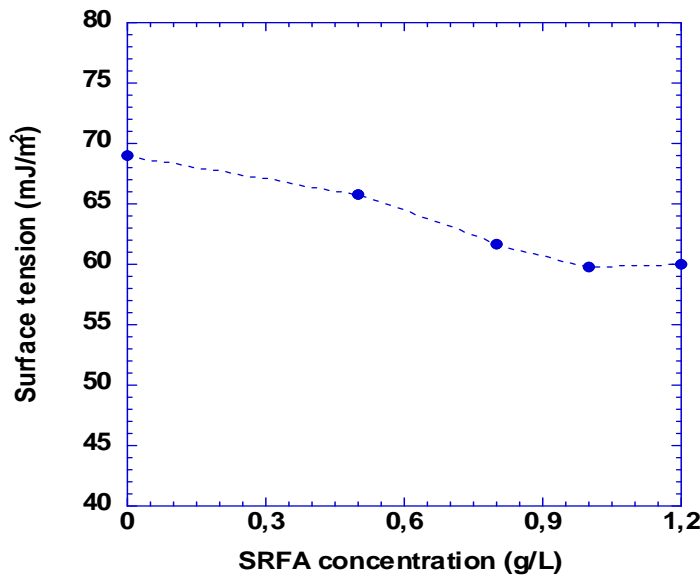


Figure III-10. Surface tension of SRFA suspensions as a function of SRFA concentration.

In our case, $\Gamma_{\max} = 2.35 \cdot 10^{-10} \text{ mol/cm}^2$ and hence $a_{SRFA} = 0.71 \text{ nm}^2$, which is consistent with previous results in the literature (Taraniuk et al., 2007). An average chain volume v_{SRFA} of SRFA constituents can also be assessed by assuming a spherical micelle organization: knowing that the volume V of the micelle is $V = n v_{SRFA} = 4/3\pi r_{SRFA}^3$ and the surface S of the micelle is $S = n a_{SRFA} = 4\pi r_{SRFA}^2$, with n the number of SRFA constituents in a micelle, $v_{SRFA} = \frac{a_{SRFA} r_{SRFA}}{3}$. Using the average radius-of-gyration r_{SRFA} of 7.5 \AA reported in the literature for SRFA (Aiken et al., 1994 ; Lead et al., 2000b), we obtained $v_{SRFA} = 0.177 \text{ nm}^3$. An estimate of the number n_c of alkyl groups in the hydrophobic portion of SRFA

constituents can also be inferred using the following expression: $v_{SRFA} = (27.4 + 26.9 n_c) \times 10^{-3} \text{ nm}^3$ (Tanford, 1972). Interestingly, the n_c value of about 5 thus obtained, is consistent with the picture of short-chained or highly branched aliphatic structures provided by NMR studies of SRFA (Thorn, 1987).

The complex formed from DTAC and SRFA constituents possesses its own packing parameter p_c . Following Manohar and Narayanan approach (Manohar and Narayanan, 2012), it is convenient to consider two cases:

(i) The anionic surfactants (N_1 moles), *i.e.* the SRFA constituents are in excess and all the cationic surfactants (N_2 moles) are complexed; the average packing parameter P is then:

$$P = \frac{2N_2}{N_1 + N_2} p_c + \frac{N_1 - N_2}{N_1 + N_2} p_{SRFA} \text{ or } P = 2xp_c + (1 - 2x)p_{SRFA} \quad (3.4)$$

where $x = \frac{N_2}{N_1 + N_2}$ is the mole fraction of cationic surfactant.

(ii) The cationic surfactants are in excess and all the SRFA constituents are complexed,

$$P = \frac{2N_1}{N_1 + N_2} p_c + \frac{N_2 - N_1}{N_2 + N_1} p_{DTAC} \text{ or } P = 2(1 - x)p_c + (2x - 1)p_{DTAC}. \quad (3.5)$$

This simple analysis readily accounts for the variety of aggregate structures (micelles, vesicles, disks) that were found in the SRFA/DTAC system, P changing with the molar fraction of cationic surfactant. Actually, both anionic and cationic surfactants should be distributed between the bulk and the self-assemblies, which complicate the exact calculation of the packing parameter. At the moment, not knowing the amount of DTAC associated in any self-assembly, it is not possible to infer the architectural characteristics of the SRFA/DTAC complex from the geometrical constraints associated with the formation of a given molecular structure. The polar head of the complex may however be determined using the Gibbs adsorption equation, *i.e.* $a_c \sim 0.17 \text{ nm}^2$ (fig. III-5). In addition, the thin thickness of vesicles, less than 1.15 nm according to the width of the dark rim on the micrographs (fig. III-7b2 and III-7f2), and hence much less than $l_{DTAC} = 1.643 \text{ nm}$, suggests (i) a mismatch in size between the cationic surfactant and the SRFA constituent, and (ii) a deformation of the DTAC hydrocarbon chain around the SRFA constituent.

III.2-6 Conclusions

The surface active behaviour of complexes formed during the interaction of SRFA with DTAC, the sequence of molecular structures observed by cryoTEM, and the size of constituents involved in those molecular structures, concur to describe SRFA as a supramolecular assembly of amphiphiles molecules. Taking into account the variety of functional groups evidenced in humic material (Sutton and Sposito, 2005), and the various compounds detected in SRFA by coupling solvent extraction with ESI FTICR MS (Tfaily et al., 2015), it seems a bit simplistic to assimilate SRFA to a single type of amphiphile molecule, and hence to consider the SRFA/DTAC mixture as a well-defined binary system. In addition, it is highly plausible that only part of SRFA constituents participate to the molecular structures observed here. Nevertheless, such comments do not fundamentally challenge the picture of SRFA as a supramolecular structure. To assess the dynamics of such molecular aggregate, *i.e.* its formation and evolution in the natural environment, or its relationships to the other DOM components, in particular humic acid, appear to be key elements for a better understanding of global carbon cycle.

III.3 Packing Parameter of the Mixed System SRFA/DTAC: Assuming Interdigitating Alkyl Chain

The theory of the packing parameter according to Israelachvili et al. (1976) is an appropriate approach in order to understand the self-aggregation of surfactants. Although SRFA constituents can not merely be described as a single type of amphiphile molecule, however, we have demonstrated the supramolecular organization of SRFA as assembly of various anionic amphiphile molecules. Hence, the SRFA/DTAC mixture is considered as a well-defined binary system as that resulting from a cationic surfactant system. Accordingly, the packing parameter can be then used to infer an average characteristic of the SRFA/DTAC complex.

Consider a vesicle (Figure III-11) made of an outer and inner layer with the following parameters: R_o (Outer radius), R_i (Inner Radius) and $t=R_o-R_i$ (Hydrophobic portion thickness).

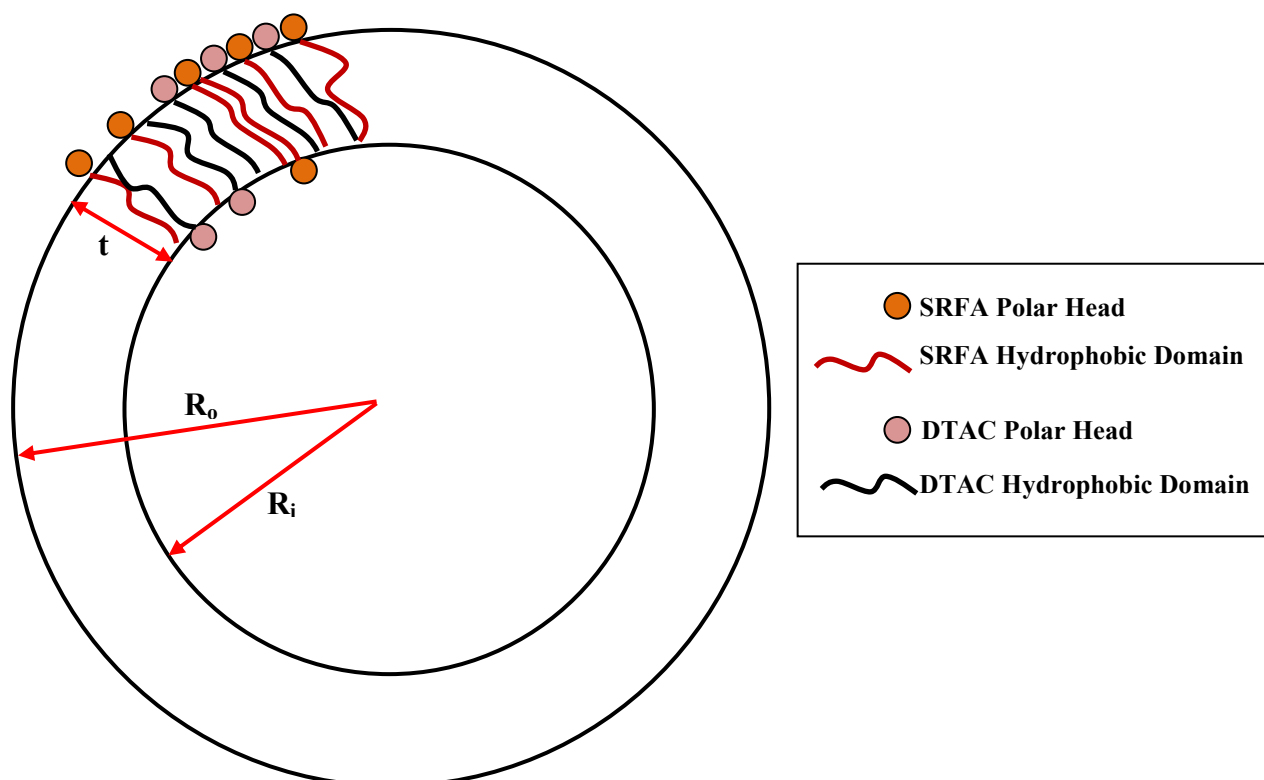


Figure III-11. Interdigitating Hydrophobic Domain Vesicle of SRFA/DTAC Mixed System.

Assuming Interdigitating Alkyl Chain, which is more reasonable than a lipid bilayer, the volume “ V_x ” and the area “ S_x ” of the vesicles of the SRFA/DTAC complexes, observed by cryo-TEM (see figure III-7), obtained by size bin distribution $d_{i+1} = 2^{1/3} d_i$ (Frappier et al., 2010) (see figure III-9) is calculated using the following equations (Table III-1) (the index “ x ” corresponds to either the inner layer “ i ”, outer layer “ o ” or the whole vesicle “ t ”):

- The volume of the vesicle depends on the hydrophobic chain of SRFA and DTAC; since we have interdigitating alkyl chains then the volume depends on the amount of SRFA and DTAC in both layers (*i.e.* outer and inner region) (Israelachvili et al., 1976 ; Israelachvili, 2011 ; Fattal et al., 1995):

$$V_t = V_o = V_i = N^{agg} v_a = (4/3) \pi (R_o^3 - R_i^3) \quad (3.6)$$

- The area of the vesicle:

$$S_t = N^{agg} a_a = S_o + S_i = 4\pi (R_o^2 + R_i^2) \quad (3.7)$$

$$S_o = N_o^{agg} a_a = 4\pi R_o^2 \quad (3.8)$$

$$S_i = N_i^{agg} a_a = 4\pi R_i^2 \quad (3.9)$$

where $N^{agg} = N_o^{agg} + N_i^{agg}$ is the sum of the number of SRFA and DTAC molecules on the outer (N_o^{agg}) and inner layer (N_i^{agg}); $N_o^{agg} = N_{So}^{agg} + N_{Fo}^{agg}$ sum of the number of SRFA “F” and DTAC “S” molecules on the outer layer; $N_i^{agg} = N_{Si}^{agg} + N_{Fi}^{agg}$ sum of the number of SRFA “F” and DTAC “S” molecules in the inner layer; “ v_a ” average chain volume and “ a_a ” the average polar head area of SRFA/DTAC complex.

Table III-1. The Volume and area of the outer layer, inner layer and the whole vesicle of SRFA/DTAC Complex.

[DTAC]=7.6 10 ⁻³ mmol/L										
	Vesicle Size Bin (diameter “d” nm)									
	6.35	8	10.08	12.71	16.01	20.17	25.42	32.02	40.35	50.84
R _o (nm)	3.18	4.00	5.04	6.36	8.01	10.09	12.71	16.01	20.18	25.42
R _i (nm)	2.03	2.85	3.89	5.21	6.86	8.94	11.56	14.86	19.03	24.27
t (nm)	1.15	1.15	1.15	1.15	1.15	1.15	1.15	1.15	1.15	1.15
V _t (nm ³)	99.83	172.18	291.68	487.93	805.51	1318.97	2147.07	3473.20	5600.29	8998.61
S _t (nm ²)	177.61	302.26	508.13	846.22	1393.33	2277.92	3704.53	5989.14	9653.63	15508.13
V _o (nm ³)	99.83	172.18	291.68	487.93	805.51	1318.97	2147.07	3473.20	5600.29	8998.61
S _o (nm ²)	126.61	200.96	319.04	507.25	804.85	1277.44	2028.99	3219.38	5112.30	8115.98
V _i (nm ³)	99.83	172.18	291.68	487.93	805.51	1318.97	2147.07	3473.20	5600.29	8998.61
S _i (nm ²)	51.00	101.30	189.08	338.97	588.49	1000.47	1675.54	2769.76	4541.32	7392.16

As previously mentioned, the polar head of the complex was determined using the Gibbs adsorption equation and $a_a \sim 0.17 \text{ nm}^2$. Using equation (3.7), (3.8) and (3.9), N^{agg} , N_o^{agg} and N_i^{agg} can be calculated respectively. This value (N^{agg}) can be use to estimate the average chain volume “ v_a ” of SRFA/DTAC complex (equation (3.6)). Concomitantly, the number of mole of SRFA/DTAC that comprises the aggregates of the outer, inner layer and the whole vesicles can be calculated using (Table III-2):

$$n_x = N_x^{agg} / N_A \quad (3.10)$$

where “ n_x ” the number of mole and “ N_A ” the Avogadro number.

In general, the case of vesicles we can mainly consider the outer layer in the molecular packing parameter, since it is where the geometrical constraints emerge (Israelachvili, 2011). The effective parameter " p_{eff} " of the mixed system can be defined by the following equation (Del Burgo et al., 2007; Xu et al., 2013 ; Junquera et al., 2004 ; Goltsov and Barsukov, 2000):

$$p_{eff} = \left(\frac{v_a}{a_a t} \right) \quad (3.11)$$

Thus, for $1/2 < p < 1$ vesicles are formed.

Table III-2. The Number of molecules N_x^{agg} , mole and the effective packing parameter of SRFA/DTAC Complex.

[DTAC]=7.6 10 ⁻³ mmol/L													
Bin size diameter (nm)	Whole Vesicles				Vesicle Outer Layer					Vesicle Inner layer			
	a_a (nm ²)	N^{agg}	v_a (nm ³)	n_t (x 10 ⁻²³ mol)	a_a (nm ²)	N_o^{agg}	v (nm ³)	n_o (x 10 ⁻²³ mol)	$P_{eff} = v_a/a_a * t$	a_a (nm ²)	N_i^{agg}	v_a (nm ³)	n_i (x 10 ⁻²³ mol)
6.35	0.17	1056	0.095	175.35	0.17	753	0.095	125.00	0.48	0.17	303	0.095	50.35
8	0.17	1797	0.096	298.41	0.17	1195	0.096	198.40	0.49	0.17	602	0.096	100.01
10.08	0.17	3021	0.097	501.66	0.17	1897	0.097	314.98	0.49	0.17	1124	0.097	186.68
12.71	0.17	5031	0.097	835.44	0.17	3016	0.097	500.79	0.50	0.17	2015	0.097	334.65
16.01	0.17	8284	0.097	1375.59	0.17	4785	0.097	794.59	0.50	0.17	3499	0.097	580.99
20.17	0.17	13543	0.097	2248.91	0.17	7595	0.097	1261.17	0.50	0.17	5948	0.097	987.73
25.42	0.17	22025	0.097	3657.35	0.17	12063	0.097	2003.15	0.50	0.17	9962	0.097	1654.20
32.02	0.17	35607	0.098	5912.86	0.17	19140	0.098	3178.38	0.50	0.17	16467	0.098	2734.49
40.35	0.17	57394	0.098	9530.68	0.17	30394	0.098	5047.19	0.50	0.17	27000	0.098	4483.48
50.84	0.17	92201	0.098	15310.62	0.17	48252	0.098	8012.61	0.50	0.17	43949	0.098	7298.01

At the moment, not knowing the amount of DTAC associated in any self-assembly, it is not possible to infer the architectural characteristics of each of the constituents (*i.e.* SRFA and DTAC) in the SRFA/DTAC complex. Nevertheless, this calculation approach can be useful with additional complementary experiments, such as Surfactants selective electrodes to identify the amount of surfactant associated in any self-assembly and phase diagram to identify the mole fraction. This will lead to the possibility to infer the architectural characteristics of each of the constituents (*i.e.* HS and Surfactant) in the SRHS/Surfactant complex from the geometrical constraints associated with the formation of a given molecular structure. Therefore, knowing the number of DTAC in the complex I can then refer the number of SRFA, hence, estimating the molar mass (average molecular weight). Concomitantly, knowing the mole fraction can help in estimating the polar head area and the chain volume of SRFA and DTAC separately.

III.4 SMALL ANGLE NEUTRON SCATTERING (SANS)

The SANS experiments were not included in the paper because they were carried out at 5g/L and the results are not completely comparable with those obtained at lower concentrations (lower pH, higher HS concentration). Vesicles were not evidenced in SANS experiments but such result is plausible in the phase diagram of a catanionic system.

III.4-1 Sample Preparation

For SANS experiments, SRFA 0.5% w/w was dissolved in D₂O in order to minimize the incoherent background from hydrogen thus yielding a higher scattering contrast. The SRFA/DTAC complexes were prepared by adding aliquots of the surfactant stock solution, prepared at 10 g/L in deionised water (Millipore-MilliQ 18.Ω.cm), to 1 mL of SRFA suspension.

III.4-2 Characterization of SRFA/DTAC Complexes

The SANS experiments were performed at the D22 SANS instrument at Institut Laue-Langevin (ILL), Grenoble, France. A range of scattering vectors q from 0.001 to 0.6 Å⁻¹ was covered by using three sample-to-detector distances (1.1, 5.6, and 17.6 m) at the neutron wavelength of 8 Å. The samples were kept in quartz cells (Hellma) with a path length of 2 mm for samples in D₂O and maintained at 25°C. The raw data were corrected for background

scattering from the sample transmission, empty sample cell (EC), detector efficiency (Cd/B₄C) and any other sources to produce the Q dependence of the intensity for each sample (Tucker et al., 2008 ; Claesson et al., 2000). The curves were then normalized using water as standard according to Grillo (2008). Data analysis benefitted from SasView software (DANSE/SANSview 2.1.0), originally developed by the DANSE project under NSF award DMR-0520547 (*SasView*, <http://www.sasview.org/>).

III.4-3 Small Angle Neutron Scattering Measurements

Figure III-12 shows the double-logarithmic plot of $I(Q)$ versus Q from SRFA_{5g/L}/DTAC mixtures in D₂O as a function of cationic surfactant concentration. Two types of patterns can be distinguished: at low DTAC concentration, $\log(I(Q))$ linearly decreases over about a decade in Q ; it then levels off because of the large incoherent scattering associated with the rather high SRFA concentration used (Diallo et al., 2005). Above a surfactant concentration of 0.189 mmol/L, in addition to the power-law decay at low Q , the scattering curves show a stronger decay at large Q that identifies a Porod regime. In all cases, the SANS curves do not exhibit a well-defined Guinier region at low Q . This implies that the characteristic size of the larger scattering objects ($R=2\pi/Q_{\min}$) is greater than 325 nm ($Q_{\min}=1.9 \cdot 10^{-3} \text{ \AA}^{-1}$).

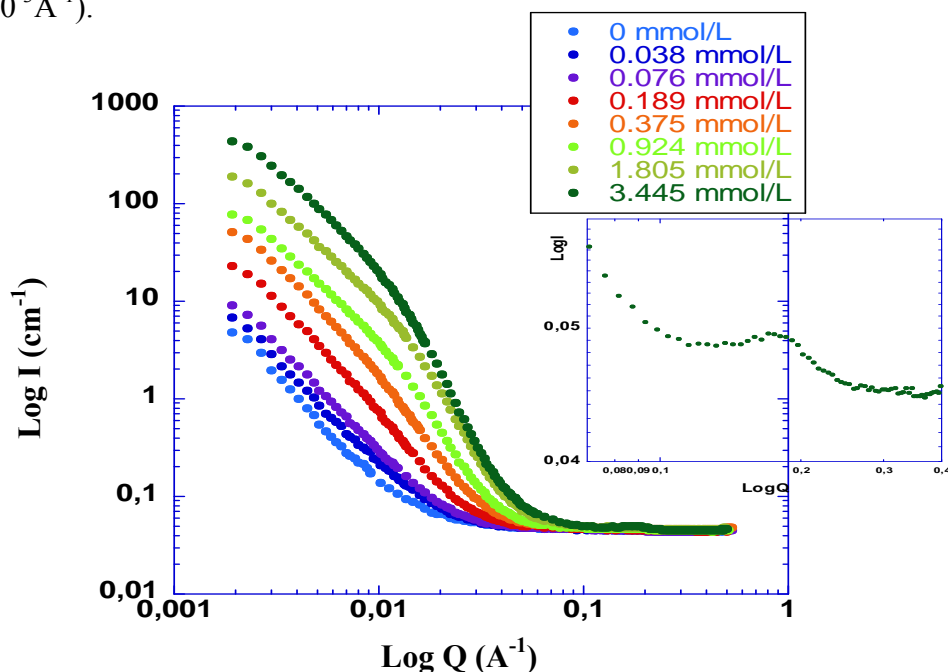


Figure III-12. Small-angle neutron scattering curves from SRFA_{5g/L} in presence of various DTAC concentrations. The inset shows the high Q behaviour of $[\text{DTAC}] = 3.445 \text{ mmol/L}$ with a small correlation peak identifying a bilayer of DTAC molecules.

The initial power-law decay of $I(Q)$ at low Q is typical of fractal aggregates (Martin and Hurd, 1987). It can be modeled with:

$$I(Q) = A Q^{-D_1} + B \quad (3.12)$$

Where A is a scale factor, D_1 is the fractal dimension, and B is the incoherent background scattered intensity. Applied to the reference SRFA solution and to the first two DTAC concentrations, fractal dimensions close to 2.2 for the SRFA/DTAC aggregates and to 2.5 for SRFA are obtained (Table III-3). The latter value is slightly higher than the fractal dimensions previously reported for SRFA in similar solution conditions (Diallo et al., 2005 ; Osterberg and Mortensen, 1994), but it remains consistent with the structure of an aggregate made from partially coalescing particles as seen by cryoTEM (inset of fig. III-7a) (Jarvie and King, 2007).

For the SANS curves that exhibit a cross-over between the fractal and Porod regimes, the scattering intensity $I(Q)$ can be fitted more adequately using the power law:

$$I(q) \begin{cases} \frac{A}{q^{D_1}} & \text{For } q \leq q_c \\ \frac{A \cdot q^{D_1}}{q^{D_2}} & \text{For } q > q_c \end{cases} \quad (3.13)$$

where q_c is the location of the crossover from one slope to the other, A is a scale factor that sets the overall intensity of the lower Q power law region, D_1 and D_2 are the fractal dimensions before and after q_c , respectively. The fitted parameters values are listed in Table III-3. If $D \leq 3$ the scattering objects are considered as mass fractal aggregates; if $D > 3$ they are described as surface fractals (Schmidt, 1989 ; Schmidt, 1995).

Table III-3. Absolute Power Law and Two Power Law Fitting parameters for SRFA_{5g/L} as a function of DTAC concentration.

SRFA g/L	DTAC mmol/L	D ₁ fractal dimension	qc (Å ⁻¹)	D ₂ Fractal dimension	A scale	B (cm ⁻¹) background	χ ² goodness of fitting ¹
Absolute Power Law							
	0	2.51±0.016			9.19e-07±7.97e-08	0.050±0.0012	3.71
	0.038	2.27±0.014			5.25e-06±4.16e-07	0.041±0.0020	1.99
	0.076	2.21±0.010			1.06e-05±6.11e-07	0.019±0.0021	2.90
Two Power Law							
5	0.189	2.21±0.0043	0.0089±5.74e-05	3.01±0.0057	2.91e-05±6.76e-07	0.045±1.81e-05	6.95
	0.375	2.18±0.0023	0.010±2.75e-05	3.30±0.0035	8.26e-05±1.02e-06	0.046±1.77e-05	15.22
	0.924	1.78±0.00202	0.012±1.32e-05	3.64±0.0026	3.90e-04±2.97e-06	0.045±1.78e-05	16.51
	1.805	1.75±0.00112	0.013±7.42e-06	3.81±0.0014	1.12e-03±5.05e-06	0.046±1.84e-05	37.39
	3.445	1.80±0.00099	0.012±5.09e-06	4.01±0.0012	1.74e-03±5.16e-06	0.046±1.81e-05	77.97

¹The goodness-of-fit parameter is given by: $\chi^2 = \frac{1}{N-p-1} \sum_i \left(\frac{y-y_i}{\sigma_i} \right)^2$

where N is the number of data points, p is the number of fitting parameter, y is the fitted value, y_i is the measured value and σ_i is the estimated standard deviation for y_i. σ_i was taken as the standard deviation of the measured scattered intensity I(Q). The magnitudes of χ² show that the power law model provides reasonably good fits of the SANS curves.

In principle, the values of D₁ can be used to identify the underlying aggregation process. Thus, the fractal dimensions close to 2.1-2.2 observed at low DTAC concentrations should be consistent with a reaction-limited cluster-cluster aggregation model (RLCA); which is a slow growth process, where the particles and clusters must overcome the repulsive energy barrier to produce dense aggregates (Meakin, 1991); whereas the fractal dimensions of 1.75-1.8 obtained at high DTAC concentrations should characterize a diffusion-limited cluster-cluster aggregation (DLCA); which is a fast growth process where the particles and clusters come in close contact, during their random motion in solution, resulting in the formation of loose aggregates (Jullien and Botet, 1987). Likewise, fractal prod exponents of 3 to 4 at low surfactant concentration should reveal a rough surface whereas the D₂ value close to 4 obtained at a DTAC concentration of 1.8 mmol/L should be associated with a smooth surface (Jarvie and King, 2007 ; King, 1999). Interestingly, a small correlation peak at Q = 0.17 Å⁻¹ can be detected at the highest DTAC concentration used, *i.e.* 3.445 mmol/L,

that identifies a characteristic length scale of 3.68 nm. Such distance corresponds precisely with the length of a bilayer of DTAC molecules, which then confirms the presence of stacks of platelets at this surfactant concentration.

In SANS data treatment, two categories can be considered, the discrete objects (vesicles, spheres...) and random system (aggregates). Dealing with natural colloidal system embraced with the difficulty that scatterings are unlikely to be from regular geometric shapes (spheres, lamellae, cylinder...) especially that they exhibited polydispersity in size distribution, thus, affecting data resolution. The validity of such analyses can nevertheless be argued from the perspective of cryoTEM results. Indeed, although the micrographs are obtained at a lower SRFA concentration (1g/L), and though most aggregates in suspension are certainly drained away during the blotting process, they reveal a variety of structures whose features do not seem to be captured by the SANS curves. Attempts to model the scattering curves as the product of a particle form factor $P(Q)$ and an interparticle structure factor $S(Q)$, *i.e.* $I(Q)=A \cdot P(Q) \cdot S(Q)+B$ (Chen and Teixeira, 1986), yielded mixed results.

III.5 INTERMEDIATE CONCLUSIONS

The organization of Suwannee River Fulvic Acid investigated through the interaction of SRFA with a cationic surfactant molecule (DTAC), using Cryo-TEM, shows sequence of molecular structures typically found in phase diagrams of catanionic systems. The geometrical constraints associated with the formation of these structures especially vesicles imply that a major component of SRFA is an individual amphiphile negatively charged of molecular size similar to that of DTAC. Hence, SRFA is viewed as a supramolecular assembly of various anionic surfactant molecules.

Furthermore, we were able to infer average geometric characteristics of SRFA/DTAC complex (*i.e.* polar head area, alkyl chain volume, alkyl chain length and the number of molecules in the aggregates) according to the framework introduced by Israelachvili.

We show that such soft matter approach provides additional tools to assess the supramolecular architecture of SRFA. In the next chapter, we extend this approach to assess the organization of Suwannee River Humic Acid.

CHAPTER

(IV)

*Association of Suwannee River Humic
Acid with a Homologous Series of
Cationic Surfactants
(C_n-trimethyl ammonium chloride):
The Self-assemblies and Rearrangements*

IV.1 PREFACE

The interaction of surfactants with humic substance has recently been a subject of growing interest due to the wide range of applications of surfactants in domestic, biochemical and pharmaceutical products. However, the interest of previous studies was focused on the binding of detergent to humic colloids in the context of contaminant transport in the environment, for which such interaction affects the fate and bioavailability of organic and inorganic contaminants. Our approach used with SRFA provides additional tools to assess the supramolecular architecture of humic substance. In this chapter, we extend this soft matter approach to assess the organization of Suwannee River Humic Acid (SRHA). The Self-assemblies and rearrangements, induced by the combination of humic acid with a homologous series of cationic surfactants (C_n-trimethylammonium chloride) with different alkyl chain length, *i.e.* Octyl (C8), Dodecyl (C12) and Hexadecyl (C16) are investigated. The results are presented in the form of an article draft entitled ***“Reconformation of Humic Acid Induced by the Addition of Cationic Surfactants of Varying Alkyl Chain Length: Evidence of the Supramolecular Organization of Humic Substances.”***

In the second part, the pH of the SRHA stock solution was adjusted to 7. Such modification will affect the charge density, *i.e.* hydrophobic/hydrophilic ratio. The variation of the pH along with the varying alkyl chain lengths of the cationic surfactant will point out the effect of the chemical composition forming humic and fulvic acid, that will lead to some geometric constraints in SRHS/surfactant aggregates formed. The results are presented in the form of Rapid Communication Letter draft.

IV.2 RECONFORMATION OF HUMIC ACID INDUCED BY THE ADDITION OF CATIONIC SURFACTANTS OF VARYING ALKYL CHAIN LENGTH: EVIDENCE OF THE SUPRAMOLECULAR ORGANIZATION OF HUMIC SUBSTANCES.

IV.2-1 Introduction

Humic substances (HS), found in soil, water and sediments, represent the major organic matter component on earth (Woodwell and Houghton, 1977 ; Woodwell et al., 1978; Hayes et al., 1989 ; Gjessing, 1976). HS are key players of all biogeochemical processes that occur in the environment (Nebbioso and Piccolo, 2012 ; Piccolo and Conte, 1999 ; Maurice et al., 1995). They are composed of a heterogeneous mixture of biochemical substances resulting in a poorly understood structure. Besides their obvious role in carbon geocycling, their amphiphilic nature plays a significant role as protons buffer (Koopal et al., 2005 ; Milne et al., 2001) and in the transportation/sequestration of metal contaminants, xenobiotic molecules and hydrophobic organic pollutants (Ishiguro et al., 2007 ; Wershaw, 1999 ; Sutton and Sposito, 2005 ; Nebbioso and Piccolo, 2012 ; Cabaniss, 1990).

The association of HS with surfactants has been a subject of interest, due to the wide use of surfactants in domestic, biochemical and pharmaceutical products (Penfold et al., 2003 ; Nieuwkerk et al., 1998 ; Cottrell and Van-Peij, 2004 ; Kato et al., 2008). The HS/surfactant interaction has been considered from two main points of view in the literature: **(i)** the surfactant is viewed as a model organic pollutant introduced into the ecosystem through wastewater or pollutant remediation (Harwell et al., 1999), and the authors investigate the adsorption properties to assess the importance of HS-surfactant interaction on contaminants transportation/sequestration. The addition of a cationic surfactant drastically enhances the surface activity of humic substances and leads to micelles at lower concentration than that of the pure materials (Gamboa and Olea, 2006). Otto et al. (2003) found that HA improves the aggregation of sodium dodecyl sulfate (SDS) while cetyltrimethylammonium bromide binds more strongly to humic acid than fulvic acid, and forms ion pairs. Traina et al. (1996) demonstrated the significance of hydrophobic interaction from the complexation of HS with alkylbenzenesulfonate, that increases with alkyl chain lengths, and in other studies a phase separation due to precipitation as a result of neutralization and formation of hydrophobic humic/surfactant complex was reported (Adou et al., 2001). Binding isotherms and

potentiometric titration have been used to estimate the amount of surfactant bound to humic substances (Shirahama, 1998 ; Rodenhiser and Kwak, 1998). Humic acids bind more strongly to dodecylpyridinium than fulvic acid with a cooperative interaction of the latter (Yee et al., 2006a) and a limited interaction when a negatively charged surfactant (e.g. Sodium Dodecyl Sulfate) was used (Yee et al., 2009 ; Koopal et al., 2004). Koopal et al. (2004) also demonstrated the effect of longer alkyl chain surfactants that increase the hydrophobicity of HS/surfactant complex and their adsorption to them. The ionic strength and pH affect the binding; an increase in pH and a decrease in ionic strength enhance the interaction by increasing the charge density and decreasing counter-ions screening effect, respectively (Yee et al., 2006b ; Yee et al., 2007 ; Ishiguro et al., 2007). In summary, low concentrations of cationic surfactants bind strongly to HS, which is sufficient to drastically modify the physicochemical properties affecting the fate of HS and sequestration/bioavailability of organic pollutant.

On the other hand, **(ii)** surfactant has also been used to probe the cationic exchange capacity (CEC) of HS and eventually their effect on their organization. The interaction of cationic surfactants with humic substances affect their conformation, hence the fate and bioavailability of metallic and organic contaminants (Bors et al., 2001). Such structural modification, from disordered to ordered structure, was investigated by X-ray diffraction in the presence of alkylammonium-based surfactants, where a coagulation of humic matter was evidenced (Tombácz et al., 1988). De Nobili et al. (1989) suggested that the interaction of HS and cetyltrimethylammonium is mainly governed by electrostatic interaction. This lead to a stoichiometric precipitation between the cationic surfactant and the carboxylate groups of HS (Nobili et al., 1990). Shang and Rice (2007) examined the structural changes of HS-Cationic surfactant complexes using small-angle X-ray scattering and reported a collapse of HS network along with precipitation/redissolution as a result of charge neutralization/charge inversion respectively.

The different fractions of humic substances can be distinguished from their solubility in aqueous solutions. Fulvic acids are richer in acidic functional groups such as carboxylic acid, phenolic and ketonic groups and their content in aromatic and aliphatic moieties is less than those of humic acids. This led to envision humic acid structure as aromatic cores linked to different materials (Schulten and Schnitzer, 1995 ; Hosse and Wilkinson, 2001 ; Lead et al., 2000) except for aquagenic fulvic acids with more aliphatic chains than humic acids

(Malcolm, 1990). This accounts for the solubility of fulvic acid at any pH value and the insolubility of humic acids at low pH where deionization and protonation of their carboxylic groups takes place that render them more hydrophobic (Pompe et al., 1996). As a result, the variation of functional groups content (i.e. hydrophobic/hydrophilic moieties) between HA and FA should give rise to a different interaction behavior in response to any variation in their surrounding environment, e.g. an addition of cationic surfactants addition. In line with the previous approaches, Chaaban et al. (2016) have investigated the behavior of Suwannee River Fulvic Acid (SRFA) in the presence of a cationic surfactant molecule (Dodecyltrimethyl ammonium Chloride, DTAC), and they presented evidences of a supramolecular organization of fulvic acid as assembly of various anionic surfactant molecules.

The interest of the previous studies was focused on the binding of detergent to humic colloids in the context of contaminant transport in the environment. In this paper, we investigate the interaction of Suwannee River Humic Acid (SRHA), a reference material, with 3 surfactants of varying alkyl chain length. This will vary the geometrical characteristics of the SRHA/Surfactant complexes formed in order to elucidate their structural organization.

IV.2-2 Experimental Section: Materials and Methods

Suwannee River Humic acid (SRHA) was purchased in solid-state powder from the IHSS (Humic Acid Standard 2S101H). All the surfactants: Octyltrimethyl ammonium chloride “OTAC” ($C_{11}H_{26}ClN$; purity $\geq 97\%$), Dodecyltrimethyl ammonium chloride “DTAC” ($C_{15}H_{34}ClN$; purity $\geq 99\%$) and Cetyltrimethyl ammonium chloride “CTAC” ($C_{19}H_{42}ClN$; purity $\geq 98\%$) were purchased from Sigma-Aldrich. DTAC is readily soluble in water at ambient temperature (Laschewsky et al., 2005 ; Prévost et al., 2011), with a Krafft temperature below $0^{\circ}C$ and its critical micelle concentration (CMC) at $30^{\circ}C$ is 21.7mM (Perger and Bešter-Rogač, 2007). With a Krafft temperature of $18^{\circ}C$, CTAC solubility in water is around 440 mg/L and CMC of 1.3mM at $30^{\circ}C$ (Tan et al., 2010 ; Singh and Hinze, 1982 ; Mata et al., 2005 ; Sakamoto et al., 2002 ; Karlstroem et al., 1990). OTAC possesses a CMC of 250mM at $28^{\circ}C$ with a Krafft temperature below $0^{\circ}C$ (Lindblom and Lindman, 1973). Both Humic acid and surfactants were used without further purification.

The DTAC and CTAC stock solutions were prepared at 10 g/L and 200mg/L in deionised water (Millipore-MilliQ 18.2 M Ω .cm), respectively. For OTAC, the stock solutions were prepared at three different concentrations, *i.e.* 10, 35 and 70g/L. The concentration of the SRHA was adapted to the technique of investigation. For Turbidity, Dynamic Light Scattering, Surface Tension and Electrophoretic Mobility measurements, a SRHA suspension of 20 mg/L, *i.e.* 12 mg C/L, was prepared by adding the appropriate mass of humic acid into 500 mL of deionised water. For Cryo-TEM, stock suspensions of 1g/L were used. The SRHA stock solutions were mechanically mixed overnight to ensure a well-dispersed suspension, and then vacuum filtered through a membrane (Membranfilter porafil) of 0.2 μ m porosity in order to remove any impurities. The pH of SRHA suspension was adjusted to 7 ± 0.05 by dropwise addition of 1N NaOH when necessary. The preparation and the methods of Characterization of SRHA/Surfactants complexes are similar to that previously described for SRFA/DTAC.

IV.2-3 Results

IV.2-3-1 Turbidity and DLS Measurements

Figure IV-1 shows the temporal evolution of the turbidity of SRHA/Surfactants mixtures obtained after various Surfactants, *i.e.* DTAC, CTAC and OTAC, additions to a 20 mg/L (*i.e.* 12mg C/L) Humic acid solution at inherent pH (4.52, 4.5 and 4.3 respectively). At the various range of concentrations, the turbidity increases to reach a plateau after about 20 minutes, except for DTAC at 4.65 and 6.32mmol/L, where the turbidity is characterized by a rapid early overshoot followed by a slow stabilizing trend (fig. IV-1a). The values measured for SRHA/OTAC (*i.e.* ~7 NTU) are very low and obtained at very high OTAC concentration (fig. IV-1b) compared to those of SRHA/DTAC (*i.e.* ~90 NTU) and of SRHA/CTAC (*i.e.* ~50 NTU) (fig. IV-1c).

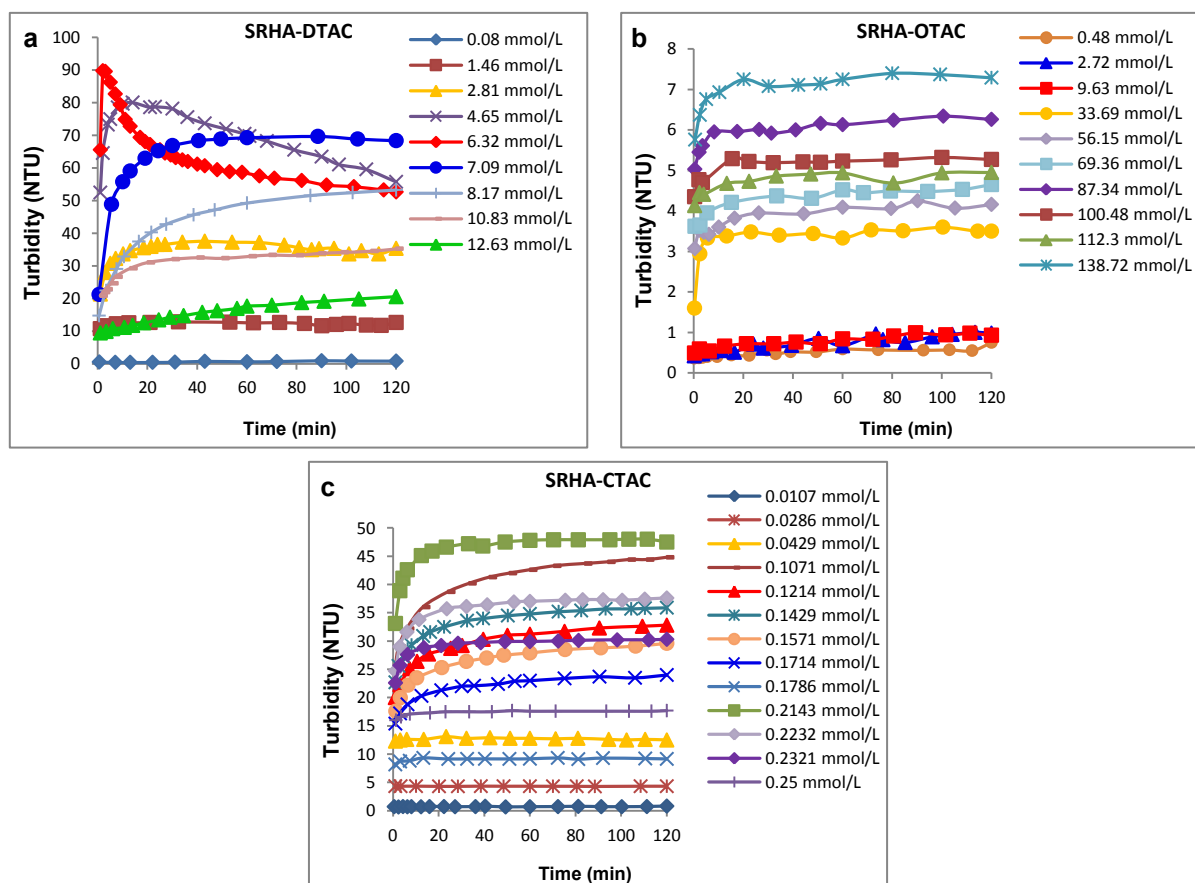


Figure IV-1. The temporal evolution of the turbidity of SRHA_{20mg/L}/Surfactant suspensions as a function of time obtained for various surfactant additions.

At steady-state, *i.e.* after one hour, the variation of turbidity with DTAC concentration is characterized by an asymmetric curve (fig. IV-2). This asymmetry confirms the presence of two different behaviors depending on the concentration of DTAC, in a way that the turbidity increases sharply to reach a maximum value after which it gradually decreases. Indeed, this observation shows the formation of one or more new structures due to the interaction between SRHA and DTAC, followed by an additional structural modification for a certain concentration of DTAC. This change could correspond to a molecular rearrangement leading to structures with less light scattering effect. Regarding SRHA/CTAC, the variation of turbidity is characterized by a noisy pattern which could be due to partial aggregation (*i.e.* small and large aggregates). For SRHA/OTAC, the interaction is not very strong with little variation in turbidity even at high OTAC concentration ($\geq 0.15\text{CMC}$).

Such behavior suggests that the interaction between humic substances and cationic surfactant is not only governed by charge neutralization, but is also due to hydrophobic

interaction between bound surfactants (Cooperative binding nature of surfactant) and between surfactant alkyl chain with other SRHA and/or SRHA/Surfactant aggregates.

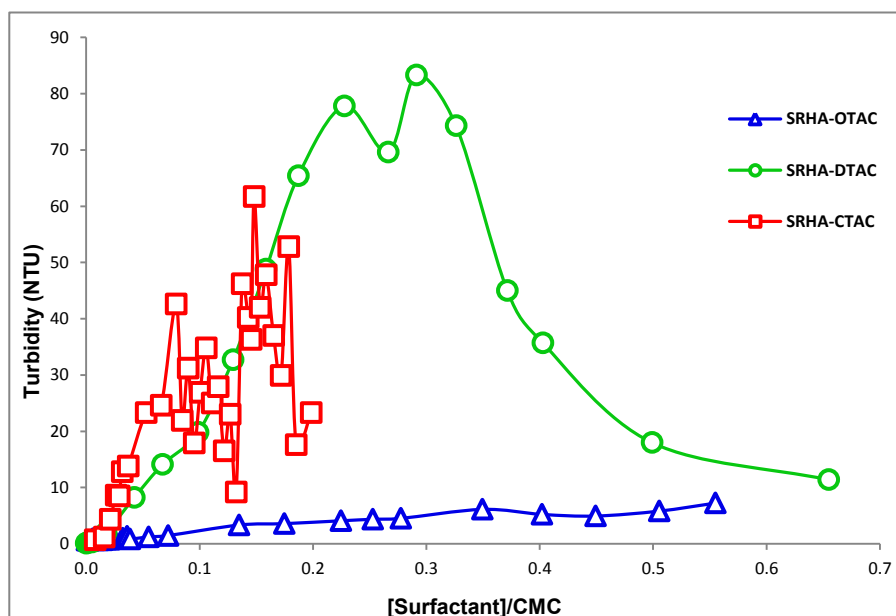


Figure IV-2. Turbidity at 1 hour of SRHA_{20mg/L}/surfactant suspensions as a function of surfactant concentration normalized by CMC.

As illustrated in Figure IV-3, the variation of particle size, measured using VASCO Particle Size Analyzer “Cordouan Technologies”, at 1 hour as a function of [surfactant]/CMC, shows a basic unit of 70 nm formed regardless of the initial DTAC concentration added. Another molecular structure of size between 200 and 400 nm is also obtained. We can clearly see that above a [surfactant]/CMC of 0.04, the particle size strongly increases, which is in agreement with the turbidity peaks. Therefore, at low DTAC concentration, the interactions between SRHA and DTAC contribute to the formation of new structures of size relatively stable regardless of the initial concentration of stock solutions. In addition, the linear increase in turbidity in this range of surfactant concentration indicates that it is the number of those molecular structures which increases and not their size or shape (inset of fig. IV-3). For CTAC an opposite pattern to DTAC can be observed. At low [CTAC]/CMC, *i.e.* 0.0013CMC, the size obtained is around 142.5nm. Upon further increase in concentration, the size decreases to about 70nm. Above 0.008CMC, the particle size drastically increased to values (>4 μ m) which is due to formation of larger aggregates. However, such values are over the detection limit of the technique used. While for SRHA/OTAC no reading was obtained, which is consistent with the limited interaction detected by turbidity measurement (fig. IV-2).

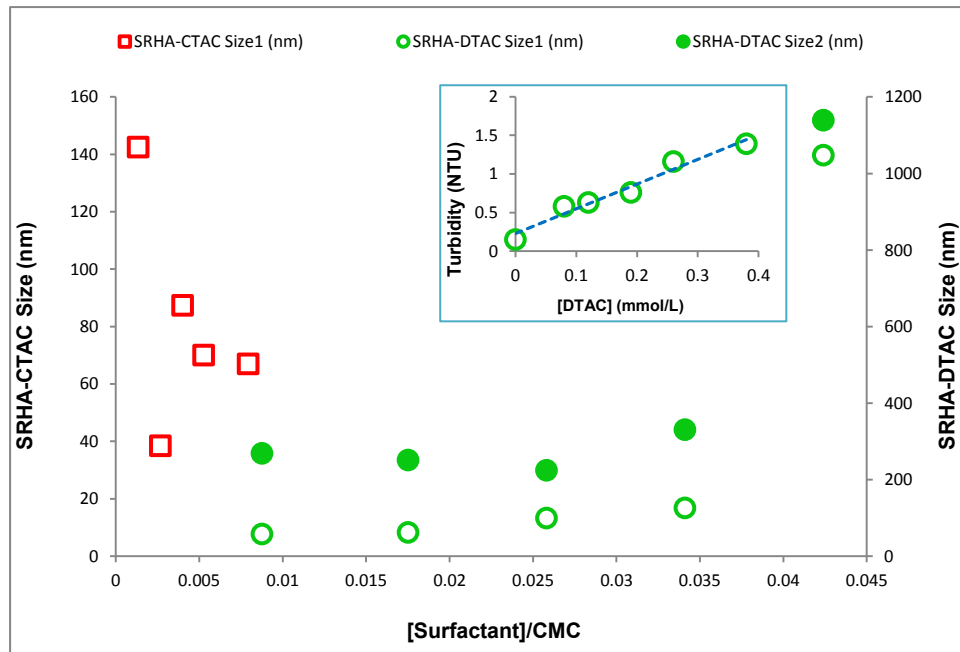


Figure IV-3. SRHA_{20mg/L}/Surfactant Particles sizes as a function of [Surfactant]/CMC. The inset is the turbidity curve of SRHA/DTAC for comparison.

The pH of the SRHA/Surfactants mixtures, slightly acidic between 4 and 5, show no considerable variation compared with that of the initial stock solution (fig. IV-4). The fluctuations noted could be due to protons released upon cationic surfactant adsorption to the humic acid (Ishiguro et al., 2007).

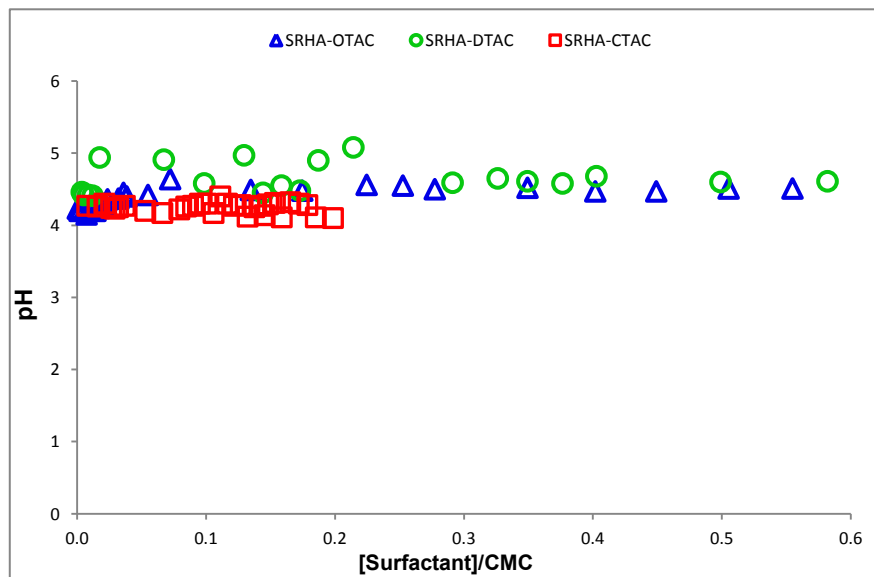


Figure IV-4. Variation of pH as a function of [Surfactant]/CMC for SRHA_{20mg/L}/Surfactant suspensions.

Figure IV-5 shows a linear increase in conductivity as a function DTAC and OTAC concentration. The change in conductivity is certainly due to the release of chloride ions by the surfactant during interactions SRHA/Surfactants. The linear increase was not seen for SRHA/CTAC, this could probably be due to the formation of microdomains that are capable of rebinding counter chloride ions.

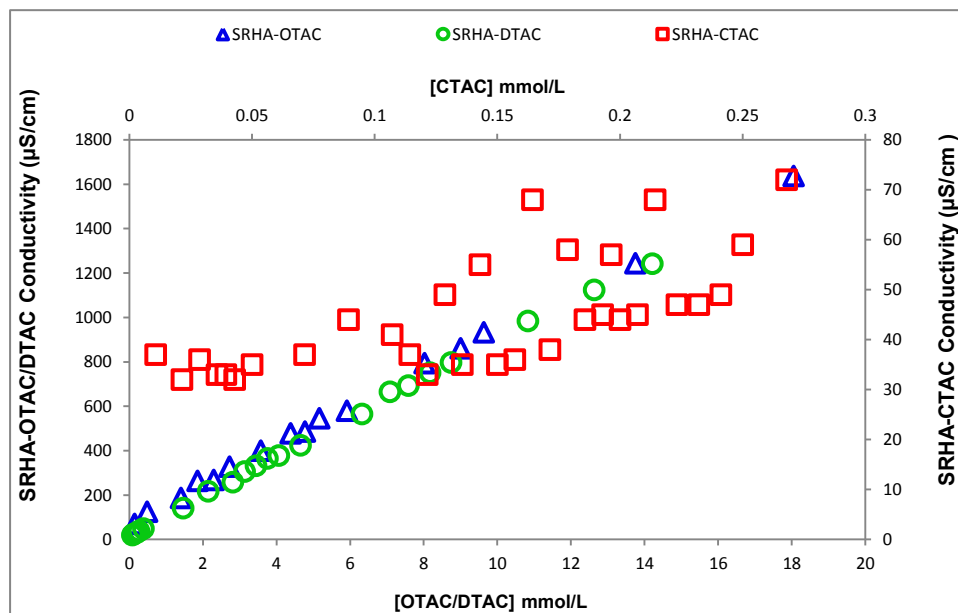


Figure IV-5. Variation of Conductivity ($\mu\text{S}/\text{cm}$) versus surfactant concentration for SRHA_{20mg/L}/Surfactant suspensions.

IV.2-3-2 Electrophoretic Mobility and Surface Tension Measurements

Figure IV-6 shows the electrophoretic mobility of SRHA/Surfactant complexes as a function of surfactant concentration normalized by CMC. For DTAC, the electrophoretic mobility increases upon surfactant addition, with a minimum at the start of the turbidity peak, then reaches positive values above 0.15CMC that coincides with the sharp increase in turbidity, and then further increases over the range of DTAC concentration used. A similar phenomenon is obtained with CTAC except at low concentration; we noted a decrease towards more negative values in the electrophoretic mobility with a minimum that coincides with the start of the first turbidity peak at 0.0107mmol/L. Such pattern suggests a significant reorganization of the humic colloid; humic acid internal hydrophobic domains could be viewed as loosely constructed and relatively accessible, the reformation allowing the detection of some internal charges (Engebretson and von Wandruszka, 1994). Indeed, a minor variation of turbidity in this concentration range along with a size reduction into

smaller subunits is observed which suggests a deaggregation of HS into smaller units as a result of a significant molecular rearrangement due to the increased electrostatic repulsion (fig. IV-7). Overall, such behavior is consistent with the charge neutralization, *i.e.* the reduction of negative charge, of humic acid functional groups with the cationic surfactant that leads to the formation of one or more new molecular structures upon the formation of SRHA/Surfactant complex as well as to the cooperative binding of surfactants that leads to the increase in electrophoretic mobility after neutralization. Such result is consistent with the SRFA/DTAC interaction reported by Chaaban et al. (2016)

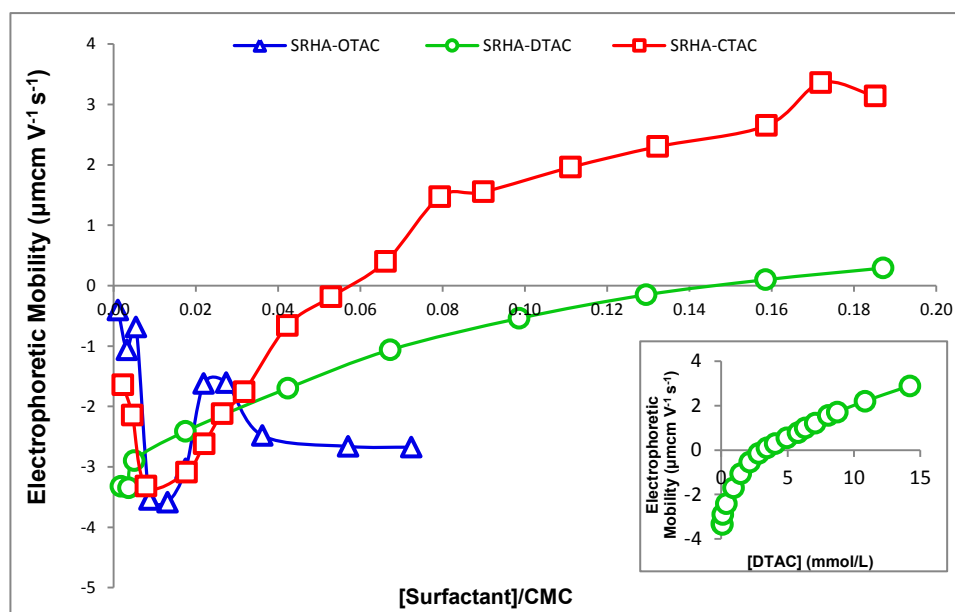


Figure IV-6. Electrophoretic mobility of SRHA_{20mg/L}/Surfactant suspensions versus surfactant concentration normalized by CMC. The inset is the electrophoretic mobility of SRHA/DTAC over the range of concentration used.

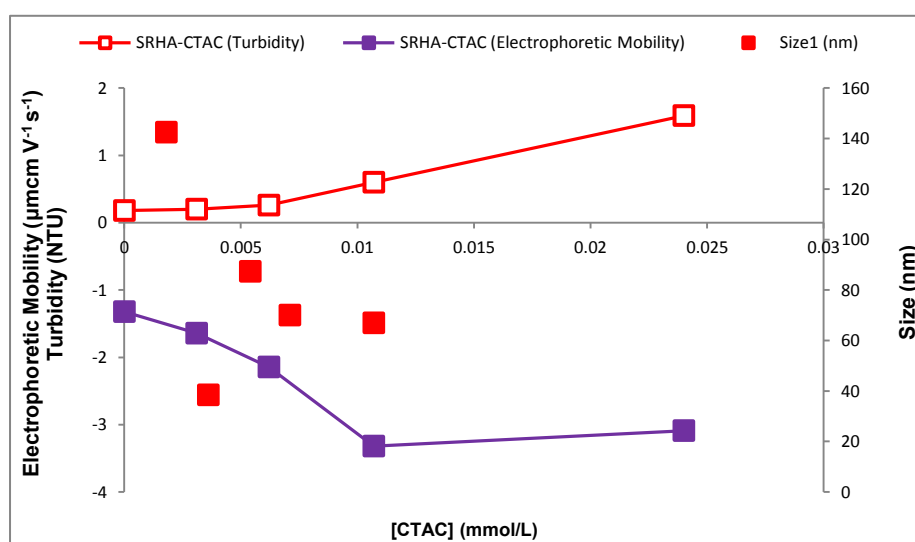


Figure IV-7. Electrophoretic mobility of SRHA_{20mg/L}/CTAC suspensions at low concentration. The turbidity and size curves are shown in order to locate the main variations of electrophoretic mobility.

The significance of the hydrophobic interactions can be clearly seen when OTAC is used. The electrophoretic mobility becomes more negative upon OTAC addition to reach a minimum at 0.013CMC, then increases and stabilizes over the range of concentration used. Interestingly, all the values remain negative. Such behavior might be a result of the limited hydrophobic interaction due to the short alkyl chain of the surfactant. This restricts any major rearrangement of the humic acid, and hence inaccessibility of some internal charges for neutralization. This result is in line with the turbidity measurements; where no significant variation was detected, and it is limited to very high OTAC concentration illustrating the significance of the cooperative binding nature of surfactant where HS/Surfactant interaction and the formation of aggregates is not only governed by charge neutralization, but also by a major role of the hydrophobic interactions.

Figure IV-8a shows the surface tension of SRHA/Surfactant complexes as a function of surfactant concentration normalized by CMC. The SRHA/DTAC complexes are highly surface active if compared to the pure surfactants (Figure IV-8b, IV-8c and IV-8d): indeed, at very low DTAC concentration a drastic reduction in surface tension is measured, and it then keeps decreasing gradually over the concentration range investigated (Olea et al., 2000). Such effect is due to the charge neutralization and cooperative binding resulting from the strong electrostatic attraction between the oppositely charged species (Nguyen et al., 2014 ; Hayakawa and Kwak, 1982 ; Hayakawa et al., 1990). Interestingly, although CTAC is more hydrophobic than DTAC, in other terms the SRHA/CTAC complex is expected to be more surface active, the phenomenon pointed out in the electrophoretic mobility, *i.e.* the increase in charge, enhances the amphiphilic properties of the SRHA/CTAC, producing less surface-active complexes compared with SRHA/DTAC complexes. Concomitantly, the shorter alkyl chain length of OTAC makes it more hydrophilic, and with the lesser effect on charge neutralization, the SRHA/OTAC complex is expected to be the least surface active. Surprisingly, at a given surfactant/CMC ratio, OTAC reduces the surface tension more than CTAC, which might be a result of the higher amount of counterions produced in the case of OTAC if compared with that of CTAC (see the conductivity curve) where these ions are attracted and migrated to the air/water interface, hence, lowering the surface tension (Okuda et al., 1987 ; Góralczyk, 1996 ; Adamczyk et al., 1999).

Humic substances are well known surface active compounds due to their amphiphilic nature (*i.e.* hydrophobic/hydrophilic moieties) that resembles surfactant properties (von

Wandruszka, 2000 ; Wershaw, 1999 ; Guetzloff and Rice, 1994 ; Chen and Schnitzer, 1978). Thus, SRHA has the ability to reduce the surface tension in an aqueous solution (Terashima et al., 2004a), and the formation of micellar aggregates above CMC which this material would consist of relatively small and heterogeneous molecules "building blocks" held by weak hydrophobic interaction producing supramolecular associations.

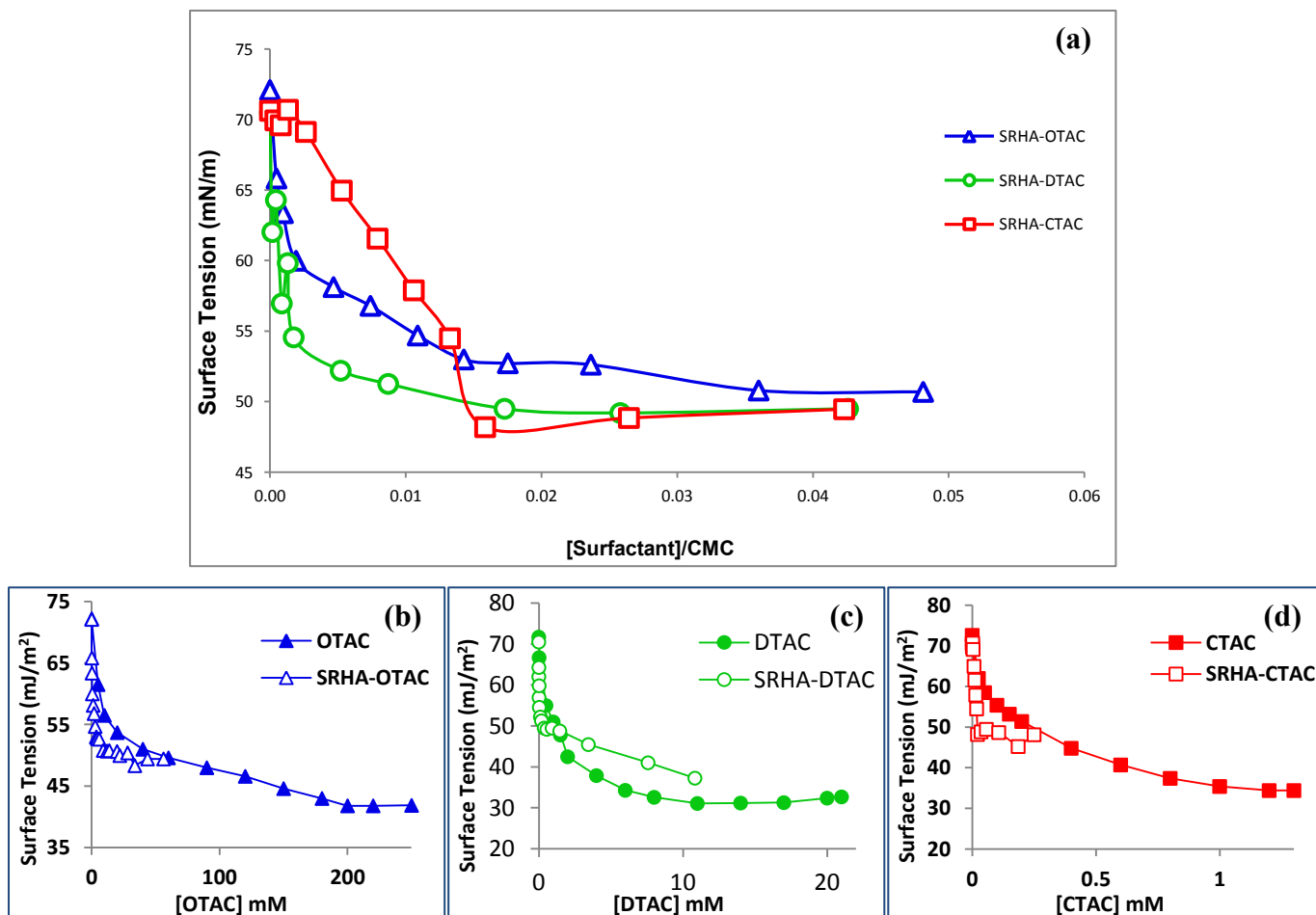


Figure IV-8. Surface Tension of: (a) SRHA_{20mg/L}/Surfactant suspensions versus surfactant concentration normalized by CMC; (b), (c) and (d) the Surfactants OTAC, DTAC and CTAC, respectively.

IV.2-3-3 Cryo-TEM Observations

The cryo-TEM experiments were conducted with a SRHA concentration of 1g/L at inherent pH (3.09). Such pH value will cause a reduction in HA initial charge and surfactant concentration required to induce any rearrangement. As illustrated in figure IV-9, various molecular structures were obtained from the mixing of SRHA with various DTAC concentrations. In the case of the reference humic acid (fig. IV-9a), *i.e.* 0 mmol/L DTAC, the cryo-TEM images show aggregate of globular structures. This type of organization may reflect an early stage of aggregation result from the low pH of the SRHA stock solution. An addition of 7.6×10^{-3} mmol/L of DTAC yields low abundant globular structures about 16-25nm in size (fig. IV-9b). These globules may represent the early stages of interaction between molecules of SRHS and DTAC. Increasing the concentration, sparse spongy networks are observed (Fig. IV-9c1) and the globules become more frequent with size segregation of small and larger globules (25-40nm) at 37.86×10^{-3} mmol/L (Fig. IV-9c2). The globules became larger in size (50nm), more frequent and close to each other and seem to merge to form aggregates usually composed of 3 to 6 aligned globules at 188.53×10^{-3} mmol/L (Fig. IV-9d1). At both concentrations, we can also observe some layer thickening of complete but more frequently open vesicles, around 2.04 nm that corresponds to the length of two DTAC alkyl chain, with formation of vesicles more evident at the latter concentration. This might point out the possibility of vesicle production in SRHA. In order to understand the effect of kinetics on aggregate formation of SRHA/DTAC complex, freezing was done at 120 minutes for 188.53×10^{-3} mmol/L (Fig. IV-9d2). No major variation can be pointed out; the globules are persisting but are more homogeneous in size and thinner because they are lighter in colour than before with 30-50nm in size as well as the layer wall thickening vesicle. This shows that after two hours, limited molecular rearrangement takes place. This is consistent with the turbidity measurements reported where the SRHA/Surfactant complex formed became stable around 20 minutes. Finally, a molecular rearrangement is observed again at the largest DTAC concentration investigated (375.19×10^{-3} mmol/L). Figure. IV-9e1 and IV-9e2, at 40 and 120 minutes respectively, show small polydisperse spheroidal particles with a size between 16-20 nm. These could be SRHA and DTAC interacting to form mixed micelles.

When longer alkyl chain surfactant was used, *i.e.* CTAC (C16), globules and aggregates of globules were the main dominant structures. An addition of 3.12×10^{-5} mmol/L

of CTAC yields few globular structures about 12-20nm in size with less developed spongy-like networks (fig. IV-9a'). With further addition of cationic surfactant, i.e. 18.7×10^{-5} mmol/L, the globules became more frequent with size segregation of small scattered and larger aggregates of globules (20-32nm). This could be due to the longer alkyl chain of the surfactant (C16) that could bind to adjacent globules through hydrophobic interaction forming the chain of the aligned globular aggregates (fig. IV-9b'). At CTAC concentration of 93.6×10^{-5} mmol/L, aggregates further increased into a spongy-like network (fig. IV-9c'). Finally, at the largest surfactant concentration investigated, i.e. 311×10^{-5} mmol/L, sparse and loosely aggregated spheroidal structures (16-25nm) are found (fig. IV-9d').

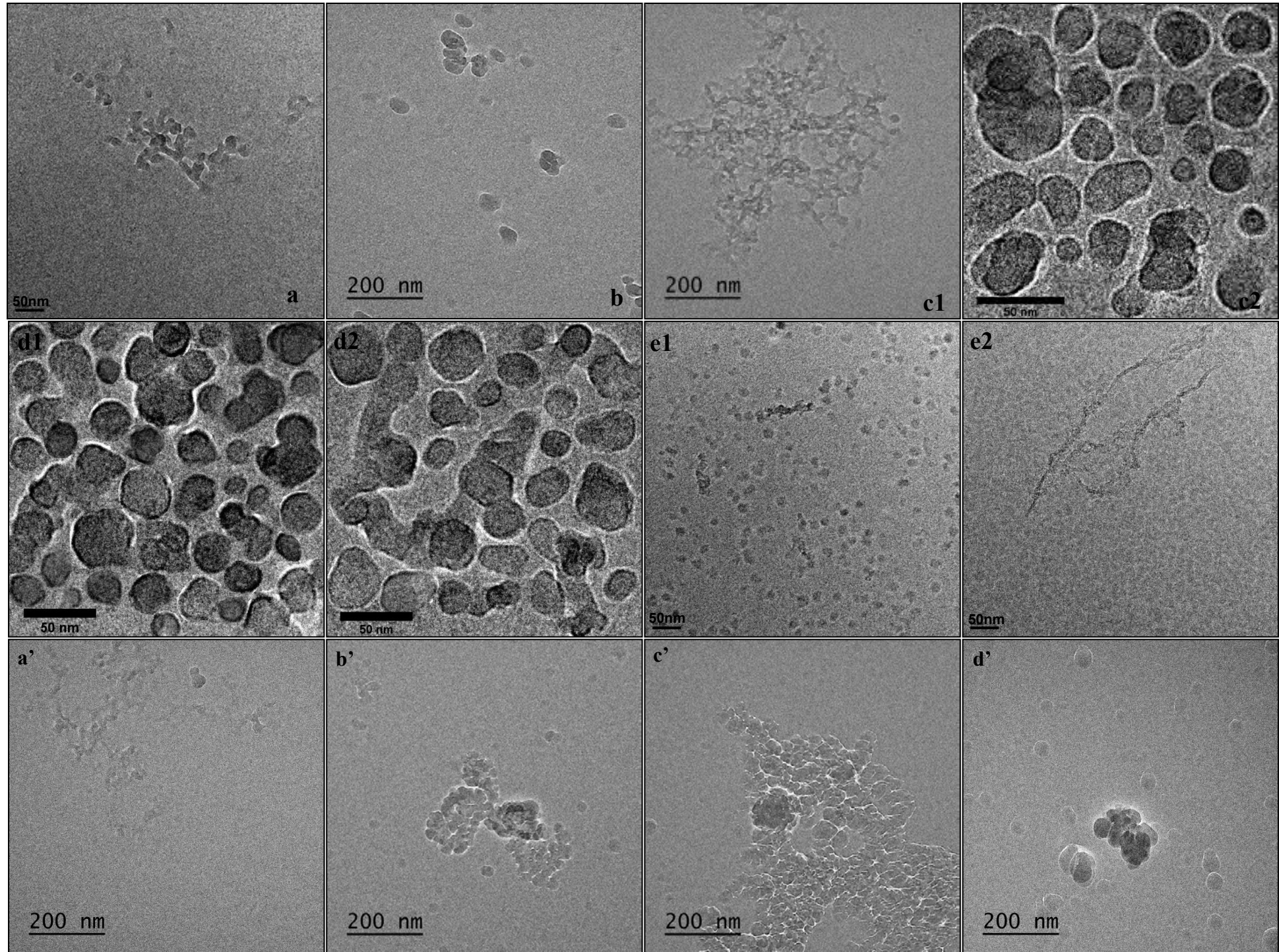


Figure IV-9. Cryo-TEM micrographs of SRHA_{1g/L}/Surfactant molecular structures. [DTAC] mmol/L: (a) 0; (b) $7.6 \cdot 10^{-3}$; (c1-2) $37.86 \cdot 10^{-3}$; (d1-2) $188.53 \cdot 10^{-3}$; (e1-2) $375.19 \cdot 10^{-3}$. [CTAC] mmol/L: (a') $3.12 \cdot 10^{-5}$; (b') $18.7 \cdot 10^{-5}$; (c') $93.6 \cdot 10^{-5}$; (d') $311 \cdot 10^{-5}$.

The size distributions of SRHA/Surfactant complexes observed by cryoTEM and their mean diameter as a function of surfactant concentration presented in Figure IV-10 and IV-11. All the distributions are unimodal. However, the blotting during sampling preparation removes large aggregates, this may lead to slight shifting towards the larger sizes every time an aggregation phenomenon has been detected on the micrographs (Lee et al., 2012).

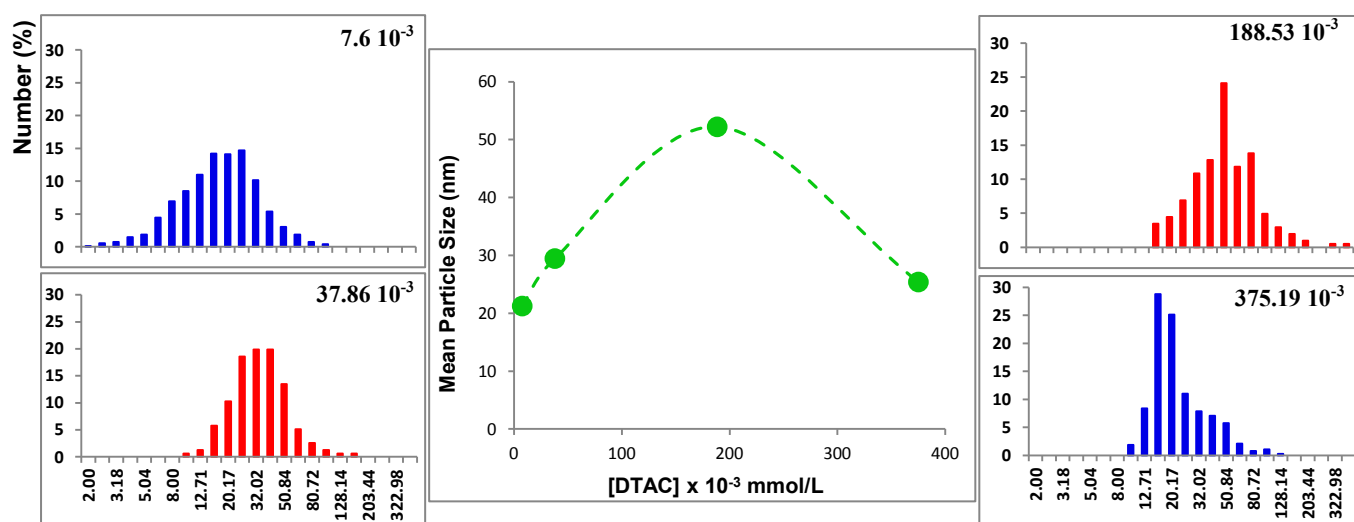


Figure IV-10. Size histograms (%) of molecular structures viewed by cryoTEM and evolution of mean particle size with DTAC concentration. The DTAC concentration is indicated in the histograms in mmol/L. The histograms in red are associated with the presence of layer thickening vesicles.

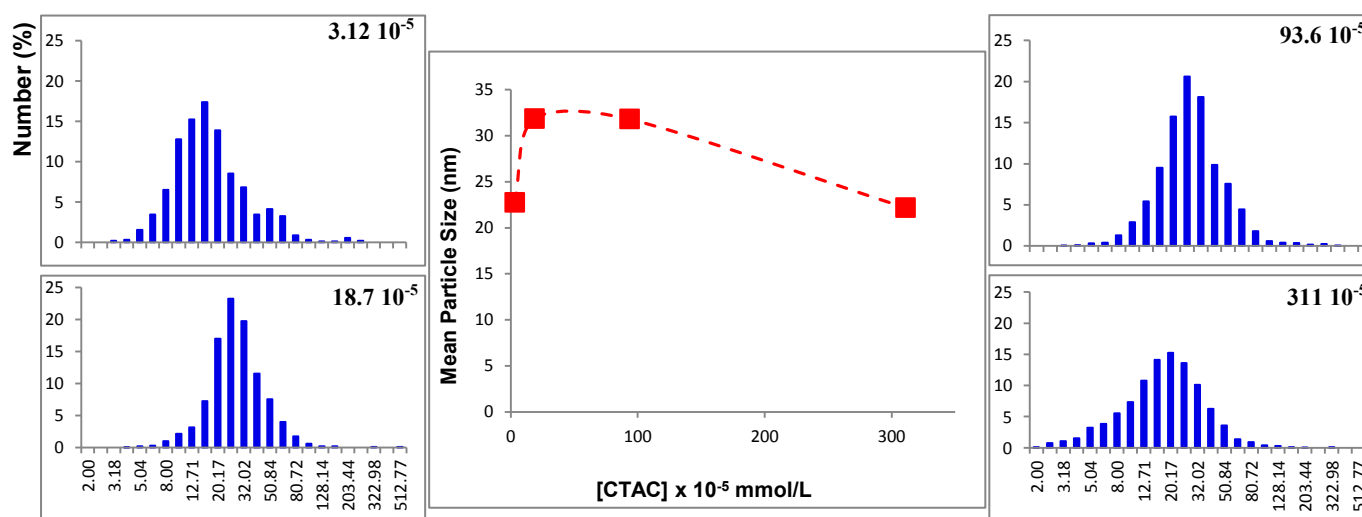


Figure IV-11. Size histograms (%) of molecular structures viewed by cryoTEM and evolution of mean particle size with CTAC concentration. The CTAC concentration is indicated in the histograms in mmol/L.

IV.2-4 Discussion

IV.2-4-1 Interaction between Humic Acid/Surfactant: Effect of Alkyl Chain Length

The amphiphilic nature of cationic surfactants makes it an appropriate candidate to assess in great detail the significance of HA interaction with organic and inorganic contaminants in the environment. It has been well-recognized that ionic surfactants bind cooperatively to oppositely charged polyelectrolytes because of electrostatic interactions and hydrophobic interactions of the bound surfactants and with the polyelectrolyte hydrophobic backbone (Shirahama et al., 1992 ; Kwak, 1998 ; Liu et al., 1999). Although the electrostatic interaction between cationic polar head of surfactant and anionic sites of SRHA molecules is one of the main driving forces in the binding of the Surfactants (DTAC, CTAC and OTAC), additional hydrophobic interactions obviously affect the binding mode. The absence of cooperative hydrophobic binding in SRHA/OTAC system might be the reason of the limited interaction of the short tailed surfactant (OTAC, C8) with SRHA when compared with that of DTAC (C12) and CTAC (C16); this is reflected in the slight increase in turbidity which might be due to the direct effect of the electrostatic interaction that is not enough to produce large aggregates through the hydrophobic binding with neighbouring surfactants and/or with adjacent SRHA/Surfactant complexes.

Increasing the alkyl chain length of surfactant, using DTAC and CTAC, improves the cooperative binding, i.e. the HS/surfactant interaction. This effect is more pronounced for C16 where the longer alkyl chain will enhance the hydrophobicity of HS/CTAC complex and their adsorption to HS and to other surrounding complexes; hence, this will lead to the formation of larger aggregates. Indeed, from the turbidity and DLS measurement much lower concentration of CTAC, compared to DTAC, was required to obtain detectable values. Such behavior suggests that low surfactant concentrations mainly reflect the binding of cationic surfactant to the oppositely charged functional groups of SRHS, whereas at high concentration, i.e. around and after neutralization, the association between SRHS and surfactant is essentially driven by hydrophobic interactions in presence of excess surfactant (Koopal et al., 2004).

In general, a low concentration of cationic surfactants is sufficient for establishing strong binding to HS. This interaction will modify their physicochemical properties such as their surface activity that leads to molecular rearrangement and the formation of micelle-like

structures. Therefore, a cationic surfactant can be used to probe the internal structure of humic colloids.

IV.2-4-2 Organization of Humic Substances

The effect of solution conditions such as pH and ionic strength have been extensively studied and found to affect the structural modifications of HS conformation (Glaser and Edzwald, 1979 ; Avena et al., 1999). HAs are somehow more aromatic, less aliphatic and are poorer in carboxylic acid and phenolic groups which make them more hydrophobic and less soluble (Gaffney et al., 1996 ; Otto et al., 2003). This result in lower density of ionic sites, and because of the large size of HA, the binding sites seem to be far apart, which in turn will prevent the cooperative binding (Davies et al., 1998). Cationic surfactants show greater binding strength to HA due to the hydrophobic interaction between the hydrocarbon tail of the surfactant and the hydrophobic moieties of HA; while the hydrophobic interaction among the bound surfactants themselves causes the cooperative binding in FA (Yee, 2006). Hence, this will result in different molecular rearrangements.

From a thermodynamic point of view, this variation will cause geometric constraint on the self-assembly of SRHA/DTAC-CTAC. The smaller negative charge in humic acid and the acidic pH, will result in lower electrostatic repulsion between the polar group “*a*” (–COOH), hence the area of the polar head is low. Concomitantly, the high aromatic content will lead to higher volume of the hydrophobic chain “*v*”. According to the packing parameter ($p=v/a*l$), the low value of “*a*” and the high value to “*v*” will lead to higher “*p*”. Therefore, the addition of DTAC or CTAC will further decrease “*a*” and increase “*p*” to a value that does not correspond to spherical vesicles formation. This could be the reason for obtaining some incomplete open vesicles and planar bilayer with no clear evidence of spontaneous spherical vesicles formation in SRHA/DTAC. These bilayer structures might be distorted spherical vesicles due to the geometric constraint where they are thermodynamically disfavoured, hence, transition into more energetically stable structures. The absence of bilayers with CTAC is due to the longer alkyl chain which will enhance the cooperative binding and the formation of larger aggregates.

The polar head area of SRHA can be obtained from surface tension measurements (fig. IV-12) using Gibbs adsorption equation at the maximal value of $d\gamma/d\ln C$ (Chen and Schnitzer, 1978), and hence $a_{SRHA} = 0.25 \text{ nm}^2$. Using the average radius-of-gyration r_{SRHA} of

25 Å reported in the literature for HA (Osterberg and Mortensen, 1992), we obtained $v_{SRHA} = 0.21 \text{ nm}^3$. The methods of calculation are reported elsewhere (Chaaban et al., 2016)

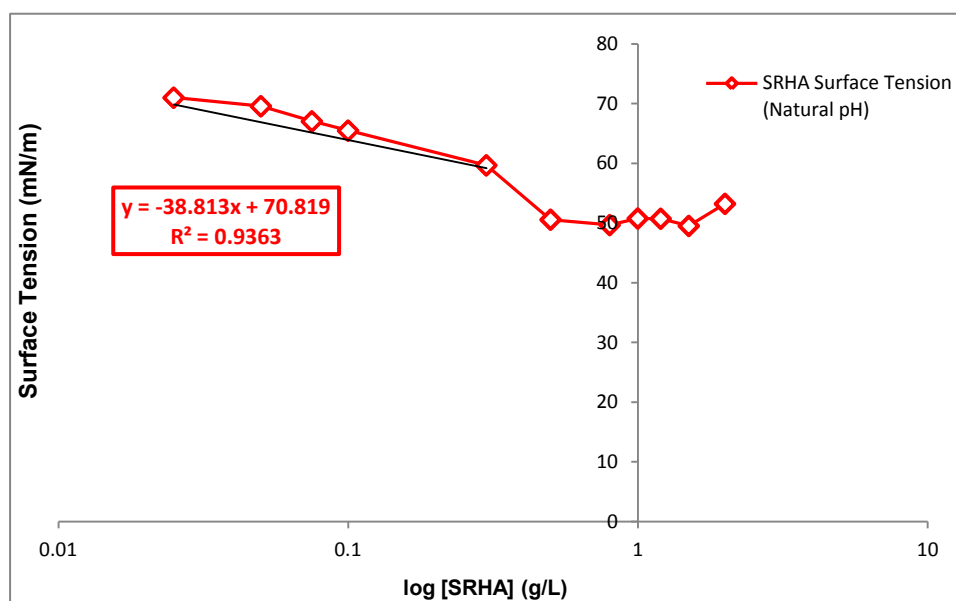


Figure IV-12. Surface tension of SRHA versus log [SRHA].

In the self-assembly, the surface contributions include the attractive hydrophobic or surface tension forces and the opposing repulsive forces, in particular of electrostatic origin. At some value of v/a^*l close to $1/2$, a spherical vesicle becomes the most favoured structure. As v/a^*l increases above $1/2$ the vesicle will grow. The values obtained in our experiments for the v and a , and upon surfactant addition, spherical vesicles are unlikely to occur in general due to packing constraint. The lower polar head area per outer amphiphile will affect the curvature; the peripheral regions will have great curvature while the central regions approach and become thicker and denser, eventually, distortions from spherical to an oblate shaped vesicles. Israelachvili et al. (1976) found that oblate shape is unacceptable due to the great curvature, hence, the central region is flattened so that locally it approaches a bilayer (open vesicles) and simultaneously the curvature of the peripheral regions is reduced, the packing criteria can be satisfied, becoming a planar bilayer when v/a^*l reaches 1.

Humic substances are detected as semipermeable spheres using atomic force microscopy (Marinsky and Ephraim, 1986 ; Kinniburgh et al., 1996). The effect of pH on peat humic acid aggregation was studied by dynamic light scattering: large aggregates were found in the 30-185nm range (Pinheiro et al., 1998, 1996). Baalousha et al. (2006) identified branched networks composed of a small number of elementary units of HS with a range of

sizes that increases with increasing ionic strength. The interaction of cationic surfactant with extracted soil HS was studied using X-ray microscopy: spherical particles of 224 nm in size were observed at low surfactant concentration; the size of the spheroid structures increased with higher concentration and the formation of some aggregates and network-like structure occurred predominately at high concentration (Thieme and Niemeyer, 1998)

Some early studies, using Zn dust distillation and hydrolysis, oxidation, reduction and spin resonance spectroscopy, performed on humic acids proposed structures made of aromatic core that is linked to different materials (peptides, metals, phenolic acids and carbohydrates) (Haworth, 1971 ; Cheshire et al., 1967). Other studies, using Liquid-NMR, have suggested the existence of a monomer subunit for humic acid based on aromatic groups with various branched functional groups (Steelink, 1985 ; Jansen et al., 1996). From pyrolysis/GC-MS analysis, a helical conformation of Temple Northeastern Birmingham (TNB) humic acid monomer was envisioned by Sein et al. (1999). More intricate structures have been suggested by Schulten and Schnitzer for the humic acid monomer using pyrolysis results (Schulten and Schnitzer, 1992a, 1992b), ^{13}C -NMR spectra (Schnitzer et al., 1991), , and electron microscopy observations (Stevenson and Schnitzer, 1982). They suggest a 2D model (Schulten and Schnitzer, 1993) and corresponding 3D structure (Schulten and Schnitzer, 1995 ; Schulten, 1995 ; Schulten and Gleixner, 1999) where it is based on aromatic fractions.

The differences in functionality and hydrophobicity/hydrophilicity balance between HA and FA, as a result of the distribution mode of the ionic binding site and the hydrophobic groups will result in variations in the binding behavior. The hydrophobic interaction can be seen through the molecular rearrangement and the generation of various molecular structures with the effect more pronounced for CTAC than DTAC. The longer tail of CTAC leads to the formation of larger aggregate through the binding of adjacent globules forming the chain of the aligned globular aggregates. Using DTAC, although no spontaneous vesicles formation is evident, we observed some layer thickening of incomplete open vesicles, globules. This might point out the possibility of vesicle production in SRHA with the appropriate experimental conditions.

The sequencing in which the different molecular structures is obtained, aggregates of globules with layer thickening and incomplete vesicle, second stage of layer thickening and

some complete and more frequent incomplete vesicles, and finally disperse globular micelles, indicates a drastic reorganization of the humic acid nanostructure. Hence, Humic acid can be viewed as supramolecular assembly of various anionic subunits. The variation between the mode of vesicles formation in SRHA compared with that found in the case of SRFA point out the difference between the constituents forming humic and fulvic acid, where HA can be viewed as aromatic core linked to different functional groups. The chemical composition causes some geometric constraints in SRHA/surfactant aggregates formed.

IV.3 EFFECT OF pH MODIFICATION

IV.3-1 Turbidity and Surface Tension Measurements

Figure IV-13 shows the variation of turbidity of SRHA/DTAC suspensions at pH=7, taken at 1 hour, as function of DTAC concentration. The variation is characterized by two well-resolved peaks at about 4 and 8mmol/L, 0.18CMC and 0.37CMC respectively, which was not found at the inherent pH (i.e. 4.52). The first peak is distinguished by a rapid overshoot and a backshift to lower concentration. Such behavior is consistent with the results reported regarding HS-cationic surfactant interaction; the binding is essentially driven by electrostatic attraction and at excess of surfactants the interaction is driven by hydrophobic interaction. Indeed, increasing the pH of SRHA increases the density of the negatively charged ionic sites through the ionization of phenolic groups; this might be the reason of the backshift of the first peak to lower concentration where the electrostatic interaction between SRHA-DTAC is enhanced. Furthermore, the ionic sites are now located close enough to each other to allow a cooperative binding of the bound surfactants, thus leading to the well-defined second peak (Yee, 2006).

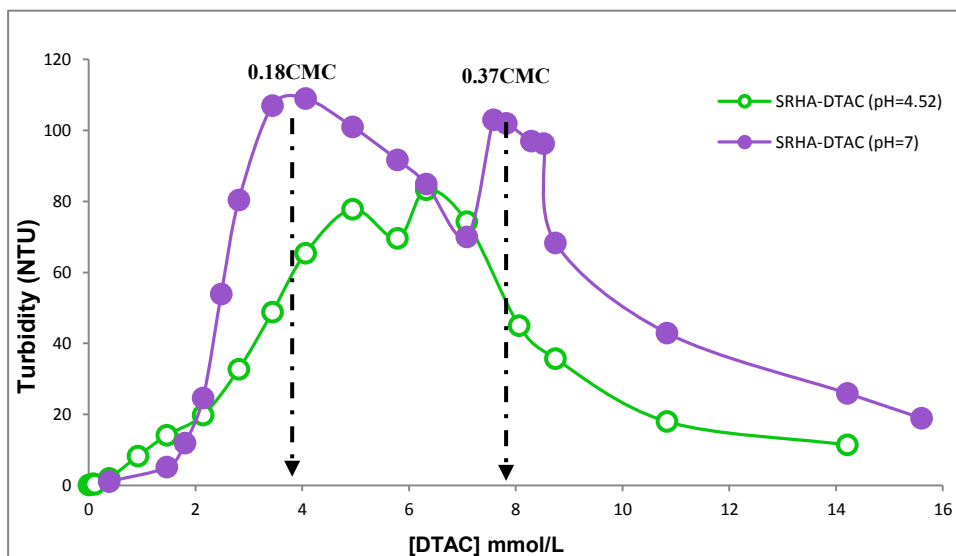


Figure IV-13. Turbidity variation of SRHA_{20mg/L}/DTAC suspensions at 1 hour as a function of DTAC concentration at pH=7. The turbidity of SRHA_{20mg/L}/DTAC suspensions at inherent pH=4.52 is added for comparison.

The enhanced cooperative binding is further confirmed when the surface tension of SRHA/DTAC complex at pH=7 is measured (Figure IV-14). The drastic reduction of surface tension, at very low DTAC concentration, reflects a highly surface active SRHA/DTAC complex. In addition, at pH 7, the surface tension is stabilized at lower value (~42mN/m) compared to that of pH 4.52 (~49mN/m).

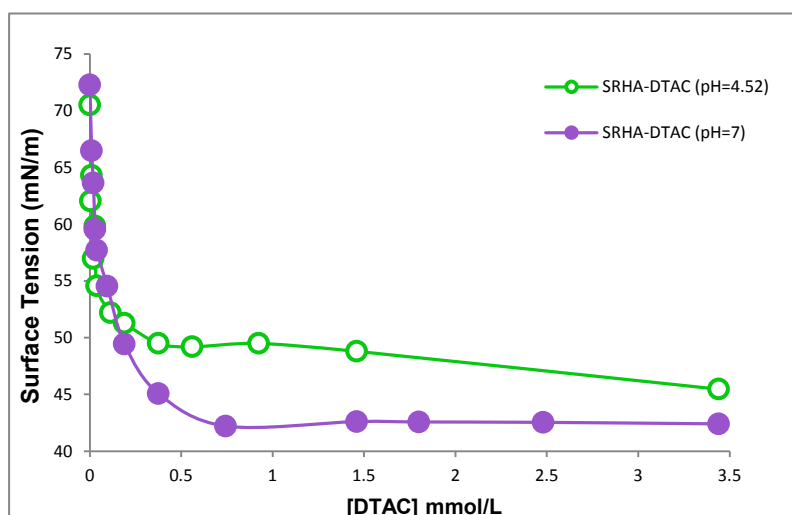


Figure IV-14. Surface Tension of SRHA_{20mg/L}/DTAC suspensions concentration at pH=7 versus surfactant concentration. The Surface tension of SRHA/DTAC suspensions at inherent pH=4.52 is added for comparison.

IV.3-2 Cryo-TEM Observations

In the SRHA/DTAC complex at inherent pH (i.e. 3.09), we observed some bilayer thickening and incomplete vesicle-like structures, but with no clear or abundant spontaneous vesicles formation. Increasing the pH of SRHA to 7, a similar turbidity pattern is obtained as that reported by Chaaban et al. (2016) for SRFA, with a slight shift to higher DTAC concentration of the second peak. Therefore, the Cryo-TEM observations were performed at DTAC concentrations similar to those where SRFA/DTAC complexes lead to vesicles (same concentration at fulvic-rich vesicles region and slightly higher concentration at DTAC-rich vesicles).

An addition of 7.58×10^{-3} mmol/L of DTAC yields unilamellar vesicles, both complete and open, mostly around 20 nm (fig. IV-15a and IV-15b), as well as sparse spongy networks with budding vesicles attached on the branches (fig. IV-15c). When the surfactant concentration is further increased (226×10^{-3} mmol/L), unilamellar and multilamellar vesicles, mean size of 30 nm, are again spontaneously formed (fig. IV-15d and IV-15e). Less developed spongy-like networks with nascent vesicles are also frequently observed (fig. IV-15f and inset of IV-15f). At low DTAC concentration we have humic-rich vesicles whereas the DTAC-rich vesicles obtained at higher surfactant concentration.

The functional groups composing the humic colloid affect the packing parameter of the SRHA/DTAC self assembly. The lower electrostatic repulsion of SRHA, due to the low content in carboxylic acid and phenolic groups, and the higher aromatic content will reduce the polar head area “ a ” and increase volume of the hydrophobic chain “ v ”, respectively. Hence, the value of the packing parameter ($p=v/a*l$) is high, the addition of DTAC will further reduce “ a ” and increase “ p ” that will add some constraint to the spontaneously formation of vesicles. The ionization of more functional group at pH 7, will increase the electrostatic repulsion and the polar head area, and on the other hand reduce the “ p ” to a value similar to that of SRFA where we had globular aggregates, *i.e.* $p \leq 1/3$ (Chaaban et al., 2016). Therefore, the DTAC addition will reduce the “ a ” and increase “ p ” where we could have structural transition to vesicles ($0.5 < p < 1$) as that obtained for SRFA/DTAC at inherent pH.

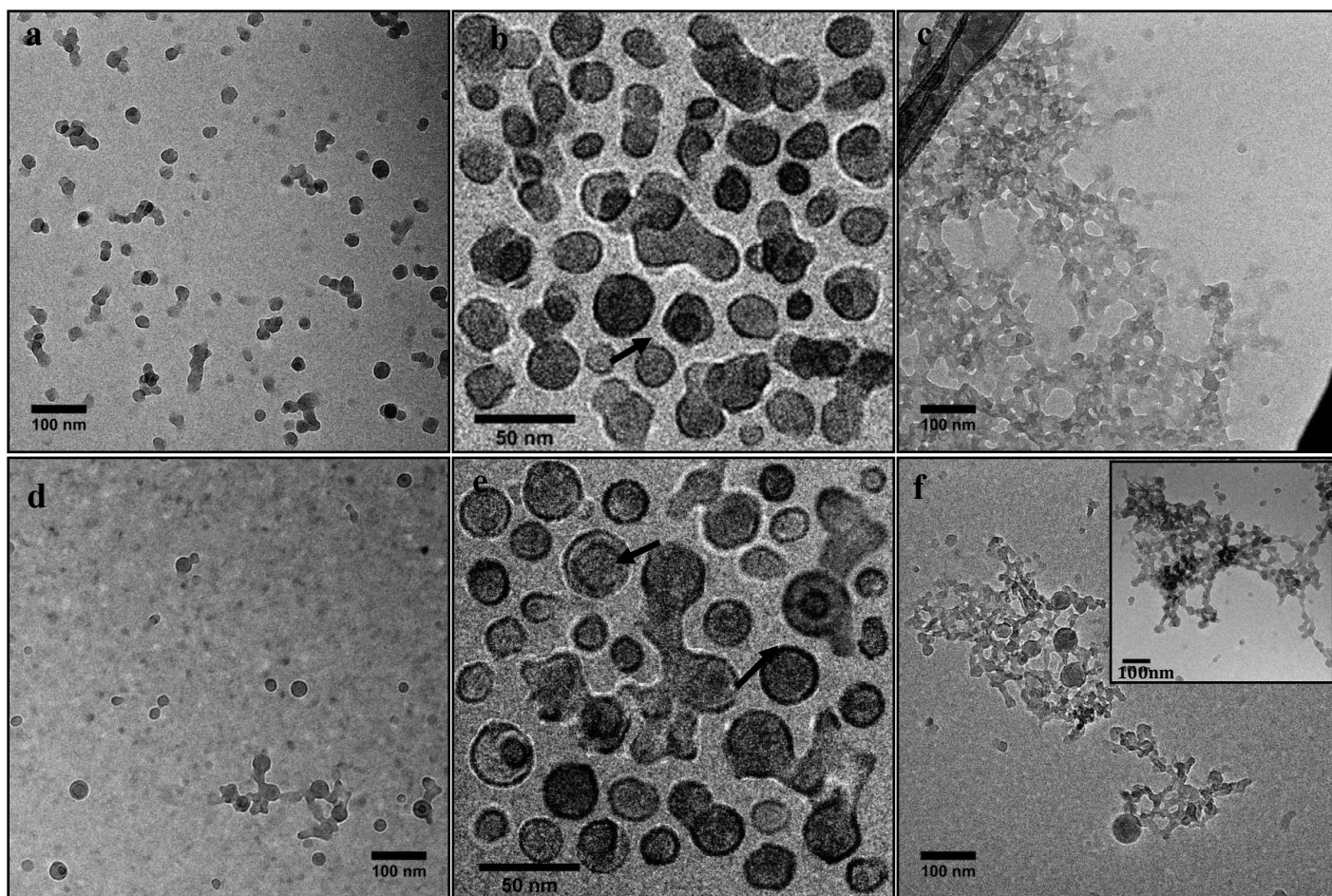


Figure IV-15. Cryo-TEM micrographs of SRHA_{1g/L}/DTAC molecular structures at pH=7. [DTAC] mmol/L: (a-c) $7.58 \cdot 10^{-3}$; (d-f) $226 \cdot 10^{-3}$. The arrow indicates the multilamellar vesicles.

The difference in the chemical constituents between HA and FA will affect their interaction with their surrounding environment (organic and inorganic compound). The variation of the hydrophobic/hydrophilic ratio seems to be a controlling factor, through which HA can be distinguished from FA. However, our results show that, with the appropriate experimental conditions, the mode of interaction seems to be similar. This raises questions about the boundary between the different fractions of humic substances.

IV.4 SMALL ANGLE NEUTRON SCATTERING (SANS)

The analysis of SANS data is carried out using two approaches: indirect model-independent and direct model-dependent. The latter gives detailed structural information, where a particular shape function (e.g. sphere, cylinder, vesicles...) is presumed to fit the experimental data. In many cases, the numerous adjustable parameters used for fitting may

raise some ambiguity. Under certain conditions, when a precise model is not available or too complex to use, an indirect model-independent approach is applied using empirical models that reproduce the observed trends in the SANS data. However, the shape of the aggregates cannot adequately determine where some detailed structural information will be lost and mainly the gross morphology is identified. For more reliable and unambiguous result, both approaches, model-independent and model-dependent, are combined (Kucerka et al., 2010 ; Mullins and Sheu, 2013).

IV.4-1 Small Angle Neutron Scattering Measurements

Figure IV-16 shows the double-logarithmic plot of $I(Q)$ versus Q from SRHA_{5g/L}/DTAC mixtures in D₂O as a function of cationic surfactant concentration. A typical SANS patterns can be distinguished: $\log(I(Q))$ linearly decreases over about a decade in Q at low DTAC concentration; it then levels off because of the large incoherent scattering associated with the rather high SRHA concentration used (Diallo et al., 2005). The evolution of shape is not evident at low DTAC concentration until 0.375mmol/L. In addition to the power-law decay at low Q , the scattering curves show decay at large Q that identifies a Porod regime.

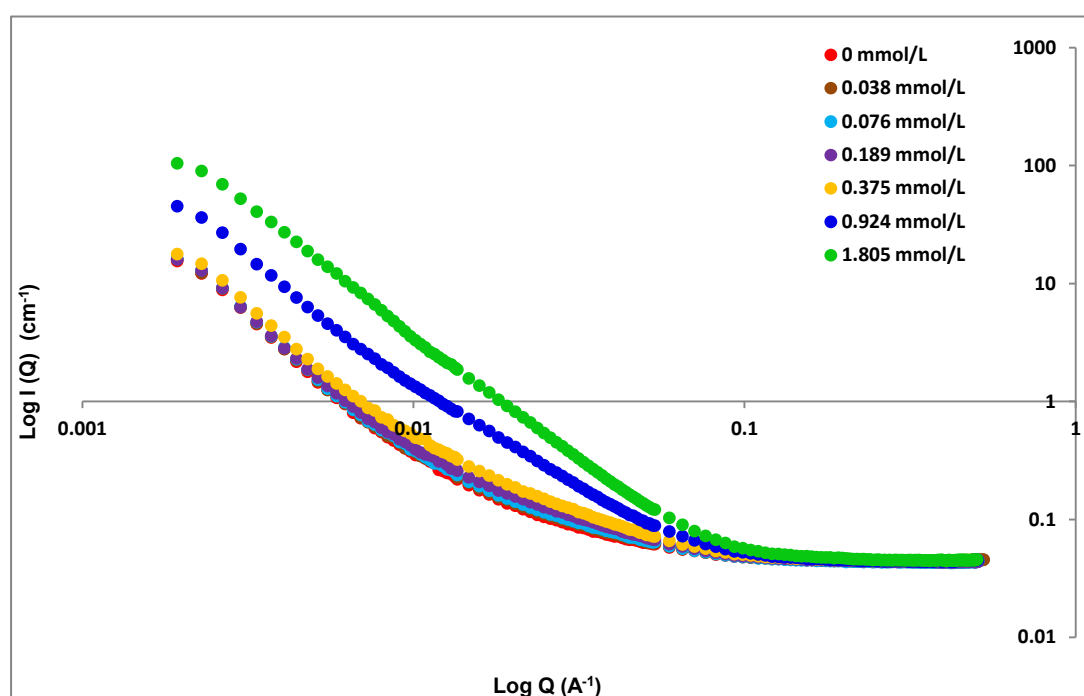


Figure IV-16. The double-logarithmic plot of $I(Q)$ versus Q from SRHA_{5g/L}/DTAC suspensions in D₂O as a function of cationic surfactant concentration.

The cryo-TEM experiments of SRHA_{1g/L}/DTAC show various discrete molecular structures such as globules, aligned globules and vesicles. In this case, using the model-dependent method, vesicle or globule functional model can yield detailed structural information. This can be also combined with model-independent approach as previously mention. However, the higher concentration of SRHA (i.e. 5g/L) used in SANS measurements led to discrepancies with the cryo-TEM, where most of the reported structures in the cryo-micrographs do not seem to be modeled by the SANS data using direct model-dependent approach. Therefore, the indirect approach using different empirical models was employed in order to extract as many parameters as possible that can help identifying possible structures.

IV.4-1-1 Two Power Law

The linear relationship is a characteristic feature of a fractal object (Martin and Hurd, 1987 ; Schmidt, 1991). Due to the presence of two range of decade in Q with a cross over from one slope to another between the fractal and Porod regimes, the scattering intensity I(Q) can be fitted using Two Power Law:

$$I(q) \begin{cases} \frac{A}{q^{D_1}} & \text{For } q \leq q_c \\ \frac{A \cdot q^{D_1}}{q^{D_2}} & \\ \frac{A}{q^{D_2}} & \text{For } q \geq q_c \end{cases} \quad (4.1)$$

Where q_c is the location of the crossover from one slope to the other, A is a scale factor that sets the overall intensity of the lower Q power law region, D_1 and D_2 are the fractal dimensions before and after q_c , respectively. The fitted parameters values are listed in Table IV-1.

Table IV-1. Two Power Law fitting parameters of SRHA_{5g/L}/DTAC suspensions for the various DTAC additions.

Two Power Law							
SRHA g/L	DTAC mmol/L	D ₁ fractal dimension	D ₂ fractal dimension	A scale	B (cm ⁻¹) background	qc (Å ⁻¹)	χ ² goodness of fitting
5	0	2.58 ±0.0076	1.85 ±0.01	1.82e-06±7.62e-08	0.048 ±0.00027	0.0083 ±9.33e-05	7.69
	0.038	2.57 ±0.0075	1.76 ±0.0098	1.96e-06 ±8.12e-08	0.047 ±0.00032	0.0083 ±8.0904e-05	8.60
	0.076	2.58 ±0.0074	1.72 ±0.01	1.94e-06 ±7.88e-08	0.046 ±0.00035	0.0082 ±7.73e-05	9.74
	0.189	2.50 ±0.0070	1.54 ±0.0098	2.97e-06 ±1.14e-07	0.041 ±0.00046	0.0086 ±6.78e-05	9.77
	0.375	2.44 ±0.0065	1.57 ±0.0072	5.01e-06 ±1.78e-07	0.04 ±0.00042	0.0082 ±6.13e-05	11.86
	0.924	2.33 ±0.0040	1.817 ±0.0032	2.52e-05 ±5.66e-07	0.021 ±0.0004	0.0070 ±4.93e-05	16.03
	1.805	2.26 ±0.0020	2.10 ±0.0025	1.06e-04 ±1.11e-06	0.014 ±0.00043	0.00013±1.11e-06	23.29

The aggregation process is identified from the value of D. All the values obtained are less than 3 which correspond to mass fractal aggregates of subunits such as branched systems of networks (Jarvie and King, 2007 ; Beaucage, 1996 ; Rice et al., 1999). At low DTAC concentrations (0-0.375mmol/L), the fractal dimension close to 2.5 described weakly segregated networks and percolating cluster; whereas the fractal dimensions of 2.25-2.3 obtained at high DTAC concentrations (0.924-1.805mmol/L) should be consistent with a reaction-limited cluster-cluster aggregation model (RLCA) (Jullien and Botet, 1987 ; Tombacz et al., 1997 ; Meakin, 1991). As for D₂, the fractal dimensions of 1.75-1.8 obtained at low DTAC concentrations (0-0.076mmol/L) should characterize a diffusion-limited cluster-cluster aggregation (DLCA), where the aggregates grow larger as particles and clusters come in close contact as they randomly move in solution (Diallo et al., 2005). Those values are closed to that of D=5/3=1.667 which is a signature for fully swollen coils in good solvent. At the highest concentration investigated, i.e. 1.805mmol/L, the fractal porod exponent of 2 reflects a Gaussian chains, lamellae, platelets or discs (Figure. IV-17) (Jarvie and King, 2007). These values are consistent with the fractal dimensions previously reported for humic acid (Diallo et al., 2005 ; Osterberg and Mortensen, 1992 ; Osterberg and Mortensen, 1994).

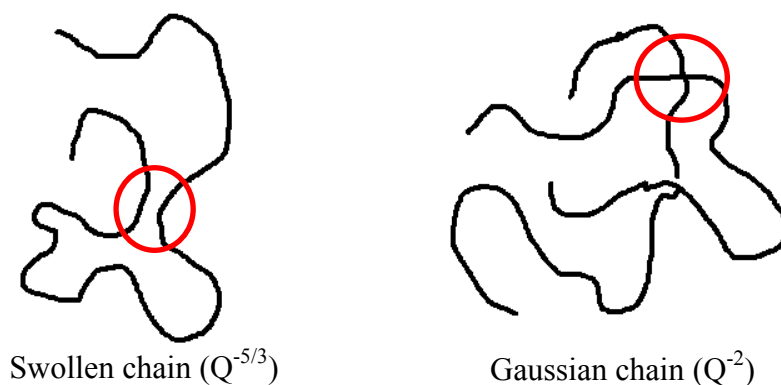


Figure IV-17. Illustration of swollen and Gaussian chain (Teixeira, 1988 ; Jarvie and King, 2007).

The presence of the swollen coils and Gaussian chains properties, Lorentzian or correlation length functions are invoked to describe the scattering from such structure of network or wormlike chains (Li et al., 2001 ; Griffiths et al., 2004), and to study the swollen and shrinkage in solution (Cosgrove et al., 1995 ; Karino et al., 2007 ; Nasimova et al., 2004), (Karino et al., 2004 ; Clark et al., 2010 ; Matsunaga et al., 2009).

IV.4-1-2 Two Correlation-Length Model (Two Lorentzian Model)

Following other SANS investigations of similar structures, two correlation-length model (Two Lorentzian Model) is used (Horkay et al., 1998 ; Zhou et al., 1998). The scattered intensity is fitted to the following functional form:

$$I(Q) = \frac{A}{1+(Q\xi_1)^n} + \frac{C}{1+(Q\xi_2)^m} + B \quad (4.2)$$

The first and second term are used to describe the low-Q (Cluster features) and high-Q (Chain network scattering) behavior, respectively. A and C are the relative weighting coefficients (Lorentzian scale), ξ_1 and ξ_2 are the long-range and short-range correlation lengths, respectively, and B is the incoherent scattering background, that refers to the standard deviation of the function. All DTAC concentrations are well fitted except for 0.924mmol/L. The absence of linear Guinier region at low-Q, the radii of gyration could not be estimated. Instead, we focused on the two correlation lengths ξ_1 - representing cluster sizes- and ξ_2 - representing network chain correlations (Figure IV-18).

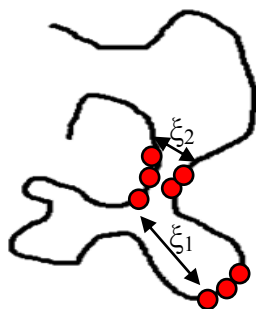


Figure IV-18. Illustration of the long range (ξ_1) and the short range (ξ_2) correlation length.

The fitted parameters values are listed in Table IV-2. The increasing or decreasing of ξ_1 and ξ_2 with concentration is when the clusters and network chain correlations get larger or smaller, respectively (Hammouda et al., 2002).

Table IV-2. The fitted parameters of SRHA_{5g/L}/DTAC suspensions for the various DTAC additions using Two Lorentzian Model.

Two Lorentzian Model									
SRHA (g/L)	DTAC (mmol/L)	B (cm ⁻¹)	m	ξ_2 (Å)	C	n	ξ_1 (Å)	A	χ^2
	0	0.044±2.99e-05	2.11±0.026	39.71±1.19	0.084±0.0039	2.69±0.02	1114.1±109.89	156.68±36.26	5.01
	0.038	0.044±2.4582e-05	2.50±0.032	31.05±0.61	0.067±0.0022	2.59±0.015	2348.7±1180.9	932.73±116.3	7.95
	0.076	0.043±2.71e-05	2.31±0.025	34.94±0.73	0.088±0.003	2.69±0.018	1468.9±260.08	317.79±138.4	4.20
5	0.189	0.043±2.63e-05	2.36±0.022	34.99±0.6	0.107±0.0031	2.64±0.018	1361.8±203.51	254.68±91.97	3.5
	0.375	0.044±2.46e-05	2.5±0.021	34.51±0.49	0.119±0.0033	2.51±0.016	2190.6±833.37	803.59±736.19	8.35
	0.924	0.045±1.81 e-04	2.56±0.21	4.41±0.11	0.006±0.0004	2.02±0.002	2987.3±466.11	1424.6±439.68	77.84
	1.805	0.044±2.05e-05	2.94±0.022	47.27±0.51	0.529±0.018	2.56±0.008	558.9±5.16	247.95±3.89	14.01

IV.4-1-3 Corrlength Model

Corrlength model is mainly used for the studying of polymer and gels. The scattered intensity is fitted to the following functional form:

$$I(Q) = \frac{A}{Q^n} + \frac{C}{1+(Q\xi)^m} + B \quad (4.3)$$

The first term describes Porod scattering from clusters, and the second term is a Lorentzian function describing scattering from the network chains. This second term characterizes the network/solvent interactions and therefore the thermodynamics. The solvation strength A and C , the incoherent background B , and the two exponents' n and m are used as fitting parameters, and ξ is a correlation length for the entangled network chains, that is equal to average distance between entanglements for semi-dilute solution and it is equal to the end-to-end distance for very dilute solution (Hammouda et al., 2004). The fitted parameters values are listed in Table IV- 3.

Table IV-3. Corrlength Model fitted parameters of SRHA_{5g/L}/DTAC suspensions for the various DTAC additions.

Corrlength Model								
SRHA (g/L)	DTAC (mmol/L)	B (cm ⁻¹)	n	m	ξ (Å)	C	A	χ^2
5	0	0.044 ± 2.87e-05	2.18 ± 0.027	2.61 ± 0.0085	35.41 ± 0.89	0.069 ± 0.0023	1.54e-06 ± 7.31e-08	5.09
	0.038	0.044 ± 2.41e-05	2.52 ± 0.031	2.58 ± 0.0075	30.67 ± 0.50	0.065 ± 0.0016	1.83e-06 ± 7.67e-08	7.95
	0.076	0.043 ± 2.64e-05	2.34 ± 0.024	2.62 ± 0.0082	33.61 ± 0.57	0.082 ± 0.0021	1.51e-06 ± 6.91e-08	4.23
	0.189	0.043 ± 2.57e-05	2.4 ± 0.021	2.59 ± 0.0083	33.79 ± 0.47	0.100 ± 0.0021	1.74e-06 ± 8.03e-08	3.54
	0.375	0.044 ± 2.41e-05	2.51 ± 0.02	2.49 ± 0.0072	34.07 ± 0.39	0.116 ± 0.0023	3.67e-06 ± 1.48e-07	8.36
	0.924	0.044 ± 2.12e-05	2.63 ± 0.014	2.44 ± 0.0057	51.40 ± 0.52	0.405 ± 0.0092	1.32e-05 ± 4.28e-07	10.96
	1.805	0.044 ± 2.25e-05	4.23 ± 0.065	2.30 ± 0.0017	40.51 ± 0.34	0.196 ± 0.0055	8.11e-05 ± 7.77e-07	76.47

The correlation length ξ is inversely related to the network volume or entanglement length. For low network volume fraction and high- Q , the chains radius of gyration is given by $R_g = \sqrt{2}\xi$ and the end-to-end chain distance is $R_{end} = \sqrt{6}R_g$ (Hammouda and Ho, 2007 ; Flory, 1953) (Table IV-4). The clustering strength is defined as A/Q^n , where $Q=0.004\text{Å}^{-1}$ (a low enough Q -value). High clustering strength corresponds to networks (where both chain-ends stick to other chains), and low clustering strength corresponds to dissolved chains (no chain-end sticking). The intermediate case corresponds to branched structures (only one chain-end is tethered to other chains) (Hammouda, 2009).

Table IV-4. The radius of gyration of globules that made up the network entanglement.

DTAC (mmol/L)	0	0.038	0.076	0.189	0.375	0.924	1.805
ξ (Å)	35.41	30.67	33.61	33.79	34.07	51.40	40.51
$R_g = \sqrt{2} \xi$ (Å)	50.07	43.37	47.54	47.79	48.18	72.69	57.29
$R_{end} = \sqrt{6} R_g$ (Å)	122.66	106.23	116.44	117.06	118.02	178.06	140.34

The cryo-micrographs show various molecular shape, however, the concentration used in the SANS experiments seems to affect the formed shape, that differ from that obtained with cryo-TEM. Using the shape-independent models, structure of network or wormlike chains was modeled and correlation-length was estimated that gives idea about cluster sizes and network chain interaction. All DTAC concentrations are well fitted and we can find a consistence between the fitted parameters of all empirical models used. The radius of gyration calculated range from 4-7nm, knowing that the radius of gyration are larger than the actual particle size, the calculated sizes are consistent with the characteristic size reported in the literature, this gives further evidence of the supramolecular nature of SRHA composed of small basic subunits which are interconnected by weak hydrophobic interactions.

IV.5 INTERMEDIATE CONCLUSIONS

The binding of cationic surfactants to humic substances is governed by the strong electrostatic attraction and the cooperative hydrophobic interactions, and starts at a very low concentration. The cooperative binding is enhanced with an increased alkyl chain length. These interactions induced drastic molecular rearrangements of the humic acid, producing sequence of different molecular structures including layer thickening and complete/incomplete vesicles. The geometrical constraint in SRHA/surfactant aggregates formed is due to the aromatic core of HA; which leads to the variation in the mode of vesicles formation in SRHA compared to SRFA. Therefore, there is a supramolecular assembly of various anionic subunits in the organization of humic acids.

It is of an interest to understand the effects of the drastic molecular rearrangements, upon the addition of cationic surfactant to HS, on the native chromophoric and fluorophoric groups in HS. In the next chapter, single-scan fluorescence emission spectroscopy is used to investigate and further confirm HS structural reformation and supramolecularity.

CHAPTER (V)

*The Effect of Molecular Rearrangement
on the Chromophores and Fluorophores
within Humic Substances upon
Interaction with Cationic Surfactant:
A Fluorimetric Study*

V.1 PREFACE

Fluorescence is a sensitive technique applied for the study of selective chromophore that fluoresces efficiently. Humic substance and dissolved organic matter have been extensively studied; the major fluorescent components that have been identified are those that correspond to humic-like substance and the other attributed to protein-like group (Mounier et al., 1999 ; De Souza Sierra et al., 1994). In Chapter V fluorescence spectroscopy is used to investigate and further confirm HS structural reformation and supramolecularity. The interactions between Suwannee river humic substances (SRFA and SRHA) with cationic surfactant (DTAC) are investigated to detect any molecular rearrangements that affect the native chromophoric and fluorophoric groups. The approach is then extended, for generalization of our results, with humic substances of different origins (Nyong humic acid, and a modeled humic-like substance) and dissolved organic matter from the Amazonas-Brazil (Rio-Negro and Rio-Jutai). The results are presented in the form of an article draft entitled *“Addition of DTAC Cationic Surfactant to Humic Substances Triggers the So-called Protein-like Fluorescence.”*

V.2 ADDITION OF DTAC CATIONIC SURFACTANT TO HUMIC SUBSTANCES TRIGGERS THE SO-CALLED PROTEIN-LIKE FLUORESCENCE.

V.2-1 Abstract

The interaction between a cationic surfactant (DodecyltrimethylAmmonium Chloride, (DTAC)) with various humic substances (HS) and with Dissolved Organic matter (DOM) from two Blackwater Rivers of the Central Amazon (Rio Negro and Rio Jutai) was investigated using single-scan fluorescence emission spectra. The addition of DTAC cationic surfactant to HS-DOM provokes drastic molecular rearrangements that unveil an unexpected fine structure of humic fluorescence. The newly emerged bands might result from a destacking of a possible supramolecular structure of HS. After DTAC addition, the fluorescence emission at 318/326 nm ($\lambda_{\text{ex}} = 230$ nm), generally attributed to protein-like fluorescence, is strongly enhanced and found to be roughly proportional to the humic-like fluorescence. Such result questions the use of protein fluorescence to assess anthropogenic inputs of wastewater in the environment.

V.2-2 Introduction

Fluorescence spectroscopy has recently emerged as a powerful technique for identifying and monitoring various sources of Dissolved Organic Matter (DOM) in aquatic systems (Hudson et al., 2007; Yamashita et al., 2008; Fellman et al., 2010). Two main components, humic-like and protein-like, are traditionally identified in fluorescent DOM (Coble, 1996; Mounier et al., 1999; Parlanti et al., 2000; De Souza Sierra et al., 1994). According to the nomenclatures proposed by Coble (1996) and Parlanti et al. (2000), humic-like substances are characterized by fluorophores A(α'), C(α) and M(β) that are excited in the UV and visible regions, respectively, whereas protein-like matter is described from B(γ) Tyrosine-like and T(δ) Tryptophan-like fluorophores (Table V-1). The humic fluorophores are detected regardless of the humic substances origin, *i.e.* organic matter from freshwater, coastal or marine water (Matthews et al., 1996 ; Baker, 2002a ; Sierra et al., 2005; Sheng and Yu, 2006), although at a given λ_{ex} the fluorescence of fulvic acid, the most soluble component of humic substances, is more intense and blue-shifted compared with that of humic acid (Coble, 1996; Sierra et al., 2000).

Table V-1. Typical Fluorophores detected in Dissolved organic matter according to the Excitation/Emission wavelengths at maximum intensity (Coble, 1996; Parlanti et al., 2000).

Peak	λ_{ex} (nm)	λ_{em} (nm)	Fluorescent Component
B (γ)	230/275	310	Tyrosine, protein
T (δ)	230/290	350	Tryptophan, protein or phenolic group
A (α')	260	380-480	Humic Substances
C (α)	300-350	420-480	Humic Substances (terrestrial or lignin origin)
M (β)	310-320	380-420	Marine Humic Substances

The tryptophan fluorescence was first used as an indicator of biological activity in sea waters, an intense T(δ) peak being related to bacterial and/or algal blooming (Traganza, 1969; Mopper and Schultz, 1993; Determann et al., 1998 ; Matthews et al., 1996). Further studies confirmed that T(δ) can be related to freshly produced DOM and provides an estimate of proteinaceous matter in coastal environments (Mayer et al., 1999; Yamashita and Tanoue, 2003). High intensity B(γ) (Tyrosine-like) and T(δ) peaks were also identified in various effluents, *i.e.* treated wastewater (Baker, 2002a; Baker, 2002b; Galapate et al., 1998; Reynolds, 2003), diffuse landfill leachates (Baker et al., 2004), combined sewer overflows (Baker et al., 2004 ; Ahmad and Reynolds, 1995), thus providing attractive tracers for following anthropogenic discharges in the natural environment (Baker et al., 2004). On the other hand, the fluorescence of the humic-like signal has provided a marker of humification (Zsolnay et al., 1999; Ohno, 2002), and it has been used to assess the amount of terrestrial DOM in surface waters (Smart et al., 1976) and in coastal and estuarine environments (Laane and Koole 1982; Matthews et al. 1996). The fluorescence properties of HS have also been used to discriminate between microbially-derived, terrestrially-derived, and anthropogenically-derived organic material (McKnight et al., 2001; Spencer et al., 2007).

Monitoring of water quality using DOM fluorescence is not however straightforward since various environmental effects such as a change in pH (Myneni et al., 1999; Westerhoff et al., 2001; Patel-Sorrentino et al., 2002; Chen and Kenny, 2007), ionic strength (Gao et al., 2015), temperature (Baker, 2005), or complexation of DOM with metal ions (Ryan and Weber, 1982; Reynolds and Ahmad, 1995), may significantly enhance or quench the fluorescence intensity. A change in the conformation of organic molecules, thus revealing or hiding fluorophores, is the explanation generally given for a modification in fluorescence intensity. Moreover, the exclusive attribution of B(γ) or T(δ) signals to proteinaceous

material has been argued since polyphenolic compounds may also present similar fluorescence emission characteristics (Sierra et al., 2005; Maie et al., 2007).

In this study, we show that the interaction of a cationic surfactant - Dodecyltrimethyl ammonium chloride (DTAC) - with various humic substances and DOM from blackwater sources- strongly enhances the protein-like fluorescence and reveals an unexpected fine structure of humic fluorescence. The implications of the use of protein-like fluorescence as a tool to monitor anthropogenic inputs in aquatic systems are rapidly discussed.

V.2-3 Materials and Methods

Two reference materials from the International Humic Substances Society (IHSS), Suwannee River Fulvic acid (SRFA) and Suwannee River Humic acid (SRHA), an aquatic humic acid extracted from Nyong River sediments (NHA), a model of a humic substance (MHS) obtained from auto-oxidation of catechol and glycine (Andreux et al., 1980), and surface samples of Rio Negro water (RN) collected upstream of Manaus (Brasil) and Rio Jutai (RJ) collected near the confluence with Solimoes, were used in this study. SRFA (Standard 2S101F) and SRHA (Standard 2S101H) were purchased in solid-state powder from the IHSS and used as received. Details of the isolation procedure and the main characteristics of NHA can be found in Sieliechi *et al.* (2008). The preparation procedure, characterization, and relevancy of MHS to natural humic substances are discussed in Jung *et al.* (2005) and Kazpard *et al.* (2006). Sampling of RN and RJ were conducted in March 2014 during a HYBAM campaign (<http://www.ore-hybam.org>). 1 L samples of blackwaters (DOC of 16.56 mg C/L for RN and of 10.16 mg C/L for RJ) were collected from 50 cm below the water surface, vacuum-filtered on-site through a 0.2 µm pore-sized membrane filter to remove particles and microorganisms in suspension, and then stored in cool conditions in a glass bottle wrapped in an aluminium foil.

Dodecyltrimethylammonium chloride (DTAC) was purchased from Sigma-Aldrich (purity 99%) and used without further purification. DTAC possesses a Critical Micelle Concentration of 21.7 mmol/L at 30 °C (Perger and Bešter-Rogač, 2007), and is readily soluble in water at ambient temperature (Krafft temperature below 0 °C (Laschewsky et al., 2005, Prevost et al., 2011)).

The DTAC stock solution was prepared at 10 g/L in deionized water (Millipore, MilliQ 18.2 M Ω cm). The SRFA, SRHA, NHA and MHS suspensions were obtained by dissolving 20 mg of humic material in 1L of deionized water, thus leading to DOC concentrations of 12 mg C/L (SRFA and SRHA) and 12.5 mg C/L (NHA and MHS). SRFA and SRHA suspensions were investigated at natural pH, *i.e.* pH \sim 4.3, whereas the pH of NHA and MHS suspensions was adjusted to 7 ± 0.05 by dropwise addition of 1N NaOH to facilitate the dispersion of humic material. All the stock solutions were mechanically mixed overnight in the dark to ensure a well-dispersed suspension, and then vacuum-filtered through a membrane (Membranfilter porafil) of 0.2 μ m porosity to remove any impurities. The dissolved organic carbon was checked for all stock solutions and river waters (Shimadzu TOC-Vcsn).

The HS-DOM/DTAC complexes were prepared by adding various aliquots of the surfactant concentrated solution to 10 mL of HS suspension and by submitting the mixture to gentle overhead agitation (3 times). The suspensions were then incubated for 1 hour before turbidity, UV/visible absorbance, and fluorescence measurements. The one-hour incubation time was chosen based on the temporal evolution of HS-DOM/DTAC suspensions turbidity (figure V-1). Both DTAC and HS-DOM stock solutions as well as the HS-DOM/DTAC samples were maintained at 30°C in a heating bath during the experiments.

The turbidity of HS-DOM/DTAC suspensions was measured using a HACH LANGE 2100Q turbidimeter. The UV/visible absorbance measurements were carried out on a HEWLETT PACKARD 8452A Diode Array spectrophotometer in the range from 190 to 820 nm in steps of 2 nm. For HS-DOM initial suspensions, deionized water (Millipore, MilliQ-18.2M Ω .cm) was used as the blank, whereas for HS-DOM/DTAC suspensions, the HS-DOM investigated served as the reference background so that any change in absorbance can be related to the formation of HS-DOM/DTAC complexes. All measurements were made in 5 mL quartz cuvettes with a 1 cm path length.

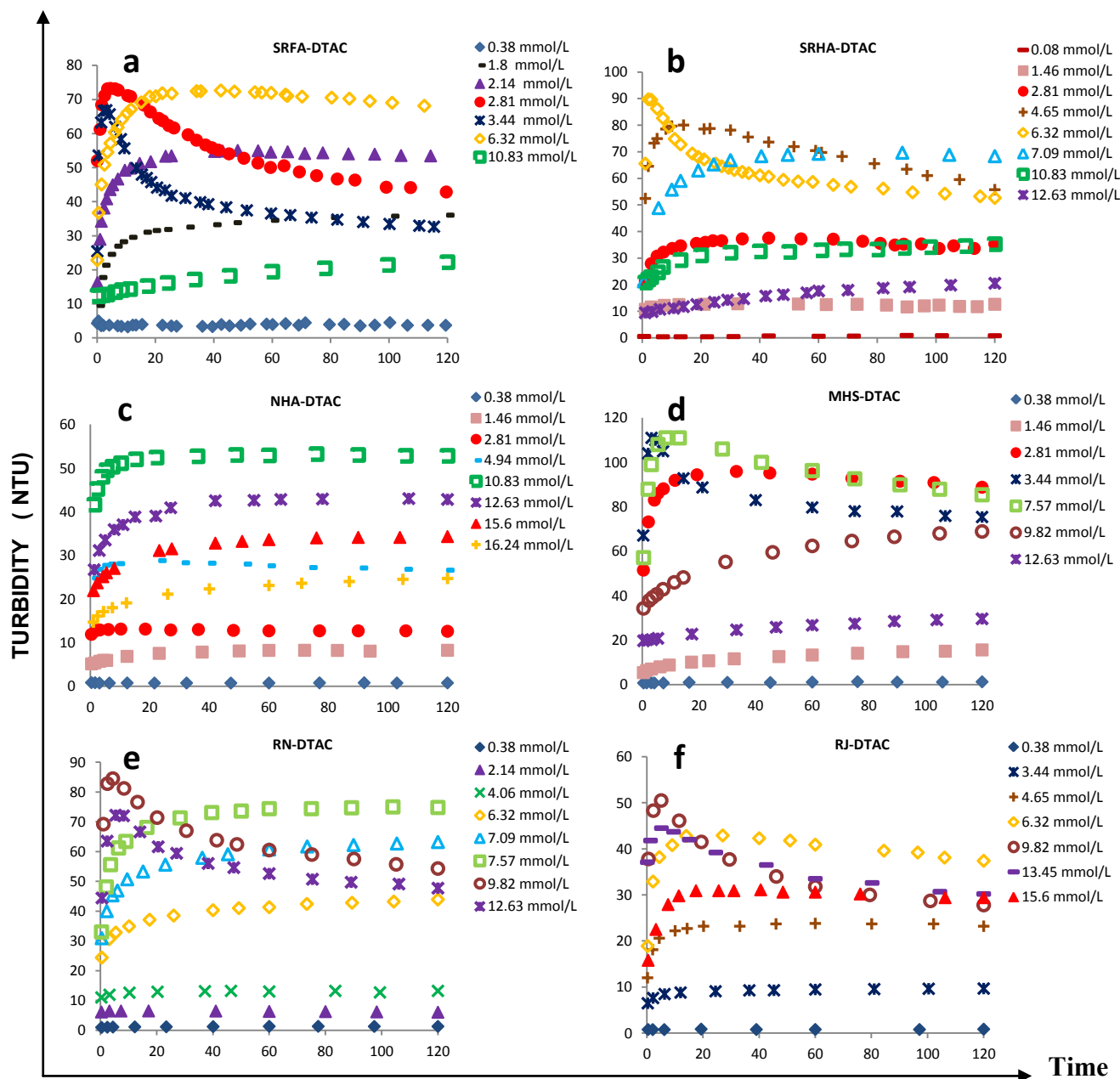


Figure V-1. Temporal evolution of turbidity for various HS-DOM/DTAC suspensions as a function of time for the various DTAC additions.

The emission Fluorescence Spectra were obtained with a Photon Technology International spectrofluorimeter (PTI, QuantaMaster 30 Plus) equipped with a high power Xenon flash lamp as the light source. The emission spectra were recorded with a slit width set at 5nm band-pass for both excitation and emission monochromators. To avoid photo-bleaching, each sample was exposed to a single excitation wavelength. The 5 mL quartz cuvette (optical path length of 1 cm) was then cleaned and a new sample was used for the following excitation wavelength (Hur et al., 2011). The temperature was regulated at 30 °C

by a thermostat. The choices of excitation wavelengths, *i.e.* $\lambda = 230, 264, 270, 350, 380$ and 400 nm, were based on previous literature on DOM fluorescence, as well as on UV/visible absorbance measurements of HS/DOM solutions (figure V-2). The absorbance spectra were used for correction of inner-filtering effects according to:

$$I_{cor} = I_{mea} 10^{\frac{A_{Ex} + A_{Em}}{2}} \quad (5.1)$$

where I_{cor} and I_{mea} are the corrected and the measured fluorescence intensities, and A_{Ex} and A_{Em} are the absorbances values at the current excitation and emission wavelengths (Lakowicz, 2010).

V.2-4 Results

All the absorbance spectra of initial HS-DOM suspensions exhibit the classical exponential monotonic decrease with increasing wavelength reported in the literature (Chin et al. 1994; Del Vecchio and Blough 2004; Fu et al. 2007). Very weak shoulders can nevertheless be detected at 260 nm for SRFA, NHA, RN and RJ, at 250 nm for SRHA, and at 270 and 320 nm for MHS (figure V-2).

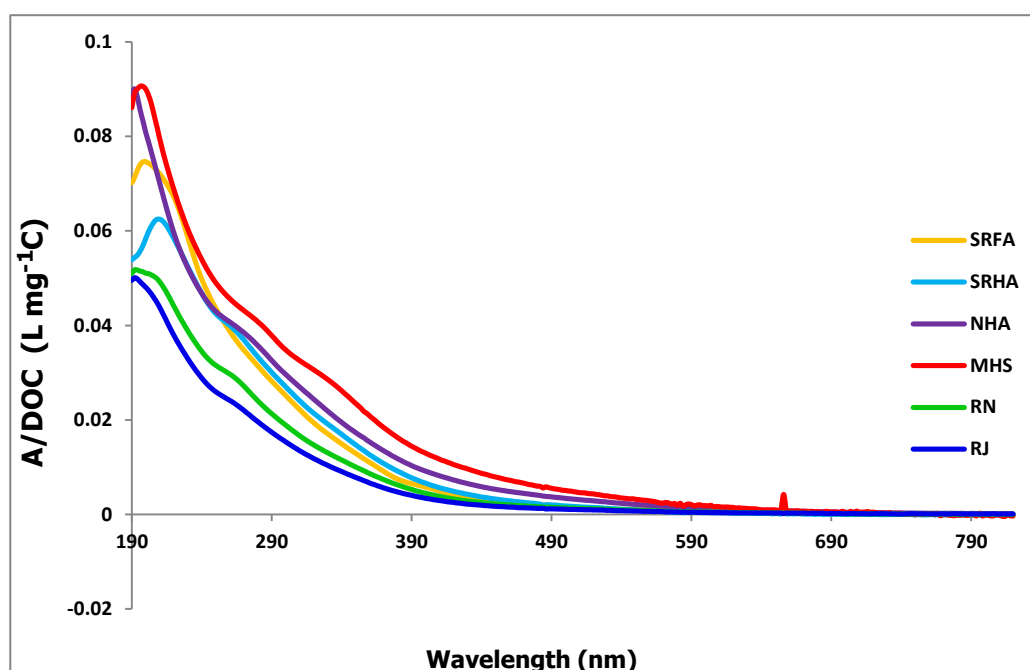


Figure V-2. UV/visible spectra (Absorbance normalized by DOC in mg C L^{-1}) of the various HS-DOM.

In the presence of low DTAC concentrations up to 0.38mmol/L, the absorbance spectra remain essentially unchanged (figure V-3).

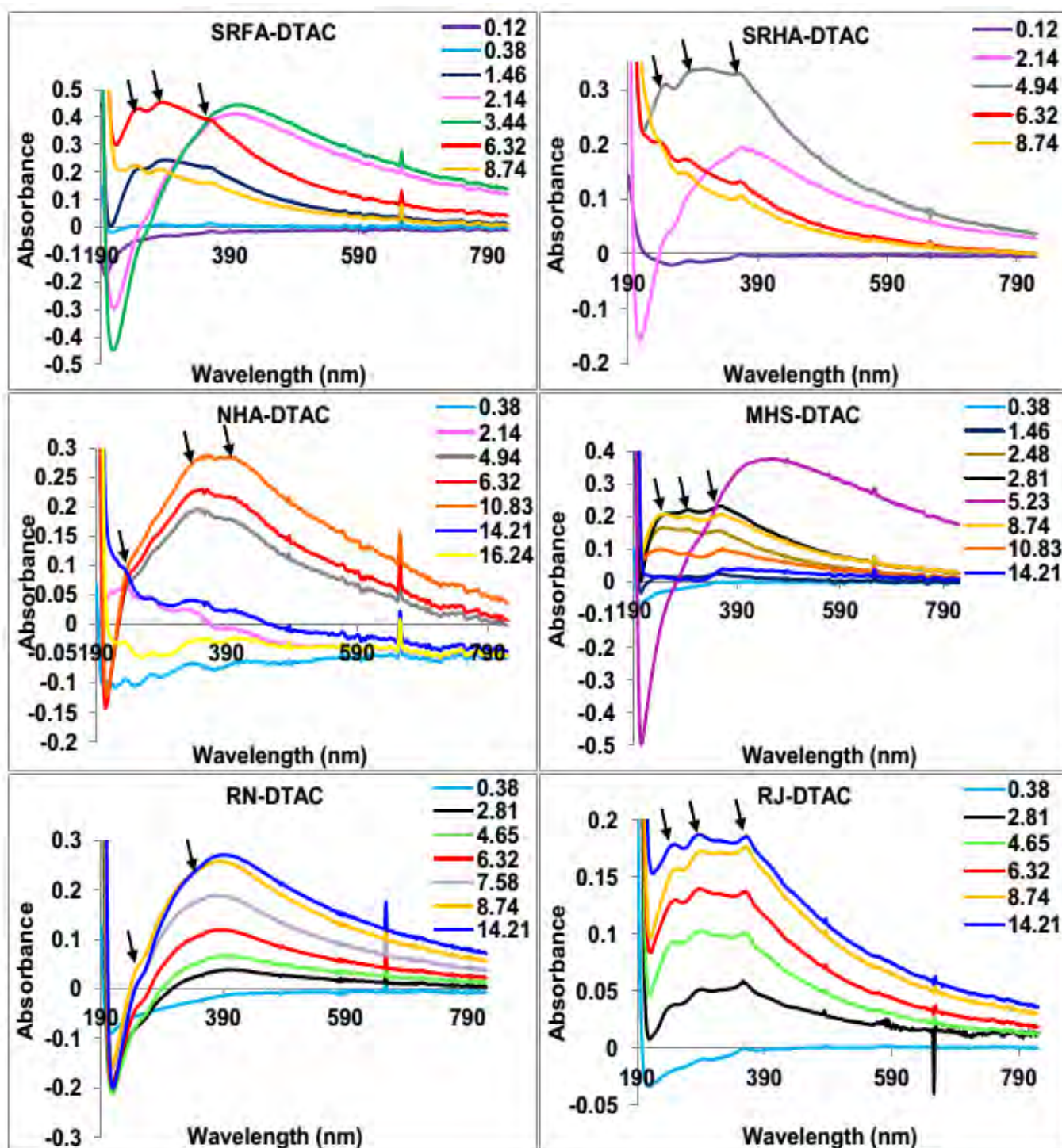


Figure V-3. UV/Visible spectra of HS-DOM/DTAC suspensions after various DTAC additions. The arrows indicate the newly emerged bands. DTAC Concentrations are indicated in the graph in mmol/L.

Upon further addition of DTAC, the spectral profiles change drastically with the emergence of new broad bands or simple shoulder bands approximately centered on 234, 280, and 350 nm that generally become slightly better, resolved with increasing DTAC concentration except for RN and NHA. Such absorbance bands might identify quinone-like components (Cory and Mcknight 2005). The sharp peak at 656 nm is a deuterium line of the UV lamp. The bands intensity increases with surfactant concentration to reach maxima around the peak in turbidity. At high DTAC concentration, the absorbance declines for all extracted humic substances whereas it remains almost constant for DOM from RJ and RN. Such patterns are in line with the changes in turbidity of the respective HS-DOM recorded in this concentration range (see fig. V-6).

Figure V-4 presents the fluorescence emission spectra of HS-DOM/DTAC suspensions for excitation wavelengths of 230, 264, and 380 nm (The emission spectra obtained with λ_{EX} of 270, 350 and 400 nm are reported in figure V-5). Initially, the HS-DOM suspensions are characterized by the classical humic-like fluorescence (HLF) broad bands A(α') in the 380-540 nm region for a λ_{EX} of 264 nm and C(α) in the 420-550 nm region for a λ_{EX} of 380 nm. A barely detectable Tryptophan-like T(δ) peak at 318/326-328 nm, depending on the type of HS/DOM, can also be observed for a λ_{EX} of 230 nm. Such poorly featured T(δ) fluorescence signal has previously been reported in humic substances extracted from natural sediments and aquagenic suspended matter in which the presence of aromatic amino acids is very plausible (Sierra et al., 2005; Chen and Kenny, 2007).

The addition of low DTAC concentrations to the HS-DOM suspensions, *i.e.* less than 0.38mmol/L, does not significantly affect the fluorescence emission spectra. However, further addition of cationic surfactant dramatically changes the fluorescence of HS-DOM with the emergence within the A(α') band ($\lambda_{\text{EX}} = 264$ nm) of well-resolved peaks at 445-448 nm (HLF-1) and at 465-468 nm (HLF-2), a pronounced shoulder around 395 nm, and minor peaks or shoulder around 420, 480, and 490 nm. For NHA, those peaks are slightly blue-shifted by about 5-10 nm. Likewise, for a λ_{EX} of 380 nm, the C(α) broad band leads to a series of fluorescence emission peaks centered around 437, 466, 480 and 540 nm, that are poorly resolved in the case of SFRA and blackwaters, but much better structured in the case of humic acids although NHA bands are slightly blue-shifted by about 9 nm. Concomitantly, the intensity of T(δ) at 318/326-328 nm ($\lambda_{\text{EX}} = 230$ nm) sharply increases with the appearance of minor peaks at 286/296 and 332/340 nm.

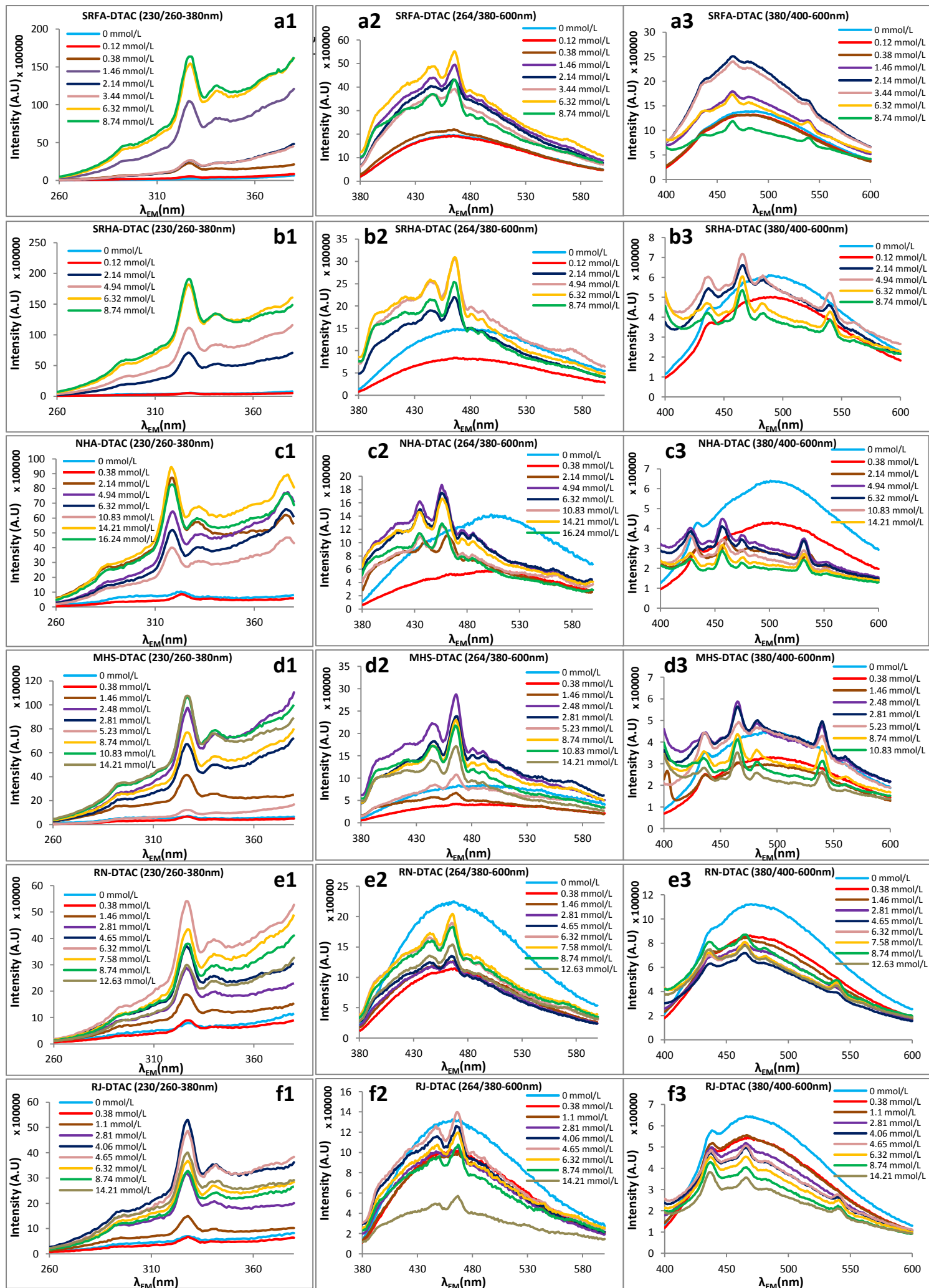


Figure V-4. Fluorescence emission spectra (excitation wavelengths of 230, 264 and 380nm) of HS-DOM/DTAC suspensions after various DTAC additions.

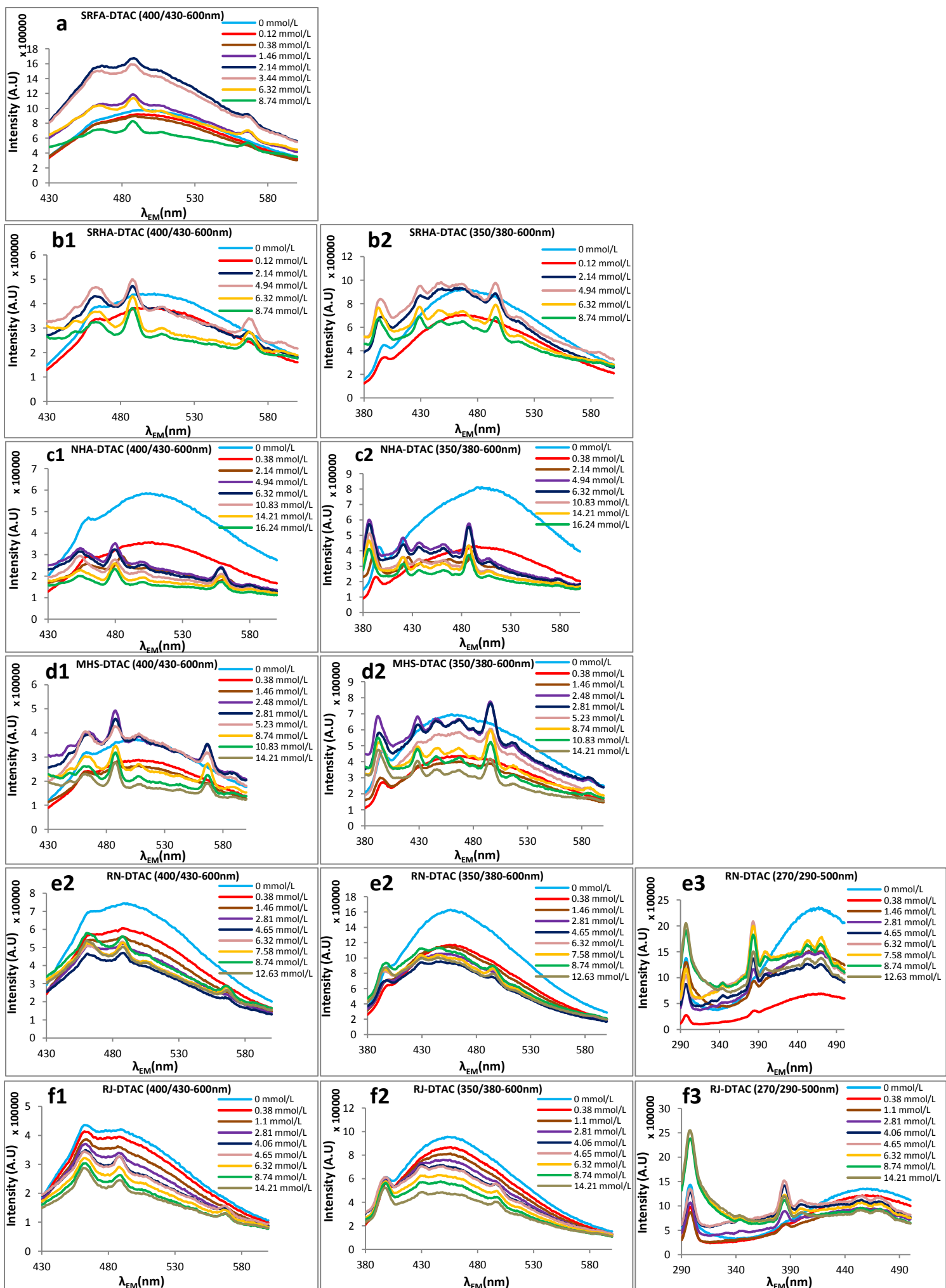


Figure V-5. Fluorescence emission spectra (excitation wavelengths of 270, 350 and 400nm) of HS-DOM/DTAC suspensions after various DTAC additions.

The general spectral features remain essentially unchanged in the DTAC concentration range investigated. However, the fluorescence intensity of the newly emerged peaks significantly evolves with the surfactant concentration. As illustrated in figure V-6, the intensity of the Tryptophan-like T(δ) peak at 318/326 nm ($\lambda_{\text{Ex}} = 230$ nm) initially increases with DTAC concentration, reaches a maximum and then substantially decreases to either stabilize in the case of DOM from Rio Negro and Rio Jutai, or re-increases at high DTAC concentration in the case of SRFA, MHS, and NHA. Only the SRHA curve shows a continuing increase in T(δ) intensity in the DTAC concentration range studied. The intensity of other peaks such as HLF-1 follows a pattern similar to that of T(δ) but on a smaller scale. Comparison with the turbidity curves, also plotted with the fluorescence intensity graphs in figure V-6, explains much of the fluorescence variability. Indeed, except for SRHA, the initial maximum in fluorescence intensity occurs before the first turbidity increase, whereas the recovery of fluorescence signals at high surfactant concentration coincides with the decrease in turbidity.

According to previous literature, the relatively slight increase in pH detected after the addition of surfactant - about 0.4 pH unit at the highest DTAC concentration used - is not expected to significantly influence the variability in fluorescence intensity (Pullin and Cabaniss, 1995; Mobed et al., 1996; Patel-Sorrentino et al., 2002; Chen and Kenny, 2007; Gao et al., 2015). Likewise, the change in ionic strength brought by the addition of surfactant counterions, known to increase the absorbance of HS-DOM especially at high pH (Mobed et al., 1996; Gao et al., 2015), should not be sufficient to significantly affect the fluorescence emission intensity.

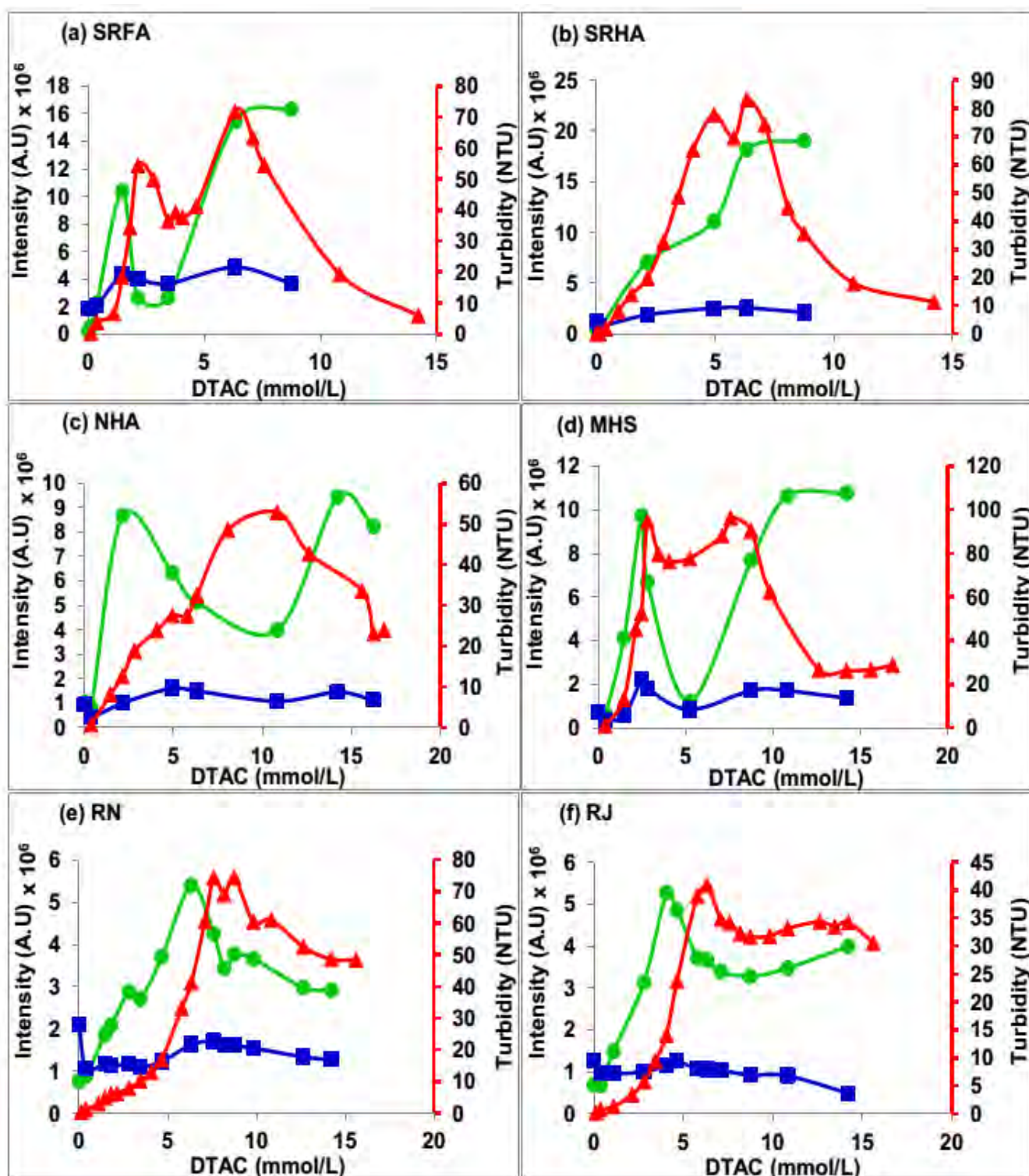


Figure V-6. Variation of Tryptophan-like (●) (I_{Try} ($\lambda_{\text{Ex}}=230\text{nm}$ / $\lambda_{\text{Em}}=327\text{nm}$)) and Humic-Like (■) ($I_{\text{HLF-1}}$ ($\lambda_{\text{Ex}}=264\text{nm}/\lambda_{\text{Em}}=445\text{nm}$)) Fluorescence intensity of HS-DOM/DTAC suspensions for excitation wavelengths of 230 and 264 nm as a function of DTAC concentration. The corresponding turbidity curves (▲) are shown in order to locate the main variations.

V.2-5 Discussion

V.2-5-1 Significance of Newly Formed Fluorescence Signals

Previous fluorescence investigations of HS-DOM/surfactant interactions had not reported such enhanced structure of fluorescence emission spectra (Subbiah and Misra, 2009; Muroi *et al.*, 2008; Jung *et al.*, 2015). Those studies were essentially conducted with CTAB (Cetyltrimethylammonium bromide), a cationic surfactant of longer alkyl chain (C16) with Br⁻ counterion known for quenching fluorescence. Nevertheless, although not discussed by the authors, an obvious sharp increase in T(δ) fluorescence can be observed upon CTAB addition to a natural humic acid from Moselle river in Jung *et al.* (2015).

At first approximation, the emergence of new fluorescence signals reflects a significant change in the molecular environment of initially quenched fluorophores brought by the cationic surfactant. According to the literature, the association between HS-DOM and cationic surfactants is driven by both electrostatic and hydrophobic intermolecular interactions (Otto *et al.*, 2003; Ishiguro *et al.*, 2007; Chaaban *et al.*, 2016): In a first step, the binding of cationic surfactant to the negatively charged functional groups of HS-DOM triggers the formation of poorly soluble complexes; further addition of surfactant then redissolve the complexes by interaction with the hydrophobic alkyl chains in excess, most often before reaching the micellar range of surfactant concentration (Ishiguro *et al.*, 2007; Subbiah and Misra, 2009; Muroi *et al.*, 2008). A more detailed description of the complexes formed was reported in the particular case of SRFA/DTAC system: using Cryogenic Transmission Electron Microscopy, Chabaan *et al.* (2016) revealed that increasing concentrations of DTAC to a SRFA suspension lead to a sequence of molecular structures comprising fulvic-rich vesicles, globules, disks, surfactant-rich vesicles, and mixed micelles. Similar HS-DOM/DTAC complexes are certainly obtained here, the extensive reorganization of HS-DOM upon DTAC binding allowing previously quenched fluorophores to manifest within the newly formed molecular structures.

Synchronous fluorescence spectroscopy of HS-DOM is also known to provide more structured spectra (Senesi, 1990; Pullin and Cabaniss, 1995; Peuravuori *et al.*, 2002). In that case, various fluorophores such as aromatic amino acids and conjugated aliphatic structures, naphthalene, aromatic rings of increasing degree of condensation, have been successively assigned to the various distinct peaks and shoulders observed with increasing excitation

wavelength (Senesi, 1990; Peuravuori *et al.*, 2002). Similar plausible assignments might be made here. However, the literature on aggregates of fluorescent dye molecules provides examples of new fluorescence peaks formed upon the addition of an oppositely charged surfactant (Mishra *et al.*, 2000). In the case of Thiocyanine/aerosol-OT system, the sharp emission peaks that develop with surfactant concentration correspond to the formation of dye/surfactant oligomers following the destacking of initial dye aggregates (Mandal and Pal, 2000). Applied to our HS-DOM/DTAC systems, such interpretation would imply that (i) the emergence of new fluorescence bands of HS-DOM in the presence of DTAC cationic surfactant could be interpreted as a reorganization of a supramolecular structure of HS leading to oligomers of HS-DOM/DTAC complexes (Piccolo, 2001); (ii) a limited number of fluorophores would be sufficient to explain the numerous peaks obtained after DTAC addition. Actually, previous phase-resolved fluorescence emission studies of SRFA indicated the presence of at least two fluorescing components (Goldberg and Weiner, 1994). Moreover, as illustrated in figure V-7, for a given excitation wavelength, the fluorescence emission peaks remain strictly proportional to each other, thus suggesting that the fluorophores could be borne by the same molecule.

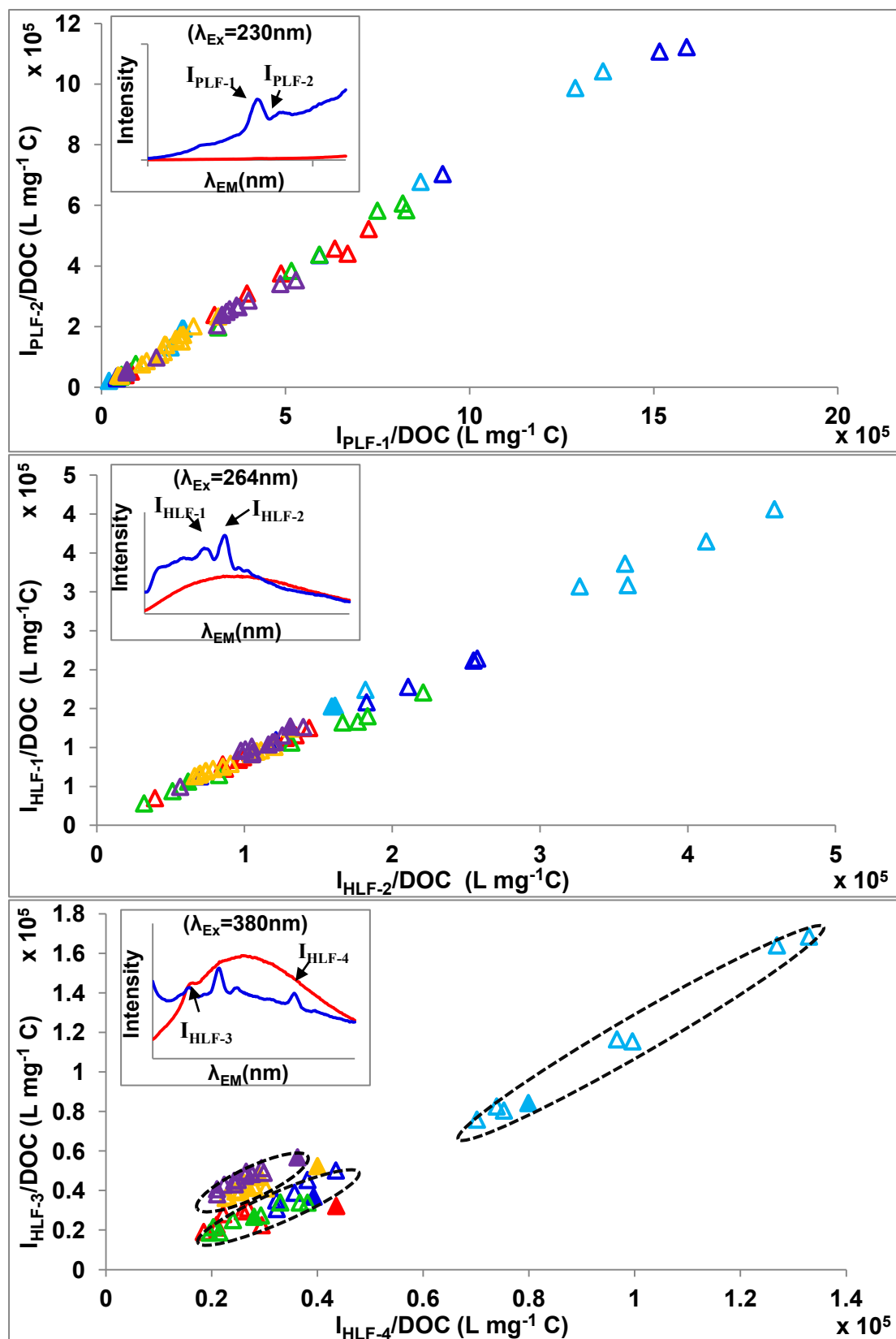


Figure V-7. Relationship between the intensities of Protein-like and the Humic-like Fluorescence peaks, $I_{\text{PLF-1}}-I_{\text{PLF-2}}$, $I_{\text{HLF-1}}-I_{\text{HLF-2}}$ and $I_{\text{HLF-3}}-I_{\text{HLF-4}}$ (see inset) at excitation wavelength of 230nm, 264nm and 380nm respectively. The Fluorescence Intensities in arbitrary unity (A.U) are normalized by DOC (in mg C L^{-1}). The filled marker (\blacktriangle) corresponds to HS-DOM and the empty marker (\triangle) designates HS-DOM with DTAC. (\blacktriangle) SRFA; (\blacktriangle) SRHA; (\blacktriangle) NHA; (\blacktriangle) MHS; (\blacktriangle) RN; (\blacktriangle) RJ.

V.2-5-2 Potential spectral fingerprinting of HS-DOM after DTAC addition

Fluorescence emission spectra have been used to define a relative degree of organic matter humification or to characterize the origin of humic material (Zsolnay et al., 1999; McKnight et al., 2001; Ohno, 2002). In both cases, an appropriate indicator was developed from the ratio of fluorescence intensity measured at specified locations on the spectra for a given excitation wavelength. Such outcome was not a primary objective of the study, which explains the limited range of HS-DOM sources investigated and in particular the absence of microbially derived humic samples. Nevertheless, if the emission spectra of HS-DOM/DTAC complexes are rather similar to each other for excitation wavelengths of 230 nm and 264 nm, a clear discrimination between humic or fulvic origin can be established for an excitation wavelength of 380 nm (figure V-4 and V-7). Indeed, in the case of SRFA and DOM from black waters, which ratios of fulvic to humic compounds have been reported to vary between 1.5 to 2 (Ertel et al., 1986; K uchler et al., 1994), the emission spectra after DTAC addition are less structured than those obtained with humic suspensions. Further work is nevertheless needed with appropriate end-members to develop an index characterizing the origin of humic material.

V.2-5-3 Assignment of T(δ) Signal

Until now, the fluorescence signal detected in the 310 to 340 nm range within HS and DOM has been mainly attributed to protein-like compounds (Coble 1996; Parlanti et al. 2000, Baker 2001; Baker and Spencer 2004; Baker and Inverarity, 2004; Reynolds, 2003). An alternative hypothesis in the literature, in line with the polyhydroxyaromatic structure of HS, has ascribed the T(δ) fluorescence emission peaks to mono-aromatic phenolic and/or polyphenolic compounds (Senesi 1990; Ferrari and Mingazzini 1995). Using Size Exclusion Chromatography, Maie et al. (2007) confirmed that part of the T(δ) fluorescence of DOM collected in estuarine environments should indeed be related to phenolic compounds. In our case, unlike natural HS, the model of humic substance MHS cannot be suspected to contain initial traces of aromatic amino acid, and hence, the fluorescence peak at $\lambda_{\text{Ex/Em}} = 230/326\text{nm}$ should identify the presence of those phenolic compounds. A direct formation of tryptophan-like molecular structures upon the addition of the DTAC quaternary amine to the carboxylic groups of HS, *i.e.* formation of amide bonds in the vicinity of phenolic moieties, seems very unlikely taking into account the rather low reactivity of carboxylic acids with amines under

our experimental conditions (Goossen et al., 2009). Furthermore, the presence of supplementary amide groups would quench the fluorescence of aromatic amino acids (Wiczek et al. 2001).

While the attribution of the **T(δ)** tryptophan-like fluorescence signal to proteinaceous compounds remains certainly valid for most natural environments (Reynolds 2003; Yamashita and Tanoue 2003), such attribution must be discussed more precisely in the case of anthropogenic-impacted waters where complexes between surfactants and humic substances can be expected. Indeed, biologically treated effluents contain dominant amounts of humic substances (Imai et al. 2002) and various surfactants in the mg/L range (Holt et al., 1998 ; Ivanković and Hrenović, 2010 ; Ying et al., 2002 ; Ying, 2006 ; Merino et al., 2001). In particular, the concentrations of free cationic surfactants, such as quaternary ammonium and benzalkylammonium chloride, are found in the 0.062 to 6mg/L range in the effluent. As the elimination of free cationic surfactants from wastewater may reach 99% in an activated sludge process (Geerts et al., 2015), it is very likely that HS/surfactant complexes, formed during the treatment, contribute to the tryptophan-like fluorescence peak in the discharge of treated wastewater. Still, such HS-surfactant complexes correspond in some way to anthropogenic DOM and therefore, the **T(δ)** signal remains an appropriate tracer of sewage-derived organic matter. On the other hand, a direct attribution of the tryptophan-like fluorescence to the bioavailable or labile DOM pool (Baker and Inverarity 2004) may be misleading, since part of the **T(δ)** signal corresponds to humic substances and hence, refractory matter (Maie et al. 2007).

V.3 Conclusions

The addition of DTAC to HS-DOM suspensions offers interesting new perspectives for studying the fluorescent properties of humic substances. From the rather featureless emission spectrum emerge new bands that imply a drastic reorganization of HS-DOM upon the interaction with the cationic surfactant. The unveiled fine structure of spectra is consistent with a destacking of a possible HS supramolecular structure. The emission spectra obtained for an excitation wavelength of 380 nm offer some potential for fingerprinting the origin of humic materials. Moreover, the interaction of HS-DOM with DTAC determines a significant increase of the so-called tryptophan-like fluorescence signal that questions its usual assignment to proteinaceous compounds. Obviously, the effect of other cationic surfactants,

varying either the alkyl chain length or the nature of polar head, should be examined to better exploit all the characteristics of the fluorescence behaviour of HS-DOM in the presence of surfactants.

CHAPTER
(VI)

General Conclusion
and
Perspectives

This study focused on identifying which of the two structural concepts, polymeric or supramolecular, is actually appropriate for describing the structure of humic substances. For that purpose, we have investigated the association between a series of HS/DOM and various concentrations of cationic surfactant with different alkyl chain lengths. Adding an oppositely charged amphiphilic molecule to HS/DOM was expected to induce drastic restructurations of humic colloids driven by both electrostatic and hydrophobic interactions. Our results demonstrate that HS/DOM can be considered as supramolecular assemblies of various amphiphilic molecules. The average geometric characteristics of SRFA/DTAC complex (polar head area and alkyl chain length) were also inferred according to the framework introduced by Israelachvili et al., (1976). However, at the moment, not knowing the amount of DTAC associated in any self-assembly, it is not possible to infer the architectural characteristics of the SRFA/DTAC complex from the geometrical constraints associated with the formation of a given molecular structure.

Single-scan fluorescence emission spectroscopy was also used to investigate and further confirm both structural reformation and supramolecularity of HS. The drastic molecular rearrangements brought by the addition of cationic surfactant to HS/DOM affect the native chromophoric and fluorophoric groups with the appearance of various fluorescence emission peaks not previously detected in the reference HS. The reformation gives the basis for identifying the chemical groups responsible for the fluorescence properties of HS. The approach also permitted the generalization of our results with humic substances of various origins and dissolved organic matter (DOM), an excitation wavelength of 380 nm being useful to fingerprint the various humic substances.

Many complementary experiments can be carried out: First, our approach has focused on aquagenic humic substances, and should be extended to soil humic substances and natural organic matter, eventually to understand the whole image of organic matter in all its fractions and origins. If the same array of techniques can obviously be applied, it would be interesting to obtain adsorption isotherms of surfactants on humic substances by using surfactants selective electrodes. In that case, the amount of surfactant associated with any self-assembly can be calculated, and hence the architectural characteristics of HS-DOM/surfactant complexes can be obtained from the geometrical constraints associated with the formation of a given molecular structure. Moreover, it will be of an interest to understand the highly surface active HS/Surfactant complex. For that, a Numerical Molecular Dynamic Simulations

can be used to identify the various binding positions for the surfactant and the partnership upon HS/Surfactant interaction. This will eventually help in predicting the structure of the HS/Surfactant complex, the appropriate experimental conditions, and as well as the thermodynamic stability of the complexes formed. The use of Isothermal Titration Calorimetry (ITC) will further help in understanding the drastic molecular rearrangement and the conformational changes evident in the supramolecular assembly of HS upon surfactant addition.

However, evidencing the supramolecular nature of humic substances opens a new field of investigation in relation with a better understanding of carbon geocycling. To precise the dynamics of such supramolecular assemblies seems fundamental, *i.e.* how it is formed, what limits the size of the molecular aggregate, does it evolve with time or in other terms is humic acid really a humified fulvic acid? If the addition of various surfactant concentrations to samples collected in the field, coupled with the array of characterization techniques, can certainly provide some information about a possible evolution of the supramolecular assembly with time (e.g. samples collected along the Rio Negro), it would also be very interesting to disperse the humic assemblies to identify the various constituents; breaking H-bonds with products such as urea or chaotropic salts should be tried in combination with chromatographic and Fluorescence techniques. Once the individual constituents are separated, ^{13}C geochemistry or ^{14}C age determination may provide useful insights into the carbon dynamics in soils and continental waters.

Finally, humic substances are well-known to be difficult to eliminate during water treatment operations. The remaining humics react with chlorine during the disinfection step to form direct-acting mutagenic product (trihalomethanes “THM”). The knowledge of the structural organization of humic substances can certainly help to improve their removal, perhaps by designing new polymers with moieties that could insert within the humic assemblies without dispersing them.

***BIBLIOGRAPHIC
REFERENCES***

Abbt-Braun, G. (1992). Spectroscopic characterization of humic substances in the ultraviolet and visible region and by Infrared spectroscopy. (In: Matthes, G., Frimmel, F. H., Hirsch, P., Schulz, H. D., Usdowski, E. (eds). *Progress in hydrogeochemistry: organics – carbonate systems – silicate systems – microbiology – models*. Berlin: Springer-Verlag, 29–36.),.

Abbt-Braun, G., and Frimmel, F.H. (2002). Setting the Scene: The Relevance of Reference Materials - Isolation and General Characterization. In *Refractory Organic Substances in the Environment*, F.H. Frimmel, G. Abbt-Braun, K.G. Heumann, B. Hock, H.-D. Lüdemann, and M. Spittler, eds. (Wiley-VCH Verlag GmbH & Co. KGaA), pp. 1–38.

Abbt-Braun, G., Frimmel, F.H., and Schulten, H.-R. (1989). Structural investigations of aquatic humic substances by pyrolysis-field ionization mass spectrometry and pyrolysis-gas chromatography/mass spectrometry. *Water Res.* 23, 1579–1591.

Abbt-Braun, G., Lankes, U., and Frimmel, F.H. (2004). Structural characterization of aquatic humic substances ? The need for a multiple method approach. *Aquat. Sci. - Res. Boundaries* 66, 151–170.

Acharya, D.P., and Kunieda, H. (2003). Formation of viscoelastic wormlike micellar solutions in mixed nonionic surfactant systems. *J. Phys. Chem. B* 107, 10168–10175.

Adamczyk, Z., Para, G., and Warszyński, P. (1999). Influence of Ionic Strength on Surface Tension of Cetyltrimethylammonium Bromide. *Langmuir* 15, 8383–8387.

Adani, F., and Spagnol, M. (2008). Humic acid formation in artificial soils amended with compost at different stages of organic matter evolution. *J. Environ. Qual.* 37, 1608–1616.

Adani, F., Tambone, F., Davoli, E., and Scaglia, B. (2010). Surfactant properties and tetrachloroethene (PCE) solubilisation ability of humic acid-like substances extracted from maize plant and from organic wastes: A comparative study. *Chemosphere* 78, 1017–1022.

Adou, A.F., Muhandiki, V.S., Shimizu, Y., and Matsui, S. (2001). A new economical method to remove humic substances in water: adsorption onto a recycled polymeric material with surfactant addition. *Water Sci. Technol. J. Int. Assoc. Water Pollut. Res.* 43, 1–7.

Ahmad, S.R., and Reynolds, D.M. (1995). Synchronous fluorescence spectroscopy of wastewater and some potential constituents. *Water Res.* 29, 1599–1602.

Aiken, G.R. (1985). Isolation and concentration techniques for aquatic humic substances. (In: *Humic Substances in Soil, Sediment, and Water*, ed. G.R. Aiken, D.M. McKnight, R.L. Wershaw & P. MacCarthy, pp. 363-385. New York: Wiley),.

Aiken, G.R., and Gillam, A.H. (1989). Determination of Molecular Weights of Humic Substances by Colligative Property Measurements. (In: *Humic Substances II: In Search of Structure*. M. H. B. Hayes, P. MacCarthy, R. L. Malcolm, and R. S. Swift (eds), Wiley, Chichester, New York, pp. 515-544),.

Aiken, G.R., and Malcolm, R.L. (1987). Molecular weight of aquatic fulvic acids by vapor pressure osmometry. *Geochim. Cosmochim. Acta* 51, 2177–2184.

Aiken, G.R., and Wershaw, R.L. (1985). Molecular size and weight measurements of humic substances (In: *Humic Substances in Soil, Sediment, and Water: Geochemistry, Isolation and Characterization*. G. R. Aiken, D. M. McKnight, R. L. Wershaw, and P. MacCarthy (eds). Wiley, New York, pp. 477-492).

Aiken, G.R., McKnight, D.M., Wershaw, R.L., and MacCarthy, P. (1985). *Humic substances in soil, sediment, and water: geochemistry, isolation and characterization*. (John Wiley & Sons, 0-471-88274-7, pp. 692).

Aiken, G.R., Brown, P.A., Noyes, T.I., and Pinckney, D.J. (1994). Molecular Size and Weight of Fulvic and Humic Acids from the Suwannee River (In: *Humic substances in the Suwannee River, Georgia; interactions, properties, and proposed structures*. p. 89-98, United States Geological Survey), WSP - 2373.

Albani, J.R. (2008). *Principles and applications of fluorescence spectroscopy* (John Wiley & Sons).

Alvarez-Puebla, R.A., Valenzuela-Calahorra, C., and Garrido, J.J. (2006). Theoretical study on fulvic acid structure, conformation and aggregation: A molecular modelling approach. *Sci. Total Environ.* 358, 243–254.

Amalfitano, C., Pignalosa, V., Auriemma, L., and Ramunni, A. (1992). The contribution of lignin to the composition of humic acids from a wheat-straw amended soil during 3 years of incubation in pots. *J. Soil Sci.* 43, 495–504.

Amon, R.M., and Benner, R. (1996). Bacterial utilization of different size classes of dissolved organic matter. *Limnol. Oceanogr.* 41, 41–51.

Amy, G.L., Collins, M.R., Kuo, C.J., and King, P.H. (1987). Comparing gel permeation chromatography and ultrafiltration for the molecular weight characterization of aquatic organic matter. *J. Am. Water Works Assoc.* 43–49.

Anderson, H.A., Bick, W., Hepburn, A., and Stewart, M. (1989). Nitrogen in Humic Substances. (In: *Humic Substances II: In Search of Structure*. M. H. B. Hayes, P. MacCarthy, R. L. Malcolm, and R. S. Swift (eds), Wiley, Chichester, New York, pp. 223-253),.

Anderson, M., Hung, A., Mills, D., and Scott, M. (1995). Factors Affecting the Surface-Tension of Soil Solutions and Solutions of Humic Acids. *Soil Sci.* 160, 111–116.

Andreux, F., Golebiowska, D., and Metche, M. (1980). Oxydative polymerization of O-diphenols in presence or absence of amino-acids. Topics on (catechol-glycocolle) and (catecholdiglycylglycine). (General Assembly of Polyphenols Group Report, Logrono, Spain, Bulletin, vol. 9, pp.178–188),.

Antunes, F.E., Marques, E.F., Gomes, R., Thuresson, K., Lindman, B., and Miguel, M.G. (2004). Network Formation of Catanionic Vesicles and Oppositely Charged Polyelectrolytes. Effect of Polymer Charge Density and Hydrophobic Modification. *Langmuir* 20, 4647–4656.

Aswal, V.K., and Goyal, P.S. (2002). Role of counterion distribution on the structure of micelles in aqueous salt solutions: small-angle neutron scattering study. *Chem. Phys. Lett.* *357*, 491–497.

Aswal, V.K., and Goyal, P.S. (2003). Role of different counterions and size of micelle in concentration dependence micellar structure of ionic surfactants. *Chem. Phys. Lett.* *368*, 59–65.

Atkins, P.W., and Jones, L. (1998). *Chimie: molécules, matière, métamorphoses* (De Boeck Supérieur).

Attwood, D., and Florence, A.T. (1983). *Surfactant Systems: Their Chemistry, Pharmacy and Biology* (Chapman and Hall).

Avena, M.J., and Wilkinson, K.J. (2002). Disaggregation kinetics of a peat humic acid: mechanism and pH effects. *Environ. Sci. Technol.* *36*, 5100–5105.

Avena, M.J., Vermeer, A.W.P., and Koopal, L.K. (1999). Volume and structure of humic acids studied by viscometry: pH and electrolyte concentration effects. *Colloids Surf. Physicochem. Eng. Asp.* *151*, 213–224.

Averett, R.C., Leenheer, J.A., McKnight, D.M., and Thorn, K.A. (1994). Humic substances in the Suwannee River, Georgia; interactions, properties, and proposed structures (United States Geological Survey), WSP - 2373.

Azam, F., and Malfatti, F. (2007). Microbial structuring of marine ecosystems. *Nat. Rev. Microbiol.* *5*, 782–791.

B

Baalousha, M., Motelica-Heino, M., Galaup, S., and Le Coustumer, P. (2005). Supramolecular structure of humic acids by TEM with improved sample preparation and staining. *Microsc. Res. Tech.* *66*, 299–306.

Baalousha, M., Motelica-Heino, M., and Le Coustumer, P. (2006). Conformation and size of humic substances: Effects of major cation concentration and type, pH, salinity, and residence time. *Colloids Surf. -Physicochem. Eng. Asp.* *272*, 48–55.

Babi, K.G., Koumenides, K.M., Nikolaou, A.D., Makri, C.A., Tzoumerkas, F.K., and Lekkas, T.D. (2007). Pilot study of the removal of THMs, HAAs and DOC from drinking water by GAC adsorption. *Desalination* *210*, 215–224.

Baigorri, R., Fuentes, M., González-Gaitano, G., and García-Mina, J.M. (2007a). Analysis of molecular aggregation in humic substances in solution. *Colloids Surf. Physicochem. Eng. Asp.* *302*, 301–306.

Baigorri, R., Fuentes, M., Gonzalez-Gaitano, G., and Garcia-Mina, J.M. (2007b). Simultaneous presence of diverse molecular patterns in humic substances in solution. *J. Phys. Chem. B* *111*, 10577–10582.

- Baker, A. (2001). Fluorescence Excitation–Emission Matrix Characterization of Some Sewage-Impacted Rivers. *Environ. Sci. Technol.* *35*, 948–953.
- Baker, A. (2002a). Fluorescence properties of some farm wastes: implications for water quality monitoring. *Water Res.* *36*, 189–195.
- Baker, A. (2002b). Fluorescence Excitation–Emission Matrix Characterization of River Waters Impacted by a Tissue Mill Effluent. *Environ. Sci. Technol.* *36*, 1377–1382.
- Baker, A. (2005). Thermal fluorescence quenching properties of dissolved organic matter. *Water Res.* *39*, 4405–4412.
- Baker, A., and Genty, D. (1999). Fluorescence wavelength and intensity variations of cave waters. *J. Hydrol.* *217*, 19–34.
- Baker, A., and Inverarity, R. (2004). Protein-like fluorescence intensity as a possible tool for determining river water quality. *Hydrol. Process.* *18*, 2927–2945.
- Baker, A., and Spencer, R.G.M. (2004). Characterization of dissolved organic matter from source to sea using fluorescence and absorbance spectroscopy. *Sci. Total Environ.* *333*, 217–232.
- Baker, A., Ward, D., Lieten, S.H., Periera, R., Simpson, E.C., and Slater, M. (2004). Measurement of protein-like fluorescence in river and waste water using a handheld spectrophotometer. *Water Res.* *38*, 2934–2938.
- Bales, B.L., Benrraou, M., and Zana, R. (2002). Krafft Temperature and Micelle Ionization of Aqueous Solutions of Cesium Dodecyl Sulfate. *J. Phys. Chem. B* *106*, 9033–9035.
- Balnois, E., Wilkinson, K.J., Lead, J.R., and Buffle, J. (1999). Atomic force microscopy of humic substances: effects of pH and ionic strength. *Environ. Sci. Technol.* *33*, 3911–3917.
- Banerjee, S.K. (1979). Humic fraction of Soil humus. *J. Indian Chem Soc* *56* 1094-1097.
- Beaucage, G. (1996). Small-Angle Scattering from Polymeric Mass Fractals of Arbitrary Mass-Fractal Dimension. *J. Appl. Crystallogr.* *29*, 134–146.
- Becher, G., Carlberg, G.E., Gjessing, E.T., Hongslo, J.K., and Monarca, S. (1985). High-performance size exclusion chromatography of chlorinated natural humic water and mutagenicity studies using the microscale fluctuation assay. *Environ. Sci. Technol.* *19*, 422–426.
- Beck, A.J., Jones, K.C., Hayes, M.H.B., and Mingelgrin, U. (1993). Organic substances in soil and water. Natural constituents and their influences on contaminant behaviour. (Royal Society of Chemistry (RSC)).
- Beckett, R., Jue, Z., and Giddings, J.C. (1987). Determination of molecular weight distributions of fulvic and humic acids using flow field-flow fractionation. *Environ. Sci. Technol.* *21*, 289–295.
- Ben-Naim, A. (1980). Hydrophobic interactions. N. Y. Plenum *3*, 1.

- Bennett, E. (1949). Fixation of ammonia by lignin. *Soil Sci.* 68, 399–400.
- Benzing-Purdie, L., and Ripmeester, J.A. (1983). Melanoidins and Soil Organic Matter: Evidence of Strong Similarities Revealed by ^{13}C CP-MAS NMR. *Soil Sci. Soc. Am. J.* 47, 56.
- Benzing-Purdie, L., Cheshire, M.V., Williams, B.L., Ratcliffe, C.I., Ripmeester, J.A., and Goodman, B.A. (1992). Interactions between peat and sodium acetate, ammonium sulphate urea or wheat straw during incubation studied by ^{13}C and ^{15}N NMR spectroscopy. *J. Soil Sci.* 43, 113–125.
- Berdén, M., and Berggren, D. (1990). Gel filtration chromatography of humic substances in soil solutions using HPLC-determination of the molecular weight distribution. *J. Soil Sci.* 41, 61–72.
- Berkovic, A.M., García Einschlag, F.S., Gonzalez, M.C., Pis Diez, R., and Mártire, D.O. (2013). Evaluation of the Hg^{2+} binding potential of fulvic acids from fluorescence excitation–emission matrices. *Photochem. Photobiol. Sci.* 12, 384.
- Berne, B.J., and Pecora, R. (2000). *Dynamic Light Scattering: With Applications to Chemistry, Biology, and Physics* (Courier Dover Publications).
- Bertoncini, E.I., D’Orazio, V., Senesi, N., and Mattiazzo, M.E. (2005). Fluorescence analysis of humic and fulvic acids from two Brazilian oxisols as affected by biosolid amendment. *Anal. Bioanal. Chem.* 381, 1281–1288.
- Blaakmeer, J., Bohmer, M.R., Stuart, M.A.C., and Fler, G.J. (1990). Adsorption of weak polyelectrolytes on highly charged surfaces. Poly(acrylic acid) on polystyrene latex with strong cationic groups. *Macromolecules* 23, 2301–2309.
- Bloom, P.R., and Leenheer, J.A. (1989). Vibrational, Electronic, and High-energy Spectroscopic Methods for Characterizing Humic Substances. (In: *Humic Substances II: In Search of Structure*. M. H. B. Hayes, P. MacCarthy, R. L. Malcolm, and R. S. Swift (eds), Wiley, Chichester, New York, pp. 409–446),.
- Boggs, S., Livermore, D.G., and Seitz, M.G. (1985). Humic Macromolecules in Natural Waters. *J. Macromol. Sci. Part C Polym. Rev.* 25, 599–657.
- Bohmer, M.R., Evers, O.A., and Scheutjens, J.M.H.M. (1990). Weak polyelectrolytes between two surfaces: adsorption and stabilization. *Macromolecules* 23, 2288–2301.
- Bors, J., Patzkó, Á., and Dékány, I. (2001). Adsorption behavior of radioiodides in hexadecylpyridinium–humate complexes. *Appl. Clay Sci.* 19, 27–37.
- Bowles, E.C., and Antweiler, R.C. (1994). Acid-Base Utration and Hydrolysis of Fulvic Acid from the Suwannee River (In: *Humic substances in the Suwannee River, Georgia; interactions, properties, and proposed structures*. p. 115–128, United States Geological Survey), WSP - 2373.
- Bracewell, J.M., Haider, K., Larter, S.R., and Schulten, H.-R. (1989). Thermal Degradation Relevant to Structural Studies of Humic Substances. (In: *Humic Substances II: In Search of*

- Structure. M. H. B. Hayes, P. MacCarthy, R. L. Malcolm, and R. S. Swift (eds), Wiley, Chichester, New York, pp. 181-222),.
- Brar, S.K., and Verma, M. (2011). Measurement of nanoparticles by light-scattering techniques. *TrAC Trends Anal. Chem.* *30*, 4–17.
- Breger, I.A. (1960). Diagenesis of metabolites and a discussion of the origin of petroleum hydrocarbons. *Geochim. Cosmochim. Acta* *19*, 297–308.
- Bromberg, L., Temchenko, M., and Colby, R.H. (2000). Interactions among hydrophobically modified polyelectrolytes and surfactants of the same charge. *Langmuir* *16*, 2609–2614.
- Brown, T.L., and Rice, J.A. (2000). Effect of Experimental Parameters on the ESI FT-ICR Mass Spectrum of Fulvic Acid. *Anal. Chem.* *72*, 384–390.
- Brumberger, H., Stein, R.S., and Rowell, R. (1968). *Light Scattering*. (Science and Technology, pp. 34-60),.
- Bryant, G., Abeynayake, C., and Thomas, J.C. (1996). Improved particle size distribution measurements using multiangle dynamic light scattering. 2. Refinements and applications. *Langmuir* *12*, 6224–6228.
- Buffle, J. (1977). Les substances humiques et leur interactions avec les ions minéraux. *Conf. Proc. Comm. Hydrol. Appl. G H T M Univ. Orsay* Pp 3-10.
- Buffle, J. (1984). Natural organic matter and metal-organic interactions in aquatic systems. *Met. Ions Biol. Syst. Met. Environ.* Ed H Sigel Pp 165—221 N. Y. Marcel Dekker *18*, 165–221.
- Buffle, J. (1990). *Complexation Reactions in Aquatic Systems: An Analytical Approach* (E. Horwood).
- Buffle, J., and Leppard, G.G. (1995a). Characterization of Aquatic Colloids and Macromolecules. 1. Structure and Behavior of Colloidal Material. *Environ. Sci. Technol.* *29*, 2169–2175.
- Buffle, J., and Leppard, G.G. (1995b). Characterization of Aquatic Colloids and Macromolecules. 2. Key Role of Physical Structures on Analytical Results. *Environ. Sci. Technol.* *29*, 2176–2184.
- Buffle, J., Deladoey, P., and Haerdi, W. (1978). The use of ultrafiltration for the separation and fractionation of organic ligands in fresh waters. *Anal. Chim. Acta* *101*, 339–357.
- Buffle, J., Altmann, R.S., Filella, M., and Tessier, A. (1990). Complexation by natural heterogeneous compounds: Site occupation distribution functions, a normalized description of metal complexation. *Geochim. Cosmochim. Acta* *54*, 1535–1553.
- Burdon, J. (2001). Are the traditional concepts of the structures of humic substances realistic? *Soil Sci.* *166*, 752–769.
- Burges, A., Hurst, H.M., Walkden, S.B., Dean, F.M., and Hirst, M. (1963). Nature of Humic Acids. *Nature* *199*, 696–697.

Del Burgo, P., Aicart, E., and Junquera, E. (2007). Mixed vesicles and mixed micelles of the cationic–cationic surfactant system: didecyldimethylammonium bromide/dodecylethyldimethylammonium bromide/water. *Colloids Surf. Physicochem. Eng. Asp.* 292, 165–172.

Burov, S.V., Obrezkov, N.P., Vanin, A.A., and Piotrovskaya, E.M. (2008). Molecular dynamic simulation of micellar solutions: A coarse-grain model. *Colloid J.* 70, 1–5.

C

Cabaniss, S.E. (1990). pH and ionic strength effects on nickel-fulvic acid dissociation kinetics. *Environ. Sci. Technol.* 24, 583–588.

Cabaniss, S.E. (1992). Synchronous fluorescence spectra of metal-fulvic acid complexes. *Environ. Sci. Technol.* 26, 1133–1139.

Cabaniss, S.E., and Shuman, M.S. (1988). Copper binding by dissolved organic matter: I. Suwannee River fulvic acid equilibria. *Geochim. Cosmochim. Acta* 52, 185–193.

Cabaniss, S.E., Zhou, Q., Maurice, P.A., Chin, Y.-P., and Aiken, G.R. (2000). A Log-Normal Distribution Model for the Molecular Weight of Aquatic Fulvic Acids. *Environ. Sci. Technol.* 34, 1103–1109.

Cameron, R.S., and Posner, A.M. (1974). Molecular weight distributions of humic acid from density gradient ultracentrifugation profiles corrected for diffusion (Trans. 10th Int. Congr. Soil Sci., Moscow 2, 325–331).

Cameron, R.S., Swift, R.S., Thornton, B.K., and Posner, A.M. (1972a). Calibration of Gel Permeation Chromatography Materials for Use with Humic Acid. *J. Soil Sci.* 23, 342–349.

Cameron, R.S., Thornton, B.K., Swift, R.S., and Posner, A.M. (1972). Molecular Weight and Shape of Humic Acid from Sedimentation and Diffusion Measurements on Fractionated Extracts. *J. Soil Sci.* 23, 394–408.

Cane, R.F. (1976). The Origin and Formation of Oil Shale. In *Oil Shale: Developments in Petroleum Science*, T. F. Yen and G. V. Chilingarian, ed. (Elsevier), pp. 27–60.

Canellas, L.P., Zandonadi, D.B., Busato, J.G., Baldotto, M.A., Simões, M.L., Martin-Neto, L., Façanha, A.R., Spaccini, R., and Piccolo, A. (2008). BIOACTIVITY AND CHEMICAL CHARACTERISTICS OF HUMIC ACIDS FROM TROPICAL SOILS SEQUENCE. *Soil Sci.* 173, 624–637.

Carstea, E.M. (2012). Fluorescence Spectroscopy as a Potential Tool for In-Situ Monitoring of Dissolved Organic Matter in Surface Water Systems. *INTECH Open Access Publ.*

Carter, C. W. and Suffet, I. H. (1982). “Binding of DDT to dissolved humic materials,” *Environ. Sci. Technol.*, vol. 16, no. 11, pp. 735–740.

Cavalier, A., Spohner, D., and Humbel, B.M. (2008). *Handbook of Cryo-Preparation Methods for Electron Microscopy* (Taylor & Francis).

- Cawley, K.M., Korak, J.A., and Rosario-Ortiz, F.L. (2015). Quantum Yields for the Formation of Reactive Intermediates from Dissolved Organic Matter Samples from the Suwannee River. *Environ. Eng. Sci.* *32*, 31–37.
- Ceccanti, B., Calcinai, M., Bonmati-Pont, M., Ciardi, C., and Tarsitano, R. (1989). Molecular size distribution of soil humic substances with ionic strength. *Sci. Total Environ.* *81–82*, 471–479.
- Chaaban, A.A., Lartiges, B., Kazpard, V., Plisson-Chastang, C., Michot, L., Bihannic, I., Caillet, C., and Prelot, B. (2016). Probing the organization of fulvic acid using a cationic surfactant. *Colloids Surf. Physicochem. Eng. Asp.* *504*, 252–259.
- Chakraborty, T., Chakraborty, I., and Ghosh, S. (2006). Sodium Carboxymethylcellulose–CTAB Interaction: A Detailed Thermodynamic Study of Polymer–Surfactant Interaction with Opposite Charges. *Langmuir* *22*, 9905–9913.
- Chen, H., and Kenny, J.E. (2007). A Study of pH Effects on Humic Substances Using Chemometric Analysis of Excitation–Emission Matrices. *Ann. Environ. Sci.* *1*, 1–9.
- Chen, Y., and Schnitzer, M. (1976). Viscosity measurements on soil humic substances. *Soil Sci. Soc. Am. J.* *40*, 866–872.
- Chen, Y., and Schnitzer, M. (1978). Surface-Tension of Aqueous-Solutions of Soil Humic Substances. *Soil Sci.* *125*, 7–15.
- Chen, Y., and Schnitzer, M. (1989). Sizes and Shapes of Humic Substances by Electron Microscopy. (In: *Humic Substances II: In Search of Structure*. M. H. B. Hayes, P. MacCarthy, R. L. Malcolm, and R. S. Swift (eds), Wiley, Chichester, New York, pp. 621–638),.
- Chen, S.-H., and Teixeira, J. (1986). Structure and fractal dimension of protein-detergent complexes. *Phys. Rev. Lett.* *57*, 2583–2586.
- Chen, J., LeBoeuf, E.J., Dai, S., and Gu, B. (2003a). Fluorescence spectroscopic studies of natural organic matter fractions. *Chemosphere* *50*, 639–647.
- Chen, Z., Wannere, C.S., Corminboeuf, C., Puchta, R., and Schleyer, P. von R. (2005). Nucleus-Independent Chemical Shifts (NICS) as an Aromaticity Criterion. *Chem. Rev.* *105*, 3842–3888.
- Chen, W., Westerhoff, P., Leenheer, J.A., and Booksh, K. (2003b). Fluorescence excitation-emission matrix regional integration to quantify spectra for dissolved organic matter. *Environ. Sci. Technol.* *37*, 5701–5710.
- Cheshire, M.V. (1979). *Nature and origin of carbohydrates in soils*. (Academic Press, London and New York).
- Cheshire, M.V., Cranwell, P.A., Falshaw, C.P., Floyd, A.J., and Haworth, R.D. (1967). Humic acid—II: Structure of humic acids. *Tetrahedron* *23*, 1669–1682.

- Cheshire, M.V., Cranwell, P.A., and Haworth, R.D. (1968). Humic acid—III. *Tetrahedron* *24*, 5155–5167.
- Chew, C.H., Gan, L.M., Liu, J., and Lindman, B. (1995). Interactions of polymerized surfactants and a polymer. *Langmuir* *11*, 3312–3315.
- Chien, Y.-Y., and Bleam, W.F. (1998). Two-Dimensional NOESY Nuclear Magnetic Resonance Study of pH-Dependent Changes in Humic Acid Conformation in Aqueous Solution. *Environ. Sci. Technol.* *32*, 3653–3658.
- Chilom, G., and Rice, J.A. (2009). Structural Organization of Humic Acid in the Solid State. *Langmuir* *25*, 9012–9015.
- Chilom, G., Bruns, A.S., and Rice, J.A. (2009). Aggregation of humic acid in solution: Contributions of different fractions. *Org. Geochem.* *40*, 455–460.
- Chin, Y., and Gschwend, P.M. (1991). The abundance, distribution, and configuration of porewater organic colloids in recent sediments. *Geochim. Cosmochim. Acta* *55*, 1309–1317.
- Chin, W.-C., Orellana, M.V., and Verdugo, P. (1998). Spontaneous assembly of marine dissolved organic matter into polymer gels. *Nature* *391*, 568–572.
- Chin, Y., Aiken, G., and Oloughlin, E. (1994). Molecular-Weight, Polydispersity, and Spectroscopic Properties of Aquatic Humic Substances. *Environ. Sci. Technol.* *28*, 1853–1858.
- Chiou, C.T., Malcolm, R.L., Brinton, T.I., and Kile, D.E. (1986). Water solubility enhancement of some organic pollutants and pesticides by dissolved humic and fulvic acids. *Environ. Sci. Technol.* *20*, 502–508.
- Chiou, C.T., Kile, D.E., Brinton, T.I., Malcolm, R.L., Leenheer, J.A., and MacCarthy, P. (1987). A comparison of water solubility enhancements of organic solutes by aquatic humic materials and commercial humic acids. *Environ. Sci. Technol.* *21*, 1231–1234.
- Christl, I., Knicker, H., Kögel-Knabner, I., and Kretzschmar, R. (2000). Chemical heterogeneity of humic substances: characterization of size fractions obtained by hollow-fibre ultrafiltration. *Eur. J. Soil Sci.* *51*, 617–625.
- Christl, I., Metzger, A., Heidmann, I., and Kretzschmar, R. (2005). Effect of humic and fulvic acid concentrations and ionic strength on copper and lead binding. *Environ. Sci. Technol.* *39*, 5319–5326.
- Christman, R.F., and Gjessing, E.T. (1983). Aquatic and terrestrial humic materials (Ann Arbor Science Michigan).
- Christman, R.F., Norwood, D.L., Seo, Y., and Frimmel, F.H. (1989). Oxidative Degradation of Humic Substances From Freshwater Environments. (In: *Humic Substances II: In Search of Structure*. M. H. B. Hayes, P. MacCarthy, R. L. Malcolm, and R. S. Swift (eds), Wiley, Chichester, New York, pp. 33-68),.

- Claesson, P.M., Bergström, M., Dedinaite, A., Kjellin, M., Legrand, J.-F., and Grillo, I. (2000). Mixtures of cationic polyelectrolyte and anionic surfactant studied with small-angle neutron scattering. *J. Phys. Chem. B* *104*, 11689–11694.
- Clapp, C.E., and Hayes, M.H.B. (1999a). Sizes and shapes of humic substances. *Soil Sci.* *164*, 777–789.
- Clapp, C.E., and Hayes, M.H.B. (1996). Isolation of Humic Substances from an Agricultural Soil using a Sequential and Exhaustive Extraction Process. (In: *Humic Substances and Organic Matter in Soil and Water Environments*. C. E. Clapp, M. H. B. Hayes, N. Senesi, and S. M. Griffith (eds). IHSS, University of Minnesota, St. Paul, MN, pp. 3-11.),.
- Clapp, C.E., and Hayes, M.H.B. (1999). Characterization of Humic Substances Isolated From Clay-and Silt-Sized Fractions of a Corn Residue-Amended Agricultural Soil. *Soil Sci.* *164*, 899–913.
- Clapp, C.E., Emerson, W.W., and Olness, A.E. (1989). Sizes and Shapes of Humic Substances by Viscosity Measurements. (In: *Humic Substances II: In Search of Structure*. M. H. B. Hayes, P. MacCarthy, R. L. Malcolm, and R. S. Swift (eds), Wiley, Chichester, New York, pp. 497-514),.
- Clapp, C.E., Hayes, M.H.B., Senesi, N., Bloom, P.R., Jardine, P.M., Piccolo, A., Conte, P., Cozzolino, A., and Spaccini, R. (2001). Molecular Sizes and Association Forces of Humic Substances in Solution. In ACSESS Publications, (Soil Science Society of America),.
- Clark, G.N.I., Hura, G.L., Teixeira, J., Soper, A.K., and Head-Gordon, T. (2010). Small-angle scattering and the structure of ambient liquid water. *Proc. Natl. Acad. Sci.* *107*, 14003–14007.
- Cleven, R.F.M.J. (1984). Heavy metal/polyacid interaction : an electrochemical study of the binding of Cd(II), Pb(II) and Zn(II) to polycarboxylic and humic acids / (Ph.D. Thesis, Wageningen University, Wageningen, The Netherlands),.
- Cloos, P., Badot, C., and Herbillon, A. (1981). Interlayer formation of humin in smectites. *Nature* *289*, 391–393.
- Coble, P.G. (1996). Characterization of marine and terrestrial DOM in seawater using excitation-emission matrix spectroscopy. *Mar. Chem.* *51*, 325–346.
- Conte, P., and Piccolo, A. (1999). Conformational arrangement of dissolved humic substances. Influence of solution composition on association of humic molecules. *Environ. Sci. Technol.* *33*, 1682–1690.
- Conte, P., and Piccolo, A. (2002). Effect of concentration on the self-assembling of dissolved humic substances. In *Soil Mineral-Organic Matter-Microorganism Interactions and Ecosystem Health, Vol 28a: Dynamics, Mobility and Transformation of Pollutants and Nutrients*, A. Violante, P.M. Huang, J.M. Bollag, and L. Gianfreda, eds. pp. 409–417.
- Conte, P., Agretto, A., Spaccini, R., and Piccolo, A. (2005). Soil remediation: humic acids as natural surfactants in the washings of highly contaminated soils. *Environ. Pollut.* *135*, 515–522.

- Conte, P., Spaccini, R., and Piccolo, A. (2006). Advanced CPMAS-¹³C NMR techniques for molecular characterization of size-separated fractions from a soil humic acid. *Anal. Bioanal. Chem.* *386*, 382–390.
- Conte, P., Spaccini, R., Smejkalová, D., Nebbioso, A., and Piccolo, A. (2007). Spectroscopic and conformational properties of size-fractions separated from a lignite humic acid. *Chemosphere* *69*, 1032–1039.
- Cook, R. L., and Langford, C. H. (1998). “Structural Characterization of a Fulvic Acid and a Humic Acid Using Solid-State Ramp-CP-MAS ¹³C Nuclear Magnetic Resonance,” *Environ. Sci. Technol.*, vol. 32, no. 5, pp. 719–725.
- Cornel, P.K., Summers, R.S., and Roberts, P.V. (1986). Diffusion of humic acid in dilute aqueous solution. *J. Colloid Interface Sci.* *110*, 149–164.
- Corrado, G., Sanchez-Cortes, S., Francioso, O., and Garcia-Ramos, J.V. (2008). Surface-enhanced Raman and fluorescence joint analysis of soil humic acids. *Anal. Chim. Acta* *616*, 69–77.
- Cory, R.M., and McKnight, D.M. (2005). Fluorescence Spectroscopy Reveals Ubiquitous Presence of Oxidized and Reduced Quinones in Dissolved Organic Matter. *Environ. Sci. Technol.* *39*, 8142–8149.
- Cosgrove, T., White, S.J., Zorbakhsh, A., Heenan, R.K., and Howe, A.M. (1995). Small-angle scattering studies of sodium dodecyl sulfate interactions with gelatin. 1. *Langmuir* *11*, 744–749.
- da Costa Saab, S., Carvalho, E.R., Bernardes Filho, R., de Moura, M.R., Martin-Netob, L., and Mattosob, L.H.C. (2010). pH effect in aquatic fulvic acid from a Brazilian river. *J Braz Chem Soc* *21*, 1490–1496.
- Cottrell, T., and Van-Peij, J. (2004). Sorbitan Esters and Polysorbates. (In: *Emulsifiers in Food Technology*; Whitehurst, R. J., Ed.; Blackwell Publishing Ltd.: Oxford, pp 162-185),.
- Cozzolino, A., and Piccolo, A. (2002). Polymerization of dissolved humic substances catalyzed by peroxidase. Effects of pH and humic composition. *Org. Geochem.* *33*, 281–294.
- Cozzolino, A., Conte, P., and Piccolo, A. (2001). Conformational changes of humic substances induced by some hydroxy-, keto-, and sulfonic acids. *Soil Biol. Biochem.* *33*, 563–571.
- Cronan, C.S., and Aiken, G.R. (1985). Chemistry and transport of soluble humic substances in forested watersheds of the Adirondack Park, New York. *Geochim. Cosmochim. Acta* *49*, 1697–1705.
- Cui, Z., Qiu, F., and Sloat, B.R. (2006). Lecithin-based cationic nanoparticles as a potential DNA delivery system. *Int. J. Pharm.* *313*, 206–213.
- Curvetto, N.R., and Orioli, G.A. (1982). Electrophoretic subfractionation of low and high molecular weight humic acids fractions. *Plant Soil* *66*, 205–215.

Cyrański, M.K. (2005). Energetic Aspects of Cyclic Pi-Electron Delocalization: Evaluation of the Methods of Estimating Aromatic Stabilization Energies. *Chem. Rev.* 105, 3773–3811.

D

Dauben, H.J., Wilson, J.D., and Laity, J.L. (1968). Diamagnetic susceptibility exaltation as a criterion of aromaticity. *J. Am. Chem. Soc.* 90, 811–813.

Davies, G., Fataftah, A., Cherkasskiy, A., Ghabbour, E.A., Radwan, A., Jansen, S.A., Kolla, S., Paciolla, M.D., Sein, L.T.J., Buermann, W., et al. (1997). Tight metal binding by humic acids and its role in biomineralization†. *J. Chem. Soc. Dalton Trans.* 4047–4060.

Davies, G., Ghabbour, E.A., Khairy, K.A., and Britain), R.S. of C. (Great (1998). *Humic Substances: Structures, Properties and Uses* (RSC).

Davies, G., Ghabbour, E.A., and Steelink, C. (2001). Humic acids: Marvelous products of soil chemistry. *J. Chem. Educ.* 78, 1609.

Davis, J.A., and Gloor, R. (1981). Adsorption of dissolved organics in lake water by aluminum oxide. Effect of molecular weight. *Environ. Sci. Technol.* 15, 1223–1229.

Dearlove, J.P.L., Longworth, G., Ivanovich, M., Kim, J.I., Delakowitz, B., and Zeh, P. (1991). A study of groundwater-colloids and their geochemical interactions with natural radionuclides in Gorleben aquifer systems. *Radiochim. Acta* 52, 83–90.

DeBorger, R., and DeBacker, H. (1968). Determination des poids moleculaire moyen des acides fulviques per cryoscopie en milieu aqueux. *CR Acad Sci Ser* 266 2052—2055.

Deo, P., Deo, N., and Somasundaran, P. (2005). Complexation of hydrophobically modified polyelectrolytes with surfactants: Anionic poly (maleic acid/octyl vinyl ether)/anionic sodium dodecyl sulfate. *Langmuir* 21, 9998–10003.

Determann, S., Lobbes, J.M., Reuter, R., and Rullkötter, J. (1998). Ultraviolet fluorescence excitation and emission spectroscopy of marine algae and bacteria. *Mar. Chem.* 62, 137–156.

Detmer, V. (1871). Natural humic substances of the soil and their importance in agriculture. *Istor. Agrikultury IZD Akad Nauk SSSR*.

Diallo, M.S., Glinka, C.J., Goddard, W.A., and Johnson, J.H. (2000). Small angle neutron scattering investigations of Suwanee River fulvic acid aggregates in aqueous solutions. *Abstr. Pap. Am. Chem. Soc.* 220, U345–U345.

Diallo, M.S., Glinka, C.J., Iii, W.A.G., and Jr, J.H.J. (2005). Characterization of Nanoparticles and Colloids in Aquatic Systems 1. Small Angle Neutron Scattering Investigations of Suwanee River Fulvic Acid Aggregates in Aqueous Solutions. *J. Nanoparticle Res.* 7, 435–448.

Dixon, A.M., and Larive, C.K. (1997). Modified Pulsed-Field Gradient NMR Experiments for Improved Selectivity in the Measurement of Diffusion Coefficients in Complex Mixtures: Application to the Analysis of the Suwanee River Fulvic Acid. *Anal. Chem.* 69, 2122–2128.

Dixon, J.B., Weed, S.B., and Dinaure, R.C. (1989). Minerals in soil environments. (Soil Science Society of America Inc. 1244pp.).

Dobro, M.J., Melanson, L.A., Jensen, G.J., and McDowall, A.W. (2010). Plunge Freezing for Electron Cryomicroscopy. In *Methods in Enzymology*, G.J. Jensen, ed. (Academic Press), pp. 63–82.

Driver, S.J., and Perdue, E.M. (2015). Acid-Base Chemistry of Natural Organic Matter, Hydrophobic Acids, and Transphilic Acids from the Suwannee River, Georgia, as Determined by Direct Potentiometric Titration. *Environ. Eng. Sci.* 32, 66–70.

Duarte, R.M.B.O., Santos, E.B.H., and Duarte, A.C. (2003). Spectroscopic characteristics of ultrafiltration fractions of fulvic and humic acids isolated from an eucalyptus bleached Kraft pulp mill effluent. *Water Res.* 37, 4073–4080.

Durand, B., and Nicaise, G. (1980). Procedures for kerogen isolation. *Kerogen Insoluble Org. Matter Sediment. Rocks* 35–53.

Duval, J.F., Wilkinson, K.J., Van Leeuwen, H.P., and Buffle, J. (2005). Humic substances are soft and permeable: evidence from their electrophoretic mobilities. *Environ. Sci. Technol.* 39, 6435–6445.

E

Edzwald, J.K., Becker, W.C., and Wattier, K.L. (1985). Surrogate parameters for monitoring organic matter and THM precursors. *J. Am. Water Works Assoc.* 122–132.

Ehrhardt, M. (1984). Marine Gelbstoff. In *The Natural Environment and the Biogeochemical Cycles*, (Springer Berlin Heidelberg), pp. 63–77.

Einstein, A. (1956). *Investigations on the Theory of the Brownian Movement*. R. Furth (Ed.), Dover Publ., Inc., New York, USA.

Elkins, K.M., and Nelson, D.J. (2001). Fluorescence and FT-IR spectroscopic studies of Suwannee river fulvic acid complexation with aluminum, terbium and calcium. *J. Inorg. Biochem.* 87, 81–96.

ELLIS, G.P. (1959). The Maillard reaction. *Adv. Carbohydr. Chem.* 14, 63–134.

Engebretson, R.R., and von Wandruszka, R. (1994). Micro-Organization in Dissolved Humic Acids. *Environ. Sci. Technol.* 28, 1934–1941.

Engebretson, R.R., and von Wandruszka, R. (1998). Kinetic aspects of cation-enhanced aggregation in aqueous humic acids. *Environ. Sci. Technol.* 32, 488–493.

Engebretson, R.R., Amos, T., and von Wandruszka, R. (1996). Quantitative Approach to Humic Acid Associations. *Environ. Sci. Technol.* 30, 990–997.

Ephraim, J., Alegret, S., Mathuthu, A., Bicking, M., Malcolm, R.L., and Marinsky, J.A. (1986). A unified physicochemical description of the protonation and metal ion complexation equilibria of natural organic acids (humic and fulvic acids). 2. Influence of polyelectrolyte

properties and functional group heterogeneity on the protonation equilibria of fulvic acid. *Environ. Sci. Technol.* *20*, 354–366.

Ertel, J.R., Hedges, J.I., Devol, A.H., Richey, J.E., and Ribeiro, M. de N.G. (1986). Dissolved humic substances of the Amazon River system. *Limnol. Oceanogr.* *31*, 739–754.

F

Fagbenro, J., Hayes, M.H.B., Law, I.A., and Agboola, A.A. (1985). Extraction of Soil Organic Matter and Humic Substances from Two Nigerian Soils Using Three Solvent Mixtures. *Volunt. Pap. 2nd Intern Conf IHSS Birm. UK 1984 M H B Hayes R Swift Eds Pp 22-26.*

Fattal, D.R., Andelman, D., and Ben-Shaul, A. (1995). The vesicle-micelle transition in mixed lipid-surfactant systems: a molecular model. *Langmuir* *11*, 1154–1161.

Fava, F., and Piccolo, A. (2002). Effects of humic substances on the bioavailability and aerobic biodegradation of polychlorinated biphenyls in a model soil. *Biotechnol. Bioeng.* *77*, 204–211.

Feigin, L.A., Svergun, D.I., and Taylor, G.W. (1987). General Principles of Small-Angle Diffraction. In *Structure Analysis by Small-Angle X-Ray and Neutron Scattering*, G.W. Taylor, ed. (Springer US), pp. 25–55.

Fellman, J.B., Hood, E., and Spencer, R.G.M. (2010). Fluorescence spectroscopy opens new windows into dissolved organic matter dynamics in freshwater ecosystems: A review. *Limnol. Oceanogr.* *55*, 2452–2462.

Ferrari, G.M., and Mingazzini, M. (1995). Synchronous fluorescence spectra of dissolved organic matter (DOM) of algal origin in marine coastal waters. *Mar. Ecol.-Prog. Ser. - MAR ECOL-PROGR SER 125*, 305–315.

Fetsch, D., Hradilová, M., Peña Méndez, E.M., and Havel, J. (1998). Capillary zone electrophoresis study of aggregation of humic substances. *J. Chromatogr. A* *817*, 313–323.

Fievre, A., Solouki, T., Marshall, A.G., and Cooper, W.T. (1997). High-Resolution Fourier Transform Ion Cyclotron Resonance Mass Spectrometry of Humic and Fulvic Acids by Laser Desorption/Ionization and Electro spray Ionization. *Energy Fuels* *11*, 554–560.

Figini, R.V., and Marx-Figini, M. (1981). On the molecular weight determination by vapour pressure osmometry, 3. Relationship between diffusion coefficient of the solute and non-colligative behaviour. *Makromol. Chem.* *182*, 437–443.

Fischer, F., and Schrader, H. (1921). The origin and chemical structure of coal. *Brennst.-Chem V2 Pp 37–45.*

Fischer, H., Sachse, A., Steinberg, C.E., and Pusch, M. (2002). Differential retention and utilization of dissolved organic carbon by bacteria in river sediments. *Limnol. Oceanogr.* *47*, 1702–1711.

Flaig, W. (1964). Effects of micro-organisms in the transformation of lignin to humic substances. *Geochim. Cosmochim. Acta* 28, 1523–1535.

Flaig, W. (1988). Generation of model chemical precursors. (In: Humic substances and their role in the environment. F. H. Frimmel and R. F. Christman (eds). Wiley, Chichester, UK, pp. 59-74.).

Flaig, W. (1990). Effects of some organic substances from humus on plant growth and metabolism. (In: humic substances III. Interactions with Metals, Minerals and Organic Chemicals. P. MacCarthy, M. H. B. Hayes, R.L Malcolm, and R.S. Swift (eds), Wiley, Chichester, New York, in press.),.

Flaig, W., and Beutelspacher, H. (1968). Investigations of humic acids with the analytical ultracentrifuge. In: *Isotopes and Radiation in Soil Organic-matter Studies* (International Atomic Energy Agency, Vienna, pp. 23-30).

Flaig, W., Beutelspacher, H., and Rietz, E. (1975). Chemical Composition and Physical Properties of Humic Substances. In *Soil Components*, J.E. Gieseking, ed. (Springer Berlin Heidelberg), pp. 1–211.

Flory, P.J. (1953). *Principles of polymer chemistry* (Cornell University Press).

Frank, J. (1996). Electron Microscopy of Macromolecular Assemblies. In *Three-Dimensional Electron Microscopy of Macromolecular Assemblies*, J. Frank, ed. (Burlington: Academic Press), pp. 12–53.

Frappier, G., Lartiges, B.S., and Skali-Lami, S. (2010). Floc Cohesive Force in Reversible Aggregation: A Couette Laminar Flow Investigation. *Langmuir* 26, 10475–10488.

Frimmel, F.H., Christman, R.F., Bracewell, J.M., and Wissenschaft, S. für die D. (1988). Humic substances and their role in the environment: report of the Dahlem Workshop on Humic Substances and Their Role in the Environment, Berlin (Chichester [West Sussex]; New York : Wiley).

Fu, P., Wu, F., Liu, C., Wang, F., Li, W., Yue, L., and Guo, Q. (2007). Fluorescence characterization of dissolved organic matter in an urban river and its complexation with Hg(II). *Appl. Geochem.* 22, 1668–1679.

Fu, Q., Pan, X., Zhang, D., and Zhou, B. (2011). Effects of heat treatment on fluorescence properties of humic substances from sandy soil in arid land and their Hg(II) binding behaviors. *Environ. Earth Sci.* 66, 2273–2279.

Funasaka, W., and Yokokawa, C. (1953). Coal Chemistry. X. Formation of Humin-Substance from Cellulose. *J. Soc. Chem. Ind. Jpn.* 56, 34–36.

G

Gaffney, J.S., Marley, N.A., and Clark, S.B. (1996). Humic and Fulvic Acids and Organic Colloidal Materials in the Environment. In *Humic and Fulvic Acids*, (American Chemical Society), pp. 2–16.

- Galapate, R.P., Baes, A.U., Ito, K., Mukai, T., Shoto, E., and Okada, M. (1998). Detection of domestic wastes in Kurose river using synchronous fluorescence spectroscopy. *Water Res.* *32*, 2232–2239.
- Gamboa, C., and Olea, A.F. (2006). Association of cationic surfactants to humic acid: Effect on the surface activity. *Colloids Surf. Physicochem. Eng. Asp.* *278*, 241–245.
- Gan, L., Chen, S., and Jensen, G.J. (2008). Molecular organization of Gram-negative peptidoglycan. *Proc. Natl. Acad. Sci. pnas.0808035105*.
- Gao, Y., Yan, M., and Korshin, G.V. (2015). Effects of Ionic Strength on the Chromophores of Dissolved Organic Matter. *Environ. Sci. Technol.*
- Geerts, R., van Ginkel, C.G., and Plugge, C.M. (2015). Accurate assessment of the biodegradation of cationic surfactants in activated sludge reactors (OECD TG 303A). *Ecotoxicol. Environ. Saf.* *118*, 83–89.
- George, J., Sudheesh, P., Reddy, P.N., and Sreejith, L. (2009). Influence of Salt on Cationic Surfactant-Biopolymer Interactions in Aqueous Media. *J. Solut. Chem.* *38*, 373–381.
- Ghosh, K., and Schnitzer, M. (1980). Macromolecular structures of humic substances. *Soil Sci.* *129*, 266–276.
- Ghosh, K., Das, I., Das, D.K., and Sanyal, S.K. (2012). Evaluation of humic and fulvic acid extracts of compost, oilcake, and soils on complex formation with arsenic. *Soil Res.* *50*, 239–248.
- Giannissis, D. (1987). Etude des interactions des substances humiques avec les cations de métaux lourds (Thèse de 3ème cycle Etat Univ.Rennes, p. 152).
- Giasuddin, A.B.M., Kanel, S.R., and Choi, H. (2007). Adsorption of Humic Acid onto Nanoscale Zerovalent Iron and Its Effect on Arsenic Removal. *Environ. Sci. Technol.* *41*, 2022–2027.
- Gillam, A.H., and Riley, J.P. (1981). Correction of osmometric number-average molecular weights of humic substances for dissociation. *Chem. Geol.* *33*, 355–366.
- Gjessing, E.T. (1965). Use of “Sephadex” Gel for the Estimation of Molecular Weight of Humic Substances in Natural Water. *Nature* *208*, 1091–1092.
- Gjessing, E.T. (1976). Physical and chemical characteristics of aquatic humus (Ann Arbor Science Publishers).
- Gjessing, E.T., Alberts, J., Bruchet, A., Egeberg, P.K., Lydersen, E., McGown, L.B., Mobed, J.J., Münster, U., Pempkowiak, J., Perdue, M., et al. (1998). Multi-method characterisation of natural organic matter isolated from water: characterisation of reverse osmosis-isolates from water of two semi-identical dystrophic lakes basins in Norway. *Water Res.* *32*, 3108–3124.
- Glaser, H.T., and Edzwald, J.K. (1979). Coagulation and direct filtration of humic substances with polyethylenimine. *Environ. Sci. Technol.* *13*, 299–305.

- Glaser, B., Haumaier, L., Guggenberger, G., and Zech, W. (1998). Black carbon in soils: the use of benzenecarboxylic acids as specific markers. *Org. Geochem.* *29*, 811–819.
- Glover, C.A. (1975). Absolute Colligative Property Measurements (In: *Polymer Molecular Weights, Part I* (P. E. Slade, Jr ed.). Marcel Dekker, New York, pp. 79-159).
- Goldberg, M.C., and Weiner, E.R. (1994). Fluorescence Measurements of the Volume, Shape, and Fluorophore Composition of Fulvic Acid from the Suwannee River (In: *Humic substances in the Suwannee River, Georgia; interactions, properties, and proposed structures.* p. 99-114, United States Geological Survey, WSP - 2373).
- Goltsov, A.N., and Barsukov, L.I. (2000). Synergetics of the membrane self-assembly: a micelle-to-vesicle transition. *J. Biol. Phys.* *26*, 27–41.
- Goossen, L.J., Ohlmann, D.M., and Lange, P.P. (2009). The thermal amidation of carboxylic acids revisited. *Synthesis* *2009*, 160–164.
- Gopal, K., Tripathy, S.S., Bersillon, J.L., and Dubey, S.P. (2007). Chlorination byproducts, their toxicodynamics and removal from drinking water. *J. Hazard. Mater.* *140*, 1–6.
- Góralczyk, D. (1996). Influence of Inorganic Electrolyte Concentration on Properties of Anionic–Cationic Adsorption Films. *J. Colloid Interface Sci.* *179*, 211–217.
- Goring, D.A.I. (1971). Lignins: occurrence, formation, structure and reactions (In: *Lignins: Occurrence, Formation, Structure and Reactions.* K. V. Sarkanen and C. H. Ludwig (eds). Wiley, New York, pp. 695-768).
- Green, N.W., McInnis, D., Hertkorn, N., Maurice, P.A., and Perdue, E.M. (2015). Suwannee River Natural Organic Matter: Isolation of the 2R101N Reference Sample by Reverse Osmosis. *Environ. Eng. Sci.* *32*, 38–44.
- Gregor, J.E., and Powell, H.K.J. (1987). Effects of extraction procedures on fulvic acid properties. *Sci. Total Environ.* *62*, 3–12.
- Griffith, S.M., and Schnitzer, M. (1989). Oxidative Degradation of Soil Humic Substances. (In: *Humic Substances II: In Search of Structure.* M. H. B. Hayes, P. MacCarthy, R. L. Malcolm, and R. S. Swift (eds), Wiley, Chichester, New York, pp. 69-98),.
- Griffiths, P.C., Fallis, I.A., Teerapornchaisit, P., and Grillo, I. (2001). Hydrophobically modified gelatin and its interaction in aqueous solution with sodium dodecyl sulfate. *Langmuir* *17*, 2594–2601.
- Griffiths, P.C., Hirst, N., Paul, A., King, S.M., Heenan, R.K., and Farley, R. (2004). Effect of ethanol on the interaction between poly (vinylpyrrolidone) and sodium dodecyl sulfate. *Langmuir* *20*, 6904–6913.
- Grillo, I. (2008). *13 Small-Angle Neutron Scattering and Applications in Soft Condensed Matter.*
- Guéguen, C., and Cuss, C.W. (2011). Characterization of aquatic dissolved organic matter by asymmetrical flow field-flow fractionation coupled to UV–Visible diode array and excitation emission matrix fluorescence. *J. Chromatogr. A* *1218*, 4188–4198.

Guetzloff, T., and Rice, J. (1994). Does Humic-Acid Form a Micelle. *Sci. Total Environ.* 152, 31–35.

Guo, J., and Ma, J. (2006). AFM study on the sorbed NOM and its fractions isolated from River Songhua. *Water Res.* 40, 1975–1984.

Guthrie, J.W., Hassan, N.M., Salam, M.S.A., Fafous, I.I., Murimboh, C.A., Murimboh, J., Chakrabarti, C.L., and Grégoire, D.C. (2005). Complexation of Ni, Cu, Zn, and Cd by DOC in some metal-impacted freshwater lakes: a comparison of approaches using electrochemical determination of free-metal-ion and labile complexes and a computer speciation model, WHAM V and VI. *Anal. Chim. Acta* 528, 205–218.

H

De Haan, H., Jones, R.I., and Salonen, K. (1987). Does ionic strength affect the configuration of aquatic humic substances, as indicated by gel filtration? *Freshw. Biol.* 17, 453–459.

Haiber, S., Herzog, H., Burba, P., Gosciniak, B., and Lambert, J. (2001a). Quantification of carbohydrate structures in size fractionated aquatic humic substances by two-dimensional nuclear magnetic resonance. *Fresenius J. Anal. Chem.* 369, 457–460.

Haiber, S., Herzog, H., Burba, P., Gosciniak, B., and Lambert, J. (2001b). Two-dimensional NMR studies of size fractionated Suwannee River fulvic and humic acid reference. *Environ. Sci. Technol.* 35, 4289–4294.

Haider, K., Frederick, L.R., and Flaig, W. (1965). Reactions between amino acid compounds and phenols during oxidation. *Plant Soil* 22, 49–64.

Haider, K., Martin, J.P., and Filip, Z. (1975). Humus biochemistry. (In *Soil Biochemistry*. Ed. E. A. Paul, S. D. McLaren. New York: Marcel Dekker, pp. 195–244.),.

Hammouda, B. (2009). The mystery of clustering in macromolecular media. *Polymer* 50, 5293–5297.

Hammouda, B., and Ho, D.L. (2007). Insight into chain dimensions in PEO/water solutions. *J. Polym. Sci. Part B Polym. Phys.* 45, 2196–2200.

Hammouda, B., Ho, D.L., and Kline, S. (2002). SANS from Poly(ethylene oxide)/Water Systems. *Macromolecules* 35, 8578–8585.

Hammouda, B., Ho, D.L., and Kline, S. (2004). Insight into Clustering in Poly(ethylene oxide) Solutions. *Macromolecules* 37, 6932–6937.

Han, S., Hou, W., Dang, W., Xu, J., Hu, J., and Li, D. (2003). Synthesis of rod-like mesoporous silica using mixed surfactants of cetyltrimethylammonium bromide and cetyltrimethylammonium chloride as templates. *Mater. Lett.* 57, 4520–4524.

Hänninen, K.I., Klöcking, R., and Helbig, B. (1987). Synthesis and characterization of humic acid-like polymers. *Sci. Total Environ.* 62, 201–210.

- Hansen, E.H., and Schnitzer, M. (1966). The Alkaline Permanganate Oxidation of Danish Illuvial Organic Matter. *Soil Sci. Soc. Am. J.* *30*, 745.
- Hansen, E.H., and Schnitzer, M. (1969). Zn-dust distillation and fusion of a soil humic and fulvic acid. *Soil Sci. Soc. Am. J.* *33*, 29–36.
- Hansson, P., and Almgren, M. (1994). Interaction of Alkyltrimethylammonium Surfactants with Polyacrylate and Poly(styrenesulfonate) in Aqueous Solution: Phase Behavior and Surfactant Aggregation Numbers. *Langmuir* *10*, 2115–2124.
- Hargreaves, A.E., and Hargreaves, T. (2003). Chemical formulation: an overview of surfactant-based preparations used in everyday life (Royal Society of Chemistry).
- Harvey, G.R., Boran, D.A., Chesal, L.A., and Tokar, J.M. (1983). The structure of marine fulvic and humic acids. *Mar. Chem.* *12*, 119–132.
- Harwell, J.H., Sabatini, D.A., and Knox, R.C. (1999). Surfactants for ground water remediation. *Colloids Surf. Physicochem. Eng. Asp.* *151*, 255–268.
- Hatcher, P.G., and Spiker, E.C. (1988). Selective degradation of plant biomolecules. (In: Humic substances and their role in the environment. F. H. Frimmel and R. F Christman (eds). Wiley, Chichester, UK, pp. 59-74.).
- Hatcher, P.G., Rowan, R., and Mattingly, M.A. (1980a). ¹H and ¹³C NMR of marine humic acids. *Org. Geochem.* *2*, 77–85.
- Hatcher, P.G., VanderHart, D.L., and Earl, W.L. (1980b). Use of solid-state ¹³C NMR in structural studies of humic acids and humin from Holocene sediments. *Org. Geochem.* *2*, 87–92.
- Hatcher, P.G., Breger, I.A., Maciel, G., and Szeverenyi, N. (1985). Geochemistry of Humin. (In: Humic substances in soil, sediment, and water: geochemistry, isolation and characterization. G. R. Aiken, D. M. McKnight, R.L. Wershaw, and P. MacCarthy (eds). John Wiley, New York, pp. 275-302).
- Hausler, M.J., and Hayes, M.H.B. (1996). Uses of XAD-8 Resin and Acidified Dimethylsulfoxide in Studies of Humic Acids. (In: Humic Substances and Organic Matter in Soil and Water Environments. C. E. Clapp, M. H. B. Hayes, N. Senesi, and S. M. Griffith (eds). IHSS, University of Minnesota, St. Paul, MN, pp. 13-24.).
- Haworth, R.D. (1971). The chemical nature of humic acid. *Soil Sci.* *111*, 71–79.
- Hayakawa, K., and Kwak, J.C. (1982). Surfactant-polyelectrolyte interactions. 1. Binding of dodecyltrimethylammonium ions by sodium dextransulfate and sodium poly(styrenesulfonate) in aqueous solution in the presence of sodium chloride. *J. Phys. Chem.* *86*, 3866–3870.
- Hayakawa, K., Fukutome, T., and Satake, I. (1990). Solubilization of water-insoluble dye by a cooperative binding system of surfactant and polyelectrolyte. *Langmuir* *6*, 1495–1498.
- Hayano, S., Shinozuka, N., and Hyakutake, M. (1982). Surface Active Properties of Marine Humic Acids. *J. Jpn. Oil Chem. Soc.* *31*, 357–362.

Hayase, K., and Tsubota, H. (1983). Sedimentary humic acid and fulvic acid as surface active substances. *Geochim. Cosmochim. Acta* 47, 947–952.

Hayes, M.H.B. (1985). Extraction of Humic Substances from Soil (In: *Humic Substances in Soil, Sediment, and Water*, ed. G.R. Aiken, D.M. McKnight, R.L. Wershaw & P. MacCarthy, pp. 329–362. New York: Wiley.).

Hayes, M.H.B. (1989). *Humic substances II: in search of structure* (J. Wiley).

Hayes, M.H.B. (1997). Emerging concepts of the compositions and structures of humic substances (In: *Humic Substances, Peats and Sludges: Health and Environmental Aspects*. M. H. B. Hayes and W. S. Wilson (eds). The Royal Society of Chemistry, Cambridge, UK, pp. 3-30).

Hayes, M.H.B. (1998). Humic Substances: Progress towards more realistic concepts of structures (In: *Humic Substances: Structures, Properties and Uses*. G. Davies and E. A. Ghabbour (eds). The Royal Society of Chemistry, Cambridge. UK, pp. 1-27).

Hayes, M.H.B., and Malcolm, R.L. (2001). Structures of Humic Substances. (In: *Humic Substances and Chemical Contaminants*. C. E. Clapp, M. H. B. Hayes, N. Senesi, P. Bloom, and P. M. Jardine (eds). Soil Science Society of America, Madison, WI, pp. 3-40.),.

Hayes, M.H.B., and O’Callaghan, M.R. (1989). Degradations with Sodium Sulfide and with Phenol. (In: *Humic Substances II: In Search of Structure*. M. H. B. Hayes, P. MacCarthy, R. L. Malcolm, and R. S. Swift (eds), Wiley, Chichester, New York, pp. 143-180),.

Hayes, M.H.B., and Swift, R.S. (1978). The chemistry of soil organic colloids. *Chem. Soil Const. J Greenl.* M H B Hayes Eds Wiley Chichester N. Y. Pp 179-320.

Hayes, M.H.B., and Swift, R.S. (1990). Genesis, Isolation, Composition and Structures of Soil Humic Substances. In *Soil Colloids and Their Associations in Aggregates*, M.F.D. Boodt, M.H.B. Hayes, A. Herbillon, E.B.A.D. Strooper, and J.J. Tuck, eds. (Springer US), pp. 245–305.

Hayes, M.H., and Clapp, C.E. (2001). Humic substances: considerations of compositions, aspects of structure, and environmental influences. *Soil Sci.* 166, 723–737.

Hayes, M.H.B., MacCarthy, P., Malcolm, R.L., and Swift, R.S. (1989a). Structures of Humic Substances: The Emergence of “Forms.” (In: *Humic Substances II: In Search of Structure*. M. H. B. Hayes, P. MacCarthy, R. L. Malcolm, and R. S. Swift (eds), Wiley, Chichester, New York, pp. 689-733),.

Hayes, M.H.B., MacCarthy, P., Malcolm, R.L., and Swift, R.S. (1989b). The Search for Structure: Setting the Scene. (In: *Humic Substances II: In Search of Structure*. M. H. B. Hayes, P. MacCarthy, R. L. Malcolm, and R. S. Swift (eds), Wiley, Chichester, New York, pp. 3-32),.

Hayes, T.M., Hayes, M.H.B., Skjemstad, R.S., Swift, R.S., and Malcolm, R.L. (1996). Isolation of Humic Substances from Soil using Aqueous Extractants of Different pH and XAD resins, and their Characterization by ¹³C-NMR. (In: *Humic Substances and Organic Matter in Soil and Water Environments*. C. E. Clapp, M. H. B. Hayes, N. Senesi, and S. M. Griffith (eds). IHSS, University of Minnesota, St. Paul, MN, pp. 13-24.),.

- He, Q.H., Leppard, G.G., Paige, C.R., and Snodgrass, W.J. (1996). Transmission electron microscopy of a phosphate effect on the colloid structure of iron hydroxide. *Water Res.* *30*, 1345–1352.
- Hedges, J.I. (1988). Polymerization of humic substances in natural environments. (In: Humic substances and their role in the environment. F. H. Frimmel and R. F. Christman (eds). Wiley, Chichester, UK, pp. 59-74.).
- Hedges, J.I., and Keil, R.G. (1995). Sedimentary organic matter preservation: an assessment and speculative synthesis. *Mar. Chem.* *49*, 81–115.
- Henderson, R., and Unwin, P.N.T. (1975). Three-dimensional model of purple membrane obtained by electron microscopy. *Nature* *257*, 28–32.
- Her, N., Amy, G., Foss, D., and Cho, J. (2002). Variations of Molecular Weight Estimation by HP-Size Exclusion Chromatography with UVA versus Online DOC Detection. *Environ. Sci. Technol.* *36*, 3393–3399.
- Herbert, B.E., and Bertsch, P.M. (1995). Characterization of Dissolved and Colloidal Organic Matter in Soil Solution: A Review. In ACSESS Publications, (In: Carbon Forms and Functions in Forest Soils, ed. W.W. McFee & J.M. Kelly, pp. 63—88. Madison, WI: Soil Science Society of America),.
- Hering, J.G., and Morel, F.M.M. (1989). Slow coordination reactions in seawater. *Geochim. Cosmochim. Acta* *53*, 611–618.
- Hertkorn, N., Claus, H., Schmitt-Kopplin, P., Perdue, E.M., and Filip, Z. (2002). Utilization and Transformation of Aquatic Humic Substances by Autochthonous Microorganisms. *Environ. Sci. Technol.* *36*, 4334–4345.
- Hertkorn, N., Ruecker, C., Meringer, M., Gugisch, R., Frommberger, M., Perdue, E.M., Witt, M., and Schmitt-Kopplin, P. (2007). High-precision frequency measurements: indispensable tools at the core of the molecular-level analysis of complex systems. *Anal. Bioanal. Chem.* *389*, 1311–1327.
- Hiraide, M., Shima, T., and Kawaguchi, H. (1994). Separation and determination of dissolved and particulate humic substances in river water. *Microchim. Acta* *113*, 269–276.
- Hobson, R.P. (1925). A study of the nitrogen compounds of mineral soils. PhD Thesis Univ. Lond.
- Hoff, E., Nyström, B., and Lindman, B. (2001). Polymer-surfactant interactions in dilute mixtures of a nonionic cellulose derivative and an anionic surfactant. *Langmuir* *17*, 28–34.
- H g lund, C., Birch, J., Andersen, K., Bigault, T., Buffet, J.-C., Correa, J., van Esch, P., Guerard, B., Hall-Wilton, R., Jensen, J., et al. (2012). B4C thin films for neutron detection. *J. Appl. Phys.* *111*, 104908.
- Holman, H.-Y.N., Nieman, K., Sorensen, D.L., Miller, C.D., Martin, M.C., Borch, T., McKinney, W.R., and Sims, R.C. (2002). Catalysis of PAH Biodegradation by Humic Acid Shown in Synchrotron Infrared Studies. *Environ. Sci. Technol.* *36*, 1276–1280.

- Holt, M.S., Fox, K.K., Burford, M., Daniel, M., and Buckland, H. (1998). UK monitoring study on the removal of linear alkylbenzene sulphonate in trickling filter type sewage treatment plants. Contribution to GREAT-ER project # 2. *Sci. Total Environ.* *210-11*, 255–269.
- Hopkins, D.W., Chudek, J.A., Webster, E.A., and Barraclough, D. (1997). Following the decomposition of ryegrass labelled with ^{13}C and ^{15}N in soil by solid-state nuclear magnetic resonance spectroscopy. *Eur. J. Soil Sci.* *48*, 623–631.
- Horkay, F., Hecht, A.-M., and Geissler, E. (1998). Fine Structure of Polymer Networks As Revealed by Solvent Swelling. *Macromolecules* *31*, 8851–8856.
- Hosse, M., and Wilkinson, K.J. (2001). Determination of Electrophoretic Mobilities and Hydrodynamic Radii of Three Humic Substances as a Function of pH and Ionic Strength. *Environ. Sci. Technol.* *35*, 4301–4306.
- Hsu, P.-H., and Hatcher, P.G. (2005). New evidence for covalent coupling of peptides to humic acids based on 2D NMR spectroscopy: A means for preservation. *Geochim. Cosmochim. Acta* *69*, 4521–4533.
- Hu, W.-G., Mao, J., Xing, B., and Schmidt-Rohr, K. (2000). Poly(methylene) Crystallites in Humic Substances Detected by Nuclear Magnetic Resonance. *Environ. Sci. Technol.* *34*, 530–534.
- Huang, C.-C., Li, Y.-M., Yang, H., Sun, D.-Y., Xu, L.-J., and Chen, X. (2013). Study of influencing factors to chromophoric dissolved organic matter absorption properties from fluorescence features in Taihu lake in autumn. *J. Limnol.* *72*.
- Huang, P.M., Emerson, W.W., Foster, R.C., and Oades, J.M. (1986). Interactions of soil minerals with natural organics and microbes (The Soil Science Society of America).
- Huc, A.Y., and Durand, B.M. (1977). Occurrence and significance of humic acids in ancient sediments. *Fuel* *56*, 73–80.
- Hudson, N., Baker, A., and Reynolds, D. (2007). Fluorescence analysis of dissolved organic matter in natural, waste and polluted waters—a review. *River Res. Appl.* *23*, 631–649.
- Huffman, E.W.D., and Stuber, H.A. (1985). Analytical methodology for elemental analysis of humic substances. (In: Aiken, G. R., McKnight, D. M., Wershaw, R. L., MacCarthy, P. (eds). *Humic substances in soil, sediment and water*. New York: John Wiley & Sons, 433–455.),.
- Hur, J., and Schlautman, M.A. (2003). Molecular weight fractionation of humic substances by adsorption onto minerals. *J. Colloid Interface Sci.* *264*, 313–321.
- Hur, J., Jung, K.-Y., and Jung, Y.M. (2011). Characterization of spectral responses of humic substances upon UV irradiation using two-dimensional correlation spectroscopy. *Water Res.* *45*, 2965–2974.

I

Ikan, R., Ioselis, P., Rubinsztain, Y., Aizenshtat, Z., Miloslavsky, I., Yariv, S., Pugmire, R., Anderson, L.L., Woolfenden, W.R., Kaplan, I.R., et al. (1992). Chemical, isotopic, spectroscopic and geochemical aspects of natural and synthetic humic substances. *Sci. Total Environ.* 117–118, 1–12.

Insam, H. (1996). Chapter 6 - Microorganisms and Humus in Soils. In *Humic Substances in Terrestrial Ecosystems*, A. Piccolo, ed. (Amsterdam: Elsevier Science B.V.), pp. 265–292.

Imai, A., Fukushima, T., Matsushige, K., Kim, Y.-H., and Choi, K. (2002). Characterization of dissolved organic matter in effluents from wastewater treatment plants. *Water Res.* 36, 859–870.

Ishiguro, M., Tan, W., and Koopal, L.K. (2007). Binding of cationic surfactants to humic substances. *Colloids Surf. Physicochem. Eng. Asp.* 306, 29–39.

Ishiwatari, R. (1985). Geochemistry of Humic Substances in Lake Waters. (In: *Humic substances in soil, sediment, and water: geochemistry, isolation and characterization*. G. R. Aiken, D. M. McKnight, R.L. Wershaw, and P. MacCarthy (eds). John Wiley, New York, pp. 147-180).

Israelachvili, J.N. (2011). *Intermolecular and surface forces: revised third edition* (Academic press).

Israelachvili, J. N., Mitchell, D. J., and Ninham, B. W. (1976). “Theory of self-assembly of hydrocarbon amphiphiles into micelles and bilayers,” *J Chem Soc Faraday Trans 2*, vol. 72, pp. 1525–1568.

Ivanković, T., and Hrenović, J. (2010). Surfactants in the Environment. *Arch. Ind. Hyg. Toxicol.* 61.

J

Jacrot, B. (1976). The study of biological structures by neutron scattering from solution. *Rep. Prog. Phys.* 39, 911.

Jansen, S.A., Malaty, M., Nwabara, S., Johnson, E., Ghabbour, E., Davies, G., and Varnum, J.M. (1996). Structural modeling in humic acids. *Mater. Sci. Eng. C* 4, 175–179.

Jarvie, H.P., and King, S.M. (2007). Small-angle neutron scattering study of natural aquatic nanocolloids. *Environ. Sci. Technol.* 41, 2868–2873.

Jellinek, H.H.G. (1974). *Soil Organics: 1. Complexation of Heavy Metals*. (Special Report, No. 212, Cold Regions Research and Engineering Laboratory, Hanover, NH, pp. 1-51.).

Jenkinson, D.S. (1981). The fate of plant and animal residues in soil. *Chem. Soil Process.* 505–561.

Jensen, H.L. (1931). The Microbiology of Farmyard Manure Decomposition in Soil I. Changes in the Microflora, and their Relation to Nitrification. *J. Agric. Sci.* *21*, 38–80.

Johnson, C.S. (1999). Diffusion ordered nuclear magnetic resonance spectroscopy: principles and applications. *Prog. Nucl. Magn. Reson. Spectrosc.* *34*, 203–256.

Jones, M.N., and Bryan, N.D. (1998). Colloidal properties of humic substances. *Adv. Colloid Interface Sci.* *78*, 1–48.

Jores, K., Mehnert, W., Drechsler, M., Bunjes, H., Johann, C., and Mäder, K. (2004). Investigations on the structure of solid lipid nanoparticles (SLN) and oil-loaded solid lipid nanoparticles by photon correlation spectroscopy, field-flow fractionation and transmission electron microscopy. *J. Controlled Release* *95*, 217–227.

Jullien, R., and Botet, R. (1987). *Aggregation and Fractal Aggregates* (World Scientific).

Juma, N.G. (1999). The pedosphere and its dynamics. A systems approach to soil science. Volume 1: introduction to soil science and soil resources. (Salman productions, University of Alberta, Edmonton. 1999. Hardcover, 315 pp. ISBN 1-896263-10-0. Web site: <http://www.pedosphere.com>).

Jung, A.-V. (2004). Interaction de la matière organique avec les micropolluants anthropiques et devenir lors de la coagulation (Vandoeuvre-les-Nancy, INPL).

Jung, A.-V., Chanudet, V., Ghanbaja, J., Lartiges, B.S., and Bersillon, J.-L. (2005a). Coagulation of humic substances and dissolved organic matter with a ferric salt: An electron energy loss spectroscopy investigation. *Water Res.* *39*, 3849–3862.

Jung, A.-V., Frochot, C., and Bersillon, J.-L. (2015). Fluorescence spectroscopy as a specific tool for the interaction study of two surfactants with natural and synthetic organic compounds. *Colloids Surf. Physicochem. Eng. Asp.* *481*, 567–576.

Jung, A.-V., Frochot, C., Parant, S., Lartiges, B.S., Selve, C., Viriot, M.-L., and Bersillon, J.-L. (2005b). Synthesis of amino-phenolic humic-like substances and comparison with natural aquatic humic acids: A multi-analytical techniques approach. *Org. Geochem.* *36*, 1252–1271.

Jung, A.-V., Frochot, C., Villieras, F., Lartiges, B.S., Parant, S., Viriot, M.-L., and Bersillon, J.-L. (2010). Interaction of pyrene fluoroprobe with natural and synthetic humic substances: Examining the local molecular organization from photophysical and interfacial processes. *Chemosphere* *80*, 228–234.

Junquera, E., Arranz, R., and Aicart, E. (2004). Mixed vesicle formation on a ternary surfactant system: Didodecyldimethylammonium bromide/dodecylethyldimethylammonium bromide/water. *Langmuir* *20*, 6619–6625.

K

Kalbitz, K., Geyer, W., and Geyer, S. (1999). Spectroscopic properties of dissolved humic substances—a reflection of land use history in a fen area. *Biogeochemistry* *47*, 219–238.

- Kalbitz, K., Geyer, S., and Geyer, W. (2000). A comparative characterization of dissolved organic matter by means of original aqueous samples and isolated humic substances. *Chemosphere* *40*, 1305–1312.
- Kam, S.-K., and Gregory, J. (2001). The interaction of humic substances with cationic polyelectrolytes. *Water Res.* *35*, 3557–3566.
- Karino, T., Okumura, Y., Ito, K., and Shibayama, M. (2004). SANS Studies on Spatial Inhomogeneities of Slide-Ring Gels. *Macromolecules* *37*, 6177–6182.
- Karino, T., Ikeda, Y., Yasuda, Y., Kohjiya, S., and Shibayama, M. (2007). Nonuniformity in Natural Rubber As Revealed by Small-Angle Neutron Scattering, Small-Angle X-ray Scattering, and Atomic Force Microscopy. *Biomacromolecules* *8*, 693–699.
- Karlstroem, G., Carlsson, A., and Lindman, B. (1990). Phase diagrams of nonionic polymer-water systems: experimental and theoretical studies of the effects of surfactants and other cosolutes. *J. Phys. Chem.* *94*, 5005–5015.
- Karsa, D.R. (1999). *Industrial applications of surfactants IV* (Elsevier).
- Kasha, M., Rawls, H.R., and El-Bayoumi, M.A. (1965). The exciton model in molecular spectroscopy. *Pure Appl Chem* *11*, 371–392.
- Kato, K., Walde, P., Koine, N., Ichikawa, S., Ishikawa, T., Nagahama, R., Ishihara, T., Tsujii, T., Shudou, M., and Omokawa, Y. (2008). Temperature-sensitive nonionic vesicles prepared from Span 80 (sorbitan monooleate). *Langmuir* *24*, 10762–10770.
- Kawahigashi, M., Fujitake, N., Azuma, J., Takahashi, T., Kajiwara, K., and Urakawa, H. (1995). The Shape of Humic-Acid in Solution as Observed by Small-Angle X-Ray-Scattering (vol 41, Pg 363, 1995). *Soil Sci. Plant Nutr.* *41*, 624–624.
- Kawahigashi, M., Sumida, H., and Yamamoto, K. (2005). Size and shape of soil humic acids estimated by viscosity and molecular weight. *J. Colloid Interface Sci.* *284*, 463–469.
- Kazpard, V., Lartiges, B.S., Frochot, C., d'Espinose de la Caillerie, J.B., Viriot, M.L., Portal, J.M., Görner, T., and Bersillon, J.L. (2006). Fate of coagulant species and conformational effects during the aggregation of a model of a humic substance with Al13 polycations. *Water Res.* *40*, 1965–1974.
- Kelleher, B.P., and Simpson, A.J. (2006). Humic substances in soils: are they really chemically distinct? *Environ. Sci. Technol.* *40*, 4605–4611.
- Khalaf, M., Kohl, S. D., Klumpp, E., Rice, J. A., and Tombácz, E. (2003). “Comparison of Sorption Domains in Molecular Weight Fractions of a Soil Humic Acid Using Solid-State ¹⁹F NMR,” *Environ. Sci. Technol.*, vol. 37, no. 13, pp. 2855–2860.
- Khan, S.U., and Sowden, F.J. (1971). Distribution of nitrogen in the black solonchic and black chernozemic soils of alberta. *Can. J. Soil Sci.* *51*, 185–193.
- Kim, H.-C., and Yu, M.-J. (2007). Characterization of aquatic humic substances to DBPs formation in advanced treatment processes for conventionally treated water. *J. Hazard. Mater.* *143*, 486–493.

- Kim, Y.-J., and Osako, M. (2004). Investigation on the humification of municipal solid waste incineration residue and its effect on the leaching behavior of dioxins. *Waste Manag.* *24*, 815–823.
- King, S.M. (1999). Small-angle neutron scattering. (In: *Modern Techniques for Polymer Characterisation*. Chapter 7. Pethrick, R. A. ; Dawkins, J. V. (editors). John Wiley & Sons.).
- Kinniburgh, D.G., Milne, C.J., Benedetti, M.F., Pinheiro, J.P., Filius, J., Koopal, L.K., and Van Riemsdijk, W.H. (1996). Metal Ion Binding by Humic Acid: Application of the NICA-Donnan Model. *Environ. Sci. Technol.* *30*, 1687–1698.
- Klang, V., Matsko, N.B., Valenta, C., and Hofer, F. (2012). Electron microscopy of nanoemulsions: An essential tool for characterisation and stability assessment. *Micron* *43*, 85–103.
- Klaus, U., Pfeifer, T., and Spiteller, M. (2000). APCI-MS/MS: A Powerful Tool for the Analysis of Bound Residues Resulting from the Interaction of Pesticides with DOM and Humic Substances. *Environ. Sci. Technol.* *34*, 3514–3520.
- Klavins, M., and Purmalis, O. (2010). Humic substances as surfactants. *Environ. Chem. Lett.* *8*, 349–354.
- Klucáková, M., Kargerová, A., and Novácková, K. (2012). Conformational changes in humic acids in aqueous solutions. *Chem. Pap.* *66*, 875–880.
- Knicker, H. (2000). Double dross polarization magic angle spinning ^{15}N ^{13}C NMR spectroscopic studies for characterization of immobilized nitrogen in soils. *Proc. 10th Int. Humic Subst. Soc. Toulouse Fr. July 24-28 2000* Pp 1105-1108.
- Knicker, H., and Hatcher, P.G. (1997). Survival of Protein in an Organic-Rich Sediment: Possible Protection by Encapsulation in Organic Matter. *Naturwissenschaften* *84*, 231–234.
- Knicker, H., and Lüdemann, H.-D. (1995). N-15 and C-13 CPMAS and solution NMR studies of N-15 enriched plant material during 600 days of microbial degradation. *Org. Geochem.* *23*, 329–341.
- Knicker, H., Fründ, R., and Lüdemann, H.D. (1997). Characterization of nitrogen in plant composts and native humic material by natural-abundance ^{15}N CPMAS and solution NMR spectra (In: *Nuclear Magnetic Resonance Spectroscopy in Environmental Chemistry*. M. A. Nanny, R. A. Minear, J. A. Leenheer (eds), Oxford University Press, Chp. 15, pp. 272-294).
- Kögel-Knabner, I., Zech, W., and Hatcher, P.G. (1988). Chemical composition of the organic matter in forest soils: The humus layer. *Z. Für Pflanzenernähr. Bodenk.* *151*, 331–340.
- Kolla, S., Sein, L.T., Paciolla, M.D., and Jansen, S.A. (1998). Physical insights in humic acid research. *Recent Res. Dev. Phys. Chem.* 765–786.
- Kononova, M.M. (1966). *Soil organic matter; its nature, its role in soil formation and in soil fertility*, (Oxford; New York: Pergamon Press).
- Koopal, L.K., Goloub, T.P., and Davis, T.A. (2004). Binding of ionic surfactants to purified humic acid. *J. Colloid Interface Sci.* *275*, 360–367.

- Koopal, L.K., Saito, T., Pinheiro, J.P., and van Riemsdijk, W.H. (2005). Ion binding to natural organic matter: General considerations and the NICA–Donnan model. *Colloids Surf. Physicochem. Eng. Asp.* 265, 40–54.
- Kreller, D.I., Wu, Y., Sutton, S., and Furio, A. (2015). Adsorption and Fractionation of Suwannee River Organic Matter on Metal (Fe, Al) Oxide-Coated Quartz: A Liquid Chromatographic Investigation. *Environ. Eng. Sci.* 32, 45–53.
- Van Krevelen, D.W. (1963). *Geochemistry of coal*. Org. Geochem. Breger Ed Pergamon Press Oxf. Pp 183–247.
- Kucerka, N., Nieh, M.-P., and Katsaras, J. (2010). Small-angle scattering from homogenous and heterogeneous lipid bilayers. *Adv. Planar Lipid Bilayers Liposomes* 201.
- Küchler, I.L., Miekeley, N., and Forsberg, B.R. (1994). Molecular mass distributions of dissolved organic carbon and associated metals in waters from Rio Negro and Rio Solimões. *Sci. Total Environ.* 156, 207–216
- Kuhn, K.M., Neubauer, E., Hofmann, T., Kammer, F. von der, Aiken, G.R., and Maurice, P.A. (2015). Concentrations and Distributions of Metals Associated with Dissolved Organic Matter from the Suwannee River (GA, USA). *Environ. Eng. Sci.* 32, 54–65.
- Kujawinski, E.B., Freitas, M.A., Zang, X., Hatcher, P.G., Green-Church, K.B., and Jones, R.B. (2002). The application of electrospray ionization mass spectrometry (ESI MS) to the structural characterization of natural organic matter. *Org. Geochem.* 33, 171–180.
- Kumke, M.U., Abbt-Braun, G., and Frimmel, F.H. (1998). Time-resolved Fluorescence Measurements of Aquatic Natural Organic Matter (NOM). *Acta Hydrochim. Hydrobiol.* 26, 73–81.
- Kuntsche, J., Horst, J.C., and Bunjes, H. (2011). Cryogenic transmission electron microscopy (cryo-TEM) for studying the morphology of colloidal drug delivery systems. *Int. J. Pharm.* 417, 120–137.
- Kurková, M., Klika, Z., Kliková, C., and Havel, J. (2004). Humic acids from oxidized coals: I. Elemental composition, titration curves, heavy metals in HA samples, nuclear magnetic resonance spectra of HAs and infrared spectroscopy. *Chemosphere* 54, 1237–1245.
- Kwak, J.C.T. (1998). *Polymer-Surfactant Systems* (CRC Press).

L

- Laane, R.W.P.M., and Koole, L. (1982). The relation between fluorescence and dissolved organic carbon in the Ems-Dollart estuary and the Western Wadden Sea. *Neth. J. Sea Res.* 15, 217–227.
- Lähdesmäki, P., and Piispanen, R. (1988). Degradation products and the hydrolytic enzyme activities in the soil humification processes. *Soil Biol. Biochem.* 20, 287–292.
- Lakowicz, J.R. (2010). *Principles of fluorescence spectroscopy* (New York, NY: Springer).

Lal, R. (2004). Soil Carbon Sequestration Impacts on Global Climate Change and Food Security. *Science* 304, 1623–1627.

Lal, R., Griffin, M., Apt, J., Lave, L., and Morgan, M.G. (2004). Ecology. Managing soil carbon. *Science* 304, 393.

Lambert, J., Burba, P., and Buddrus, J. (1992). Quantification of partial structures in aquatic humic substances by volume integration of two-dimensional ¹³C nuclear magnetic resonance spectra. Comparison of one- and two-dimensional techniques. *Magn. Reson. Chem.* 30, 221–227.

Langevin, D., (2009). “Complexation of oppositely charged polyelectrolytes and surfactants in aqueous solutions. A review,” *Adv. Colloid Interface Sci.*, vol. 147, pp. 170–177, 2009.

Lansing, W.D., and Kraemer, E.O. (1935). Molecular Weight Analysis of Mixtures by Sedimentation Equilibrium in the Svedberg Ultracentrifuge. *J. Am. Chem. Soc.* 57, 1369–1377.

Largeau, C., Casadevall, E., Kadouri, A., and Metzger, P. (1984). Formation of Botryococcus-derived kerogens—Comparative study of immature torbanites and of the extent alga Botryococcus braunii. *Org. Geochem.* 6, 327–332.

Laschewsky, A., Wattebled, L., Arotçaréna, M., Habib-Jiwan, J.-L., and Rakotoaly, R.H. (2005). Synthesis and Properties of Cationic Oligomeric Surfactants. *Langmuir* 21, 7170–7179.

Lead, J.R., Hamilton-Taylor, J., Hesketh, N., Jones, M.N., Wilkinson, A.E., and Tipping, E. (1994). A comparative study of proton and alkaline earth metal binding by humic substances. *Anal. Chim. Acta* 294, 319–327.

Lead, J.R., Balnois, E., Hosse, M., Menghetti, R., and Wilkinson, K.J. (1999). Characterization of Norwegian natural organic matter: Size, diffusion coefficients, and electrophoretic mobilities. *Environ. Int.* 25, 245–258.

Lead, J.R., Wilkinson, K.J., Starchev, K., Canonica, S., and Buffle, J. (2000a). Determination of Diffusion Coefficients of Humic Substances by Fluorescence Correlation Spectroscopy: Role of Solution Conditions. *Environ. Sci. Technol.* 34, 1365–1369.

Lead, J.R., Wilkinson, K.J., Balnois, E., Cutak, B.J., Larive, C.K., Assemi, S., and Beckett, R. (2000b). Diffusion Coefficients and Polydispersities of the Suwannee River Fulvic Acid: Comparison of Fluorescence Correlation Spectroscopy, Pulsed-Field Gradient Nuclear Magnetic Resonance, and Flow Field-Flow Fractionation. *Environ. Sci. Technol.* 34, 3508–3513.

Ledl, F., and Schleicher, E. (1990). New Aspects of the Maillard Reaction in Foods and in the Human Body. *Angew. Chem. Int. Ed. Engl.* 29, 565–594.

Lee, J., Saha, A., Pancera, S.M., Kempter, A., Rieger, J., Bose, A., and Tripathi, A. (2012). Shear free and blotless cryo-TEM imaging: a new method for probing early evolution of nanostructures. *Langmuir ACS J. Surf. Colloids* 28, 4043–4046.

- Leenheer, J.A. (1981). Comprehensive approach to preparative isolation and fractionation of dissolved organic carbon from natural waters and wastewaters. *Environ. Sci. Technol.* *15*, 578–587.
- Leenheer, J.A. (1994). Methods for Determination of Structural Models of Fulvic Acid from the Suwannee River by Convergent Independent Analyses (In: Humic substances in the Suwannee River, Georgia; interactions, properties, and proposed structures. p. 75-80, United States Geological Survey), WSP - 2373.
- Leenheer, J.A. (2007). Progression from model structures to molecular structures of natural organic matter components. *Ann. Environ. Sci.* *1*, 15.
- Leenheer, J.A., and Noyes, T.I. (1989). Derivatization of Humic Substances for Structural Studies. (In: Humic Substances II: In Search of Structure. M. H. B. Hayes, P. MacCarthy, R. L. Malcolm, and R. S. Swift (eds), Wiley, Chichester, New York, pp. 257-280),.
- Leenheer, J.A., McKnight, D.M., Thurman, E.M., and MacCarthy, P. (1989). Structural components and proposed structural models of fulvic acid from the Suwannee River. (In: Humic Substances in the Suwannee River, Georgia: Interactions, Properties and Proposed Structures, USGS Open File Report 87—557, ed. R.C. Averett, J.A. Leenheer, D.M. McKnight & K.A. Thorn, pp. 331—359. Denver, CO: US Geological Survey.),.
- Leenheer, J.A., Rostad, C.E., Gates, P.M., Furlong, E.T., and Ferrer, I. (2001). Molecular resolution and fragmentation of fulvic acid by electrospray ionization/multistage tandem mass spectrometry. *Anal. Chem.* *73*, 1461–1471.
- Leenheer, J.A., Wershaw, R.L., Brown, G.K., and Reddy, M.M. (2003). Characterization and diagenesis of strong-acid carboxyl groups in humic substances. *Appl. Geochem.* *18*, 471–482.
- Lehmann, J., and Kleber, M. (2015). The contentious nature of soil organic matter. *Nature* *528*, 60–68.
- Leppard, G.G., Kent Burnison, B., and Buffle, J. (1990). Transmission electron microscopy of the natural organic matter of surface waters. *Anal. Chim. Acta* *232*, 107–121.
- Li, Y., Xu, R., Couderc, S., Bloor, D.M., Warr, J., Penfold, J., Holzwarth, J.F., and Wyn-Jones, E. (2001). Structure of the complexes formed between sodium dodecyl sulfate and a charged and uncharged ethoxylated polyethyleneimine: small-angle neutron scattering, electromotive force, and isothermal titration calorimetry measurements. *Langmuir* *17*, 5657–5665.
- Lienemann, C., Heissenberger, A., Leppard, G.G., and Perret, D. (1998). Optimal preparation of water samples for the examination of colloidal material by transmission electron microscopy. *Aquat. Microb. Ecol.* *14*, 205–213.
- Lindblom, G., and Lindman, B. (1973). Interaction between halide ions and amphiphilic organic cations in aqueous solutions studied by nuclear quadrupole relaxation. *J. Phys. Chem.* *77*, 2531–2537.
- Lindqvist, I. (1967). Adsorption effects in gel filtration of humic acid. *Acta Chem Scand* *21*, 2564–2566.

Lingafelter, E.C. (1949). Aqueous Solutions of Paraffin-Chain Salts. *Chem. Rev.* *44*, 135–140.

Linn, D.M., Carski, T.H., Brusseau, M.L., and Chang, F.H. (1993). Sorption and degradation of pesticides and organic chemicals in soil. (Soil Science Society of America).

Liu, A.L. (2011). *Advances in planar lipid bilayers and liposomes* (Academic Press).

Liu, J., Takisawa, N., and Shirahama, K. (1999). The interaction of mixed surfactants with polyelectrolytes. *Colloid Polym. Sci.* *277*, 247–251.

Lucassen-Reynders, E.H. (1982). Anionic Surfactants: Physical Chemistry of Surfactant Action. *J. Dispers. Sci. Technol.* Marcel Dekker N. Y. *3*, 211–212.

Łuczak, J., Jungnickel, C., Joskowska, M., Th mi ng, J., and Hupka, J. (2009). Thermodynamics of micellization of imidazolium ionic liquids in aqueous solutions. *J. Colloid Interface Sci.* *336*, 111–116.

Lyvén, B., Hassellöv, M., Turner, D.R., Haraldsson, C., and Andersson, K. (2003). Competition between iron- and carbon-based colloidal carriers for trace metals in a freshwater assessed using flow field-flow fractionation coupled to ICPMS. *Geochim. Cosmochim. Acta* *67*, 3791–3802.

M

MacCarthy, P. (2001). The principles of humic substances. *Soil Sci.* *166*, 738–751.

MacCarthy, P., Clapp, C.E., Malcolm, R.L., and Bloom, P.R. (1990). An Introduction to Soil Humic Substances. In ACSESS Publications, (Soil Science Society of America),.

Madaeni, S.S., Sedeh, S.N., and De Nobili, M. (2006). Ultrafiltration of humic substances in the presence of protein and metal ions. *Transp. Porous Media* *65*, 469–484.

Magee, B.R., Lion, L.W., and Lemley, A.T. (1991). Transport of dissolved organic macromolecules and their effect on the transport of phenanthrene in porous media. *Environ. Sci. Technol.* *25*, 323–331.

Magid, L.J., Han, Z., Li, Z., and Butler, P.D. (2000). Tuning the Contour Lengths and Persistence Lengths of Cationic Micelles: The Role of Electrostatics and Specific Ion Binding. *J. Phys. Chem. B* *104*, 6717–6727.

Magny, B., Iliopoulos, I., Zana, R., and Audebert, R. (1994). Mixed micelles formed by cationic surfactants and anionic hydrophobically modified polyelectrolytes. *Langmuir* *10*, 3180–3187.

Maie, N., Scully, N.M., Pisani, O., and Jaffé, R. (2007). Composition of a protein-like fluorophore of dissolved organic matter in coastal wetland and estuarine ecosystems. *Water Res.* *41*, 563–570.

Maillard, L.C. (1912). Action des acides amines sur le sucres; formation des melanoidines par voie methodique. *C R Acad Sci* *154* 66-68.

- Maillard, L.C. (1917). Identite des materieres humiques de synthese avec les matieres humiques naturelles. *Ann Chim Paris* 7 113-152.
- Malcolm, R.L. (1989). Application of Solid-State ^{13}C NMR Spectroscopy to Geochemical Studies of Humic Substances. (In: *Humic Substances II: In Search of Structure*. M. H. B. Hayes, P. MacCarthy, R. L. Malcolm, and R. S. Swift (eds), Wiley, Chichester, New York, pp. 339-372),.
- Malcolm, R.L. (1990). The uniqueness of humic substances in each of soil, stream and marine environments. *Anal. Chim. Acta* 232, 19–30.
- Malcolm, R.L., and MacCarthy, P. (1992). Quantitative evaluation of XAD-8 and XAD-4 resins used in tandem for removing organic solutes from water. *Environ. Int.* 18, 597–607.
- Malcolm, R.L., McKnight, D.M., and Averett, R.C. (1994a). History and Description of the Okefenokee Swamp Origin of the Suwannee River (In: *Humic substances in the Suwannee River, Georgia; interactions, properties, and proposed structures*. p. 2-12, United States Geological Survey), WSP - 2373.
- Malcolm, R.L., Aiken, G.R., Bowles, E.C., and Malcolm, J.D. (1994b). Isolation of Fulvic and Humic Acids from the Suwannee River (In: *Humic substances in the Suwannee River, Georgia; interactions, properties, and proposed structures*. p. 13-19, United States Geological Survey), WSP - 2373.
- Mandal, A.K., and Pal, M.K. (2000). Strong fluorescence emissions by H-aggregates of the dye thiacyanine in the presence of the surfactant aerosol-OT. *Chem. Phys.* 253, 115–124.
- Manning, T.J., and Bennett, T. (2000). Aggregation studies of humic acid using multiangle laser light scattering. *Sci. Total Environ.* 257, 171–176.
- Manohar, C., and Narayanan, J. (2012). “Average packing factor approach for designing micelles, vesicles and gel phases in mixed surfactant systems,” *Colloids Surf. Physicochem. Eng. Asp.*, vol. 403, pp. 129–132.
- Mao, J.-D., Hundal, L.S., Thompson, M.L., and Schmidt-Rohr, K. (2002). Correlation of Poly(methylene)-Rich Amorphous Aliphatic Domains in Humic Substances with Sorption of a Nonpolar Organic Contaminant, Phenanthrene. *Environ. Sci. Technol.* 36, 929–936.
- Marques, E.F., Regev, O., Khan, A., da Graça Miguel, M., and Lindman, B. (1999). “Vesicle Formation and General Phase Behavior in the Catanionic Mixture SDS–DDAB–Water. The Cationic-Rich Side,” *J. Phys. Chem. B*, vol. 103, no. 39, pp. 8353–8363.
- Marques, E.F., Regev, O., Khan, A., da Graça Miguel, M., and Lindman, B. (1998). “Vesicle formation and general phase behavior in the catanionic mixture SDS-DDAB-water. The anionic-rich side,” *J. Phys. Chem. B*, vol. 102, no. 35, pp. 6746–6758.
- March, J. (1992). *Advanced organic chemistry: reactions, mechanisms, and structure* (Wiley).
- Marcusson, J. (1926). Lignin and oxycellulose theory. *Z Angew Chem* 39 898-900.
- Marinsky, J.A., and Ephraim, J. (1986). A unified physicochemical description of the protonation and metal ion complexation equilibria of natural organic acids (humic and fulvic

acids). 1. Analysis of the influence of polyelectrolyte properties on protonation equilibria in ionic media: fundamental concepts. *Environ. Sci. Technol.* *20*, 349–354.

Marley, N.A., Gaffney, J.S., Orlandini, K.A., and Dugue, C.P. (1991). An evaluation of an automated hollow-fibre ultrafiltration apparatus for the isolation of colloidal materials in natural waters. *Hydrol. Process.* *5*, 291–299.

Marley, N.A., Gaffney, J.S., Orlandini, K.A., Picel, K.C., and Choppin, G.R. (1992). Chemical characterization of size-fractionated humic and fulvic materials in aqueous samples. *Sci. Total Environ.* *113*, 159–177.

Marley, N.A., Gaffney, J.S., Orlandini, K.A., and Cunningham, M.M. (1993). Evidence for radionuclide transport and mobilization in a shallow, sandy aquifer. *Environ. Sci. Technol.* *27*, 2456–2461.

Martin, R.B. (1964). *Introduction to biophysical chemistry*. Acad. Med. McGraw-Hill N. Y. *39*, 867.

Martin, F., Almendros, G., González-Vila, F.J., and Verdejo, T. (2001). Experimental reappraisal of flash pyrolysis and low-temperature thermally assisted hydrolysis and methylation using tetramethylammonium hydroxide for the molecular characterization of humic acids. *J. Anal. Appl. Pyrolysis* *61*, 133–145.

Martin, J.P., Haider, K., and Kassim, G. (1980). Biodegradation and Stabilization after 2 Years of Specific Crop, Lignin, and Polysaccharide Carbons in Soils¹. *Soil Sci. Soc. Am. J.* *44*, 1250.

Martin, J.E., and Hurd, A.J. (1987). Scattering from fractals. *J. Appl. Crystallogr.* *20*, 61–78.

Mata, J., Varade, D., and Bahadur, P. (2005). Aggregation behavior of quaternary salt based cationic surfactants. *Thermochim. Acta* *428*, 147–155.

Mata, J., Patel, J., Jain, N., Ghosh, G., and Bahadur, P. (2006). Interaction of cationic surfactants with carboxymethylcellulose in aqueous media. *J. Colloid Interface Sci.* *297*, 797–804.

Matsuda, M., Kaminaga, A., Hayakawa, K., Takisawa, N., and Miyajima, T. (2009). Surfactant binding by humic acids in the presence of divalent metal salts. *Colloids Surf. Physicochem. Eng. Asp.* *347*, 45–49.

Matsunaga, T., Sakai, T., Akagi, Y., Chung, U., and Shibayama, M. (2009). SANS and SLS Studies on Tetra-Arm PEG Gels in As-Prepared and Swollen States. *Macromolecules* *42*, 6245–6252.

Matthews, B.J.H., Jones, A.C., Theodorou, N.K., and Tudhope, A.W. (1996). Excitation-emission-matrix fluorescence spectroscopy applied to humic acid bands in coral reefs. *Mar. Chem.* *55*, 317–332.

Maurdev, G., Gee, M.L., and Meagher, L. (2002). Controlling the adsorbed conformation and desorption of polyelectrolyte with added surfactant via the adsorption mechanism: a direct force measurement study. *Langmuir* *18*, 9401–9408.

- Maurice, P.A. (2015). Special Issue Introduction: Dissolved Organic Matter from the Suwannee River (GA, USA). *Environ. Eng. Sci.* 32, 1–3.
- Maurice, P.A., and Namjesnik-Dejanovic, K. (1999). Aggregate structures of sorbed humic substances observed in aqueous solution. *Environ. Sci. Technol.* 33, 1538–1541.
- Maurice, P.A., Hochella, M.F.J., Parks, D.A., SPOSITO, G., and SCHWERTMANN, U. (1995). Evolution of hematite surface microtopography upon dissolution by simple organic acids. *Clays Clay Miner.* 43, 29–38.
- Maximov, O.B., and Krasovskaya, N.P. (1977). Action of metallic sodium on humic acids in liquid ammonia. *Geoderma* 18, 227–228.
- Maxit, B. Particle size measurements of dark and concentrated dispersions by dynamic light scattering. Cordouan Technol. 33400 Pessac Fr.
- May, R.P., Ibel, K., and Haas, J. (1982). The forward scattering of cold neutrons by mixtures of light and heavy water. *J. Appl. Crystallogr.* 15, 15–19.
- Mayer, L.M. (1994). Relationships between mineral surfaces and organic carbon concentrations in soils and sediments. *Chem. Geol.* 114, 347–363.
- Mayer, L.M., Schick, L.L., and Loder III, T.C. (1999). Dissolved protein fluorescence in two Maine estuaries. *Mar. Chem.* 64, 171–179.
- McBain, M.E.L., and Hutchinson, E. (1955). Solubilization and related phenomena. *Acad. Press N. Y.* 33, 190.
- McCarthy, J.F., Czerwinski, K.R., Sanford, W.E., Jardine, P.M., and Marsh, J.D. (1998). Mobilization of transuranic radionuclides from disposal trenches by natural organic matter. *J. Contam. Hydrol.* 30, 49–77.
- McDonald, S., Bishop, A.G., Prenzler, P.D., and Robards, K. (2004). Analytical chemistry of freshwater humic substances. *Anal. Chim. Acta* 527, 105–124.
- McInnis, D.P., Bolster, D., and Maurice, P.A. (2015). Mobility of Dissolved Organic Matter from the Suwannee River (Georgia, USA) in Sand-Packed Columns. *Environ. Eng. Sci.* 32, 4–13.
- McKnight, D.M., Boyer, E.W., Westerhoff, P.K., Doran, P.T., Kulbe, T., and Andersen, D.T. (2001). Spectrofluorometric characterization of dissolved organic matter for indication of precursor organic material and aromaticity. *Limnol. Oceanogr.* 46, 38–48.
- Meakin, P. (1991). Fractal aggregates in geophysics. *Rev. Geophys.* 29, 317–354.
- Meier, M., Namjesnik-Dejanovic, K., Maurice, P.A., Chin, Y.-P., and Aiken, G.R. (1999). Fractionation of aquatic natural organic matter upon sorption to goethite and kaolinite. *Chem. Geol.* 157, 275–284.
- Merino, F., Rubio, S., and Pérez-Bendito, D. (2001). Determination of dialkyldimethylammonium surfactants in sewage based on the formation of premicellar aggregates. *Analyst* 126, 2230–2234.

- Mendez, J., and Stevenson, F.J. (1966). REDUCTIVE CLEAVAGE OF HUMIC ACIDS WITH SODIUM AMALGUM. *Soil Sci.* *102*, 85–93.
- Meuzelaar, H.L., Haverkamp, J., and Hileman, F.D. (1982). Pyrolysis mass spectrometry of recent and fossil biomaterials (Elsevier).
- Milne, C.J., Kinniburgh, D.G., and Tipping, E. (2001). Generic NICA-Donnan Model Parameters for Proton Binding by Humic Substances. *Environ. Sci. Technol.* *35*, 2049–2059.
- Minkin, V.I., Glukhovtsev, M.N., and Simkin, B.I. (1994). Aromaticity and antiaromaticity: electronic and structural aspects (J. Wiley & Sons).
- Mishra, A., Behera, R.K., Behera, P.K., Mishra, B.K., and Behera G.B. (2000). Cyanines during the 1990s: A review. *Chem. Rev.* *100*(6), 1973–2012.
- Mobed, J.J., Hemmingsen, S.L., Autry, J.L., and McGown, L.B. (1996). Fluorescence characterization of IHSS humic substances: total luminescence spectra with absorbance correction. *Environ. Sci. Technol.* *30*, 3061–3065.
- Mondal, P.P., and Diaspro, A. (2013). *Fundamentals of Fluorescence Microscopy: Exploring Life with Light* (Springer Science & Business Media).
- Moore, W.J. (1972). *Physical Chemistry* (4th Edition. Prentice-Hall, Englewood Cliffs, NJ).
- Mopper, K., and Schultz, C.A. (1993). Fluorescence as a possible tool for studying the nature and water column distribution of DOC components. *Mar. Chem.* *41*, 229–238.
- Moraes, S.L. de, and Rezende, M.O.O. (2008). Capillary electrophoresis (CE): a powerful tool to characterize humic acid (HA). *J. Braz. Chem. Soc.* *19*, 24–28.
- Morishima, Y., Mizusaki, M., Yoshida, K., and Dubin, P. (1999). Interactions of micelles with fluorescence-labeled polyelectrolytes. *Colloids Surf. Physicochem. Eng. Asp.* *147*, 149–159.
- Moroi, Y. (1988). Relationship between solubility and micellization of surfactants: The temperature range of micellization. In *Dispersed Systems*, K. Hummel, and J. Schurz, eds. (Steinkopff), pp. 55–61.
- Morris, C.E.M. (1977). Aspects of vapor pressure osmometry. *J. Appl. Polym. Sci.* *21*, 435–448.
- Moulin, V.M., Moulin, C.M., and Dran, J.-C. (1996). Role of Humic Substances and Colloids in the Behavior of Radiotoxic Elements in Relation to Nuclear Waste Disposal. In *Humic and Fulvic Acids*, (American Chemical Society), pp. 259–271.
- Mounier, S., Patel, N., Quilici, L., Benaim, J.Y., and Benamou, C. (1999). Fluorescence 3D de la matière organique dissoute du fleuve amazon: (Three-dimensional fluorescence of the dissolved organic carbon in the Amazon river). *Water Res.* *33*, 1523–1533.
- Mukerjee, P., and Mysels, K.J. (1971). *Critical micelle concentrations of aqueous surfactant systems* (National Bureau of Standards, NSRDS-NBS 36, U.S. Government Printing Office, Washington, DC).

Mullins, O.C., and Sheu, E.Y. (2013). Structures and Dynamics of Asphaltenes (Springer Science & Business Media).

Muroi, Y., Kurawaki, J., Hayakawa, K., Takisawa, N., and Miyajima, T. (2008). Fluorescence spectroscopy of fulvic acids' interaction with surfactants. *Colloid Polym. Sci.* *287*, 57–62.

Murphy, E.M., and Zachara, J.M. (1995). The role of sorbed humic substances on the distribution of organic and inorganic contaminants in groundwater. *Geoderma* *67*, 103–124.

Myers, D. (2005). Surfactant science and technology (John Wiley & Sons).

Myneni, S.C.B., Brown, J.T., Martinez, G.A., and Meyer-Ilse, W. (1999). Imaging of humic substance macromolecular structures in water and soils. *Science* *286*, 1335–1337.

N

Nagarajan, R., and Ruckenstein, E. (1991). Theory of surfactant self-assembly: a predictive molecular thermodynamic approach. *Langmuir* *7*, 2934–2969.

Nakashima, K., Xing, S., Gong, Y., and Miyajima, T. (2008). Characterization of humic acids by two-dimensional correlation fluorescence spectroscopy. *J. Mol. Struct.* *883-884*, 155–159.

Nam, K., and Kim, J.Y. (2002). Role of loosely bound humic substances and humin in the bioavailability of phenanthrene aged in soil. *Environ. Pollut.* *118*, 427–433.

Namjesnik-Dejanovic, K., and Maurice, P.A. (1997). Atomic force microscopy of soil and stream fulvic acids. *Colloids Surf. Physicochem. Eng. Asp.* *120*, 77–86.

Namjesnik-Dejanovic, K., Maurice, P.A., Aiken, G.R., Cabaniss, S., Chin, Y.-P., and Pullin, M.J. (2000). Adsorption and fractionation of a muck fulvic acid on kaolinite and goethite at pH 3.7, 6, and 8. *Soil Sci.* *165*, 545–559.

Nardi, S., Muscolo, A., Vaccaro, S., Baiano, S., Spaccini, R., and Piccolo, A. (2007). Relationship between molecular characteristics of soil humic fractions and glycolytic pathway and krebs cycle in maize seedlings. *Soil Biol. Biochem.* *39*, 3138–3146.

Nasimova, I., Karino, T., Okabe, S., Nagao, M., and Shibayama, M. (2004). Small-Angle Neutron Scattering Investigation of Pressure Influence on the Structure of Weakly Charged Poly(*N*-isopropylacrylamide) Solutions and Gels. *Macromolecules* *37*, 8721–8729.

Nebbioso, A., and Piccolo, A. (2009). Molecular rigidity and diffusivity of Al³⁺ and Ca²⁺ humates as revealed by NMR spectroscopy. *Environ. Sci. Technol.* *43*, 2417–2424.

Nebbioso, A., and Piccolo, A. (2011). Basis of a humeomics science: chemical fractionation and molecular characterization of humic biosuprastructures. *Biomacromolecules* *12*, 1187–1199.

Nebbioso, A., and Piccolo, A. (2012). Advances in humeomics: Enhanced structural identification of humic molecules after size fractionation of a soil humic acid. *Anal. Chim. Acta* *720*, 77–90.

- Neiswender, D.D., Moniz, W.B., and Dixon, J.A. (1960). The Oxidation of Methylene and Methyl Groups by Sodium Hypochlorite. *J. Am. Chem. Soc.* *82*, 2876–2878.
- Newman, R.H., Tate, K.R., Barron, P.F., and Wilson, M.A. (1980). Towards a Direct, Non-Destructive Method of Characterising Soil Humic Substances Using ¹³C N.m.r. *J. Soil Sci.* *31*, 623–631.
- Nguyen, K. T., Nguyen, T. D., and Nguyen, A. V., (2014). “Strong Cooperative Effect of Oppositely Charged Surfactant Mixtures on Their Adsorption and Packing at the Air–Water Interface and Interfacial Water Structure,” *Langmuir*, vol. 30, no. 24, pp. 7047–7051.
- Niemeyer, J., Chen, Y., and Bollag, J.-M. (1992). Characterization of humic acids, composts, and peat by diffuse reflectance Fourier-transform infrared spectroscopy. *Soil Sci. Soc. Am. J.* *56*, 135–140.
- Nieuwkerk, A.C., Marcelis, A.T.M., and Sudhoelter, E.J.R. (1998). Interactions between hydrophobically modified poly (maleic acid-co-alkyl vinyl ether) s and dodecyltrimethylammonium bromide. In *Trends in Colloid and Interface Science XII*, (Springer), pp. 114–118.
- Nip, M., Tegelaar, E.W., Brinkhuis, H., De Leeuw, J.W., Schenck, P.A., and Holloway, P.J. (1986). Analysis of modern and fossil plant cuticles by Curie point Py-GC and Curie point Py-GC-MS: Recognition of a new, highly aliphatic and resistant biopolymer. *Org. Geochem.* *10*, 769–778.
- De Nobili, M., and Chen, Y. (1999). SIZE EXCLUSION CHROMATOGRAPHY OF HUMIC SUBSTANCES: LIMITS, PERSPECTIVES AND PROSPECTIVES. *Soil Sci.* *164*, 825–833.
- De Nobili, M., Contin, M., and Leita, L. (1989). Investigation of the interactions between humic substances and a cationic detergent (Cetiltrimethylammonium bromide). *Sci. Total Environ.* *81–82*, 635–642.
- De Nobili, M., Contin, M., and Leita, L. (1990). Alternative method for carboxyl group determination in humic substances. *Can. J. Soil Sci.* *70*, 531–536.
- De Nobili, M., Gjessing, E., and Sequi, P. (1989). Sizes and Shapes of Humic Substances by Gel Chromatography. (In: *Humic Substances II: In Search of Structure*. M. H. B. Hayes, P. MacCarthy, R. L. Malcolm, and R. S. Swift (eds), Wiley, Chichester, New York, pp. 561-592),.
- Nordén, M., and Dabek-Zlotorzynska, E. (1996). Study of metal—fulvic acid interactions by capillary electrophoresis. *J. Chromatogr. A* *739*, 421–429.
- Norwood, D.L., Johnson, J.D., Christman, R.F., Hass, J.R., and Bobenrieth, M.J. (1980). Reactions of chlorine with selected aromatic models of aquatic humic material. *Environ. Sci. Technol.* *14*, 187–190.
- Novotny, F.J., Rice, J.A., and Weil, D.A. (1995). Characterization of Fulvic Acid by Laser-Desorption Mass Spectrometry. *Environ. Sci. Technol.* *29*, 2464–2466.

Noyes, T.I., and Leenheer, J.A. (1994). Proton Nuclear-Magnetic-Resonance Studies of Fulvic Acid from the Suwannee River (In: Humic substances in the Suwannee River, Georgia; interactions, properties, and proposed structures. p. 129-140, United States Geological Survey), WSP - 2373.

Nwosu, U.G., and Cook, R.L. (2015). ¹³C Nuclear Magnetic Resonance and Electron Paramagnetic Spectroscopic Comparison of Hydrophobic Acid, Transphilic Acid, and Reverse Osmosis May 2012 Isolates of Organic Matter from the Suwannee River. *Environ. Eng. Sci.* 32, 14–22.

O

O'Brien, R.W., and Hunter, R.J. (1981). The electrophoretic mobility of large colloidal particles. *Can. J. Chem.* 59, 1878–1887.

Ochs, M., Brunner, I., Stumm, W., and Čosović, B. (1993). Effects of root exudates and humic substances on weathering kinetics. *Water. Air. Soil Pollut.* 68, 213–229.

Ohshima, H. (1995). Electrophoretic mobility of soft particles. *Colloids Surf. Physicochem. Eng. Asp.* 103, 249–255.

Ohno, T. (2002). Fluorescence Inner-Filtering Correction for Determining the Humification Index of Dissolved Organic Matter. *Environ. Sci. Technol.* 36, 742–746.

Okuda, H., Ozeki, S., and Ikeda, S. (1987). Adsorption of ions on aqueous surfaces of NaBr solutions of dodecyldimethylammonium chloride. *J. Colloid Interface Sci.* 115, 155–166.

Olea, A.F., Gamboa, C., Acevedo, B., and Martinez, F. (2000). Synergistic Effect of Cationic Surfactant on Surface Properties of Anionic Copolymers of Maleic Acid and Styrene. *Langmuir* 16, 6884–6890.

Olendzki, R.N., Ignácio, A.C., and Mangrich, A.S. (2009). The use of total luminescence spectroscopy in the investigation of the effects of different rice management practices on humic substances of a planosol. *Rev. Bras. Ciênc. Solo* 33, 1147–1152.

Orlov, D.S. (1985). Humus acids of soils (Balkema).

Orlov, D.S. (1990). Humic substances of soils and general theory of humification. (AA Balkema, Moscow State University Publisher: Moscow, 1990).

Orlov, D.S., Ammosova, Y.M., and Glebova, G.I. (1975). Molecular parameters of humic acids. *Geoderma* 13, 211–229.

Orsetti, S., Marco-Brown, J.L., Andrade, E.M., and Molina, F.V. (2013). Pb(II) Binding to Humic Substances: An Equilibrium and Spectroscopic Study. *Environ. Sci. Technol.* 130717064732001.

Osterberg, R., and Mortensen, K. (1992). Fractal Dimension of Humic Acids - a Small-Angle Neutron-Scattering Study. *Eur. Biophys. J. Biophys. Lett.* 21, 163–167.

Osterberg, R., and Mortensen, K. (1994). The Growth of Fractal Humic Acids - Cluster Correlation and Gel Formation. *Radiat. Environ. Biophys.* 33, 269–276.

Osterberg, R., Lindqvist, I., and Mortensen, K. (1993). Particle-Size of Humic-Acid. *Soil Sci. Soc. Am. J.* 57, 283–285.

Otto, W.H., Britten, D.J., and Larive, C.K. (2003). NMR diffusion analysis of surfactant–humic substance interactions. *J. Colloid Interface Sci.* 261, 508–513.

Owen, D.M., Amy, G.L., Chowdhury, Z.K., Paode, R., Mccoy, G., and Viscosil, K. (1995). NOM: characterization and treatability: Natural organic matter. *J. - Am. Water Works Assoc.* 87, 46–63.

P

Paciolla, M.D., Kolla, S., Sein Jr., L.T., Varnum, J.M., Malfara, D.L., Davies, G., Ghabbour, E.A., and Jansen, S.A. (1998). GENERATION OF FREE RADICALS BY HUMIC ACID: IMPLICATIONS FOR BIOLOGICAL ACTIVITY. In *Humic Substances*, G.D.A. Ghabbour, ed. (Woodhead Publishing), pp. 203–214.

Palmer, N.E., and von Wandruszka, R. (2001). Dynamic light scattering measurements of particle size development in aqueous humic materials. *Fresenius J. Anal. Chem.* 371, 951–954.

Parlanti, E., Wörz, K., Geoffroy, L., and Lamotte, M. (2000). Dissolved organic matter fluorescence spectroscopy as a tool to estimate biological activity in a coastal zone submitted to anthropogenic inputs. *Org. Geochem.* 31, 1765–1781.

Parsons, J.W. (1989). Hydrolytic Degradations of Humic Substances. (In: *Humic Substances II: In Search of Structure*. M. H. B. Hayes, P. MacCarthy, R. L. Malcolm, and R. S. Swift (eds), Wiley, Chichester, New York, pp. 99-120),.

Patel-Sorrentino, N., Mounier, S., and Benaim, J.Y. (2002). Excitation–emission fluorescence matrix to study pH influence on organic matter fluorescence in the Amazon basin rivers. *Water Res.* 36, 2571–2581.

Pavlik, J.W., and Perdue, E.M. (2015). Number-Average Molecular Weights of Natural Organic Matter, Hydrophobic Acids, and Transphilic Acids from the Suwannee River, Georgia, as Determined Using Vapor Pressure Osmometry. *Environ. Eng. Sci.* 32, 23–30.

Pecora, R. (1985). *Dynamic Light Scattering: Applications of Photon Correlation Spectroscopy* (Springer).

Pecora, R. (2000). Dynamic Light Scattering Measurement of Nanometer Particles in Liquids. *J. Nanoparticle Res.* 2, 123–131.

Penfold, J., Taylor, D.J.F., Thomas, R.K., Tucker, I., and Thompson, L.J. (2003). Adsorption of Polymer/Surfactant Mixtures at the Air–Water Interface: Ethoxylated Poly(ethyleneimine) and Sodium Dodecyl Sulfate†. *Langmuir* 19, 7740–7745.

Perdue, E.M., Gjessing, E.T., and Glaze, W. (1990). *Organic Acids in Aquatic Ecosystems* (Dahlem Konferenzen, J. Wiley, Chichester,).

Perger, T.-M., and Bešter-Rogač, M. (2007). Thermodynamics of micelle formation of alkyltrimethylammonium chlorides from high performance electric conductivity measurements. *J. Colloid Interface Sci.* *313*, 288–295.

Perkampus, H.-H. (2013). *UV-VIS Spectroscopy and Its Applications* (Springer Science & Business Media).

Perminova, I.V. (1999). SIZE EXCLUSION CHROMATOGRAPHY OF HUMIC SUBSTANCES: COMPLEXITIES OF DATA INTERPRETATION ATTRIBUTABLE TO NON-SIZE EXCLUSION EFFECTS. *Soil Sci.* *164*, 834–840.

Perret, D., Leppard, G.G., Müller, M., Belzile, N., De Vitre, R., and Buffle, J. (1991). Electron microscopy of aquatic colloids: Non-perturbing preparation of specimens in the field. *Water Res.* *25*, 1333–1343.

Pestke, F.M., Bergmann, C., Rentrop, B., Maassen, H., and Hirner, A.V. (1997). Mobilization potential of hydrophobic organic compounds (HOCs) in contaminated soils and waste materials. Part 1. Mobilization potential of PCBs, PAHs, and aliphatic hydrocarbons in the presence of solubilizing substances. *Acta Hydrochim. Hydrobiol. Acta Hydrochim.* *25*, 242–247.

Peters, K.E., Rohrback, B.G., and Kaplan, I.R. (1981). Geochemistry of Artificially Heated Humic and Sapropelic Sediments--I: Protokerogen. *AAPG Bull.* *65*, 688–705.

Pettit, R.E. (2004). Organic matter, humus, humate, humic acid, fulvic acid and humin: Their importance in soil fertility and plant health. *CTI Res.*

Peuravuori, J. (2005). NMR Spectroscopy Study of Freshwater Humic Material in Light of Supramolecular Assembly. *Environ. Sci. Technol.* *39*, 5541–5549.

Peuravuori, J., and Pihlaja, K. (1997). Molecular size distribution and spectroscopic properties of aquatic humic substances. *Anal. Chim. Acta* *337*, 133–149.

Peuravuori, J., Koivikko, R., and Pihlaja, K. (2002). Characterization, differentiation and classification of aquatic humic matter separated with different sorbents: synchronous scanning fluorescence spectroscopy. *Water Res.* *36*, 4552–4562.

Piccolo, A. (2001). The supramolecular structure of humic substances. *Soil Sci.* *166*, 810–832.

Piccolo, A. (2002). The supramolecular structure of humic substances: A novel understanding of humus chemistry and implications in soil science. In *Advances in Agronomy*, (Academic Press), pp. 57–134.

Piccolo, A., and Conte, P. (1999). Molecular size of humic substances. Supramolecular associations versus macromolecular polymers (Reprinted from *Advances in Environmental Research*, vol 3, pg 508-521, 2000). *Adv. Environ. Res.* *3*.

- Piccolo, A., Conte, P., Spaccin, R., and Chiarella, M. (2003). "Effects of some dicarboxylic acids on the association of dissolved humic substances," *Biol. Fertil. Soils*, vol. 37, no. 4, pp. 255–259.
- Piccolo, A., and Spiteller, M. (2003). Electrospray ionization mass spectrometry of terrestrial humic substances and their size fractions. *Anal. Bioanal. Chem.* 377, 1047–1059.
- Piccolo, A., Nardi, S., and Concheri, G. (1996a). Micelle-like conformation of humic substances as revealed by size exclusion chromatography. *Chemosphere* 33, 595–602.
- Piccolo, A., Nardi, S., and Concheri, G. (1996b). Macromolecular changes of humic substances induced by interaction with organic acids. *Eur. J. Soil Sci.* 47, 319–328.
- Piccolo, A., Conte, P., and Cozzolino, A. (1999). Effects of mineral and monocarboxylic acids on the molecular association of dissolved humic substances. *Eur. J. Soil Sci.* 50, 687–694.
- Piccolo, A., Cozzolino, A., Conte, P., and Spaccini, R. (2000). Polymerization of humic substances by an enzyme-catalyzed oxidative coupling. *Naturwissenschaften* 87, 391–394.
- Piccolo, A., Conte, P., and Cozzolino, A. (2001). Chromatographic and spectrophotometric properties of dissolved humic substances compared with macromolecular polymers. *Soil Sci.* 166, 174–185.
- Piccolo, A., Conte, P., Trivellone, E., and Van Lagen, B. (2002). Reduced heterogeneity of a lignite humic acid by preparative HPSEC following interaction with an organic acid. Characterization of size-separates by Pyr-GC-MS and H-1-NMR spectroscopy. *Environ. Sci. Technol.* 36, 76–84.
- Piccolo, A., Spaccini, R., Nieder, R., and Richter, J. (2004). Sequestration of a Biologically Labile Organic Carbon in Soils by Humified Organic Matter. *Clim. Change* 67, 329–343.
- Pierce, R.H.J., and Felbeck, G.T.J. (1972). A comparison of three methods of extracting organic matter from soils and marine sediments. *Proc Int Mtg Humic Subst.* Niewersluis 217–232.
- Ping, C.L., Michaelson, G.J., and Malcolm, R.L. (1995). Fractionation and carbon balance of soil organic matter in selected cryic soils in Alaska. *Soils Glob. Change Adv. Soil Sci.* CRC Lewis Publ. USA 307–314.
- Pinheiro, J.P., Mota, A.M., d'Oliveira, J.M.R., and Martinho, J.M.G. (1996). Dynamic properties of humic matter by dynamic light scattering and voltammetry. *Anal. Chim. Acta* 329, 15–24.
- Pinheiro, J.P., Mota, A.M., Simões Gonçalves, M.L.S., and van Leeuwen, H.P. (1998). The pH effect in the diffusion coefficient of humic matter: influence in speciation studies using voltammetric techniques. *Colloids Surf. Physicochem. Eng. Asp.* 137, 165–170.
- PIRET, E.L., WHITE, R.G., WALTHER, H.C.J., and ET AL. (1960). Some physico-chemical properties of peat humic acids. *Sci. Proc. R. Dublin Soc. Ser. A* 69–79.

- Pirkle, E.C., Pirkle, W.A., and Yoho, W.H. (1977). The Highland heavy-mineral sand deposit on Trail Ridge in northern peninsular Florida: Florida Bureau of Geology. Rep. Investig. 84 50 P.
- Plancque, G., Amekraz, B., Moulin, V., Toulhoat, P., and Moulin, C. (2001). Molecular structure of fulvic acids by electrospray with quadrupole time-of-flight mass spectrometry. *Rapid Commun. Mass Spectrom.* 15, 827–835.
- Plaschke, M., Römer, J., Klenze, R., and Kim, J.I. (1999). In situ AFM study of sorbed humic acid colloids at different pH. *Colloids Surf. Physicochem. Eng. Asp.* 160, 269–279.
- Pompe, S., Heise, K.-H., and Nitsche, H. (1996). Capillary electrophoresis for a “fingerprint” characterization of fulvic and humic acids. *J. Chromatogr. A* 723, 215–218.
- Posner, A.M., and Creeth, J.M. (1972). A Study of Humic Acid by Equilibrium Ultracentrifugation. *J. Soil Sci.* 23, 333–341.
- Pranzas, P.K., Willumeit, R., Gehrke, R., Thieme, J., and Knochel, A. (2003). Characterisation of structure and aggregation processes of aquatic humic substances using small-angle scattering and X-ray microscopy. *Anal. Bioanal. Chem.* 376, 618–625.
- Presley, D.E. (1984). Life and lore of the swampers. (In: Cohen, A.D., Casagrande, D.J., Andrejko, M.J., and Best, G.R., eds., *The Okefenokee Swamp- Its Natural History, Geology, and Geochemistry*: Los Alamos, New Mexico, Wetland Surveys, p. 18-37),.
- Preston, W.C. (1948). Some Correlating Principles of Detergent Action. *J. Phys. Colloid Chem.* 52, 84–97.
- Preston, C.M., Schnitzer, M., and Ripmeester, J.A. (1989). A Spectroscopic and Chemical Investigation on the De-ashing of a Humin. *Soil Sci. Soc. Am. J.* 53, 1442.
- Prévost, S., Wattebled, L., Laschewsky, A., and Gradzielski, M. (2011). Formation of Monodisperse Charged Vesicles in Mixtures of Cationic Gemini Surfactants and Anionic SDS. *Langmuir* 27, 582–591.
- Primer, A. (1996). *Fundamentals of UV-visible spectroscopy*. Copyr. Hewlett-Packard Co. Hewlett-Packard Publ.
- Pullin, M.J., and Cabaniss, S.E. (1995). Rank Analysis of the pH-Dependent Synchronous Fluorescence Spectra of Six Standard Humic Substances. *Environ. Sci. Technol.* 29, 1460–1467.

Q

- Quadri, G., Chen, X., Jawitz, J.W., Tambone, F., Genevini, P., Faoro, F., and Adani, F. (2008). Biobased Surfactant-Like Molecules from Organic Wastes: The Effect of Waste Composition and Composting Process on Surfactant Properties and on the Ability to Solubilize Tetrachloroethene (PCE). *Environ. Sci. Technol.* 42, 2618–2623.

Quagliotto, P., Montoneri, E., Tambone, F., Adani, F., Gobetto, R., and Viscardi, G. (2006). Chemicals from Wastes: Compost-Derived Humic Acid-like Matter as Surfactant. *Environ. Sci. Technol.* *40*, 1686–1692.

R

Rauen, T.G., Debacher, N.A., Sierra, M.M.D., and Sierra, E.J.S. (2002). Tensioactivity of humic acids from distinct environments. *Quimica Nova* *25*, 909–913.

Rauen, T.G., Debacher, N.A., Madureira, L. a. S., and Sierra, M.M.D. (2006). Factors affecting the surfactant properties of humic acids. *J. Coast. Res.* 1058–1061.

Reckhow, D.A., Singer, P.C., and Malcolm, R.L. (1990). Chlorination of humic materials: byproduct formation and chemical interpretations. *Environ. Sci. Technol.* *24*, 1655–1664.

Reddy, M.M., Leenheer, J.A., and Malcolm, R.L. (1994). Elemental Analysis and Heat of Combustion of Fulvic Acid from the Suwannee River (In: Humic substances in the Suwannee River, Georgia; interactions, properties, and proposed structures. p. 81-88, United States Geological Survey), WSP - 2373.

Redwood, P.S., Lead, J.R., Harrison, R.M., Jones, I.P., and Stoll, S. (2005). Characterization of humic substances by environmental scanning electron microscopy. *Environ. Sci. Technol.* *39*, 1962–1966.

Reemtsma, T., and These, A. (2005). Comparative investigation of low-molecular-weight fulvic acids of different origin by SEC-Q-TOF-MS: New insights into structure and formation. *Environ. Sci. Technol.* *39*, 3507–3512.

Reemtsma, T., These, A., Springer, A., and Linscheid, M. (2006a). Fulvic acids as transition state of organic matter: indications from high resolution mass spectrometry. *Environ. Sci. Technol.* *40*, 5839–5845.

Reemtsma, T., These, A., Venkatachari, P., Xia, X., Hopke, P.K., Springer, A., and Linscheid, M. (2006b). Identification of Fulvic Acids and Sulfated and Nitrated Analogues in Atmospheric Aerosol by Electrospray Ionization Fourier Transform Ion Cyclotron Resonance Mass Spectrometry. *Anal. Chem.* *78*, 8299–8304.

Reid, P.M., Wilkinson, A.E., Tipping, E., and Jones, M.N. (1990). Determination of molecular weights of humic substances by analytical (UV scanning) ultracentrifugation. *Geochim. Cosmochim. Acta* *54*, 131–138.

Reid, P.M., Wilkinson, A.E., Tipping, E., and Jones, M.N. (1991). Aggregation of humic substances in aqueous media as determined by light-scattering methods. *J. Soil Sci.* *42*, 259–270.

Relan, P.S., Girdhar, K.K., and Khanna, S.S. (1984). Molecular configuration of compost's humic acid by viscometric studies. *Plant Soil* *81*, 203–208.

Ren, S., Tombácz, E., and Rice, J. (1996). Dynamic light scattering from power-law polydisperse fractals: Application of dynamic scaling to humic acid. *Phys. Rev. E* *53*, 2980–2983.

- Reuter, J.H., and Perdue, E.M. (1981). Calculation of molecular weights of humic substances from colligative data: Application to aquatic humus and its molecular size fractions. *Geochim. Cosmochim. Acta* 45, 2017–2022.
- Reynolds, D.M. (2003). Rapid and direct determination of tryptophan in water using synchronous fluorescence spectroscopy. *Water Res.* 37, 3055–3060.
- Reynolds, D.M., and Ahmad, S.R. (1995). The effect of metal ions on the fluorescence of sewage wastewater. *Water Res.* 29, 2214–2216.
- Rice, J.A. (2001). Humins. *Soil Sci.* 166, 848–857.
- Rice, J.A., and MacCarthy, P. (1989b). Characterization of a Stream Sediment Humin (The American Chemical Society).
- Rice, J.A., and MacCarthy, P. (1988). Comments on the literature of the humin fraction of humus. *Geoderma* 43, 65–73.
- Rice, J.A., and MacCarthy, P. (1991). Statistical evaluation of the elemental composition of humic substances. *Org. Geochem.* 17, 635–648.
- Rice, J., and MacCarthy, P. (1989a). Isolation of humin by liquid-liquid partitioning. *Sci. Total Environ.* 81–82, 61–69.
- Rice, J.A., Tombacz, E., and Malekani, K. (1999). Applications of light and X-ray scattering to characterize the fractal properties of soil organic matter. *Geoderma* 88, 251–264.
- Richardson, S. (2003). Disinfection by-products and other emerging contaminants in drinking water. *TrAC Trends Anal. Chem.* 22, 666–684.
- Richardson, S., Plewa, M., Wagner, E., Schoeny, R., and Demarini, D. (2007). Occurrence, genotoxicity, and carcinogenicity of regulated and emerging disinfection by-products in drinking water: A review and roadmap for research. *Mutat. Res. Mutat. Res.* 636, 178–242.
- Rieger, M.M., and Rhein, L.D. (1997). *Surfactants in cosmetics* (CRC Press).
- Riley, J.P., and Taylor, D. (1969). The analytical concentration of traces of dissolved organic materials from sea water with Amberlite XAD-1 resin. *Anal. Chim. Acta* 46, 307–309.
- Ritchie, G.S.P., and Posner, A.M. (1982). The effect of pH and metal binding on the transport properties of humic acids. *J. Soil Sci.* 33, 233–247.
- Ritchie, J.D., and Perdue, E.M. (2003). Proton-binding study of standard and reference fulvic acids, humic acids, and natural organic matter. *Geochim. Cosmochim. Acta* 67, 85–96.
- Robards, K., McKelvie, I.D., Benson, R.L., Worsfold, P.J., Blundell, N.J., and Casey, H. (1994). Determination of carbon, phosphorus, nitrogen and silicon species in waters. *Anal. Chim. Acta* 287, 147–190.
- Rodenhiser, A.P., and Kwak, J.C.T. (1998). Polymer-Surfactant Systems, Overview. (In: J. C. T. Kwak (Eds), *Polymer-Surfactant Systems*, Surfactant Science Series, Marcel Dekker, New York, Vol. 77, p. 1),.

- Roger, G.M., Durand-Vidal, S., Bernard, O., Mériguet, G., Altmann, S., and Turq, P. (2010). Characterization of humic substances and polyacrylic acid: A high precision conductimetry study. *Colloids Surf. Physicochem. Eng. Asp.* 356, 51–57.
- Rook, J.J. (1977). Chlorination reactions of fulvic acids in natural waters. *Environ. Sci. Technol.* 11, 478–482.
- Rosa, A.H., Rocha, J.C., and Furlan, M. (2000). Humic substances of peat: study of the parameters that influence on the process of alkaline extraction. *Quím. Nova* 23, 472–476.
- Rose, R.E., and Lisse, M.W. (1917). The Chemistry of Wood Decay. Paper I—Introductory. *J. Ind. Eng. Chem.* 9, 284–287.
- Rosen, M.J., and Kunjappu, J.T. (2012). *Surfactants and interfacial phenomena* (John Wiley & Sons).
- Rowell, D.L. (1994). *Soil Science: Methods & Applications* (Longman Scientific and Technical and John Wiley, New York.).
- Rubingh, D.N., and Holland, P.M. (1990). *Cationic surfactants: physical chemistry* (CRC Press, Surfactant Science Ser., Vol. 37 Marcel Dekker, New York).
- Russell, E.W. (1962). Soil conditions and plant growth. *Soil Sci.* 93, 73.
- Ryan, D.K., and Weber, J.H. (1982). Fluorescence quenching titration for determination of complexing capacities and stability constants of fulvic acid. *Anal. Chem.* 54, 986–990.

S

- Sadar, M.J. (1996). *Understanding Turbidity Science*. Tech. Inf. Ser. – Bookl. No 11 Hach Co.
- Sadiq, R., and Rodriguez, M. (2004). Disinfection by-products (DBPs) in drinking water and predictive models for their occurrence: a review. *Sci. Total Environ.* 321, 21–46.
- Saiz-Jimenez, C., Haider, K., and Martin, J.P. (1975). Anthraquinones and Phenols as Intermediates in the Formation of Dark-Colored, Humic Acid-Like Pigments by *Eurotium echinulatum*. *Soil Sci. Soc. Am. J.* 39, 649.
- Sakamoto, M., Kanda, Y., Miyahara, M., and Higashitani, K. (2002). Origin of long-range attractive force between surfaces hydrophobized by surfactant adsorption. *Langmuir* 18, 5713–5719.
- Salati, S., Papa, G., and Adani, F. (2011). Perspective on the use of humic acids from biomass as natural surfactants for industrial applications. *Biotechnol. Adv.* 29, 913–922.
- Saleh, F.Y., Theriot, L.J., Amani, S.K., and Kim, I. (1994). Electron-Spin Resonance of Fulvic and Humic Acids from the Suwannee River (In: *Humic substances in the Suwannee River, Georgia; interactions, properties, and proposed structures*. p. 67-74, United States Geological Survey), WSP - 2373.

Samrani, A.G. El, Lartiges, B.S., Montargès-Pelletier, E., Kazpard, V., Barrès, O., and Ghanbaja, J. (2004). Clarification of municipal sewage with ferric chloride: the nature of coagulant species. *Water Res.* 38, 756–768.

Santschi, P.H., Lenhart, J.J., and Honeyman, B.D. (1997). Heterogeneous processes affecting trace contaminant distribution in estuaries: The role of natural organic matter. *Mar. Chem.* 58, 99–125.

Sauer, M., Hofkens, J., and Enderlein, J. (2010). *Handbook of Fluorescence Spectroscopy and Imaging: From Ensemble to Single Molecules* (Wiley-VCH).

Schnitzer, M. (1990). Selected Methods for the Characterization of Soil Humic Substances. In ACSESS Publications, (In: *Humic Substances in Soil and Crop Sciences: Selected Readings*, ed. P. MacCarthy, C.E. Clapp, R.L. Malcolm & P.R. Bloom, pp. 65–89, by permission of John Wiley & Sons, Inc., Soil Science Society of America),.

Schlautman, M.A., and Morgan, J.J. (1993). Binding of a fluorescent hydrophobic organic probe by dissolved humic substances and organically-coated aluminum oxide surfaces. *Environ. Sci. Technol.* 27, 2523–2532.

Schmidt, P. (1989). Use of scattering to determine the fractal dimension (In: Avnir, D. Ed. , *The Fractal Approach to Heterogeneous Chemistry*. Wiley Interscience, Chichester, UK, pp. 67–79).

Schmidt, P.W. (1991). Small-angle scattering studies of disordered, porous and fractal systems. *J. Appl. Crystallogr.* 24, 414–435.

Schmidt, P.W. (1995). Some Fundamental Concepts and Techniques Useful in Small-Angle Scattering Studies of Disordered Solids. In *Modern Aspects of Small-Angle Scattering*, H. Brumberger, ed. (Springer Netherlands), pp. 1–56.

Schmitt, P., Kettrup, A., Freitag, D., and Garrison, A.W. (1996). Flocculation of humic substances with metal ions as followed by capillary zone electrophoresis. *Fresenius J. Anal. Chem.* 354, 915–920.

Schnitzer, M. (1977). Recent findings on the characterization of humic substances extracted from soils from widely differing climatic zones. *Proc. Symp. Soil Org. Matter Stud. Braunschweig Ger.* Pp 117-131.

Schnitzer, M. (1978). Chapter 1 Humic Substances: Chemistry and Reactions. In *Developments in Soil Science*, M. Schnitzer and S.U. Khan, ed. (Elsevier), pp. 1–64.

Schnitzer, M. (1991). Soil organic matter-the next 75 years. *Soil Sci.* 151, 41–58.

Schnitzer, M., and Khan, S.U. (1972). *Humic substances in the environment* (New York: Marcel Dekker).

Schnitzer, M., and Neyroud, J.A. (1975). Further investigations on the chemistry of fungal “humic acids.” *Soil Biol. Biochem.* 7, 365–371.

Schnitzer, M., Kodama, H., and Ripmeester, J.A. (1991). Determination of the Aromaticity of Humic Substances by X-Ray Diffraction Analysis. *Soil Sci. Soc. Am. J.* 55, 745.

- Schramm, L.L., Stasiuk, E.N., and Marangoni, D.G. (2003). Surfactants and their applications. *Annu. Rep. Sect. CPhysical Chem.* 99, 3–48.
- Schroth, B.K., and Sposito, G. (1998). Effect of Landfill Leachate Organic Acids on Trace Metal Adsorption by Kaolinite. *Environ. Sci. Technol.* 32, 1404–1408.
- Schulten, H.-R. (1995). The three-dimensional structure of humic substances and soil organic matter studied by computational analytical chemistry. *Fresenius J. Anal. Chem.* 351, 62–73.
- Schulten, H.-R., and Gleixner, G. (1999). Analytical pyrolysis of humic substances and dissolved organic matter in aquatic systems: structure and origin. *Water Res.* 33, 2489–2498.
- Schulten, H.-R., and Schnitzer, M. (1992a). A contribution to solving the puzzle of the chemical structure of humic substances: pyrolysis-soft ionization mass spectrometry. *Sci. Total Environ.* 117–118, 27–39.
- Schulten, H.-R., and Schnitzer, M. (1992b). STRUCTURAL STUDIES ON SOIL HUMIC ACIDS BY CURIE-POINT PYROLYSIS-GAS CHROMATOGRAPHY/MASS SPECTROMETRY. *Soil Sci.* 153, 205–224.
- Schulten, H.-R., and Schnitzer, M. (1993). A state of the art structural concept for humic substances. *Naturwissenschaften* 80, 29–30.
- Schulten, H.-R., and Schnitzer, M. (1995). Three-dimensional models for humic acids and soil organic matter. *Naturwissenschaften* 82, 487–498.
- Schwartz, A.M., Perry, J.W., and Bartell, F.E. (1949). Surface Active Agents. *J. Phys. Colloid Chem.* 53, 1467–1467.
- Segota, S., and Tezak, D. (2006). Spontaneous formation of vesicles. *Adv. Colloid Interface Sci.* 121, 51–75.
- Sein, L.T., Varnum, J.M., and Jansen, S.A. (1999). Conformational Modeling of a New Building Block of Humic Acid: Approaches to the Lowest Energy Conformer. *Environ. Sci. Technol.* 33, 546–552.
- Selim, H.M., and Amacher, M.C. (1996). Reactivity and transport of heavy metals in soils (CRC Press).
- Senesi, N. (1990). Molecular and quantitative aspects of the chemistry of fulvic acid and its interactions with metal ions and organic chemicals : Part II. The fluorescence spectroscopy approach. *Anal. Chim. Acta* 232, 77–106.
- Senesi, N. (1999). Aggregation patterns and macromolecular morphology of humic substances: A fractal approach. *Soil Sci.* 164, 841–856.
- Senesi, N., and Loffredo, E. (2001). Soil Humic Substances. In *Biopolymers Online*, (In: *Biopolymers: Biology, Chemistry, Biotechnology, Applications - Vol.1: Lignin, Humic substances and Coal.* Ed. M. Hofrichter, A. Steinbüchel. Weinheim: Wiley-VCH, 2001, pp. 249–299),.

- Senesi, N., and Steelink, C. (1989). Application of ESR Spectroscopy to the Study of Humic Substances. (In: Humic Substances II: In Search of Structure. M. H. B. Hayes, P. MacCarthy, R. L. Malcolm, and R. S. Swift (eds), Wiley, Chichester, New York, pp. 373-408),.
- Senesi, N., Miano, T.M., and Provenzano, M.R. (1991). Fluorescence spectroscopy as a means of distinguishing fulvic and humic acids from dissolved and sedimentary aquatic sources and terrestrial sources. In Humic Substances in the Aquatic and Terrestrial Environment, B. Allard, H. Borén, and A. Grimvall, eds. (Springer Berlin Heidelberg), pp. 63–73.
- Senesi, N., Rizzi, F.R., Dellino, P., and Acquafredda, P. (1997). Fractal humic acids in aqueous suspensions at various concentrations, ionic strengths, and pH values. *Colloids Surf. Physicochem. Eng. Asp.* 127, 57–68.
- Serkiz, S.M., and Perdue, E.M. (1990). Isolation of dissolved organic matter from the suwannee river using reverse osmosis. *Water Res.* 24, 911–916.
- Serra, J.M., and Felbeck, G.T.J. (1972). Fractionation and partial analysis of the “bound” lipid fraction of muck soil organic matter. Humic Subst. Their Struct. Funct. Biosphere Povoledo H Gotterman Eds Proc. Int. Meet. Humic Subst. Nieuwersliuis PUDOC Wagening. Pp 311-319.
- Shaffer, L., and Von Wandruszka, R. (2014). The Effects of Conformational Changes on the Native Fluorescence of Aqueous Humic Materials. *Am. Chem. Sci. J.* 4, 326–336.
- Shah, R.K., Choski, M.R., and Joshi, B.C. (1975a). Development studies on soil organic matter: Humus. *ChemEra* 4-31-34.
- Shah, R.K., Choski, M.R., and Joshi, B.C. (1975b). Development studies on soil organic matter: Humin. *ChemEra* 6-1-3.
- Shang, C., and Rice, J.A. (2007). Investigation of humate-cetyltrimethylammonium complexes by small-angle X-ray scattering. *J. Colloid Interface Sci.* 305, 57–61.
- Sheng, G.-P., and Yu, H.-Q. (2006). Characterization of extracellular polymeric substances of aerobic and anaerobic sludge using three-dimensional excitation and emission matrix fluorescence spectroscopy. *Water Res.* 40, 1233–1239.
- Shimizu, Y., Sogabe, H., and Terashima, Y. (1998). The effects of colloidal humic substances on the movement of non-ionic hydrophobic organic contaminants in groundwater. *Water Sci. Technol.* 38, 159–167.
- Shin, H.S., Monsallier, J.M., and Choppin, G.R. (1999). Spectroscopic and chemical characterizations of molecular size fractionated humic acid. *Talanta* 50, 641–647.
- Shinoda, K., Nakagawa, T., Tamamushi, B.I., and Isemura, T. (1963). Colloidal surfactants: some physicochemical properties. (New York: Academic Press).
- Shinozuka, N., and Lee, C. (1991). Aggregate Formation of Humic Acids from Marine-Sediments. *Mar. Chem.* 33, 229–241.

- Shinozuka, N., Lee, C., and Hayano, S. (1987). Solubilizing action of humic acid from marine sediment. *Sci. Total Environ.* *62*, 311–314.
- Shirahama, K. (1998). The nature of polymer-surfactant interactions. (In: *Polymer-Surfactant Systems*, J. C. T. Kwak, Ed., pp. 143–191, Marcel Dekker, New York, NY, USA),.
- Shirahama, K., Kameyama, K., and Takagi, T. (1992). Bimodality in the dodecylpyridinium bromide-sodium dextran sulfate system as observed by an electrophoretic method. *J. Phys. Chem.* *96*, 6817–6820.
- Shuman, M. (1990). Carboxyl acidity of aquatic organic matter: possible systematic errors introduced by XAD extraction. (In: *Organic Acids in Aquatic Ecosystems*, ed. E.M. Perdue & E.T. Gjessing, pp. 97–109. Chichester: Wiley.).
- Sieliechi, J.-M., Lartiges, B.S., Kayem, G.J., Hupont, S., Frochot, C., Thieme, J., Ghanbaja, J., de la Caillerie, J.B. d'Espinose, Barres, O., Kamga, R., et al. (2008). Changes in humic acid conformation during coagulation with ferric chloride: Implications for drinking water treatment. *Water Res.* *42*, 2111–2123.
- Sierra, M.M.D.S., Giovanela, M., and Soriano-Sierra, E.J. (2000). Fluorescence Properties of Well-Characterized Sedimentary Estuarine Humic Compounds and Surrounding Pore Waters. *Environ. Technol.* *21*, 979–988.
- Sierra, M.M.D., Giovanela, M., Parlanti, E., and Soriano-Sierra, E.J. (2005a). Fluorescence fingerprint of fulvic and humic acids from varied origins as viewed by single-scan and excitation/emission matrix techniques. *Chemosphere* *58*, 715–733.
- Sierra, M.M.D., Rauen, T.G., Tormen, L., Debacher, N.A., and Soriano-Sierra, E.J. (2005b). Evidence from surface tension and fluorescence data of a pyrene-assisted micelle-like assemblage of humic substances. *Water Res.* *39*, 3811–3818.
- Simpson, A.J., Kingery, W.L., Spraul, M., Humpfer, E., Dvortsak, P., and Kerssebaum, R. (2001a). Separation of Structural Components in Soil Organic Matter by Diffusion Ordered Spectroscopy. *Environ. Sci. Technol.* *35*, 4421–4425.
- Simpson, A.J., Kingery, W.L., Shaw, D.R., Spraul, M., Humpfer, E., and Dvortsak, P. (2001b). The Application of ¹H HR-MAS NMR Spectroscopy for the Study of Structures and Associations of Organic Components at the Solid–Aqueous Interface of a Whole Soil. *Environ. Sci. Technol.* *35*, 3321–3325.
- Simpson, A.J., Salloum, M.J., Kingery, W.L., and Hatcher, P.G. (2002a). Improvements in the two-dimensional nuclear magnetic resonance spectroscopy of humic substances. *J. Environ. Qual.* *31*, 388–392.
- Simpson, A.J., Kingery, W.L., Hayes, M.H.B., Spraul, M., Humpfer, E., Dvortsak, P., Kerssebaum, R., Godejohann, M., and Hofmann, M. (2002b). Molecular structures and associations of humic substances in the terrestrial environment. *Naturwissenschaften* *89*, 84–88.
- Singh, H.N., and Hinze, W.L. (1982). Micellar enhanced fluorimetric determination of 1-NN-dimethylaminonaphthalene-5-sulphonyl chloride and o-phthalaldehyde-2-mercaptoethanol derivatives of amino acids. *Analyst* *107*, 1073–1080.

- Skoog, D.A.; Holler, F.J.; Crouch, S.R. "Principles of Instrumental Analysis" 6th ed (1980). Chapter 30 Thomson Brooks/Cole Publishing: Belmont, CA 2007.
- Smart, P.L., Finlayson, B.L., Rylands, W.D., and Ball, C.M. (1976). The relation of fluorescence to dissolved organic carbon in surface waters. *Water Res.* 10, 805–811.
- Šmejkalová, D., and Piccolo, A. (2007). Aggregation and disaggregation of humic supramolecular assemblies by NMR diffusion ordered spectroscopy (DOSY-NMR). *Environ. Sci. Technol.* 42, 699–706.
- Šmejkalová, D., Spaccini, R., Fontaine, B., and Piccolo, A. (2009). Binding of Phenol and Differently Halogenated Phenols to Dissolved Humic Matter As Measured by NMR Spectroscopy. *Environ. Sci. Technol.* 43, 5377–5382.
- Smith, D.S., and Kramer, J.R. (1999). Fluorescence analysis for multi-site aluminum binding to natural organic matter. *Environ. Int.* 25, 295–306.
- Smith, D.S., and Kramer, J.R. (2000). Multisite metal binding to fulvic acid determined using multiresponse fluorescence. *Anal. Chim. Acta* 416, 211–220.
- Song, J., Huang, W., Peng, P., Xiao, B., and Ma, Y. (2010). Humic Acid Molecular Weight Estimation by High-Performance Size-Exclusion Chromatography with Ultraviolet Absorbance Detection and Refractive Index Detection. *Soil Sci. Soc. Am. J.* 74, 2013.
- De Souza Sierra, M.M., Donard, O.F.X., Lamotte, M., Belin, C., and Ewald, M. (1994). Fluorescence spectroscopy of coastal and marine waters. *Mar. Chem.* 47, 127–144.
- Sowden, F.J., and Schnitzer, M. (1967). Nitrogen distribution in illuvial organic matter. *Can. J. Soil Sci.* 47, 111–116.
- Sparks, D.L. (1998). *Soil Physical Chemistry*, Second Edition (CRC Press).
- Sparks, D.L. (2003). *Environmental soil chemistry* (Academic press).
- Spencer, R.G.M., Baker, A., Ahad, J.M.E., Cowie, G.L., Ganeshram, R., Upstill-Goddard, R.C., and Uher, G. (2007). Discriminatory classification of natural and anthropogenic waters in two U.K. estuaries. *Sci. Total Environ.* 373, 305–323.
- Stach, E. (1975). *Coal Petrology*. Gebrüder Borntraeger Stuttg. Ger.
- Steelink, C. (1963). What is humic acid? *J. Chem. Educ.* 40, 379.
- Steelink, C. (1985). Implications of elemental characteristics of humic substances. (In: *Humic Substances in Soil, Sediment, and Water*, ed. G.R. Aiken, D.M. McKnight, R.L. Wershaw & P. MacCarthy, pp. 457–476. New York: Wiley),.
- Steelink, C., Wershaw, R.L., Thorn, K.A., and Wilson, M.A. (1989). Application of Liquid-State NMR Spectroscopy to Humic Substances. (In: *Humic Substances II: In Search of Structure*. M. H. B. Hayes, P. MacCarthy, R. L. Malcolm, and R. S. Swift (eds), Wiley, Chichester, New York, pp. 281-308),.

- Stevenson, F.J. (1989). Reductive Cleavage of Humic Substances. (In: Humic Substances II: In Search of Structure. M. H. B. Hayes, P. MacCarthy, R. L. Malcolm, and R. S. Swift (eds), Wiley, Chichester, New York, pp. 121-142),.
- Stevenson, F.J. (1994). Humus chemistry: genesis, composition, reactions (John Wiley & Sons).
- Stevenson, I.L., and Schnitzer, M. (1982). Transmission Electron Microscopy of Extracted Fulvic and Humic Acids. *Soil Sci.* 133, 179–185.
- Stevenson, F.J., Van Winkle, Q., and Martin, W.P. (1953). Physicochemical Investigations of Clay-adsorbed Organic Colloids: III. *Soil Sci. Soc. Am. J.* 17, 31.
- Stigter, D., and Mysels, K.J. (1955). Tracer Electrophoresis. II. The Mobility of the Micelle of Sodium Lauryl Sulfate and its Interpretation in Terms of Zeta Potential and Charge. *J. Phys. Chem.* 59, 45–51.
- Stocking, M.A. (2003). Tropical Soils and Food Security: The Next 50 Years. *Science* 302, 1356–1359.
- Stuermer, D.H., and Harvey, G.R. (1974). Humic substances from seawater. *Nature* 250, 480–481.
- Stuermer, D.H., Peters, K.E., and Kaplan, I.R. (1978). Source indicators of humic substances and proto-kerogen. Stable isotope ratios, elemental compositions and electron spin resonance spectra. *Geochim. Cosmochim. Acta* 42, 989–997.
- Subbiah, D., and Mishra, A.K. (2009). Humic acid-cetyltrimethylammonium bromide interaction: a fluorimetric study. *Luminescence* 24, 84–89.
- Suffet, I.H., and MacCarthy, P. (1988). Aquatic Humic Substances: Influence on Fate and Treatment of Pollutants (American Chemical Society).
- Sun, L., Perdue, E.M., and McCarthy, J.F. (1995). Using reverse osmosis to obtain organic matter from surface and ground waters. *Water Res.* 29, 1471–1477.
- Sun, L., Perdue, E.M., Meyer, J.L., and Weis, J. (1997). Use of elemental composition to predict bioavailability of dissolved organic matter in a Georgia river. *Limnol. Oceanogr.* 42, 714–721.
- Sutton, R., and Sposito, G. (2005). Molecular structure in soil humic substances: the new view. *Environ. Sci. Technol.* 39, 9009–9015.
- Svergun, D.I., and Koch, M.H. (2003). Small-angle scattering studies of biological macromolecules in solution. *Rep. Prog. Phys.* 66, 1735.
- Swift, R.S. (1985). Fractionation of Soil Humic Substances. (In: Humic Substances in Soil, Sediment, and Water, ed. G.R. Aiken, D.M. McKnight, R.L. Wershaw & P. MacCarthy, pp. 387-408. New York: Wiley.).
- Swift, R.S. (1989a). Molecular Weight, Size, Shape, and Charge Characteristics of Humic Substances: Some Basic Considerations. (In: Humic Substances II: In Search of Structure.

M. H. B. Hayes, P. MacCarthy, R. L. Malcolm, and R. S. Swift (eds), Wiley, Chichester, New York, pp. 449-466),.

Swift, R.S. (1989b). Molecular Weight, Shape, and Size, of Humic Substances by Ultracentrifugation. (In: Humic Substances II: In Search of Structure. M. H. B. Hayes, P. MacCarthy, R. L. Malcolm, and R. S. Swift (eds), Wiley, Chichester, New York, pp. 467-496),.

Swift, R.S. (1996). Organic Matter Characterization (In Methods of Soil Analysis: Chemical Analysis, 3rd Ed. D. L. Sparks (ed). Am. Soc. Agron., Madison, WI, pp. 1011-1070).

Swift, R.S. (1999). Macromolecular properties of soil humic substances: fact, fiction, and opinion. *Soil Sci.* 164, 790–802.

Swift, R.S., and Posner, A.M. (1971). Gel Chromatography of Humic Acid. *J. Soil Sci.* 22, 237–249.

T

Tadros, T.F., and Gregory, J. (2013). *Colloids in the Aquatic Environment* (Elsevier).

Takata, Y., Tagashira, H., Hyono, A., and Ohshima, H. (2010). “Effect of Counterion and Configurational Entropy on the Surface Tension of Aqueous Solutions of Ionic Surfactant and Electrolyte Mixtures,” *Entropy*, vol. 12, no. 4, pp. 983–995.

Tan, K.H. (2011). *Principles of Soil Chemistry, Fourth Edition* (CRC Press).

Tan, K.H. (2014). *Humic Matter in Soil and the Environment: Principles and Controversies, Second Edition* (CRC Press).

Tan, C.H., Huang, Z.J., and Huang, X.G. (2010). Rapid determination of surfactant critical micelle concentration in aqueous solutions using fiber-optic refractive index sensing. *Anal. Biochem.* 401, 144–147.

Tan, W.F., Koopal, L.K., and Norde, W. (2009). Interaction between Humic Acid and Lysozyme, Studied by Dynamic Light Scattering and Isothermal Titration Calorimetry. *Environ. Sci. Technol.* 43, 591–596.

Tanaka, T., Nagao, S., Sakamoto, Y., Ohnuki, T., Ni, S., and Senoo, M. (1997). Distribution Coefficient in the Sorption of Radionuclides onto Ando Soil in the Presence of Humic Acid. *J. Nucl. Sci. Technol.* 34, 829–834.

Tanford, C. (1980). *The Hydrophobic Effect: Formation of Micelles and Biological Membranes* 2d Ed (J. Wiley.).

Tanford, C. (1985). Monolayers, micelles, lipid vesicles and biomembranes. *Phys. Amphiphiles Micelles Vesicles Microemulsions* Vol 90 Ed V Degiorgio M Corti.

Tanford, C. (1972). “Micelle shape and size,” *J. Phys. Chem.*, vol. 76, no. 21, pp. 3020–3024.

- Tang, M., and Carter, W.C. (2013). "Branching Mechanisms in Surfactant Micellar Growth," *J. Phys. Chem. B*, vol. 117, no. 10, pp. 2898–2905.
- Taraniuk, I., Graber, E.R., Kostinski, A., and Rudich, Y. (2007). "Surfactant properties of atmospheric and model humic-like substances (HULIS)," *Geophys. Res. Lett.*, vol. 34, no. 16, p. L16807.
- Tate, R.L. (1987). *Soil organic matter: biological and ecological effects* (Wiley).
- Terashima, M., Fukushima, M., and Tanaka, S. (2004a). Influence of pH on the surface activity of humic acid: micelle-like aggregate formation and interfacial adsorption. *Colloids Surf. -Physicochem. Eng. Asp.* 247, 77–83.
- Terashima, M., Fukushima, M., and Tanaka, S. (2004b). Evaluation of solubilizing ability of humic aggregate basing on the phase-separation model. *Chemosphere* 57, 439–445.
- Teixeira, J. (1988). Small-angle scattering by fractal systems. *J. Appl. Crystallogr.* 21, 781–785.
- Tfaily, M.M., chu, R.K., Tolic, N., Roscioli, K.M., Anderton, C.R., Pasa-Tolic, L., Robinson, E.W., and Hess, N.J. (2015). "Advanced solvent based methods for molecular characterization of soil organic matter by high-resolution mass spectrometry", *Anal. Chem.* vol. 87, pp. 5206-5215.
- Theng, B.K.G. (1979). *Formation and Properties of Clay-polymer Complexes* (Elsevier, Amsterdam).
- Theng, B.K.G. (2012). *Formation and properties of clay-polymer complexes* (Elsevier).
- Thieme, J., and Niemeyer, J. (1998). Interaction of colloidal soil particles, humic substances and cationic detergents studied by X-ray microscopy. In *Structure, Dynamics and Properties of Disperse Colloidal Systems*, (Springer), pp. 193–201.
- Thorn, K.A. (1994). Nuclear-Magnetic-Resonance Spectrometry Investigations of Fulvic and Humic Acids from the Suwannee River (In: *Humic substances in the Suwannee River, Georgia; interactions, properties, and proposed structures.* p. 141-182, United States Geological Survey), WSP - 2373.
- Thorn, K.A. (1987). "Structural characteristics of the IHSS Suwannee River fulvic and humic acids determined by solution state C-13 NMR spectroscopy," *Sci. Total Environ.*, vol. 62, pp. 175–183.
- Thorn, K.A., Folan, D.W., and MacCarthy, P. (1989). Characterization of the International Humic Substances Society standard and reference fulvic and humic acids by solution state carbon-13 (¹³C) and hydrogen-1 (¹H) nuclear magnetic resonance spectrometry (United States Geological Survey), WSP - 2373.
- Thorn, K.A., Goldenberg, W.S., Younger, S.J., and Weber, E.J. (1996). Covalent Binding of Aniline to Humic Substances. In *Humic and Fulvic Acids*, (American Chemical Society), pp. 299–326.

- Thurman, E.M. (1985). *Organic geochemistry of natural waters* (Springer Science & Business Media).
- Thurman, E.M., and Malcolm, R.L. (1981). Preparative isolation of aquatic humic substances. *Environ. Sci. Technol.* *15*, 463–466.
- Thurman, E.M., and Malcolm, R.L. (1994). Nitrogen and Amino Acids in Fulvic and Humic Acids from the Suwannee River (In: *Humic substances in the Suwannee River, Georgia; interactions, properties, and proposed structures.* p. 55-66, United States Geological Survey), WSP - 2373.
- Thurman, E.M., Wershaw, R.L., Malcolm, R.L., and Pinckney, D.J. (1982). Molecular size of aquatic humic substances. *Org. Geochem.* *4*, 27–35.
- Tipping, E. (2002). *Cation Binding by Humic Substances* (Cambridge University Press).
- Tissot, B.P., and Welte, D.H. (1978). *Petroleum Formation and Occurrence: A New Approach to Oil and Gas Exploration* (Springer-Verlag, Berlin).
- Tombacz, E. (1999). Colloidal properties of humic acids and spontaneous changes of their colloidal state under variable solution conditions. *Soil Sci.* *164*, 814–824.
- Tombácz, E., Varga, K., and Szántó, F. (1988). An X-ray diffraction study of alkylammonium humate complexes. *Colloid Polym. Sci.* *266*, 734–738.
- Tombacz, E., Rice, J.A., and Ren, S.Z. (1997). Fractal structure of polydisperse humic acid particles in solution studied by scattering methods. *Ach-Models Chem.* *134*, 877–888.
- Tombácz, E., Rice, J.A., Ghabbour, E.A., and Davies, G. (1999). Changes of colloidal state in aqueous systems of humic acids. *Underst. Humic Subst. Adv. Methods Prop. Appl. R. Soc. Chem. Bodmin Corn. UK* 69–78.
- Traganza, E.D. (1969). Fluorescence excitation and emission spectra of dissolved organic matter in sea water. *Bull. Mar. Sci.* *19*, 897–904.
- Traina, S.J., McAvoy, D.C., and Versteeg, D.J. (1996). Association of Linear Alkylbenzenesulfonates with Dissolved Humic Substances and Its Effect on Bioavailability. *Environ. Sci. Technol.* *30*, 1300–1309.
- Tschapek, M., and Wasowski, C. (1976). The surface activity of humic acid. *Geochim. Cosmochim. Acta* *40*, 1343–1345.
- Tucker, I., Penfold, J., Thomas, R.K., Grillo, I., Barker, J.G., and Mildner, D.F.R. (2008). Self-Assembly in Mixed Dialkyl Chain Cationic- Nonionic Surfactant Mixtures: Dihexadecyldimethyl Ammonium Bromide- Monododecyl Hexaethylene Glycol (Monododecyl Dodecaethylene Glycol) Mixtures. *Langmuir* *24*, 7674–7687.
- Tuschall, J.R., and Brezonik, P.L. (1980). Characterization of organic nitrogen in natural waters: its molecular size, protein content, and interactions with heavy metals. *Limnol Ocean.* *25*, 495–504.

U

Underdown, A.W., Langford, C.H., and Gamble, D.S. (1985). Light scattering studies of the relationship between cation binding and aggregation of a fulvic acid. *Environ. Sci. Technol.* *19*, 132–136.

V

Vanderbrouke, M., Pelet, R., and Debyser, Y. (1985). Geochemistry of Humic Substances in Marine Environments. (In: *Humic substances in soil, sediment, and water: geochemistry, isolation and characterization*. G. R. Aiken, D. M. McKnight, R.L. Wershaw, and P. MacCarthy (eds). John Wiley, New York, pp. 249-273).

Del Vecchio, R., and Blough, N.V. (2004). On the Origin of the Optical Properties of Humic Substances. *Environ. Sci. Technol.* *38*, 3885–3891.

Vermeer, A.W.P., and Koopal, L.K. (1998). Adsorption of Humic Acids to Mineral Particles. 2. Polydispersity Effects with Polyelectrolyte Adsorption. *Langmuir* *14*, 4210–4216.

Vigneault, B., Percot, A., Lafleur, M., and Campbell, P.G.C. (2000). Permeability Changes in Model and Phytoplankton Membranes in the Presence of Aquatic Humic Substances. *Environ. Sci. Technol.* *34*, 3907–3913.

Visser, S.A. (1964). A Physico-Chemical Study of the Properties of Humic Acids and Their Changes During Humification. *J. Soil Sci.* *15*, 202–219.

Visser, S.A. (1985). Viscosimetric studies on molecular weight fractions of fulvic and humic acids of aquatic, terrestrial and microbial origin. *Plant Soil* *87*, 209–221.

Vogt, R.D., and Taugbrf, G. (1994). Humic Substances in the Global Environment and Implications on Human Health.

W

Wagoner, D.B., Christman, R.F., Cauchon, G., and Paulson, R. (1997). Molar Mass and Size of Suwannee River Natural Organic Matter Using Multi-Angle Laser Light Scattering. *Environ. Sci. Technol.* *31*, 937–941.

Waite, T.D., Wrigley, I.C., and Szymczak, R. (1988). Photoassisted dissolution of a colloidal manganese oxide in the presence of fulvic acid. *Environ. Sci. Technol.* *22*, 778–785.

Waksman, S.A. (1932). *Humus*. (Williams and Wilkins. Baltimore, MD.).

Waksman, S.A., and Iyer, K.R.N. (1932). Contribution to our knowledge of the chemical nature and origin of humus: I. on the synthesis of the “humus nucleus.” *Soil Sci.* *34*, 43–70.

- Waksman, S.A., and Iyer, K.R.N. (1933). Contribution to our knowledge of the chemical nature and origin of humus: IV. Fixation of proteins by lignins and formation of complexes resistant to microbial decomposition. *Soil Sci.* 36, 69–82.
- Wall, N.A., and Choppin, G.R. (2003). Humic acids coagulation: influence of divalent cations. *Appl. Geochem.* 18, 1573–1582.
- Von Wandruszka, R. (1998). The micellar model of humic acid: Evidence from pyrene fluorescence measurements. *Soil Sci.* 163, 921–930.
- von Wandruszka, R. (2000). Humic acids: Their detergent qualities and potential uses in pollution remediation. *Geochem. Trans.* 1, 10–15.
- Wang, L., Chin, Y.-P., and Traina, S.J. (1997). Adsorption of (poly)maleic acid and an aquatic fulvic acid by goethite. *Geochim. Cosmochim. Acta* 61, 5313–5324.
- Wang, W., Ye, B., Yang, L., Li, Y., and Wang, Y. (2007). Risk assessment on disinfection by-products of drinking water of different water sources and disinfection processes. *Environ. Int.* 33, 219–225.
- Welte, D. (1973). Recent advances in organic geochemistry of humic substances and kerogen (A review. In: *Advances in Organic Geochemistry, 1973*. B. Tissot and F. Binner (eds). Editions Techn, Paris, pp. 3-13).
- Wershaw, R. (1993). Model for humus in soils and sediments. *Environ. Sci. Technol.* 27, 814–816.
- Wershaw, R.L. (1986). A new model for humic materials and their interactions with hydrophobic organic chemicals in soil-water or sediment-water systems. *J. Contam. Hydrol.* 1, 29–45.
- Wershaw, R.L. (1989). Sizes and Shapes of Humic Substances by Scattering Techniques. (In: *Humic Substances II: In Search of Structure*. M. H. B. Hayes, P. MacCarthy, R. L. Malcolm, and R. S. Swift (eds), Wiley, Chichester, New York, pp. 545-560),.
- Wershaw, R.L. (1994). Membrane-micelle model for humus in soils and sediments and its relation to humification (United States Geological Survey), WSP - 2373.
- Wershaw, R.L. (1999). Molecular aggregation of humic substances. *Soil Sci.* 164, 803–813.
- Wershaw, R.L., and Pinckney, D. J., (1973). *The Fractionation of Humic acids from Natural Water Systems*, vol. 1. In: *Journal of research of the U.S. Geological Survey*. pp. 361-366.
- Westerhoff, P., Chen, W., and Esparza, M. (2001). Fluorescence Analysis of a Standard Fulvic Acid and Tertiary Treated Wastewater. *J. Environ. Qual.* 30, 2037.
- Wetzel, R.G., Hatcher, P.G., and Bianchi, T.S. (1995). Natural photolysis by ultraviolet irradiance of recalcitrant dissolved organic matter to simple substrates for rapid bacterial metabolism. *Limnol. Oceanogr.* 40, 1369–1380.

- Wicz, W., Rzeska, A., Łukomska, J., Stachowiak, K., Karolczak, J., Malicka, J., and Łankiewicz, L. (2001). Mechanism of fluorescence quenching of tyrosine derivatives by amide group. *Chem. Phys. Lett.* *341*, 99–106.
- Wilkinson, A.E., Hesketh, N., Higgo, J.J.W., Tipping, E., and Jones, M.N. (1993). The determination of the molecular mass of humic substances from natural waters by analytical ultracentrifugation. *Colloids Surf. Physicochem. Eng. Asp.* *73*, 19–28.
- Wilkinson, K.J., Negre, J.-C., and Buffle, J. (1997). Coagulation of colloidal material in surface waters: the role of natural organic matter. *J. Contam. Hydrol.* *26*, 229–243.
- Wilkinson, K.J., Balnois, E., Leppard, G.G., and Buffle, J. (1999). Characteristic features of the major components of freshwater colloidal organic matter revealed by transmission electron and atomic force microscopy. *Colloids Surf. Physicochem. Eng. Asp.* *155*, 287–310.
- Williams, P.S., and Giddings, J.C. (1987). Power programmed field-flow fractionation: a new program form for improved uniformity of fractionating power. *Anal. Chem.* *59*, 2038–2044.
- Wilson, M.A. (1987). *NMR techniques and applications in geochemistry and soil chemistry.* (Pergamon Press).
- Wilson, S.A., and Weber, J.H. (1977). A comparative study of number-average dissociation-corrected molecular weights of fulvic acids isolated from water and soil. *Chem. Geol.* *19*, 285–293.
- De Wit, J.C.M., van Riemsdijk, W.H., and Koopal, L.K. (1993). Proton binding to humic substances. 1. Electrostatic effects. *Environ. Sci. Technol.* *27*, 2005–2014.
- Wolfbeis, O.S. (2012). *Fluorescence Spectroscopy: New Methods and Applications* (Springer Science & Business Media).
- Won, Y.-Y. (2004). Imaging nanostructured fluids using cryo-TEM. *Korean J. Chem. Eng.* *21*, 296–302.
- Wong, H., Mok, K.M., and Fan, X.J. (2007). Natural organic matter and formation of trihalomethanes in two water treatment processes. *Desalination* *210*, 44–51.
- Woods, G.C., Simpson, M.J., Koerner, P.J., Napoli, A., and Simpson, A.J. (2011). HILIC-NMR: toward the identification of individual molecular components in dissolved organic matter. *Environ. Sci. Technol.* *45*, 3880–3886.
- Woodwell, G.M., and Houghton, R.H. (1977). Biotic influences on the world carbon budget (pp. 61-72. In W. Stumm (eds), *Global Chemical Cycles and Their Alterations by Man.* Wiley, New York).
- Woodwell, G.M., Whittaker, R.H., Reiners, W.A., Likens, G.E., Delwiche, C.C., and Botkin, D.B. (1978). The biota and the world carbon budget. *Science* *199*, 141–146.

X

Xiaoli, C., Guixiang, L., Xin, Z., Yongxia, H., and Youcai, Z. (2012). Fluorescence excitation–emission matrix combined with regional integration analysis to characterize the composition and transformation of humic and fulvic acids from landfill at different stabilization stages. *Waste Manag.* 32, 438–447.

Xing, B. (1998). NONLINEARITY AND COMPETITIVE SORPTION OF HYDROPHOBIC ORGANIC COMPOUNDS IN HUMIC SUBSTANCES. In *Humic Substances*, G.D.A. Ghabbour, ed. (Woodhead Publishing), pp. 173–183.

Xu, R., Wang, Z., Li, H., and He, X. (2013). Dynamics of Micelle Formation from Mixed Lipid Droplets. *Chin. J. Chem. Phys.* 26, 203.

Y

Yamashita, Y., Jaffé, R., Maie, N., and Tanoue, E. (2008). Assessing the dynamics of dissolved organic matter (DOM) in coastal environments by excitation emission matrix fluorescence and parallel factor analysis (EEM-PARAFAC). *Limnol. Oceanogr.* 53, 1900–1908.

Yamashita, Y., and Tanoue, E. (2003). Chemical characterization of protein-like fluorophores in DOM in relation to aromatic amino acids. *Mar. Chem.* 82, 255–271.

Yan, M., Li, M., Wang, D., and Xiao, F. (2013). Optical property of iron binding to Suwannee River fulvic acid. *Chemosphere* 91, 1042–1048.

Yates, L.M., and von Wandruszka, R. (1999). Effects of pH and metals on the surface tension of aqueous humic materials. *Soil Sci. Soc. Am. J.* 63, 1645–1649.

Yee, M.M. (2006). *Comprehensive Study of Humic Substances-Ionic Surfactant Interaction in Aqueous Solution*. Saga University.

Yee, M.M., Miyajima, T., and Takisawa, N. (2006a). Evaluation of amphiphilic properties of fulvic acid and humic acid by alkylpyridinium binding study. *Colloids Surf. Physicochem. Eng. Asp.* 272, 182–188.

Yee, M.M., Miyajima, T., and Takisawa, N. (2006b). Thermodynamic studies of dodecylpyridinium ion binding to fulvic acid. *Colloids Surf. Physicochem. Eng. Asp.* 287, 68–74.

Yee, M.M., Miyajima, T., and Takisawa, N. (2007). Thermodynamic studies of dodecylpyridinium ion binding to humic acid and effect of solution parameters on their binding. *Colloids Surf. Physicochem. Eng. Asp.* 295, 61–66.

Yee, M.M., Miyajima, T., and Takisawa, N. (2009). Study of ionic surfactants binding to humic acid and fulvic acid by potentiometric titration and dynamic light scattering. *Colloids Surf. Physicochem. Eng. Asp.* 347, 128–132.

- Ying, G.-G. (2006). Fate, behavior and effects of surfactants and their degradation products in the environment. *Environ. Int.* *32*, 417–431.
- Ying, G.-G., Williams, B., and Kookana, R. (2002). Environmental fate of alkylphenols and alkylphenol ethoxylates—a review. *Environ. Int.* *28*, 215–226.
- Yonebayashi, K., and Hattori, T. (1987). Surface active properties of soil humic acids. *Sci. Total Environ.* *62*, 55–64.
- Young, M., and Steelink, C. (1973). Peroxidase catalyzed oxidation of naturally-occurring phenols and hardwood lignins. *Phytochemistry* *12*, 2851–2861.
- Yu, J., Xu, Q., Liu, Z., Guo, X., Han, S., Yuan, S., and Tong, L. (2013). Morphological characteristics of fulvic acid fractions observed by atomic force microscopy: MORPHOLOGICAL CHARACTERISTICS OF FULVIC ACID FRACTIONS. *J. Microsc.* *252*, 71–78.

Z

- Zang, X., van Heemst, J.D.H., Dria, K.J., and Hatcher, P.G. (2000). Encapsulation of protein in humic acid from a histosol as an explanation for the occurrence of organic nitrogen in soil and sediment. *Org. Geochem.* *31*, 679–695.
- Zavarzina, A.G., Demin, V.V., Nifant'eva, T.I., Shkinev, V.M., Danilova, T.V., and Spivakov, B.Y. (2002). Extraction of humic acids and their fractions in poly(ethylene glycol)-based aqueous biphasic systems. *Anal. Chim. Acta* *452*, 95–103.
- Zech, W., Hempfling, R., Haumaier, L., Schulten, H.-R., and Haider, K. (1990). Humification in subalpine Rendzinas: chemical analyses, IR and ¹³C NMR spectroscopy and pyrolysis-field ionization mass spectrometry. *Geoderma* *47*, 123–138.
- Zech, W., Senesi, N., Guggenberger, G., Kaiser, K., Lehmann, J., Miano, T.M., Miltner, A., and Schroth, G. (1997). Factors controlling humification and mineralization of soil organic matter in the tropics. *Geoderma* *79*, 117–161.
- Zhang, H.-M., Zhou, Q.-H., Xue, M.-G., and Wang, Y.-Q. (2011). Fluorescence spectroscopic investigation of the interaction between triphenyltin and humic acids. *Spectrochim. Acta. A. Mol. Biomol. Spectrosc.* *78*, 1018–1022.
- Zhou, Q., Cabaniss, S.E., and Maurice, P.A. (2000). Considerations in the use of high-pressure size exclusion chromatography (HPSEC) for determining molecular weights of aquatic humic substances. *Water Res.* *34*, 3505–3514.
- Zhou, C., Hobbie, E.K., Bauer, B.J., and Han, C.C. (1998). Equilibrium structure of hydrogen-bonded polymer blends. *J. Polym. Sci. Part B Polym. Phys.* *36*, 2745–2750.
- Zhou, Q., Maurice, P.A., and Cabaniss, S.E. (2001). Size fractionation upon adsorption of fulvic acid on goethite: equilibrium and kinetic studies. *Geochim. Cosmochim. Acta* *65*, 803–812.

Zsolnay, A., Baigar, E., Jimenez, M., Steinweg, B., and Saccomandi, F. (1999). Differentiating with fluorescence spectroscopy the sources of dissolved organic matter in soils subjected to drying. *Chemosphere* 38, 45–50.

Zumstein, J., and Buffle, J. (1989). Circulation of pedogenic and aquagenic organic matter in an eutrophic lake. *Water Res.* 23, 229–239.

Zwiener, C., and Richardson, S.D. (2005). Analysis of disinfection by-products in drinking water by LC–MS and related MS techniques. *TrAC Trends Anal. Chem.* 24, 613–621.

*LIST OF TABLES
AND FIGURES*

LIST OF TABLES

CHAPTER I

Table I-1. Elemental compositions of humic substances and several plant materials (Kononova, 1966).	18
Table I-2. The functional chemical groups distribution (%) in humic substance fractions (Malcolm, 1990).	19
Table I-3. Humic acid/fulvic acid ratios (R) of some surface soils (Kononova, 1966).	20
Table I-4. Humic Substances Elemental Composition (Steelink, 1985 ; Thurman, 1985 ; Hatcher et al., 1985).	31
Table I-5. IHSS Humic Substances Properties (Murphy and Zachara, 1995).	34
Table I-6. Fluorescence of Organic Matter Fractions according to Excitation/Emission wavelengths.	37
Table I-7. Molecular weights of Organic matter: Fulvic and Humic Acid.	46
Table I-8. Suwannee River Fulvic Acid Molecular Weights.	46
Table I-9. Effect of Humic Concentration, Ionic Strength and pH on the Polymeric Macromolecular Structure (Ghosh and Schnitzer, 1980).	48
Table I-10. Concentration ranges of Dissolved Organic Carbon (DOC) and Humic Substances in some aquatic systems (Thurman, 1985).	57

CHAPTER II

Table II-1. Characteristics of the Various Cationic Surfactants Used.	72
---	----

CHAPTER III

Table III-1. The Volume and area of the outer layer, inner layer and the whole vesicle of SRFA/DTAC Complex.	116
Table III-2. The Number of molecules N_x^{agg} , mole and the effective packing parameter of SRFA/DTAC Complex.	118
Table III-3. Absolute Power Law and Two Power Law Fitting parameters for SRFA _{5g/L} as a function of DTAC concentration.	122

CHAPTER IV

Table IV-1. Two Power Law fitting parameters of SRHA_{5g/L}/DTAC suspensions for the various DTAC additions. 153

Table IV-2. The fitted parameters of SRHA_{5g/L}/DTAC suspensions for the various DTAC additions using Two Lorentzian Model. 155

Table IV-3. Corrlength Model fitted parameters of SRHA_{5g/L}/DTAC suspensions for the various DTAC additions. 156

Table IV-4. The radius of gyration of globules that made up the network entanglement. ... 157

CHAPTER V

Table V-1. Typical Fluorophores detected in Dissolved organic matter according to the Excitation/Emission wavelengths at maximum intensity (Coble, 1996; Parlanti et al., 2000).
..... 163

LIST OF FIGURES

CHAPTER I

Figure I-1. Distribution of Organic matter.....	14
Figure I-2. Chemical properties Humic substances fractions (Stevenson, 1994).....	18
Figure I-3. Humic Substances distribution in forest and grassland soils (Stevenson, 1994)..	19
Figure I-4. Formation pathways of humic substances (Stevenson, 1994).....	21
Figure I-5. The Lignin theory of humic substance genesis (Waksman, 1932).....	22
Figure I-6. The polyphenol theory of humic substance formation (Stevenson, 1994).....	23
Figure I-7. Sugar-Amine theory “Maillard Reaction” for humic substances genesis (Stevenson, 1994).....	24
Figure I-8. Humic Substances Isolation Procedure from Soils (Stevenson, 1994).....	27
Figure I-9. Aquatic Humic Substances Isolation Procedure (Aiken, 1985).....	28
Figure I-10. Preparation of Humic and Fulvic Acid Samples (IHSS Method).....	28
Figure I-11. Isolation of Humin Using MIKB Method (Rice and MacCarthy, 1989a).....	29
Figure I-12. The ¹³ C-NMR spectrum of a soil humic acid, showing chemical groupings and their chemical shifts (Schinitzer, 1990).....	32
Figure I-13. CPMAS ¹³ C-NMR spectra of humic samples (HA1: volcanic soil, HA2: oxidized coal, HA3: leonardite) (Piccolo et al., 1999).....	35
Figure I-14. UV/Visible Spectra of a poorly drained Mollisol Humic and Fulvic Acid (Bloom and Leenheer, 1989).....	36
Figure I-15. Excitation-Emission matrix (EEM) of DOM (upper image) (Carstea, 2012), fresh water (lower left) and marine water (lower right) (Parlanti et al., 2000).....	38
Figure I-16. EEM of marine (M) and fresh lagoon (FL) fulvic and humic acid (Sierra et al., 2005a).....	39
Figure I-17. Size distribution obtaining by DLS, corresponding to the alkaline (solid line) and the acidified–realkalinized (dot line) samples of Aldrich humic acid (HA) and whole humic system of fulvic and humic acid extracted from peat (HT) (Baigorri et al., 2007a).....	40
Figure I-18. Effect of Ionic strength and pH on the size of SRHA measured by photon correlation spectroscopy (PCS) (Baalousha et al., 2006).....	41
Figure I-19. Transmission electron microscopy of SRHA in (a) 0.01M, (b) 0.05M and (c) 0.1M CaCl ₂ at pH 7.5 (upper images) (Baalousha et al., 2006), and soil fulvic acid in 5mM	

NaOH at (a) pH=10.4; (b) pH=7.2; (c) pH=5.9; Scale bars=1 μ m (lower images) (Wilkinson et al., 1999).	42
Figure I-20. Different Molecular conformation detected by TEM of Fluka HA (right image) (Baalousha et al., 2005) and X-ray microscopy of SRFA (left image) (Myneni et al., 1999).	43
Figure I-21. HPSEC chromatogram of SRFA (left images) (Zhou et al., 2000) and Electrophoresis in pH 4-7 gradient of soil humic acid with high and low molecular weight component obtained from discontinuous pore sized gel (right image) (Curvetto and Orioli, 1982).	45
Figure I-22. Humic acids fractionation on Sephadex G-100 at different concentrations (Swift and Posner, 1971).....	47
Figure I-23. Micelle-Like Structure of Humic Substances; left (Engebretson and von Wandruszka, 1994), right (Wershaw, 1986).	48
Figure I-24. Variation of the surface tension (γ) and DDT solubility as a function of HA concentration (a) (Guetzloff and Rice, 1994), and the effect of experimental conditions; surfactant (b) (Gamboa and Olea, 2006) and pH (c) (Terashima et al., 2004a).	49
Figure I-25. Effect of different concentrations of Mg ²⁺ on the intrinsic fluorescence of LSLHA in the 300-465 nm range; λ_{ex} =245nm; 10 μ g/mL LSLHA (Shaffer and Von Wandruszka, 2014).	50
Figure I-26. Supramolecular Assembly of HS. The red spheres represent generic metal cations, the black units polysaccharides, the blue units polypeptides, the green units aliphatic chains, and the brown units aromatic lignin fragments (Simpson et al., 2002b).	51
Figure I-27. Gel permeation chromatograms of HS ₁ (I) and HS ₂ (II) humic material (left) (Piccolo et al., 1996b) and NMR spectra of humic substances (HS) isolated from oak forest HS (right) (Simpson et al., 2002b).....	52
Figure I-28. Proposed Structures for Humic Substances. (a): Humic acid from Zn dust distillation and hydrolysis, oxidation, reduction and spin resonance spectroscopy (Haworth, 1971); (b): Humic acid from alkaline permanganate degradation (Christman et al., 1989); (c): Humic acid (Stevenson, 1982); (d): Fulvic acid (Buffle, 1977).	53
Figure I-29. The Steelink (a) and Jansens (b) Model of Humic Acid Monomer and SRFA Model of Leenheer (c, d and e).	54
Figure I-30. 2D model (left: Schulten and Schnitzer, 1993) and corresponding 3D structure (right: Schulten and Schnitzer, 1995) of Humic Acid. Element colors: carbon=light blue; hydrogen=white; nitrogen=dark blue; and oxygen= red; A, B, and C are the voids).....	55
Figure I-31. Lignin Conversion (left) into Humic Acid monomer (right) (Sein et al., 1999).	55

Figure I-32. Humic Acid Model suggested by Simpson et al. (2002b) M represents the metal ion or surface.....	56
Figure I-33. Effect of Surfactant concentration (below and above cmc) on their Physico-Chemical Properties (Preston, 1948).	59
Figure I-34. Effect of Temperature (Krafft point) on Surfactant Solubility (Shinoda et al., 1963).	60
Figure I-35. Dodecyl-pyridinium chloride –HA (purified Aldrich humic acid (PAHA), Dando humic acid (DHA), Inogashira humic acid (IHA)) and –FA (Laurentian fulvic acid (LFA) and Strichen Bs fulvic acid (SFA)) binding isotherms at 0.005 M salt and pH 4.5–5 (Ishiguro et al., 2007).....	61
Figure I-36. Potentiograms of: (a) $C_{12}Py^+$ –AFA system and (b) $C_{12}Py^+$ system. (○) Without FA or HA; (●) with FA or HA; pH= 9.18, I= 0.03M and T=25 °C (Yee et al., 2006a).....	62
Figure I-37. Surfactant–PAHA titrations at pH=7 and I=0.025 M. The cell potential or EMF (mV) is plotted as a function of the logarithm of the total SDS (Koopal et al., 2004).....	62
Figure I-38. Binding isotherms for $C_{12}Py^+$ –AFA system. Left image: as a function of pH at: (a) I= 0.03 mol dm ⁻³ and (b) I= 0.10 mol dm ⁻³ , (*), pH 3.97, (○) pH 7.41, (□) pH 9.18, (△) pH 10.01. Right image: as a function of ionic strength at: (a) pH 9.18 and (b) pH 3.97. (□) I= 0.03 mol dm ⁻³ , (○) I= 0.05 mol dm ⁻³ , (△) I= 0.10 mol dm ⁻³ (Yee et al., 2006b).....	63

CHAPTER II

Figure II-1. Okefenokee Swamp and Suwannee River Location (Pirkle et al., 1977 ; Presley, 1984).	67
Figure II-2. Location of Sampling Site of Nyong River Cameroon.	68
Figure II-3. Sampling Sites of black waters from the Amazonas-Brazil.....	69
Figure II-4. The concentration of the humic substance stock solutions according to the technique of investigation used.....	70
Figure II-5. The Procedures for Sample Preparation.....	73
Figure II-6. Turbidimeter Principle and Optial Design of HACH LANGE 2100Q.	74
Figure II-7. Effect of Particle Sizes on the Scattering Pattern (Brumberger et al., 1968).....	75
Figure II-8. Dynamic Light Scattering Setup (Maxit, Cordouan Technologies, 33400 Pessac, France).	76
Figure II-9. Surface Tension assessment using Wilhelmy plate method.	78
Figure II-10. Schematic representation for a diffuse soft particle, composed of a spherical hard-core and a permeable charged polyelectrolyte layer, moving with a velocity, “U”, in an	

electrolyte subject to a “ <i>dc</i> ” electric field, “ <i>E</i> ”. For humic substances, $a=0$, and the mode corresponds to that of a spherical polyelectrolyte (Duval et al., 2005).	79
Figure II-11. LDV Principle (left) and Electroosmosis Effect (right).	80
Figure II-12. Electrophoretic Movement of Electrolytes.	80
Figure II-13. LACEY/CARBON FILM Grid Showing the Carbon Holes (Left) and Sample Distribution within the Holes (Right).	81
Figure II-14. Vitrification System, Photograph (left) and Scheme (right). (a): Forceps, (b): Grid, (c): N-vapour, (d): LN ₂ , (e): Support and Grid Receptacle, (f): Support, (g): Liquid Ethane Cuvette.	82
Figure II-15. Cryo-TEM Sample Preparation Procedures. (a): Liquid Sample on the Grid, (b): Thinning by Blotting, (c): Rapid Vitrification (Won, 2004).	82
Figure II-16. Illustration of Transmission Electron Microscopy (left) and Grid's Holder (right) (Kuntsche et al., 2011).	83
Figure II-17. Particles Size Segregation according to Carbon Film Thickness (Klang et al., 2012).	83
Figure II-18. Illustration of D22 SANS at the Institut Laue Langevin, Grenoble (Upper image) and the Scattering Vector (lower image) (Grillo, 2008).	85
Figure II-19. A Typical Scattering Curve (upper image) and the Structures Identify from Different Region (lower image). I: low- <i>q</i> ; II: Intermediate- <i>q</i> and III: High- <i>q</i> region (Nasimova et al., 2004).	86
Figure II-20. Schematic Representation of UV/Vis Spectrophotometry.	87
Figure II-21. Electromagnetic Wave Absorption (left) and Various Electronic Transitions (right).	88
Figure II-22. Transmittance and Variation of Light Intensity through a solution.	89
Figure II-23. Jablonski diagram illustrating the Various Processes during Electronic Excited State Formation (left) and the Stokes Shift (right).	90
Figure II-24. Schematic Representation of PTI "Quanta-Master 30 Plus" Fluorescence Spectroscopy. (1) Light Source, (2) Adjustable slits, (3) Excitation and emission monochromator, (4) Excitation and emission grating, (5) Sample compartment, (6) Excitation and Lamp Intensity Fluctuation correction, (7) Detector.	91

CHAPTER III

Figure III-1. Typical turbidity curves of SRFA/DTAC suspensions as a function of time for various DTAC additions; SRFA concentration = 20 mg/L.	100
Figure III-2. pH variation of SRFA/DTAC suspensions as a function of DTAC concentration.	101
Figure III-3. Interaction of SRFA with DTAC (●), OTAC (●), and NaCl (●) as a function of salt concentration: (a) Turbidity curves; (b) Conductivity curves.	101
Figure III-4. (a) Electrophoretic mobility of SRFA/DTAC complexes versus DTAC concentration (●). (b) Number-average particle size of SRFA/DTAC complexes (DLS) versus DTAC concentration (●) for a SRFA concentration of 20 mg/L. The turbidity curve (●) is superimposed for comparison. The inset shows the bimodal size distribution obtained for a DTAC addition of 0.19 mmol/L.	103
Figure III-5. Surface tension of SRFA/DTAC suspensions versus DTAC concentration (●) for a SRFA concentration of 20 mg/L. The turbidity curve (●) is shown in order to position the main variations of surface tension.	104
Figure III-6. CryoTEM micrographs of SRFA in presence of DTAC concentrations of 1.8 mmol/L and 7.58 mmol/L (red dots) showing spongy networks and vesicles. The arrows indicate the walls of the vesicles.	105
Figure III-7. CryoTEM micrographs of SRFA/DTAC molecular structures; all scale bars equal 100 nm unless otherwise indicated. (a) [DTAC] = 0 mmol/L. (b1-4) [DTAC] = $7.6 \cdot 10^{-3}$ mmol/L; the arrow indicates an open vesicle. (c) [DTAC] = $30.2 \cdot 10^{-3}$ mmol/L. (d) [DTAC] = $56.7 \cdot 10^{-3}$ mmol/L. (e1-2) [DTAC] = $75.6 \cdot 10^{-3}$ mmol/L. (f1-4) [DTAC] = $18.8 \cdot 10^{-2}$ mmol/L. (g) [DTAC] = $74.3 \cdot 10^{-2}$ mmol/L.	107
Figure III-8. CryoTEM micrographs of (a) DTAC stock solution (10g/L or 37.9 mmol/L); (b) DTAC solution at a concentration of $7.6 \cdot 10^{-3}$ mmol/L, i.e. the concentration at which fulvic-rich vesicles are formed.	108
Figure III-9. Size histograms of molecular structures viewed by cryoTEM and evolution of mean particle size with DTAC concentration. The DTAC concentration is indicated in the histograms in mmol/L. The histograms in red are associated with the presence of vesicles.	109
Figure III-10. Surface tension of SRFA suspensions as a function of SRFA concentration.	112
Figure III-11. Interdigitating Hydrophobic Domain Vesicle of SRFA/DTAC Mixed System.	115

Figure III-12. Small-angle neutron scattering curves from SRFA_{5g/L} in presence of various DTAC concentrations. The inset shows the high Q behaviour of [DTAC] = 3.445 mmol/L with a small correlation peak identifying a bilayer of DTAC molecules. 120

CHAPTER IV

Figure IV-1. The temporal evolution of the turbidity of SRHA_{20mg/L}/Surfactant suspensions as a function of time obtained for various surfactant additions. 132

Figure IV-2. Turbidity at 1 hour of SRHA_{20mg/L}/surfactant suspensions as a function of surfactant concentration normalized by CMC. 133

Figure IV-3. SRHA_{20mg/L}/Surfactant Particles sizes as a function of [Surfactant]/CMC. The inset is the turbidity curve of SRHA/DTAC for comparison. 134

Figure IV-4. Variation of pH as a function of [Surfactant]/CMC for SRHA_{20mg/L}/Surfactant suspensions. 134

Figure IV-5. Variation of Conductivity ($\mu\text{S}/\text{cm}$) versus surfactant concentration for SRHA_{20mg/L}/Surfactant suspensions. 135

Figure IV-6. Electrophoretic mobility of SRHA_{20mg/L}/Surfactant suspensions versus surfactant concentration normalized by CMC. The inset is the electrophoretic mobility of SRHA/DTAC over the range of concentration used. 136

Figure IV-7. Electrophoretic mobility of SRHA_{20mg/L}/CTAC suspensions at low concentration. The turbidity and size curves are shown in order to locate the main variations of electrophoretic mobility. 136

Figure IV-8. Surface Tension of: (a) SRHA_{20mg/L}/Surfactant suspensions versus surfactant concentration normalized by CMC; (b), (c) and (d) the Surfactants OTAC, DTAC and CTAC, respectively. 138

Figure IV-9. Cryo-TEM micrographs of SRHA_{1g/L}/Surfactant molecular structures. [DTAC] mmol/L: (a) 0; (b) $7.6 \cdot 10^{-3}$; (c1-2) $37.86 \cdot 10^{-3}$; (d1-2) $188.53 \cdot 10^{-3}$; (e1-2) $375.19 \cdot 10^{-3}$. [CTAC] mmol/L: (a') $3.12 \cdot 10^{-5}$; (b') $18.7 \cdot 10^{-5}$; (c') $93.6 \cdot 10^{-5}$; (d') $311 \cdot 10^{-5}$ 141

Figure IV-10. Size histograms (%) of molecular structures viewed by cryoTEM and evolution of mean particle size with DTAC concentration. The DTAC concentration is indicated in the histograms in mmol/L. The histograms in red are associated with the presence of layer thickening vesicles. 142

Figure IV-11. Size histograms (%) of molecular structures viewed by cryoTEM and evolution of mean particle size with CTAC concentration. The CTAC concentration is indicated in the histograms in mmol/L.	142
Figure IV-12. Surface tension of SRHA versus log [SRHA].	145
Figure IV-13. Turbidity variation of SRHA _{20mg/L} /DTAC suspensions at 1hour as a function of DTAC concentration at pH=7. The turbidity of SRHA _{20mg/L} /DTAC suspensions at inherent pH=4.52 is added for comparison.	148
Figure IV-14. Surface Tension of SRHA _{20mg/L} /DTAC suspensions concentration at pH=7 versus surfactant concentration. The Surface tension of SRHA/DTAC suspensions at inherent pH=4.52 is added for comparison.	148
Figure IV-15. Cryo-TEM micrographs of SRHA _{1g/L} /DTAC molecular structures at pH=7. [DTAC] mmol/L: (a-c) $7.58 \cdot 10^{-3}$; (d-f) $226 \cdot 10^{-3}$. The arrow indicates the multilamellar vesicles.	150
Figure IV-16. The double-logarithmic plot of I(Q) versus Q from SRHA _{5g/L} /DTAC suspensions in D ₂ O as a function of cationic surfactant concentration.	151
Figure IV-17. Illustration of swollen and Gaussian chain (Teixeira, 1988 ; Jarvie and King, 2007).	154
Figure IV-18. Illustration of the long range (ξ_1) and the short range (ξ_2) correlation length.	155

CHAPTER V

Figure V-1. Temporal evolution of turbidity for various HS-DOM/DTAC suspensions as a function of time for the various DTAC additions.	166
Figure V-2. UV/visible spectra (Absorbance normalized by DOC in mg C L ⁻¹) of the various HS-DOM.	167
Figure V-3. UV/Visible spectra of HS-DOM/DTAC suspensions after various DTAC additions. The arrows indicate the newly emerged bands. DTAC Concentrations are indicated in the graph in mmol/L.	168
Figure V-4. Fluorescence emission spectra (excitation wavelengths of 230, 264 and 380nm) of HS-DOM/DTAC suspensions after various DTAC additions.	170
Figure V-5. Fluorescence emission spectra (excitation wavelengths of 270, 350 and 400nm) of HS-DOM/DTAC suspensions after various DTAC additions.	171

Figure V-6. Variation of Tryptophan-like (●) (I_{Try} ($\lambda_{\text{Ex}}=230\text{nm}$ / $\lambda_{\text{Em}}=327\text{nm}$)) and Humic-Like (■) ($I_{\text{HLF-1}}$ ($\lambda_{\text{Ex}}=264\text{nm}/\lambda_{\text{Em}}=445\text{nm}$)) Fluorescence intensity of HS-DOM/DTAC suspensions for excitation wavelengths of 230 and 264 nm as a function of DTAC concentration. The corresponding turbidity curves (▲) are shown in order to locate the main variations..... 173

Figure V-7. Relationship between the intensities of Protein-like and the Humic-like Fluorescence peaks, $I_{\text{PLF-1}}-I_{\text{PLF-2}}$, $I_{\text{HLF-1}}-I_{\text{HLF-2}}$ and $I_{\text{HLF-3}}-I_{\text{HLF-4}}$ (see inset) at excitation wavelength of 230nm, 264nm and 380nm respectively. The Fluorescence Intensities in arbitrary unity (A.U) are normalized by DOC (in mg C L^{-1}). The filled marker (▲) corresponds to HS-DOM and the empty marker (△) designates HS-DOM with DTAC. (▲) SRFA; (▲) SRHA; (▲) NHA; (▲) MHS; (▲) RN; (▲) RJ..... 176

ANNEXES

ANNEX 1

This annex is supplement of Chapter III. Here, we investigate the effect of various conditions on the interaction of SRFA with DTAC.

1- Effect of pH on the interaction of SRFA_{20mg/L}/DTAC_{10g/L}: pH=4.32 and pH=7

Figure III-A1 shows the turbidity at 1 hour of SRFA_{20mg/L}/DTAC (i.e. 12mg C/L) suspensions as a function of DTAC concentration at the natural unmodified pH=4.32 and at the modified pH=7. The modification to neutral pH caused a shift of the two peaks to higher DTAC concentration to 0.13cmc and 0.4cmc compared to the inherent pH (4.32) at 0.1cmc and 0.29cmc, respectively. This is possibly due to increased in the negative charges where at higher pH more functional groups are ionized which require more surfactant concentration to reduce the electrostatic repulsion and neutralization. No difference was observed with the conductivity where they are superimposed (Figure III-A2b).

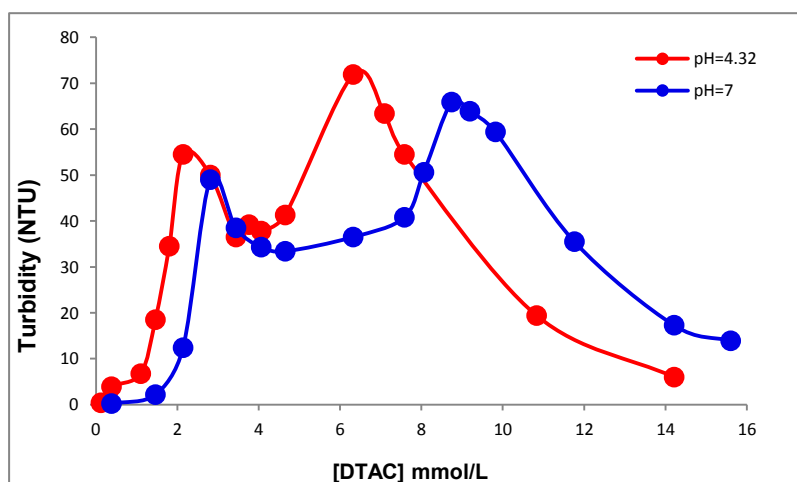


Figure III-A1. Turbidity at 1h of SRFA_{20mg/L}/DTAC suspensions as a function of surfactant concentration at pH 4.32 and 7.

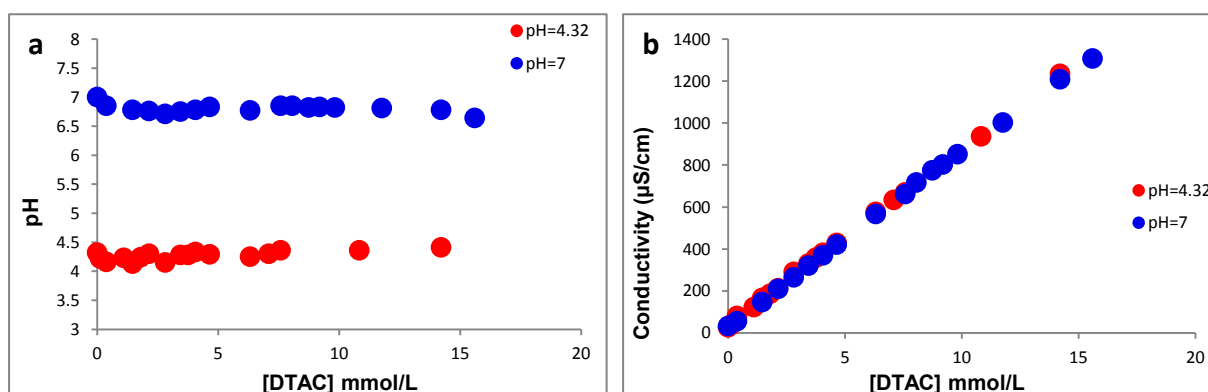


Figure III-A2. Variation of pH (a) and Conductivity (b) of SRFA_{20mg/L}/DTAC suspensions as a function of DTAC concentration at pH 4.32 and 7.

2- Influence of the initial stock concentration of DTAC: SRFA_{20mg/L}/DTAC_{10g/L} and SRFA_{20mg/L}/DTAC_{5g/L}

The concentration of DTAC stock solution previously used was 10g/L (37.89 mmol/L), which is above the CMC (21.7mmol/L). Therefore, the added DTAC to the SRFA is in the form of micelles. We wanted to identify whether it is the micelles or DTAC molecules that contribute in the formation of the various structures of fulvic acid. For this, a concentration of 5g/L of DTAC was used (18.94mmol/L). Figure III-A3 shows the variation of turbidity at 1 hour as a function of DTAC concentration for SRFA_{20mg/L}/DTAC_{5g/L} suspensions, SRFA_{20mg/L}/DTAC_{10g/L} curve is added for comparison. The two curves show similar variation with two-well resolved peaks; they are superimposed from the first addition of DTAC until the decreasing part of the first peak (i.e. 4.4mmol/L); while at the second peak, the turbidity of SRFA_{20mg/L}/DTAC_{5g/L} is lower than that of SRFA_{20mg/L}/DTAC_{10g/L}.

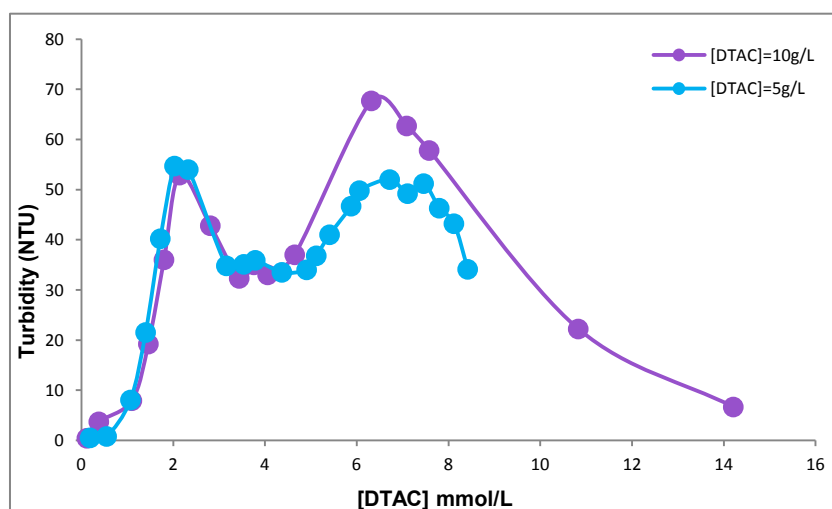


Figure III-A3. Variation of turbidity at 1 hour versus DTAC concentration for two mixtures: SRFA_{20mg/L}/DTAC_{10g/L} and SRFA_{20mg/L}/DTAC_{5g/L}.

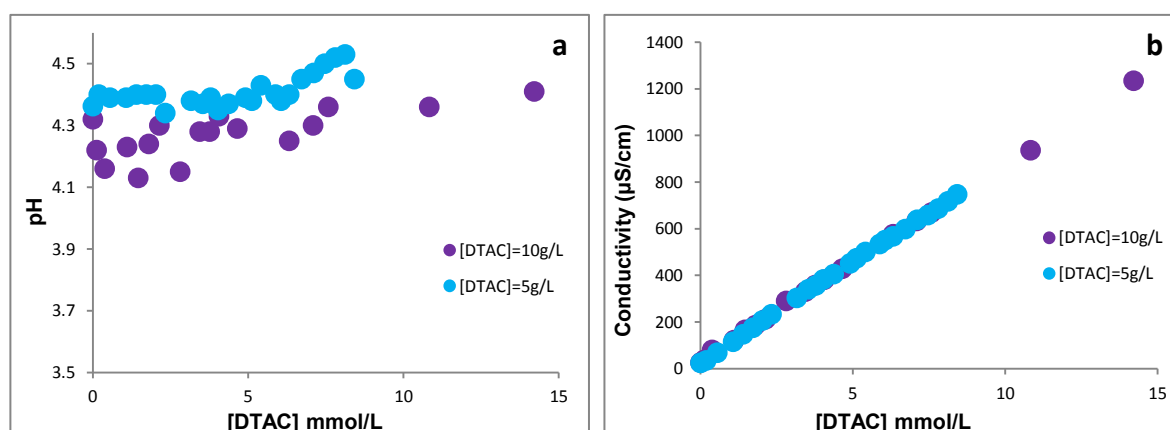


Figure III-A4. Variation of pH (a) and Conductivity (b) as a function of DTAC concentration for two mixtures: SRFA_{20mg/L}/DTAC_{10g/L} and SRFA_{20mg/L}/DTAC_{5g/L}.

Obtaining similar patterns in both cases, the initial concentration of DTAC above and one below CMC, demonstrates that it is the primarily DTAC molecule that is involved in the formation of aggregates rather than micelles, and that the process of aggregate formation is relatively stable regardless of the initial conditions although it may affect the type and amount of new structures formed and their size. Concomitantly, the pH modification didn't affect the behavior and the mode of interaction of SRFA/DTAC.

ANNEX 2

This part is supplement of Chapter IV.

1- Effect of the initial concentration of SRHA: SRHA_{10mg/L}/DTAC_{10g/L} and SRHA_{20mg/L}/DTAC_{10g/L}

1-1. Turbidity Measurement

Figures IV-A1 shows the effect of varying the initial concentration of SRHA on associations in the SRHA/DTAC suspensions. Increasing the SRHA concentration from 10 to 20 mg/L (i.e. 6 to 12 mg C/L, respectively) and because the peak of the mixture is not well determined, it is difficult to indicate a shift between the two SRHA concentrations. However, we can observe a consistent pattern at low DTAC concentration. The results presented show that the initial concentration of SRHA did not change the behavior of SRHA/DTAC associations, although it may affect the amount of new structures formed and their size.

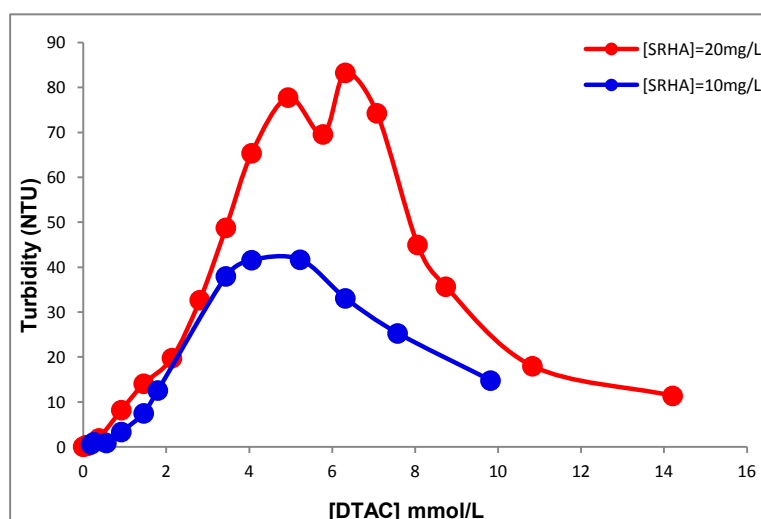


Figure IV-A1. The variation of turbidity at 1 hour of SRHA_{10mg/L}/DTAC_{10g/L} and SRHA_{20mg/L}/DTAC_{10g/L} upon DTAC addition.

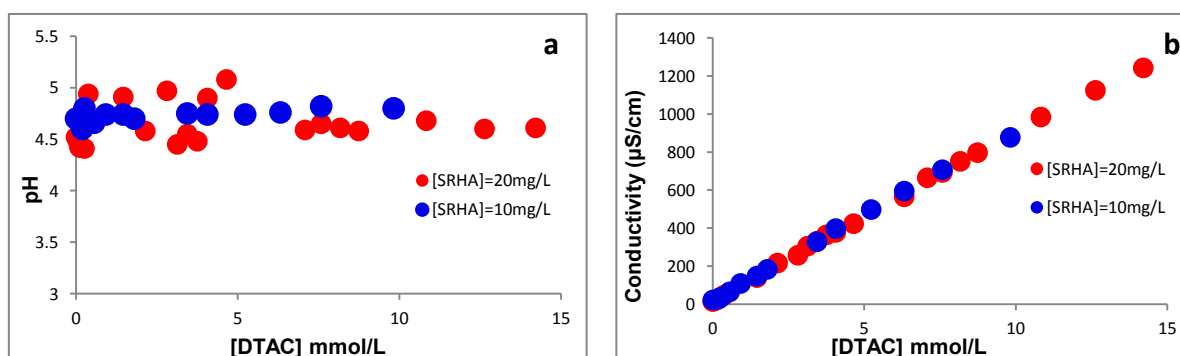


Figure IV-A2. Variation of pH (a) and Conductivity (b) as a function of DTAC concentration for two mixtures: SRHA_{10mg/L}/DTAC_{10g/L} and SRHA_{20mg/L}/DTAC_{10g/L}.

1-2. Comparison of the size of the particles obtained in the mixtures: SRHA_{10mg/L}/DTAC_{10g/L} and SRHA_{20mg/L}/DTAC_{10g/L}

Figure IV-A3 shows the variation in particle size depending on the concentration of DTAC at 1h. The same size ranges are obtained for both SRHA stock solutions studied, i.e. basic unit of 70 nm is formed regardless the initial concentration of DTAC added, and another size range between 200 and 400 nm. Therefore, at low DTAC concentration, the SRHA/DTAC interactions contribute to the formation of new structures of sizes that are relatively stable regardless of the initial concentration of the SRHA stock solutions.

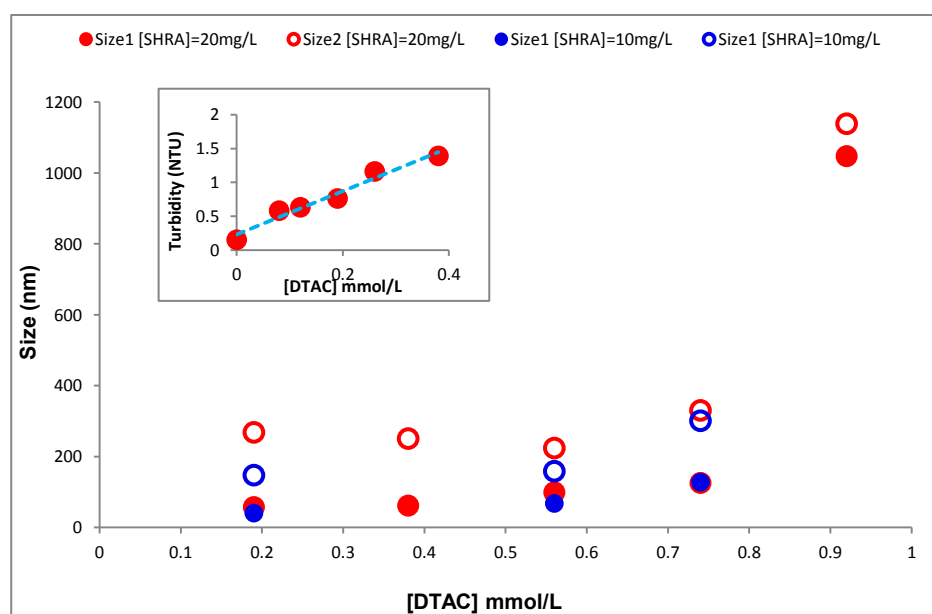


Figure IV-A3. Comparison of particles sizes obtained upon DTAC addition for SRHA_{10mg/L}/DTAC_{10g/L} and SRHA_{20mg/L}/DTAC_{10g/L} suspensions.

2- Effect of the initial stock concentration of DTAC: SRHA_{20mg/L}/DTAC_{10g/L} and SRHA_{20mg/L}/DTAC_{5g/L}

2-1. Turbidity Measurement

Figure IV-A4 shows the variation of turbidity at 1 hour as a function of DTAC concentration for SRHA_{20mg/L}/DTAC_{5g/L} and SRHA_{20mg/L}/DTAC_{10g/L} suspensions. The two curves are superimposed especially in the region of increased turbidity (in the area below 4mmol/L), with a lower turbidity value of the peak for SRHA_{20mg/L}/DTAC_{5g/L}. The variation of the initial stock concentration of DTAC did not affect the overall behavior and the mode of interaction of SRHA/DTAC where similar pattern is obtained.

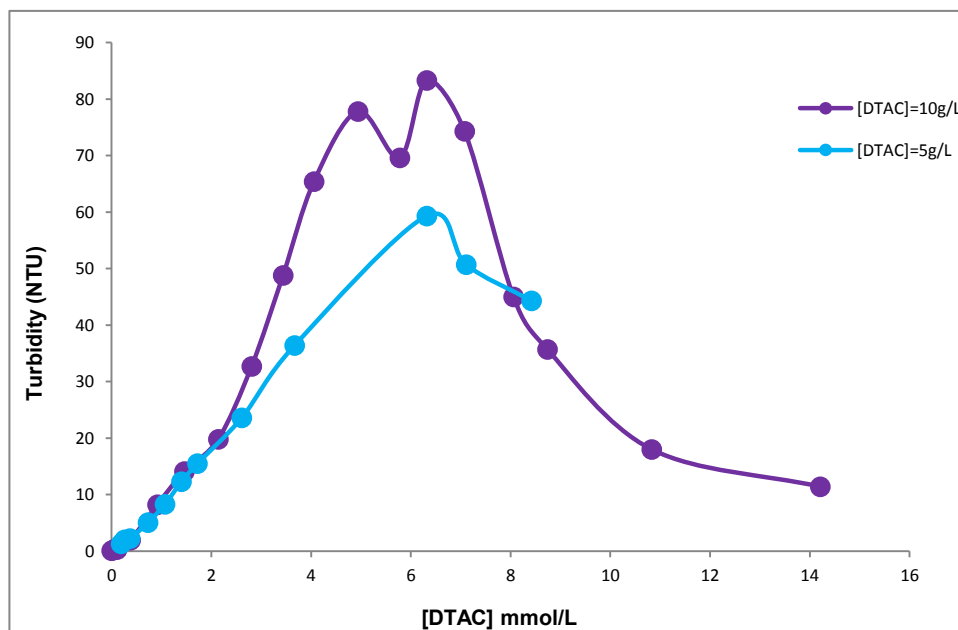


Figure IV-A4. Variation of turbidity at 1 hour versus DTAC concentration for two mixtures: SRHA_{20mg/L}/DTAC_{10g/L} and SRHA_{20mg/L}/DTAC_{5g/L}.

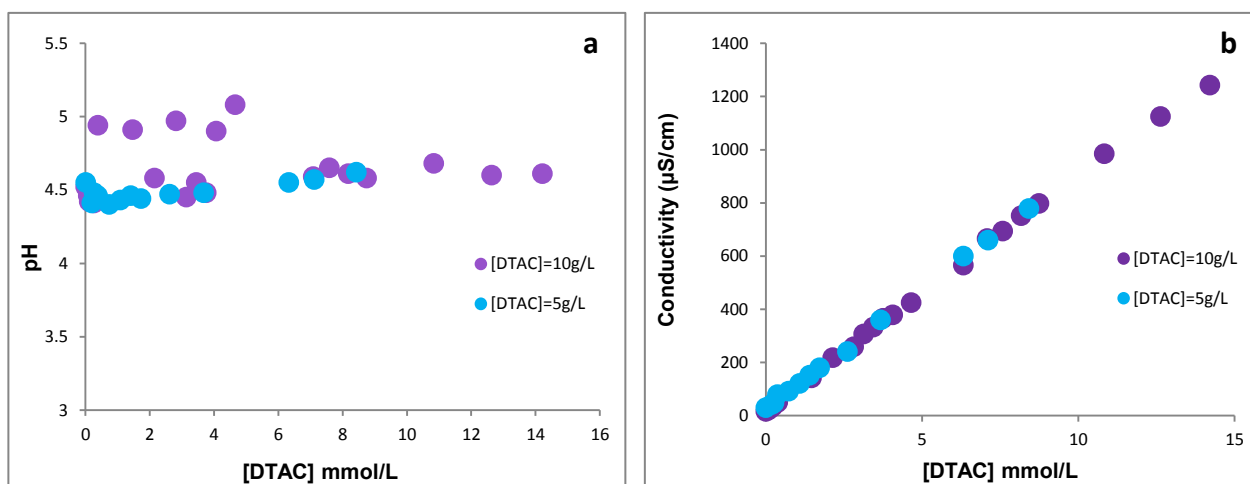


Figure IV-A5. Variation of pH (a) and Conductivity (b) as a function of DTAC concentration for two mixtures: SRHA_{20mg/L}/DTAC_{10g/L} and SRHA_{20mg/L}/DTAC_{5g/L}.

2-2. Comparison of the size of the particles obtained in the mixtures: SRHA_{20mg/L}/DTAC_{10g/L} and SRHA_{20mg/L}/DTAC_{5g/L}

Figure IV-A6 shows the variation in particle size at 1h upon DTAC addition. The same size ranges are obtained as that of the other mixtures previously studied (SRHA_{20mg/L}/DTAC_{10g/L} and SRHA_{10mg/L}/DTAC_{10g/L}).

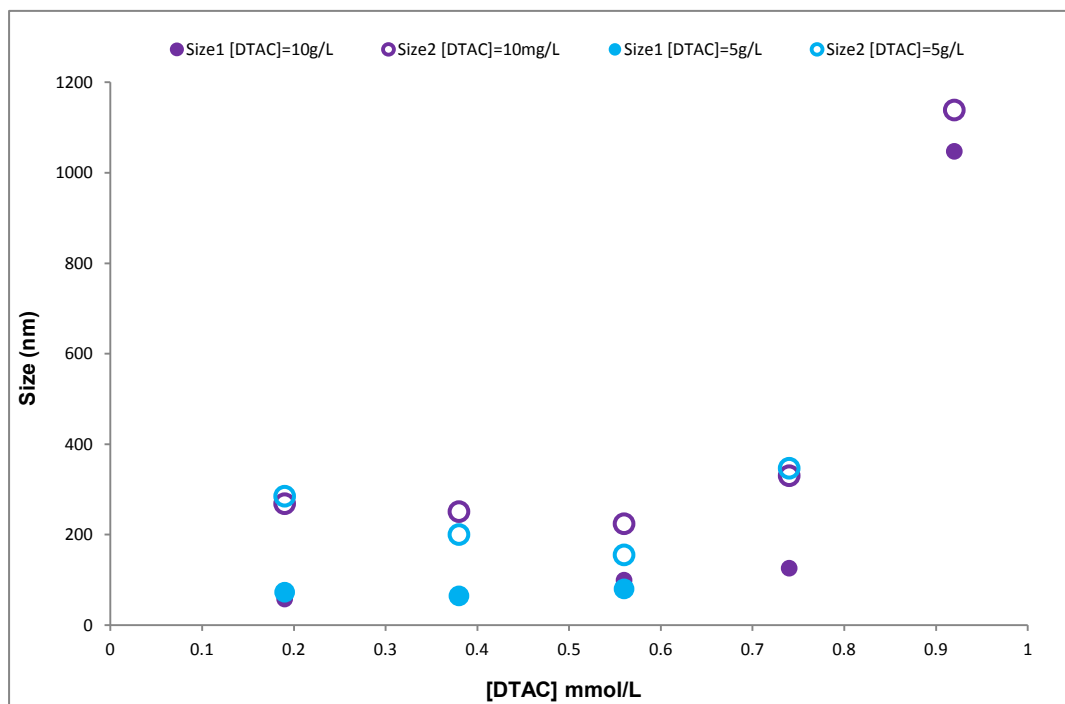


Figure IV-A6. The particles sizes obtained upon DTAC addition for SRHA_{20mg/L}/DTAC_{10g/L} and SRHA_{10mg/L}/DTAC_{5g/L} suspensions.

ANNEX 3

This annex is supplement of Chapter V. the effect of longer alkyl chain length on the fluorescence properties of SRHS is investigated

Fluorescence Intensity variation of SRHA/Surfactant (CTAC and DTAC) and SRFA/Surfactant (CTAC and DTAC) as a function of emission wavelength under various excitation wavelengths (λ_{ex} =230, 264, 350, 380 and 400nm) are shown in figures V-A1 and V-A2, respectively. Indeed the surfactant addition caused molecular rearrangement leading to the emergence of new peaks rather than the single broad band and shoulder that characterized the HS and to the variation in the intensities of the spectra with the various surfactant concentration points out conformational change upon the HS-Surfactant complexation.

In the case of SRFA, the type of surfactant (DTAC or CTAC) produced the same effect without altering the position of new peaks (figures V-A2), although the intensities cannot be compared among the spectra because each sample was measured under different detector settings in order to optimize the signal. Whereas with SRHA, CTAC induces a blue shift of 20nm if compared to DTAC (figures V-A1). This could be a result of increased isolation of certain fluorophores from the bulk aqueous solvent (Mobed et al. 1996 ; Pullin and Cabaniss 1995) while SRHA with DTAC allowed π -Conjugation and electron delocalization of different electron donating groups. Inner filtering and quenching can be also observed in the lower intensities of the emission spectra of SRHA/CTAC if compared to that of SRHA/DTAC at same excitation wavelength. This could be attributed to the high absorbance at the short wavelengths where CTAC could cause a more compact rigid structure of SRHA than that obtained with DTAC leading to proximity of the fluorophores and increasing the probability of deactivation of excited states by internal quenching.

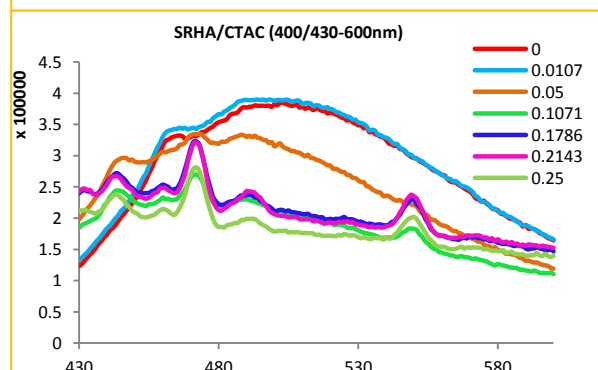
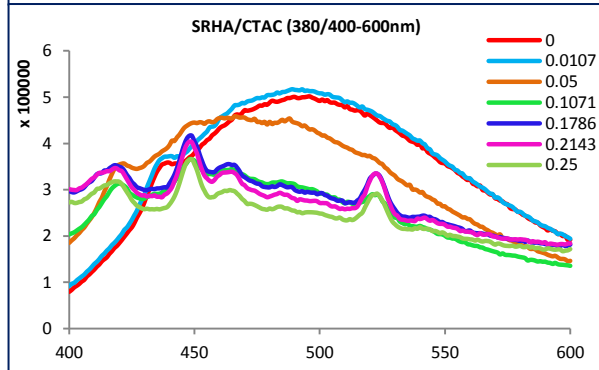
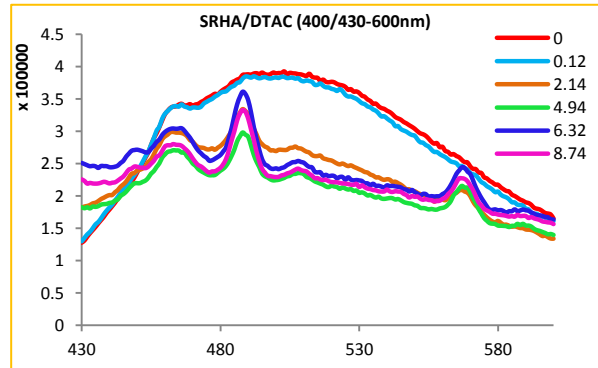
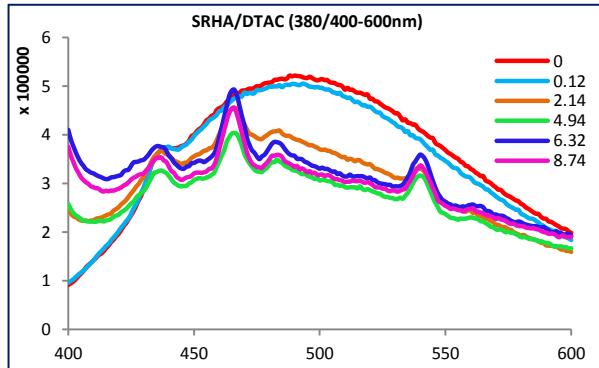
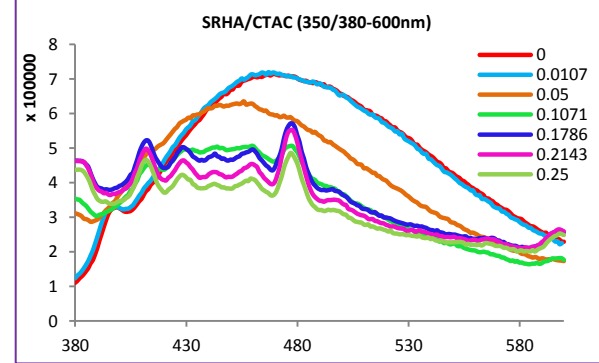
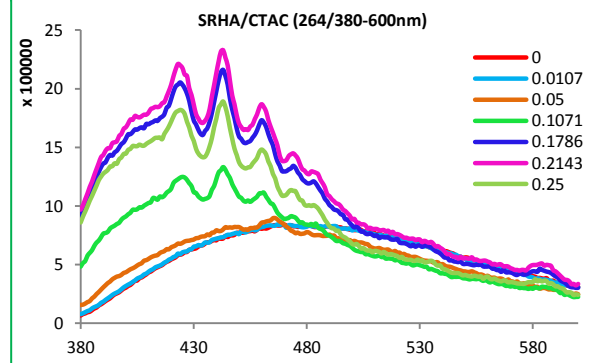
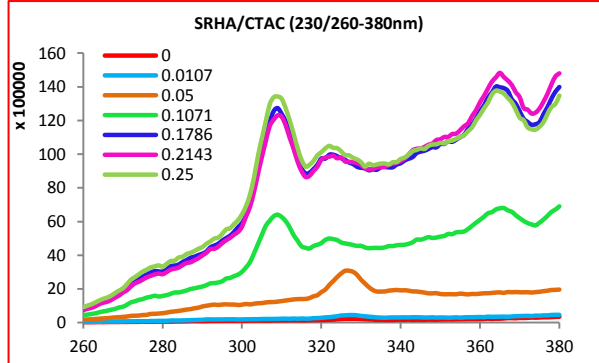
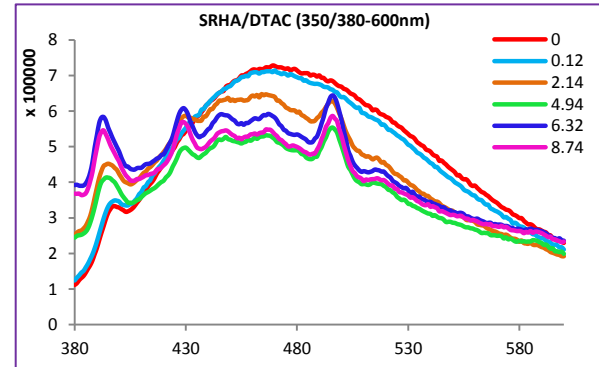
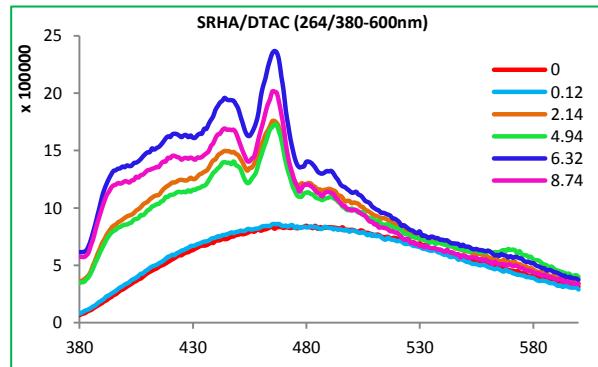
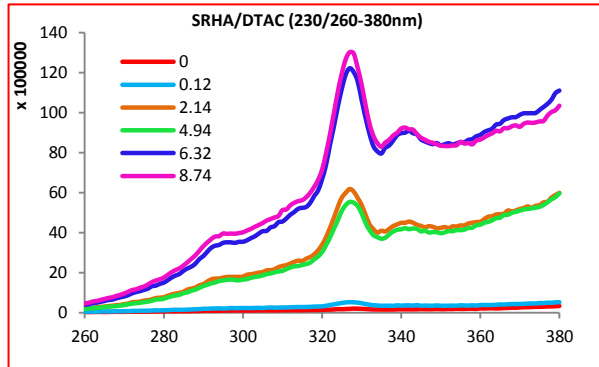


Figure V-A1. Variation Fluorescence Intensity of SRHA/DTAC and SRHA/CTAC as function of emission wavelength (nm) for various surfactant additions. The x-axis is the Emission wavelength (nm), the y-axis is the intensity, and the surfactant concentration is indicated in the graphs in mmol/L.

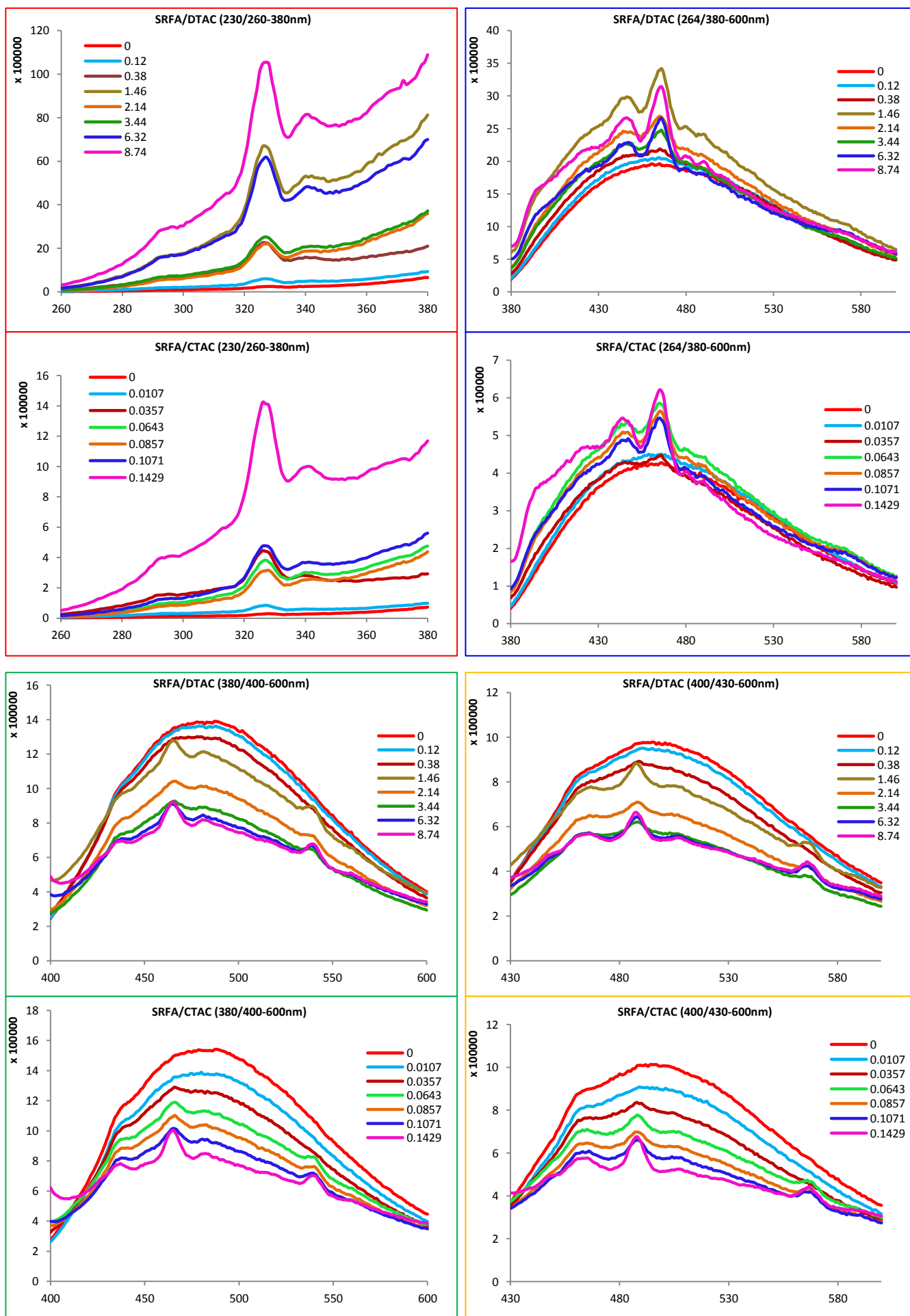


Figure V-A2. Variation Fluorescence Intensity of SRFA/DTAC and SRFA/CTAC as function of emission wavelength (nm) for various surfactant additions. The x-axis is the Emission wavelength (nm), the y-axis is the intensity, and the surfactant concentration is indicated in the graphs in mmol/L.

ABSTRACT

Study of the Structural Organization of Humic Nanocolloids

The structural organization of humic nanocolloids remains a matter of harsh debate, and surprisingly, it is yet not possible to decide between an arrangement of the humic matter in the form of randomly coiled macromolecules more or less connected, and a supramolecular organization of small heterogeneous molecules linked by hydrogen bonds and hydrophobic interactions. In this study, we investigate the reformation induced by the addition of cationic surfactants (C n-trimethylammonium chloride) of varying alkyl chain length with a series of humic substances (HS) and Dissolved Organic matter (DOM) from two blackwater rivers of the Central Amazon. Turbidity measurements, Dynamic light scattering, electrophoretic mobility, surface tension, fluorescence spectroscopy, small angle neutron scattering and cryo-transmission electron microscopy (cryo-TEM), are combined to describe the Humic Substance/Surfactant complexes obtained. The association between the oppositely charged HS and cationic surfactant is driven by both electrostatic and hydrophobic interactions. A variety of molecular structures, unilamellar vesicles, disks, globules, spheroidal micelles, are visualized by cryo-TEM depending on surfactant concentration. Such sequence, consistent with those displayed by catanionic systems, provides an independent confirmation of both the amphiphilic nature of HS and of its supramolecular organization. In addition, the molecular rearrangement was investigated using single-scan fluorescence emission spectra spectroscopy, thus identifying the chemical groups responsible for the fluorescence properties in HS and DOM. The addition of cationic surfactant to HS/DOM unveils an unexpected fine structure of humic-like fluorescence through new emission peaks that are not evidenced in the references HS/DOM. An enhanced protein-like fluorescence indicating major restructuring and structural stacking/de-stacking is observed. All our results support a supramolecular organization of humic substances and DOM.

RÉSUMÉ

Etude de l'Organisation Structurale des Nanocolloïdes Humiques.

L'organisation des substances humiques à l'échelle moléculaire reste une question largement débattue, et à ce jour, il n'a pas été possible de trancher entre une structure polymérique en pelote plus ou moins flexible et un assemblage supramoléculaire de molécules hétérogènes associées par des liaisons hydrogènes et des interactions hydrophobes. Dans cette thèse, nous étudions la reformation induite par l'addition de tensio-actifs cationiques (Chlorure de C n-triméthylammonium) sur une série de substances humiques (acides fulvique et humiques) ainsi que sur de la matière organique naturelle contenue dans des eaux noires. Des mesures de turbidité, de diffusion de lumière, mobilité électrophorétique, tension de surface, spectroscopie de fluorescence, diffusion des neutrons aux petits angles, et cryomicroscopie à transmission, permettent de décrire les complexes formés entre le tensio-actif et la matière humique. L'association matière humique/tensio-actif dépend à la fois d'interactions d'origine électrostatique et hydrophobe. Une série de structures moléculaires, vésicules, disques, globules, pseudo-micelles, est observée en cryomicroscopie selon la concentration en surfactant. La séquence obtenue est cohérente avec un système catanionique, en d'autres termes une partie de la matière humique est amphiphile et s'organise en assemblage supramoléculaire. L'addition de tensio-actif modifie également fortement le spectre de fluorescence de la matière humique, les nouvelles bandes bien résolues présentes sur le spectre indiquant une restructuration majeure de l'assemblage supramoléculaire.

Key Words: *Humic substances, Cationic Surfactant, Structural Organization, Polymer Macromolecule, Supramolecule, Cryogenic Transmission Electron Microscopy, Fluorescence spectroscopy.*